

AN ABSTRACT OF THE THESIS OF

STEPHEN JOSEPH WALSH for the degree of DOCTOR OF PHILOSOPHY

in Geography presented on August 19, 1977

Title: AN INVESTIGATION INTO THE COMPARATIVE UTILITY OF
COLOR INFRARED AERIAL PHOTOGRAPHY AND LANDSAT DATA
FOR DETAILED SURFACE COVER TYPE MAPPING WITHIN
CRATER LAKE NATIONAL PARK, OREGON

Abstract approved: -

Redacted for Privacy

James F. Laney

The identification and mapping of surface cover types within Crater Lake National Park, Oregon, has been effectively completed through the utilization of LANDSAT digital data and NASA U-2 color infrared aerial photography. Classification of LANDSAT data for surface cover type identification and mapping was accomplished through use of the Interactive Digital Image Manipulation System (IDIMS) which provided enormous classification flexibility due to the interactive capability of IDIMS and its color video display.

LANDSAT data extraction techniques employed in this research include the generation of grayscales; density slice; spectral reflectance plots versus pixel frequency and LANDSAT bands for low sun angle and medium to high sun angle LANDSAT digital tape dates; spectral relationship plots; and control clustering of training set selection.

The use of these techniques produced training statistics which show "good" class discrimination for study area classification. A covariance matrix, weighted divergence, and distance between clusters were generated for each of the 59 training classes to determine if any of the classes were statistically related and should be combined.

Slope angle, slope aspect, and surface cover type variation, and to a lesser degree, crown size and crown density are the main environmental factors which account for spectral reflectance variation of surface cover types within Crater Lake National Park. Through an understanding of the influence of environmental factors in the reflectance value of surface cover types, one can evaluate the quality of training statistics and the location of training areas in order to reduce misclassification or nonclassification possibilities. A regression analysis, analysis of variance, T-values, F-values, and beta values were used to determine the relative degree that certain environmental factors influence the spectral reflectance of surface cover types producing a change in the mean reflectance of surface cover types per LANDSAT band.

LANDSAT classification accuracy levels for 12 major surface cover types within Crater Lake National Park range from 84 to 98 percent. Accuracy levels are inversely related to the level of detail sought and obtained.

LANDSAT's primary advantages over NASA U-2 color infrared aerial photography for surface cover type identification and mapping include: repetitive coverage; computer compatibility of data without photographic digitizing; multispectral scanner capability; and the further extension of wavelengths into the near infrared. The NASA U-2 aerial photography's primary advantages (over LANDSAT) for surface cover type identification and mapping include: increased scale; greater resolution; and stereoscopic viewing. Stereoscopic viewing was accomplished through use of an Old Delft Scanning stereoscope which provided 1.5 to 4.5 magnification.

"Ground truth" is the link between LANDSAT data, aerial photography, and actual ground conditions. "Ground truth" should measure and/or observe surface cover types and parameters which are capable of influencing the spectral reflectance as detected by LANDSAT. Geologic activity, soil conditions, vegetation, and climate have in the past and do in the present influence the spectral reflectance of surface cover types within Crater Lake National Park, Oregon.

All rights reserved,

Copyright © 1977, Stephen Joseph Walsh

An Investigation into the Comparative Utility of
Color Infrared Aerial Photography and LANDSAT
Data for Detailed Surface Cover Type Mapping
within Crater Lake National Park, Oregon

by

Stephen Joseph Walsh

A THESIS

submitted to

Oregon State University

in partial fulfillment of
the requirements for the
degree of

Doctor of Philosophy

Completed August, 1977

Commencement June, 1978

APPROVED:

Redacted for Privacy

Professor of Geography
in charge of major

Redacted for Privacy

Chairman of the Department of Geography

Redacted for Privacy

Dean of Graduate School

Date thesis is presented: August 19, 1977

Typed by Deanna L. Cramer for Stephen Joseph Walsh

ACKNOWLEDGEMENTS

I would like to express my sincere appreciation to the members of my committee: Dr. James F. Lahey, Dr. A. Jon Kimerling, Dr. Gary L. Benson, Dr. Edward Starkey, Dr. Jerry Kling, and Dr. J. Granville Jensen, for sharing their time, experience, and knowledge during my pursuit of the doctoral degree. I am particularly grateful to Dr. James F. Lahey who served as major professor and advisor during my doctoral program. Dr. Lahey's enthusiasm, thoroughness, and determination in research; his guidance and concern for the individual; and his patience and motivation have truly been appreciated and have positively affected my personal development.

The scale of this research effort was made possible through the cooperation of the National Park Service; the USGS's EROS Data Center in Sioux Falls, South Dakota; the Environmental Remote Sensing Applications Laboratory (ERSAL) on the Oregon State University campus; and the Oregon State University's Computer Center and the Geography Department's Cartographic Service.

The National Park Service, particularly through Dr. Edward Starkey, Pacific Northwest Regional Research Coordinator, and Mr. Frank Betts, Superintendent of Crater Lake National Park, has been very supportive of research activities and remote sensing application to surface cover type identification and mapping within the Park.

Mr. Betts and other Crater Lake National Park personnel made available camping sites, field checking teams, personal time and involvement, and most importantly, a real concern for the research project.

Dr. Edward Starkey, besides providing personal involvement and interest, provided the funds necessary for this research project, including aerial photography, LANDSAT data, and the opportunity and cost of data processing at the EROS Data Center.

The United States Geological Service-operated EROS Data Center provided most importantly the use of the Interactive Digital Image Manipulation System (IDIMS). The Data Analysis Lab at the Center was made exclusively available for this research. Individuals such as Mr. Fred Waltz, Director of the Applications Branch of the EROS Data Center, Mr. Wayne Rodhe, forestry applications specialist, Ms. Shelley Ingle, computer operator, Mr. Dave Greenlee, computer programmer, and Mr. Chuck Nelson, our project manager, provided invaluable and quality assistance during and after our visit.

Dr. Barry J. Schrupf, Director of ERSAL, not only provided me with employment as a research assistant at the lab for two years, but also acquired, through NASA, color infrared aerial photography coverage over Crater Lake National Park for two dates. Without his effort, quality aerial photography would not have been available.

Mr. Dave Neiss, a member of the Oregon State University's Computer Center, provided great assistance in the mean reflectance and environmental factor investigation. Mr. Mark Keppinger, now a member of the Computer Center and formerly a member of the ERSAL staff, provided initial processing of LANDSAT data through use of the Oregon State University facilities.

Ms. Donna Batch and Mr. John L. Hruska, graduate students in Geography and members of the Department's cartographic service, are responsible for the fine cartographic work in this dissertation. Ms. Batch prepared the map of the vegetation of Crater Lake National Park and a few figures within the text. Mr. Hruska prepared the bulk of the figures within the text. My appreciation is offered to them.

I would also like to express my appreciation to my brother, Mr. Larry Walsh, for his assistance during field work. His patience, energy, cooperation, and durability are traits of which he can be proud and for which I am extremely grateful. To my parents, I am appreciative of their understanding and encouragement during my school years. Their concern and presence have been unwavering during the years, regardless of the many miles between us.

During my doctoral research, Mr. David L. Hawley, a doctoral candidate in Geography at OSU, has provided moral

support, cooperation, and most importantly, friendship. To him, I wish nothing but success and happiness.

Finally, I would like to express my most sincere appreciation to my wife Jeannie for her enduring patience, moral and financial support, sacrifice and love throughout these long years. This dissertation is dedicated to her.

TABLE OF CONTENTS

<u>Chapter</u>		<u>Page</u>
I	INTRODUCTION	1
	Statement of Purpose.	1
	Geographic Area	2
II	SURFACE CHARACTERISTICS OF CRATER LAKE NATIONAL PARK WHICH INFLUENCE THE SPECTRAL REFLECTIVITY OF SURFACE FEATURES WITHIN THE PARK	9
	Geology	9
	Soils	21
	Climate	30
	Temperature.	38
	Precipitation.	39
	Snow.	40
	Vegetation.	41
III	DATA ACQUISITION	51
	Sampling Strategy and Parameters.	51
	Aerial Photography Acquisition.	57
	LANDSAT Data Acquisition.	59
IV	RECONNAISSANCE TECHNIQUES.	61
	LANDSAT Satellite	61
	Parameters and Earth Coverage.	62
	Instrumentation.	62
	LANDSAT Computer Compatible Tapes.	73
	LANDSAT Products	79
	LANDSAT Surface Cover Type Differentiation Potential	80
	Aerial Photography.	89
	Instrumentation.	89
	Color Infrared Aerial Photography Surface Cover Type Differentiation Potential	90
V	CLASSIFICATION PROBLEMS AND LIMITATIONS.	95
	Environmental Factors and Spectral Reflectivity.	95
	LANDSAT Classification and Pixel Problems.134
	Spectral Reflectance Properties.135
	Pixel Integration.135
	LANDSAT Scanner Readjustment138
	Loss of Boundary and Size Definition140
	Pixel to Ground Registration144
	Atmospheric Attenuation of LANDSAT and Aerial Photography Data146

Table of Contents -- continued

<u>Chapter</u>		<u>Page</u>
VI	DATA EXTRACTION TECHNIQUES FOR LANDSAT AND NASA U-2 AERIAL PHOTOGRAPHY.149
	LANDSAT149
	Oregon State University	
	Computer System.149
	EROS Data Center171
	Tape Reformating.171
	Study Area Definition173
	Geometric Corrections173
	Control Point Selection and Digitizing.174
	Stratification Mask Generation.178
	Training Set Selection.181
	Spectral Relationship Plot.183
	Training Set Statistics191
	Classification.204
	LANDSAT Classification Accuracy.223
	Misclassification Problem230
	NASA U-2 Aerial Photography233
	Photographic Scale234
	Ecology and Plant Geography Information.235
	Photographic Interpretation Parameters236
	"Ground Truth" and Terrestrial Photography.244
	Surface Cover Type Map Generation245
	Comparison of LANDSAT Data and NASA U-2 Aerial Photography for Detailed Surface Cover Type Mapping.250
VII	SUMMARY AND CONCLUSIONS.254
	Summary254
	"Ground Truth" Activities.254
	Data Reconnaissance Techniques255
	Data Problems and Limitations.257
	Data Extraction Techniques260
	Conclusions264
	BIBLIOGRAPHY268
	APPENDIX I: Cluster Analysis.280
	APPENDIX II: Classification Key.292

LIST OF TABLES

<u>Table</u>	<u>Page</u>
1	Sequence of Events in the Crater Lake Region . . . 11
2	Estimated Soil Properties of Types within the Park 25
3	Woodland Suitability of Soil Types 26
4	Yearly Values of Direct Solar Radiation for Selected Slope Angles and Slope Aspects at 43 Degrees North Latitude. 32
5	Daily Values of Direct Solar Radiation for Selected Slope Angles and Slope Aspects on September 10 at 43 Degrees North Latitude. . . . 33
6	Daily Values of Direct Solar Radiation for Selected Slope Angles and Slope Aspects on December 22 at 43 Degrees North Latitude 34
7	Comparative Climatic Data of the Crater Lake National Park Region 36
8	Major Tree Species and Common Brush Types of Crater Lake National Park. 42
9	LANDSAT Orbit Parameters 64
10	Regression Analysis (Bands 4, 5, 6, and 7) . . .102
11	Ranking of Variables for "Full Regression" (Bands 4, 5, 6, and 7)107
12	Regression Analysis (Band 4)113
13	Ranking of Subclass Variables per Class Regression (Band 4).116
14	Regression Analysis (Band 5)118
15	Ranking of Subclass Variables per Class Regression (Band 5).121
16	Regression Analysis (Band 6)122
17	Ranking of Subclass Variables per Class Regression (Band 6).125

LIST OF FIGURES

<u>Figure</u>		<u>Page</u>
1	The Location of Crater Lake National Park within the State of Oregon	3
2	The Main Quaternary Volcanoes of the Cascade Range.	4
3	Crater Lake National Park.	6
4	Distribution of Pumice Deposits from Mount Mazama	15
5	The Evolution of Crater Lake	17
6	Generalized Geologic Map of Crater Lake National Park and Vicinity	20
7	Soil Distribution of Crater Lake National Park	23
8	Location of Climatic Data Recording Stations . .	37
9	"Ground Truth" Sample Site within Crater Lake National Park.	54
10	LANDSAT Ground Coverage Pattern.	63
11	Schematic Diagram of the LANDSAT MSS Scanning Arrangement.	65
12	LANDSAT Tracking Scheme.	67
13	LANDSAT MSS System	68
14	Ground Scan Pattern for a Single MSS Detector. .	69
15	Interleaving of LANDSAT Data	74
16	Comparison of the Constant Mirror Velocity and the Variable Mirror Velocity of LANDSAT. . .	76
17	Integration and Variable Overlapping of Pixels Corresponding to a Variable Mirror Velocity	77
18	Comparison of Distance Covered on the Ground for a Constant Mirror Velocity and a Variable Mirror Velocity.	78

List of Figures -- continued

<u>Figure</u>		<u>Page</u>
19	Ground Registration Error Due to Variable Mirror Velocity.	81
20	LANDSAT Image of Band 4.	83
21	LANDSAT Image of Band 5.	84
22	LANDSAT Image of Band 6.	86
23	LANDSAT Image of Band 7.	87
24	LANDSAT Color Composite of Bands 4, 5, 6, and 7.	88
25	Color Formation with Color Infrared Film	91
26	Color Infrared Photograph of the Southern Portion of Crater Lake National Park	93
27	Spectral Reflectance of Two Pixel Component Surface Cover Types.137
28	Functioning of the MSS in Sensing Different Surface Cover Types.139
29	Changes in Reflectance Values for Differing and Adjacent Surface Cover Types141
30	Loss of Pixel Boundary and Size Definition142
31	Shape and Size Changes of Surface Cover Types.145
32	Spectral Reflectance155
32A	Reflectance Values165
33	IDIMS Transfer Tape Format172
34	Control Point Location within Crater Lake National Park.176
35	Training Set Statistics.182
36	Spectral Reflectance Plotting.184
37	Distribution of Intensive Study Areas within Crater Lake National Park.192

List of Figures -- continued

<u>Figure</u>		<u>Page</u>
38	Color Coded Map of Crater Lake National Park .	.208
39	Combining of Classes of Color Designation. . .	.210
40	Surface Cover Types of the Generated 59 Spectral Classes	in pocket
41	Surface Cover Types.	in pocket
42	Classification Error231
43	Classification Error232
44	Surface Cover Type Map of Crater Lake National Park.	in pocket
45	Key to Appendix II, LANDSAT Classes 1 through 35294
46	Key to Appendix II, LANDSAT Classes 36 through 59296

AN INVESTIGATION INTO THE COMPARATIVE UTILITY OF
COLOR INFRARED AERIAL PHOTOGRAPHY AND LANDSAT
DATA FOR DETAILED SURFACE COVER TYPE MAPPING
WITHIN CRATER LAKE NATIONAL PARK, OREGON

I. INTRODUCTION

Statement of Purpose

The primary objective of this research is to investigate the comparative utility of National Aeronautics and Space Administration (NASA) U-2 color infrared aerial photography and LANDSAT images and digital tapes for detailed surface cover type mapping within Crater Lake National Park, Oregon. A further objective of this research is to investigate and to develop appropriate techniques to extract information from color infrared aerial photography and satellite data for forest cover type separation and subsequent mapping.

The detailed mapping and analysis of surface cover types in Crater Lake National Park requires the differentiation of brush fields, non-vegetated areas, water areas, and variations in tree species through the use of color infrared aerial photography and LANDSAT data. The tree species, brush fields, and non-vegetated areas have been analyzed as they relate to slope angle, slope aspect, surface cover type, crown density, and crown size.

The spectral reflectance of the above-mentioned surface cover types (non-vegetated areas, brush fields, water, and tree species) as registered on the U-2 color infrared aerial photography and LANDSAT data have been analyzed for

spectral differentiation. The investigation of the spectral reflectance of the desired surface cover type mapping classes will be analyzed to the pixel level.

Geographic Area

The geographic area which was studied in order to evaluate the potential utility of U-2 color infrared aerial photography and LANDSAT digital tapes and images for the differentiation and mapping of brush fields, non-vegetated areas, water areas, and various tree species is Crater Lake National Park, Oregon.

Crater Lake National Park is located in southwestern Oregon between the latitudes of N 43° 04' and N 42° 46', and between the longitudes of W 122° 15' 56" and W 121° 59' 50" (Figure 1). The Park, which is approximately 250 square miles (402.25 sq km) in area, is situated in the southern High Cascade or Eastern Cascade physiographic province, and within the Sub-Alpine forest province including: the Abies amabilis (Pacific silver fir); A. lasiocarpa (subalpine fir); A. magnifica shastensis (shasta red fir); and Tsuga mertensiana (mountain hemlock) major vegetation zones (Franklin and Dyrness, 1973).

The High Cascades which extend from Northern California to Northern Washington (Figure 2) are made up of young volcanic rocks being almost totally Pliocene and Pleistocene in age. These young volcanic rocks have been eroded and

Location of Crater Lake National Park Within The State of Oregon

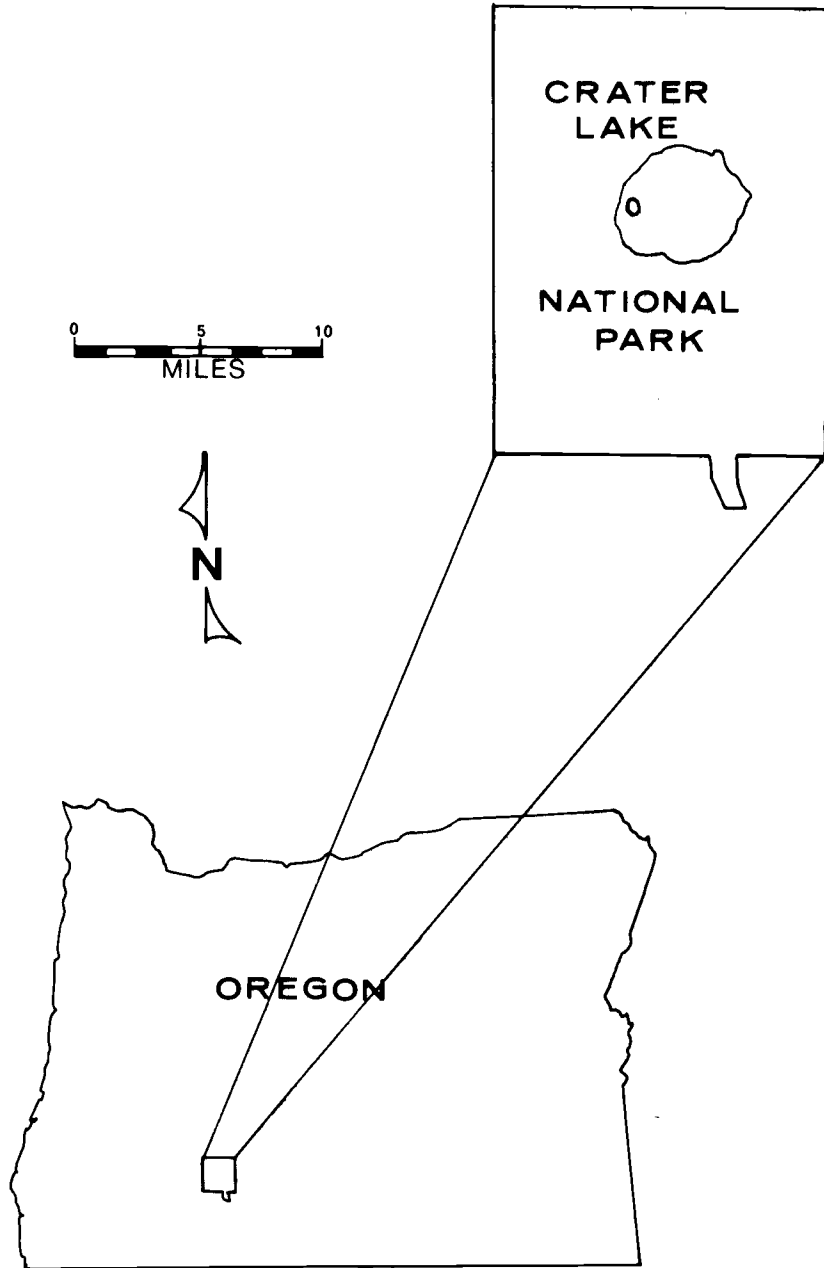


Figure 1.

The Main Quaternary Volcanoes of the Cascade Range

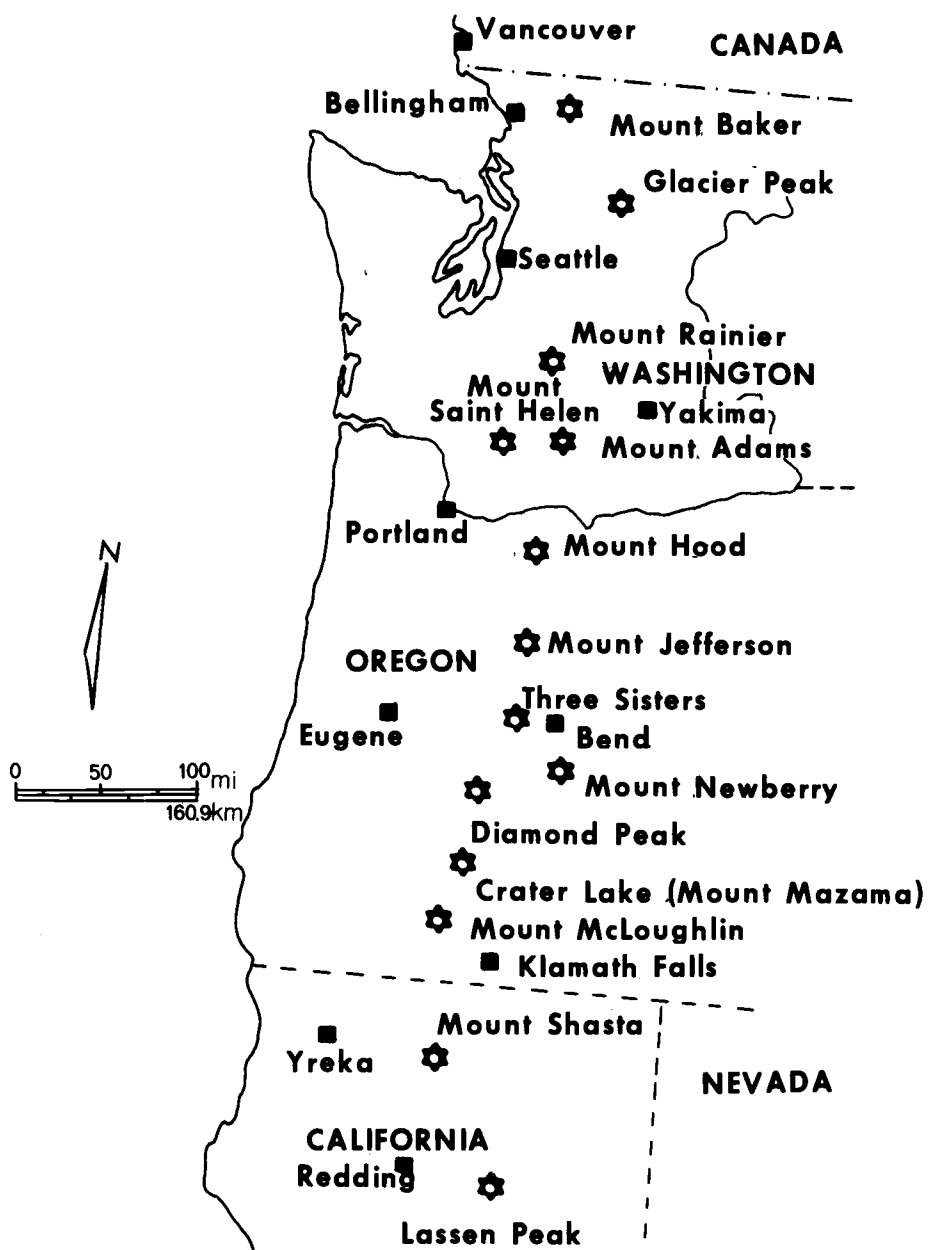


Figure 2. Adapted from McKee (1972).

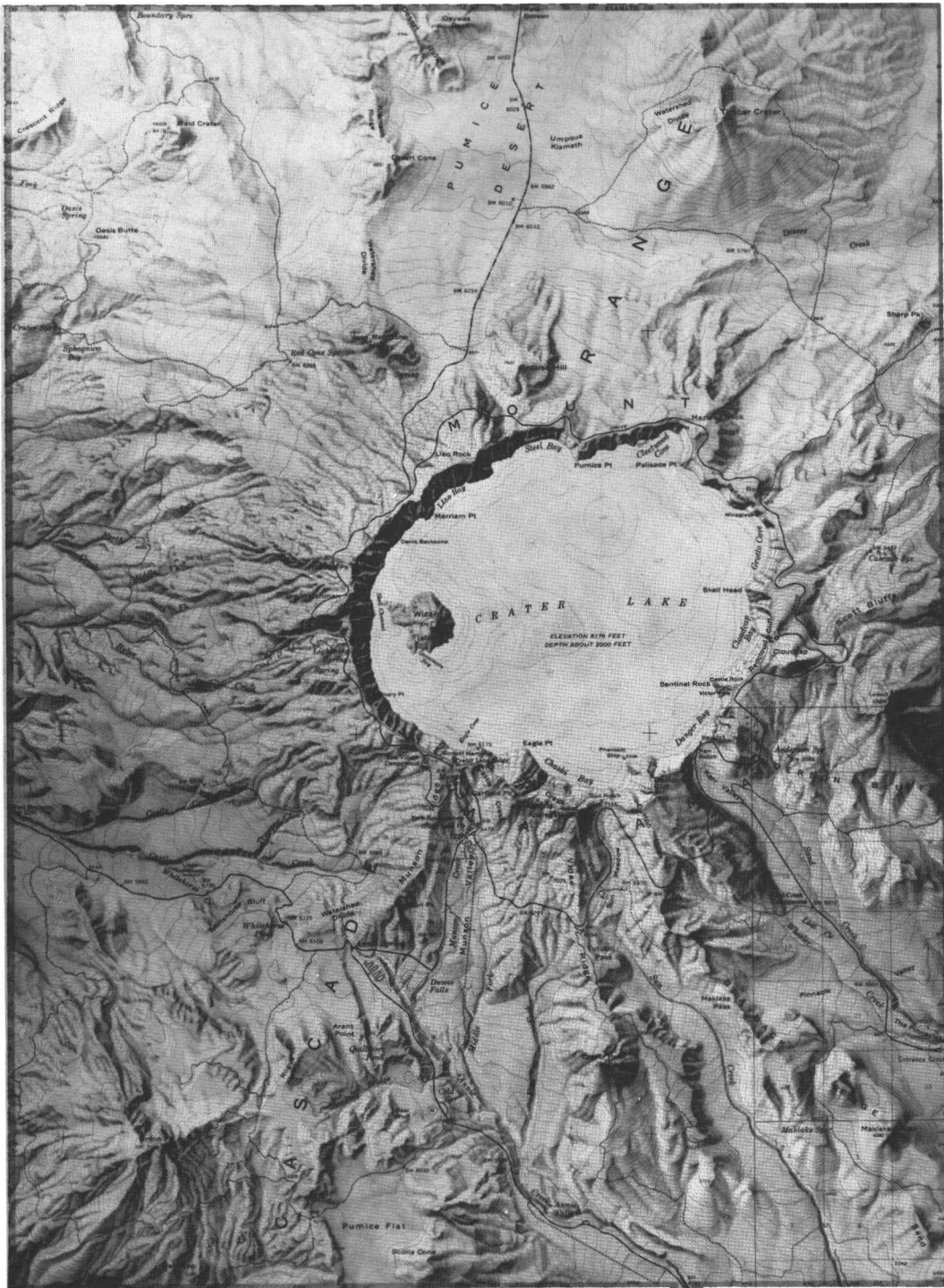
deformed little in comparison to the older Western Cascades, and thus the striking conical snowcapped peaks, glaciers, fresh lava flows, and volcanic and glacial lakes can be readily observed.

In Crater Lake National Park and its immediate vicinity, volcanic peaks are not as conspicuous as in other parts of the High Cascades. The dominant feature in and around the Park is the caldera (Crater Lake) (Figure 3). This caldera is the remnant of the ancestral Mount Mazama. The final major eruptions of Mount Mazama, occurring approximately 6,600 years ago, led to the mountain's collapse and the creation of the caldera.

The lake which formed within the caldera (Crater Lake) is 1,932 feet deep (588.88 m) at its deepest point with a shoreline of approximately 20 miles (32.18 km). The diameter of the lake varies between 4.5 (7.24 km) and 6.0 (9.65 km) miles (USGS, 1956).

The numerous creeks and streams which emanate from the slopes of the Crater Lake caldera drain either south and east into the Klamath River drainage basin or west into the Rogue River drainage basin. Nearly the entire western third of the Park drains into the Rogue River drainage, while the eastern two-thirds of the Park drains into the Klamath River drainage.

Crater Lake National Park is diverse in topography. Local relief is approximately 4,500 feet (1371.62 m) with



Crater Lake National Park



Figure 3

Mount Scott, located in the east central portion of the Park, being the highest point at 8,926 feet (2720.68 m), while the so-called "Panhandle" area, located in the south central portion of the Park, is the lowest area at 4,400 feet (1341.14 m).

Within the Park boundaries, numerous interesting landforms occur. The Pumice Desert, located in the north central part of the Park, is an area which is slightly depressed in elevation relative to its surrounding region and supports sparse herbaceous plant communities. Union Peak, which is an old, glacially-eroded shield volcano, occurs in the southwest corner of the Park. Llao Rock, which is located at the rim of the caldera, is the thickest lava flow in the Park; and Hillman Peak, which is also located on the rim, is the highest point on the caldera rim. Throughout the Park are numerous cinder and scoria cones, such as Red Cone and Desert Cone, located south and southwest of the Pumice Desert. Because of these pumice-covered flats, rocky volcanic cones, and extremely thick lava flows, the landscape, in part, has assumed a mosaic pattern of forested and open nonforested areas. Most of the Park, however, is heavily forested with a variety of tree species, brush-fields, and small concentrations of marsh and grass-fields. The dominant tree species, based upon areal extent, are shasta red fir, mountain hemlock, lodgepole pine,

white fir, and to a lesser degree, ponderosa pine (see Table 8 for scientific names).

The approximately 250 square-mile (402.25 sq km) area of the Park is bordered by National Forest land. To the south, and east, the Winema National Forest borders the Park; to the north lies the Umpqua National Forest; and to the northwest and west, the Rogue River National Forest adjoins the National Park.

The National Park Service and the U.S. Forest Service differ in their forest management practices. The Forest Service adheres to forest conservation through timber harvesting and regeneration, while the Park Service adheres to forest preservation through minimal disturbance of the forest environment. This preservation history of the Park has provided a study area which is relatively free from human manipulation and which supports a forest of numerous tree species and age classes.

II. SURFACE CHARACTERISTICS OF CRATER LAKE NATIONAL PARK WHICH INFLUENCE THE SPECTRAL REFLECTIVITY OF SURFACE FEATURES WITHIN THE PARK

In undertaking the problem of evaluating the utility of remotely-sensed data for detailed surface cover type mapping within Crater Lake National Park, one should appreciate the dynamic forces and conditions which have in the past and do in the present affect the appearance and composition of surface cover types within the Park. These forces and/or conditions include geologic activity, soil conditions, climate, and vegetation. Changes in surface cover type appearance and composition is detected by variations in reflectance as sensed by the LANDSAT satellite and by the NASA U-2 aircraft.

The following discussion describes the past geologic activity, the present soil conditions, climate and vegetation within the National Park.

Geology

Crater Lake National Park is located in the High Cascade physiographic province, a north-south occurring mountain system which is approximately 45 to 50 (72.41 to 80.45 km) wide. In Oregon, the Cascade Range includes two distinctive belts: the Western Cascades and the High or Eastern Cascades. The High Cascades are more recent than

the Western Cascades and therefore exhibit youthful topography in the form of distinct volcanic and glacial landforms. The Western Cascades have less physical relief than the High Cascades, in addition to having older mountains where the original volcanic structures are dissected and eroded.

Table 1 will aid in summarizing the events which have affected the Crater Lake region through geologic time. These events will be expanded upon in the following discussion of the Park's geologic development.

The Cascade Range began to develop into a distinct belt of mountains during the late Eocene epoch, approximately 50 million years ago. Earth movements and volcanic activity initiated the Cascade Range development. During the Miocene and Oligocene epochs, approximately 25 million years ago, widespread volcanic activity in the region of the Cascade Range occurred, causing the upheaval of the Cascade Range and developing the Range into a true and distinctive mountain system.

During the Pliocene epoch, occurring about 10 million years ago, uplifting and volcanic activity again occurred within the region of the Cascade Range. During this upheaval, many north-south facing fractures were opened along and near the crest of the already existing Western Cascades. In the course of the Pliocene epoch, the lavas that issued from these fractures built a series of new volcanic cones.

Sequence of Events in the
Crater Lake Region

Period	Epoch	Nature of events	Approximate duration in years
Quaternary	Recent	Postglacial time. Concluding activity and destruction of Mount Mazama. Formation of Crater Lake.	10,000-20,000
	Pleistocene	The Great Ice Age. The main period of growth of Mount Mazama.	1-2 million
Tertiary	Pliocene	Building of pre-Mazama volcanoes of the High Cascades, e.g. Union Peak. Climate becoming cooler. Modern forests.	10 million
	Miocene and Oligocene	Widespread volcanic activity over most of Oregon. Upheaval of Cascade Range at close of epoch. Climate becoming cooler. Redwood forests predominant.	25 million
	Eocene	Earth movements drive out the seas and volcanic activity begins at the opening of the epoch. Tropical forests cover the plains, and temperate forests exist.	50 million

Table 1. Adapted from Williams (1942).

These newly built cones formed a chain of coalescing shield and composite volcanoes extending from Mount Shasta in northern California to Mount Baker in northern Washington State (Figure 2). At the close of the Pliocene, approximately two million years ago, the crest of the Cascade Range had become a high plateau capped by towering volcanic cones. This uplifting and volcanic cone development is what constitutes the High or Eastern Cascade physiographic province (Williams, 1942).

During the Pleistocene epoch, a large number of the volcanoes of the High Cascades became more explosive in nature. Volcanoes which had been created prior to the Pleistocene epoch were now, in some cases, covered over by the flows of the more recent volcanoes. Mount Mazama, of which Crater Lake is its remnant, was one of these newly developing volcanoes which was created approximately one million years ago, on a base 5,000 to 6,000 feet (1524.02 to 1828.82 m) in elevation, between two older volcanic peaks.

Near the close of the Pliocene and the beginning of the Pleistocene epoch, the climate of the world became colder. Snow that fell on the volcanic peaks of the High Cascades no longer melted during the summer season. Snow began to linger on the peaks from year to year, and soon the small isolated patches of snow developed into permanent snowfields. The snowfields became larger and thicker, and

ultimately began extending down the mountain slopes in the form of glaciers that had tremendous erosive power. Glacial development and movement extended through the Pleistocene epoch, known as the Ice Age.

Volcanic activity occurred throughout the Ice Age. Mount Mazama grew and developed during this time period into a composite volcanic cone of approximately 12,000 feet (3657.64 m) in elevation (Williams, 1942).

While Mount Mazama grew, glacial activity was also occurring. Glaciers advanced and retreated in response to changing climatic conditions and changes in volcanic activity of Mount Mazama and its immediate vicinity. Because of the melting and growing of glaciers which existed on the volcanic peaks, glacial moraines and tills were deposited, interbedded with the lava flows on the flanks of the volcanic peaks.

Toward the end of the Ice Age, most volcanoes had gone into a period of dormancy (Williams, 1957). Glacial activity then became more dominant. It was during this period that most glacial landforms were carved into and deposited on the volcanic peaks. These landforms include, for example, the U-shaped valleys within Crater Lake National Park. During the final retreat of glaciers in the High Cascades, a semicircular line of parasitic volcanoes developed on the northern slope of Mount Mazama, approximately 5,000 feet (1524.02 m) below the summit (National

Park Service (NPS), 1970). Possibly, this northward shift of the vents, called the Northern Arc of Vents, was brought about by the enlargement of the magma chamber in the northern direction, either as a result of internal assimilation of the cone or as a consequence of ring-fracture stopping (Williams, 1942).

A long period of dormancy again affected Mount Mazama. During this quiet time, the pressure of gases within the underground magma chamber were gradually increasing. Finally, the plug which occurred in the main ejection vent was dislodged by great gas pressure within the volcanic chamber. This served as the prelude to the most violent period of volcanic activity in the history of Mount Mazama.

During the initial stages of the final eruption of Mount Mazama, the greatest amount of gas pressure from the magma chamber was released with the forming of dacite magmas into small frothy-white pumice (NPS, 1970). This pumice was discharged from Mount Mazama, high above the summit, and was dispersed by the wind, first toward the east southeast, and then toward the northeast direction (Williams, 1942). Figure 4 shows the depth and areal extent of the Mazama pumice deposition.

Explosions of Mount Mazama gradually increased in violence as the volcanic activity continued. The earlier pumice ejection, deposited by the wind, was followed by more powerful explosions in which a more pasty dacite lava

DISTRIBUTION OF PUMICE DEPOSITS FROM MOUNT MAZAMA

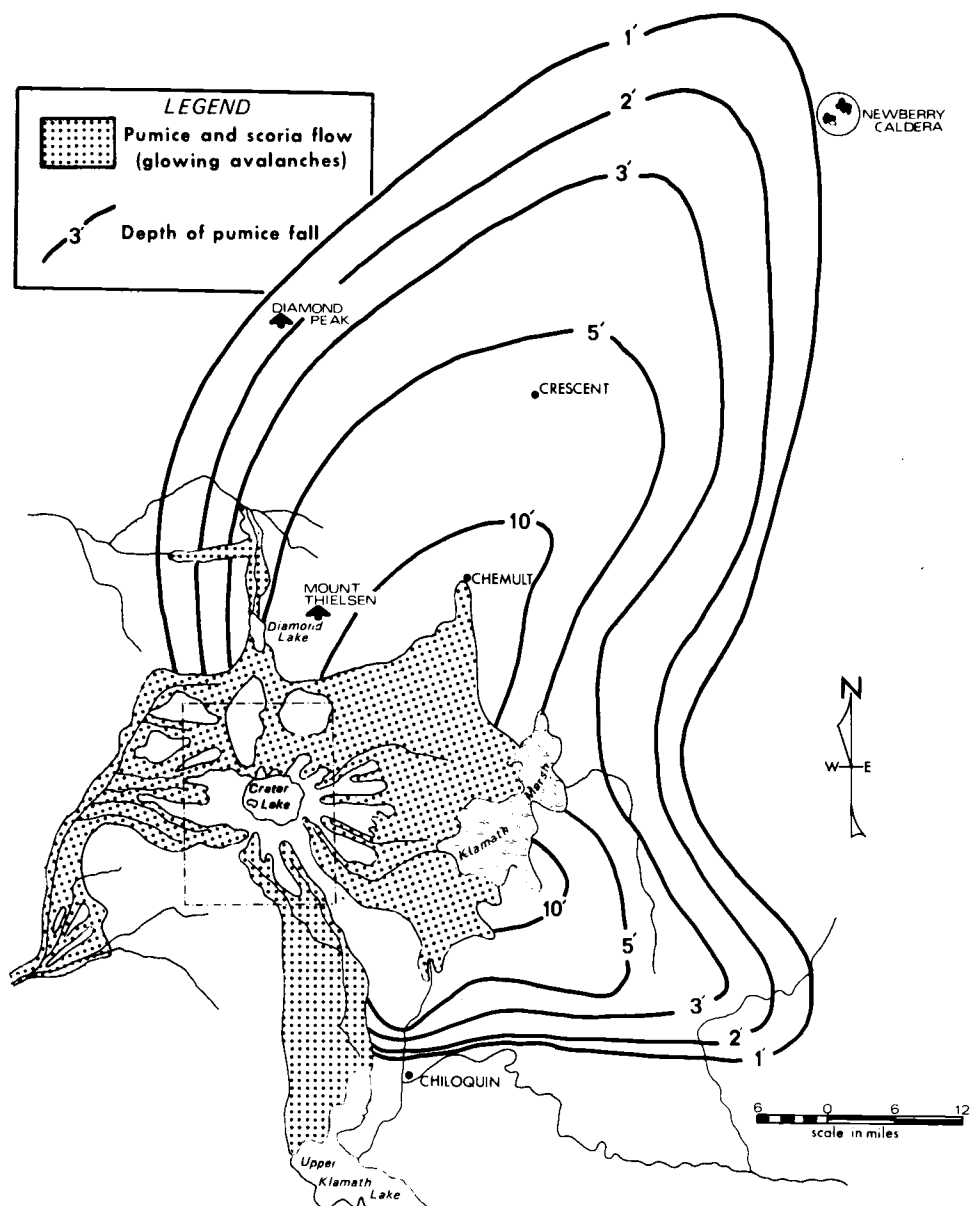
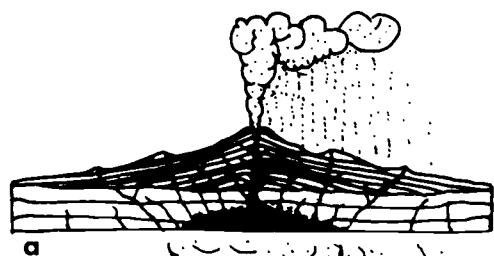


Figure 4. Adapted from Williams (1956).

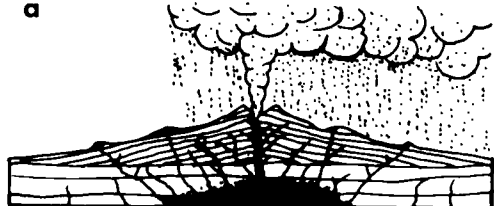
was ejected from the crater in such large volumes and sizes that the wind could not act as the agent of deposition. The ejecta fell on the upper slopes of Mount Mazama and swept down the sides of the volcano as a fiery avalanche (nuée ardentes) spreading out in wide sheets. The fiery avalanches were actually flows of incandescent magma and violently expanding gases of extremely high temperatures and pressures. The load which these avalanches carried was deposited in the canyons and on gentler slopes than those of Mount Mazama because of the high speed of the avalanche movement down the flanks of the mountain.

As depicted in Figure 5, during or shortly after the great outpouring of pumice and lava from Mount Mazama, the cone of Mazama collapsed forming the present day Crater Lake caldera. Since the beginning of the violent eruptions of Mazama, 15.0 cubic miles (24.12 cu km) of material had disappeared from the mountain's magma chamber. Only 12.0 cubic miles (19.31 cu km) of volcanic material had been ejected from the volcano (Williams and Goles, 1968). According to Howell Williams, it is probable that the forming of the caldera was brought about by the combination of explosive eruptions of magma which aided in the drainage of the magma chamber and the partial drainage of the magma reservoir by injection of the magma into cracks and fissures in the walls of the volcano, or by some other related magma withdrawal technique.

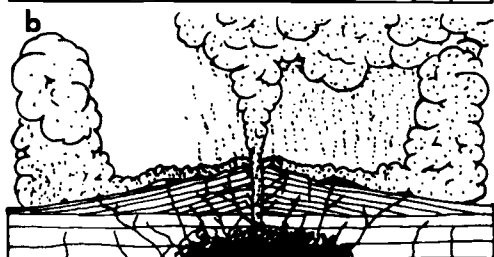
The Evolution of Crater Lake



a. Beginning of the great eruptions.



b. Eruptions become more violent and pumice showers become heavier. Lava level in volcanic pipe is falling.



c. Climax of the eruptions. Glowing avalanches sweep down the sides of the volcano. Magma chamber is being rapidly drained.



d. Summit collapses into magma chamber. Gas vents appear in the caldera floor.



e. Crater Lake today. Wizard Island and lava are shown on the lake floor. Magma in underlying chamber is in large part, or entirely, solidified.

Figure 5. Adapted from Williams (1972).

The withdrawal of the magma left a shell of a mountain which was unable to support itself. Mount Mazama then collapsed forming the 4,000 foot (1219.21 m) caldera.

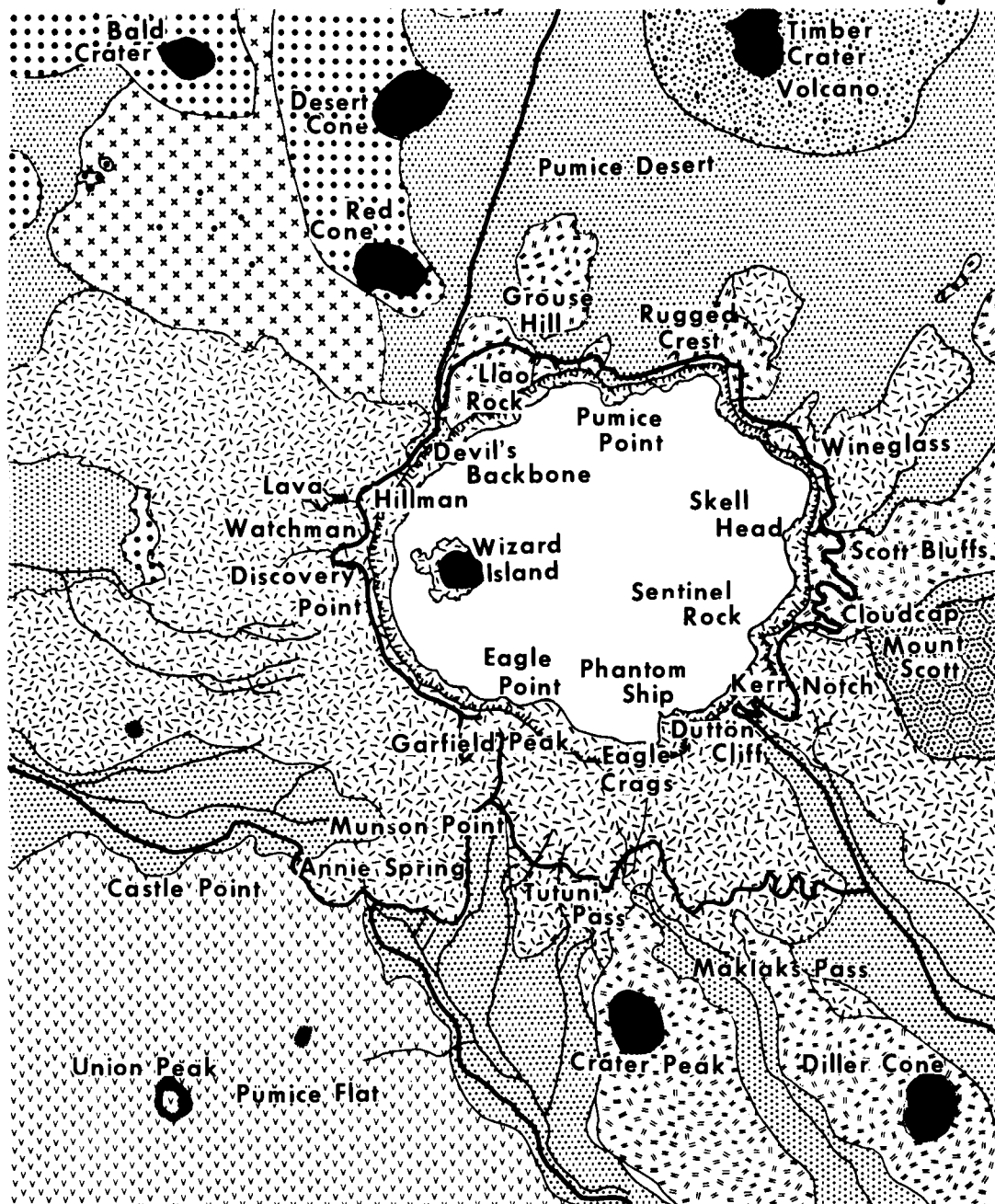
The volcanic activity of Mount Mazama did not end with the forming of the caldera approximately 6,600 years ago. Wizard Island developed about 1,000 years ago on the floor of the caldera. Of the three cones which developed due to volcanic activity, Wizard Island is the only cone which today is above the surface of the lake. Wizard Island is a symmetrical cinder cone completely encircled by dark andesitic scoriaceous lapilli and blocks (NPS, 1976). The lavas of 800 foot high (243.84 m) Wizard Island and the other two lesser cinder cones helped seal the basin of the caldera by filling in the cracks and crevasses. This sealing process created an impermeable bottom for the caldera. The caldera now has been partially filled by water through rain and snow melt. The current depth of the lake is about 2,000 feet (609.61 m), and the elevation of the lake is 6,176 feet (1882.47 m) above sea level.

Aeromagnetic and gravity surveys have been conducted throughout the region of Crater Lake National Park by the United States Geological Survey. These surveys reveal that Crater Lake lies in an area strongly affected by northwest trending, and to a lesser extent, by northeast trending lineaments. The north-south trending lineaments associated with the structure of the High Cascades have little or no

geophysical expression within the National Park. The northwest set of lineaments appear to be part of a shear zone related to the Brothers fault zone, or possibly a western extension of Basin and Range normal faulting organization (Blank, Jr., 1967). The northeast set of lineaments may reflect the stress caused by deeply buried structures in the Klamath Mountains or tensional structures associated with shearing (Blank, Jr., 1967). The location of Mount Mazama at the intersection of lineaments may have been a main ingredient into the rapid rise of magma from the chamber, which led to Mazama's volcanic eruptions that ended in the forming of the caldera.

The geology of Crater Lake National Park and its immediate vicinity is quite involved. Figure 6 is a generalized geologic map of the National Park. From this map, one can recreate the volcanic episodes which have affected this area and trace the flow of lavas and the path of the nuée ardentes as they were emitted from Mount Mazama. The glacial activity, combined with the volcanic activity which have affected the Park, have created an area of extreme topographic variation. This topographic variation, coupled with other factors such as soils, climate, and its geographic location have influenced the distribution and composition of surface cover types within the Park and have greatly affected the variation in spectral reflectance found within the National Park.

Generalized Geologic Map of Crater Lake National Park and Vicinity



- | | | |
|--------------------------|------------------------------|---|
| ••• Pre-Mazama Lavas | ⋈ Union Peak Lavas | ⋈ Mount Mazama Andesites |
| ⋈ Mount Mazama Dacites | ⋈ Mount Scott Lavas | ⋈ Timber Crater Lavas |
| ■ Parasitic cinder cones | ⋈ Glowing avalanche deposits | ⋈ Pumice and Scoria flows of Mt. Mazama |

Adapted from Carnegie Institute of Washington (1942)

Figure 6.

Soils

Within the boundaries of Crater Lake National Park, complete soil surveys have not been conducted and, therefore, little is known in detail about soil characteristics within the Park. Much of the soil within the Park, due to the Park's past geologic and glacial history, has developed on various forms of Mazama pumice, lavas, alluvium, and glacial debris.

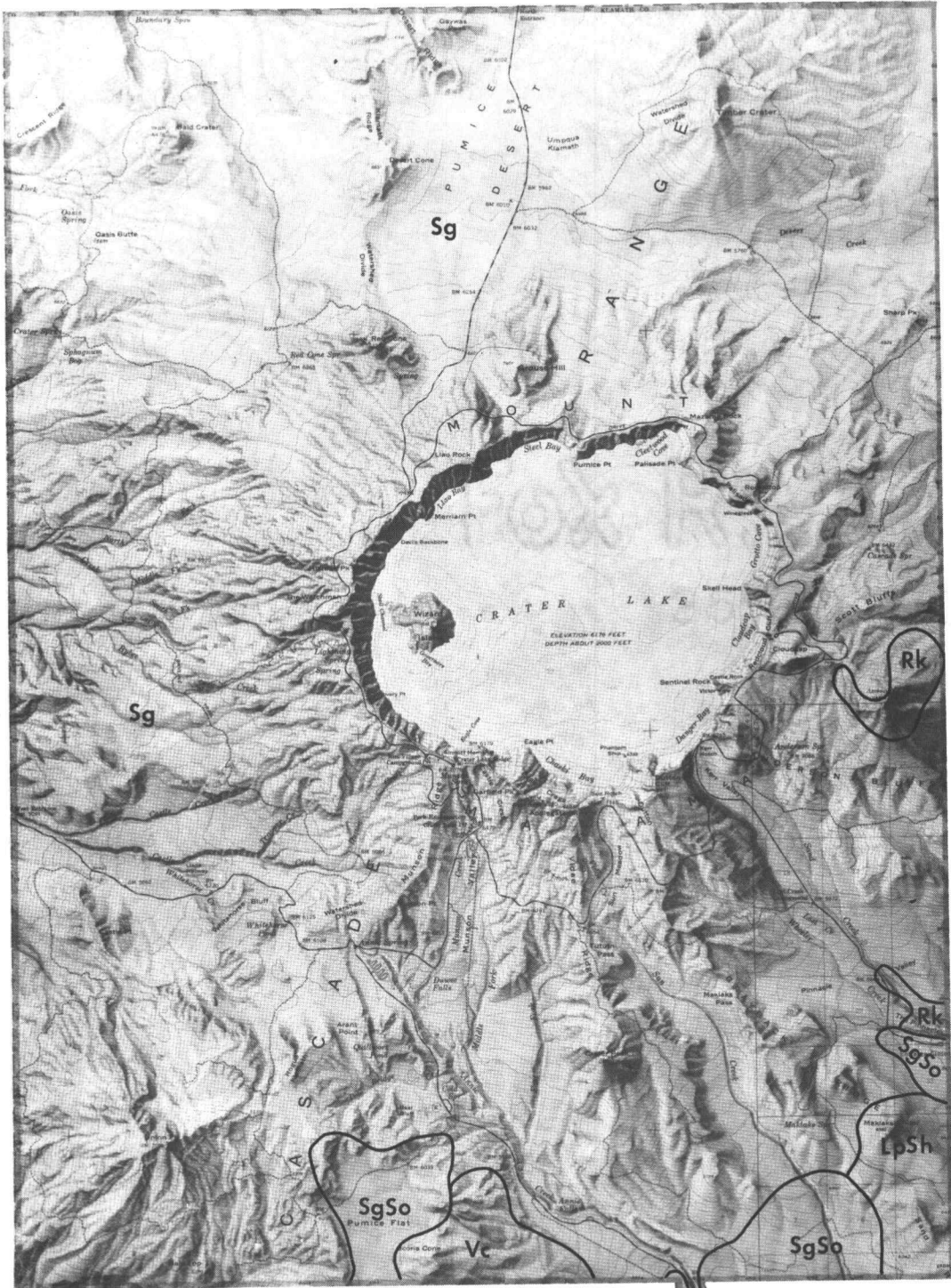
Figure 4, which shows the distribution of pumice deposits within Crater Lake National Park and its immediate vicinity, reveals that the entire Park has been affected by pumice and scoria flows and/or pumice falls. The depth of the pumice deposits throughout the Park varies from 0 to 10 feet (3.05 m). The major pumice deposits have occurred in a northeast and southeast direction from Crater Lake.

Mount Mazama, which was the dominant pumice and scoria producer of the Crater Lake region, grew predominately by eruptions of andesitic lava and ash. While Mount Mazama grew, glaciers advanced and retreated several times in conjunction with volcanic activity and climatic changes. This advancing and retreating of glaciers further altered the soil composition by the deposition of glacial moraines and tills which became interbedded within the lava flows. The combined effect of pumice, alluvium, lavas, and glacial debris have produced soils which, in general, can be described as regosols with poorly defined soil horizons.

A generalized soil map of the Park is presented in Figure 7, showing the areal extent of six soil types within the Park. Crater Lake National Park officials have located one other soil type within the borders of the Park. The soil types found within the Park include: Skellock; Lapine; Steiger; Rockland (name changed to Rockly); Shanahan; Vc (unnamed soil type); and Maklak. The soil types within the Park occur singularly and in combination with other soil types. The general characteristics of each soil type will be discussed below.

Skellock soils occur within the Pumice Flats area in the south-central portion of the Park and south of the Pinnacles, and also in the Panhandle area. In all cases, the Skellock soil type occurs in conjunction with the Steiger soil type.

The Skellock soil type occurs in areas of between 4,520 and 4,650 feet (1377.71 and 1417.34 m) in elevation with slope gradients of mostly less than 2 percent. The average annual precipitation in the region of Skellock soil is between 20 and 30 inches (50.8 and 76.2 cm) with an average annual air temperature of 42°F (5.6°C) (USDA Soil Conservation Service (SCS), 1972). The Skellock soil type consists of very deep, moderately drained soils formed in pumice and scoria flow materials. The surface layer of this soil type is very dark grayish brown, consisting of gravelly fine, sandy loam about three inches thick (State Water



Soil Distribution of
Crater Lake National Park



Figure 7

- Soil Type**
 Lp - Lapine
 Rk - Rackly
 Sg - Steiger
 Sh - Shanahan
 So - Spellock
 Vc - unnamed

Resources Board, 1969). Table 2 lists the estimated soil properties of the Skellock Soil type; Table 3 presents the woodland suitability of the Skellock soil type. Each table, besides containing Skellock soil information, has listed the respective information for each of the other five above-mentioned soil types found in the Park. The new and unnamed soil type, Vc, which occurs in the Park, is not listed in the tables due to lack of information.

The Lapine soils which occur on slopes between 5 and 15 percent and 25 and 40 percent, are found in the southeast corner of the Park, just east of Sun Creek. Lapine soils on slopes between 25 and 40 percent also occur in the southeast corner of the Park along Sand Ridge and a portion of Grayback Ridge, and north to Maklaks Crater. In both regions of Lapine soils, the Shanahan soil type occurs in conjunction.

The Lapine soil type occurs in areas which have an annual precipitation of about 18 to 35 inches (45.72 to 88.90 cm) and in areas with a mean annual air temperature of approximately 42°F (5.6°C) (State Water Resources Board, 1969). Elevation ranges of this soil type are between 4,200 and 6,000 feet (1280.18 and 1828.82 m), with slopes of 1 to 55 percent. This soil occurs on tablelands, ridges, and cinder cones.

The surface mineral layer of the Lapine soil type is very dark brown, gravelly, loamy, coarse sand about two

Estimated Soil Properties of Types within the Park

Depth from surface (in)	USDA texture	Coarse fract. over 3 in	% of material passing sieve			Liquid limit	Plasticity index	Permeability (in/hr)	Avail. water cap. (in/hr)	Soil reaction (pH)	Shrink swell potential
			#10	#40	#200						
0-20	gravelly sandy loam	0-10	55-85	35-60	15-35	nonplastic	2.0-6.0	.2-.4	6.1-7.3	low	
20-51 SKELLOCK	very gravelly loamy sand	0-25	20-50	10-40	5-15	nonplastic	0.2-0.6	.2-.4	6.1-7.3	low	
0-72 LAPINE	very gravelly coarse sand	0	15-65	0.55	0-5	nonplastic	> 20	.2-.4	5.6-7.3	low	
0-60 STEIGER	gravelly loamy coarse sand	0-5	70-95	35-70	10-30	nonplastic	6.0-20.0	.2-.4	5.6-6.5	low	
0-5	very cobbly loam	30-50	40-70	35-65	25-50	25-30	0-5	.6-2.0	.06-.11	6.1-6.5	low
0-5	gravelly loam	5-20	55-65	45-60	35-50	25-30	0-5	.6-20.0	.12-.16	6.1-6.5	low
5-12	very cobbly clay loam	30-50	40-70	35-70	30-55	35-40	10-15	.2-.6	.06-.11	6.1-6.5	low
12 ROCKLY	basalt bedrock										
0-38	gr. loamy coarse sand gr. co. sand	0	65-90	30-70	5-25	nonplastic	6.0-20.0	.2-.4	6.1-7.3	low	
38-41 SHANAHAN	silt loam, loam	0	65-95	55-95	40-85	40-50	5-10	.6-2.0	.12-.26	6.1-7.3	low
0-60 MAKLAK	very gravelly loamy coarse sand	15-25	20-75	10-55	5-20	nonplastic	6.0-20.0	.2-.4	5.6-6.5	low	

Table 2. Adapted from SCS (1972).

Woodland Suitability of Soil Types

Soil type*	Potential productivity		Management problems					Native species
	Species	Site index	Erosion hazard	Equip. limit.	Seedling Mortality	Windthrow hazard	Plant competition	
SKELLOCK	Lodgepole Pine	66± 4	slight	slight	slight	severe	slight	Lodgepole Pine
LAPINE								
1-10% slope	Ponderosa Pine	89± 7	slight	slight	slight	severe	moderate	Ponderosa Pine
10-35% slope	Sugar Pine	83± 3	slight	slight	moderate	severe	moderate	Lodgepole Pine
10-40% north slope								
35-55% slope			slight	moderate	moderate	severe	moderate	White Fir Incense Cedar
STEIGER								
1-15% slope	Ponderosa Pine	99± 10	slight	slight	moderate	severe	moderate	Ponderosa Pine White Fir
15-40% slope	Ponderosa Pine		slight	slight to moderate	slight	severe	moderate	Grand Fir Lodgepole Pine Sugar Pine
ROCKLY	none							
SHANAHAN								
12-45% north slope	Ponderosa Pine	82± 2	slight	slight to moderate	moderate	moderate	moderate	Ponderosa Pine Lodgepole Pine
12-45% slope	Ponderosa Pine	78± 6	slight	slight to moderate	severe	moderate	moderate	White Fir Sugar Pine
1-12% slope	Ponderosa Pine Lodgepole Pine	78± 6 88± 2	slight	slight	severe	moderate	moderate	Douglas Fir Incense Cedar
MAKLAK								
1-15% slope	Ponderosa Pine	104± 2	slight	slight	moderate	severe	moderate	Ponderosa Pine Lodgepole Pine Sugar Pine Douglas Fir White Fir

*Refer to Table 2--Soil type.

Table 3. Adapted from SCS (1972).

inches thick with a thin mat of loose conifer needles normally resting on the mineral soil surface (SCS, 1972). The Lapine soil, in general, is made up of deep, excessively drained soils formed in air-deposited pumice ash.

The Steiger soil type is the main soil type occurring within the Park, according to Figure 7. The Steiger soil type also occurs with the Skellock soil type in the southern portion of the Park near Pumice Flats and the Pinnacles. The Steiger soil type occurs in areas which have slope gradients ranging from less than 1 to 40 percent and elevations ranging between 4,150 and 6,000 feet (1264.94 and 1828.82 m). The average annual precipitation of the Steiger soil region is between 20 and 50 inches (50.8 and 127.0 cm) with average annual air temperature of 42°F (5.6°C) (USDA SCS, 12/1972). The surface layer of the Steiger soil type is a very dark brown, gravelly, loamy, coarse sand about two inches thick.

The Rockland (Rockly) soils occur along Sand Creek near the Pinnacles, and also includes the Pinnacles. Rockly soils also occur on the summit of Mount Scott and along its immediate flanks. The Rockly soil type occurs in areas of 16 to 30 inches (40.64 to 76.2 cm) of average annual precipitation and 47° to 50°F (8.33 to 9.90°C) average annual air temperature (SCS, 1972). Rockly soil types occur in areas ranging in elevation between 4,200 and 6,000 feet (1280.18 and 1828.82 m) with slope gradients between 40 and

65 percent. Areas which are characteristic of Rockly soil include: rock outcrops, bare bedrock, talus accumulations and scarps, fault block mountains and ridges. The surface layer of the Rockly soil series is dark reddish-brown, gravelly loam about five inches thick. The soil is very thin and runoff is slow.

The Shanahan soil type occurs in the southeast corner of the Park along Sand Ridge and Grayback Ridge north to Maklaks Crater. The Shanahan soil in these areas are combined with soil of the Lapine series.

The Shanahan series occurs in areas of 18 to 35 (45.72 to 88.90 cm) inches of average annual precipitation and 41° to 44°F (4.95 to 6.60°C) average annual air temperatures (SCS, 1972). The elevation of this soil type ranges from 4,300 to 7,000 feet (1310.66 to 2133.63 m) with slopes ranging between 3 and 45 percent. The Shanahan soil type consists of moderately deep, excessively drained soils formed in air-deposited pumice ash. These soils have thin, dark brown, and very dark grayish brown, gravelly, loamy, ashy coarse sand. The ashy part of the soil has about 10 to 35 percent cinders (State Water Resources Board, 1969).

The Maklak soil type occurs generally on plateaus and in canyons of the Park. The Maklak soil series occurs in areas of 4,350 to 7,000 feet (1325.89 to 2133.63 m) in elevation with slopes up to 15 percent. The average annual air temperature in this soil-occurring region ranges between 35° and 43°F (1.65 and 6.05°C) with average annual precipitation

amounts between 30 and 60 inches (76.20 and 152.40 cm) (SCS, 1972). The Maklak soil type consists of excessively drained, cindery soils formed in pumiceous and scoriaceous cinders and ash. Typically, a thin needle mat of forest floor litter occurs resting on a surface layer of dark brown, loamy coarse sand.

The new unnamed soil type, Vc, found within the boundaries of the Park occurs in the south-central portion of the Park in the vicinity of Scoria Cone, adjacent to Pumice Flat. In general, this soil is considered to be well to somewhat excessively drained, moderately deep to very deep, and formed largely in very stony and gravelly colluvium derived from andesite and minor pyroclastic components (SCS, 1972). For the most part, this area includes very steep mountain slopes, cinder cones, and volcanic peaks. The elevation in which this soil type occurs ranges from 4,200 to 7,000 feet (1280.18 to 2133.63 m) with very steep slopes. The annual precipitation varies between 35 and 50 inches (88.9 and 127.0 cm) with the average annual air temperature approximately 41°F (4.95°C) (State Water Resources Board, 1969).

The accurate and complete distribution of soils within Crater Lake National Park is not yet known. The general characteristics of the known soils in the Park have been strongly affected by the glacial, and even more so, by the Park's volcanic activity.

The seven soil types discussed above have different woodland suitability potential, as described in Table 3. This difference is partly due to the various degrees of which glacial and volcanic activity have affected those particular areas of known soil type occurrence. The native tree species occurrence on the particular known soil types in the Park, as listed in Table 3, is of particular interest because only a small portion of the known existing tree species of the Park has been mentioned. The six major tree species listed in Table 3 which do occur in the limited areas where soil surveys have been carried out in the Park suggests that a large tree species variation can be found within the total National Park and, therefore, a wide variation in surface cover type spectral reflectance.

Climate

The climate of Crater Lake National Park is characterized by cool summers and moist winters with the winter moisture being delivered to the Park mainly in the form of heavy snowfalls. The climatic conditions which occur within the Park is partly due to the location of the National Park near the crest of the southern High Cascade Mountains.

These climatic conditions strongly affect the development of vegetation communities. Precipitation, and not soil type, is the major factor determining vegetation types in the Park (Dyrness and Youngberg, 1958). Micro-climatological

effects occur in the Park, which also can influence the development of vegetation communities. These micro-climatological effects can be produced by the large and abrupt changes in the topography and the overall roughness of the terrain. Factors such as drainage, snow accumulation and ablation, rainfall, temperature, and wind can be affected by topographical variations which in turn influence surface cover type establishment and development.

Slope angle and slope aspect are two important topographical factors which affect surface cover type formation and composition (Muller, 1971). Due to earth-sun geometry, the intensity of the solar beam striking the earth at a particular latitude changes throughout the year and changes with variations in slope angle and slope aspect.

Table 4 shows the yearly values of direct solar radiation for selected slope angles (0, 15, 30, 45, 60, 75, 90 degrees) and slope aspects (north (N), north northeast (NNE) and north northwest (NNW), northeast (NE) and northwest (NW), east northeast (ENE) and west northwest (WNW), east (E) and west (W), east southeast (ESE) and west southwest (WSW), southeast (SE) and southwest (SW), south southeast (SSE) and south southwest (SSW), and south (S)) at 43 degrees north latitude, which occurs just north of the center of Crater Lake National Park. Tables 5 and 6 show the daily values, respectively, for 10 September and 22 December of direct solar radiation for the same slope angles and slope aspects

Yearly Values of Direct Solar Radiation for
Selected Slope Angles and Slope Aspects
at 43 Degrees North Latitude
(cal cm⁻² year⁻¹)

	0°	15°	30°	45°	60°	75°	90°
N	192,311	148,398	249,684	312,171	31,645	45,334	7,956
NNE/NNW	192,311	159,601	107,478	70,123	41,672	26,198	17,883
NE/NW	192,311	160,377	125,462	95,034	71,981	54,806	41,089
ENE/WNW	192,311	173,062	150,766	129,404	109,455	90,129	70,956
E/W	192,311	187,491	177,526	164,134	146,575	125,583	101,872
ESE/WSW	192,311	201,534	202,277	194,906	178,921	156,006	126,685
SE/SW	192,311	213,171	222,437	219,699	204,190	178,524	140,840
SSE/SSW	192,311	220,849	235,398	235,491	220,272	191,848	152,420
S	192,311	223,505	239,997	240,770	225,265	195,623	154,409

Table 4. Adapted from Buffo, Fritschen, and Murphy (1972).

Daily Values of Direct Solar Radiation for
 Selected Slope Angles and Slope Aspects
 on September 10 at 43 Degrees
 North Latitude ($\text{cal cm}^{-2} \text{ day}^{-1}$)

	0°	15°	30°	45°	60°	75°	90°
N	541	472	306	119	8	1	0
NNE/NNW	541	480	327	179	92	55	36
NE/NW	541	507	393	293	217	165	124
ENE/WNW	541	549	477	411	348	289	229
E/W	541	591	561	519	466	401	327
ESE/WSW	541	633	636	611	560	488	397
SE/SW	541	666	692	680	627	544	433
SSE/SSW	541	689	729	722	666	571	440
S	541	698	743	737	681	579	437

Table 5. Adapted from Buffo, Fritschen, and Murphy (1972).

Daily Values of Direct Solar Radiation for
 Selected Slope Angles and Slope Aspects
 on December 22 at 43 Degrees
 North Latitude (cal cm⁻² day⁻¹)

	0°	15°	30°	45°	60°	75°	90°
N	192	58	0	0	0	0	0
NNE/NNW	192	71	1	0	0	0	0
NE/NW	192	100	39	15	6	3	2
ENE/WNW	192	141	102	79	64	52	38
E/W	192	187	181	174	162	143	122
ESE/WSW	192	236	267	282	282	266	231
SE/SW	192	278	345	389	406	396	360
SSE/SSW	192	307	400	467	502	501	459
S	192	317	420	494	534	539	506

Table 6. Adapted from Buffo, Fritschen, and Murphy (1972).

as in Table 4. The daily direct solar radiation values were computed for 10 September and 22 December because LANDSAT digital tapes were utilized on or near those two particular dates. Variation in the intensity of the solar beam with changes in slope angle and slope aspect result in the establishment of differing surface cover types which produce changes in spectral reflectivity as detected by LANDSAT.

During late spring and extending through early fall at Crater Lake National Park, orographic precipitation occurs less frequently. During this high sun period, the land is being rapidly warmed. The ocean and the overlying air masses are colder than the land masses. Despite the cooling of air caused by the rising of air masses up and over the mountain slopes, the temperature at the crest of the mountain range is still higher than the air mass approaching and crossing the coastline. As a result, the air mass increases its temperature and becomes relatively drier as it approaches and ascends the mountain slopes. During this period, the polar jet stream has shifted farther north, and thus large-scale, moisture laden storms are nearly absent over the region of the National Park.

The climatic data of eight different recording stations, located within the vicinity of the Park, appears in Table 7. The data show the variation in temperature and precipitation associated with changes in elevation and geographic location. Figure 8 shows the relative location of

Comparative Climatic Data of the Crater Lake
National Park Region

Station	Elevation feet (meters)	Lati- tude	Longi- tude	Temperature			Precipitation		
				Average January	Average July	Average annual	Average annual	June through August	Average annual snowfall
				Degrees F (Degrees C)			Inches (cm)		
Medford Airport	1,312 (399.90)	42°22'	122°52'	36.7 (8.55)	71.9 (72.55)	52.2 (36.73)	20.46 (51.97)	1.40 (3.56)	7.5 (19.05)
Trail 14 NE	1,885 (574.55)	42°47'	122°40'	35.6 (6.55)	65.4 (60.73)	51.3 (35.09)	47.22 (119.94)	2.46 (6.25)	
Prospect 2 SW	2,482 (756.52)	42°44'	122°31'	35.5 (6.36)	66.7 (63.09)	50.1 (32.91)	42.87 (108.89)	2.38 (6.05)	
Klamath Falls 2	4,098 (1,249.09)	42°12'	121°47'	29.5 (-4.55)	68.1 (65.64)	47.9 (28.91)	14.18 (36.02)	1.67 (4.24)	41.0 (104.14)
Fort Klamath 7SW	4,160 (1,267.98)	42°37'	122°05'	27.0 (-9.09)	60.4 (51.64)	43.3 (20.55)	39.19 (99.54)	1.79 (4.55)	
Chiloquin	4,220 (1,286.27)	42°35'	121°52'	26.4 (-10.18)	59.1 (49.27)	42.8 (19.64)	18.34 (46.58)	1.81 (4.59)	
Chemult	4,760 (1,450.87)	43°13'	121°47'	25.2 (-12.36)	60.0 (50.91)	41.8 (17.82)	26.40 (67.06)	2.35 (5.97)	160.0 (406.40)
Crater Lake Hq.	6,475 (1,973.60)	42°54'	122°08'	24.8 (-13.09)	53.3 (38.73)	37.7 (10.36)	69.74 (177.14)	3.99 (10.13)	590.0 (1,498.60)

(Note: Data covers period 1941-1975.)

Table 7. Adapted from the National Park Service (1970).

Location of Climatic Data Recording Stations

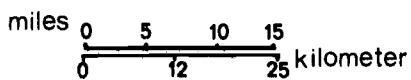
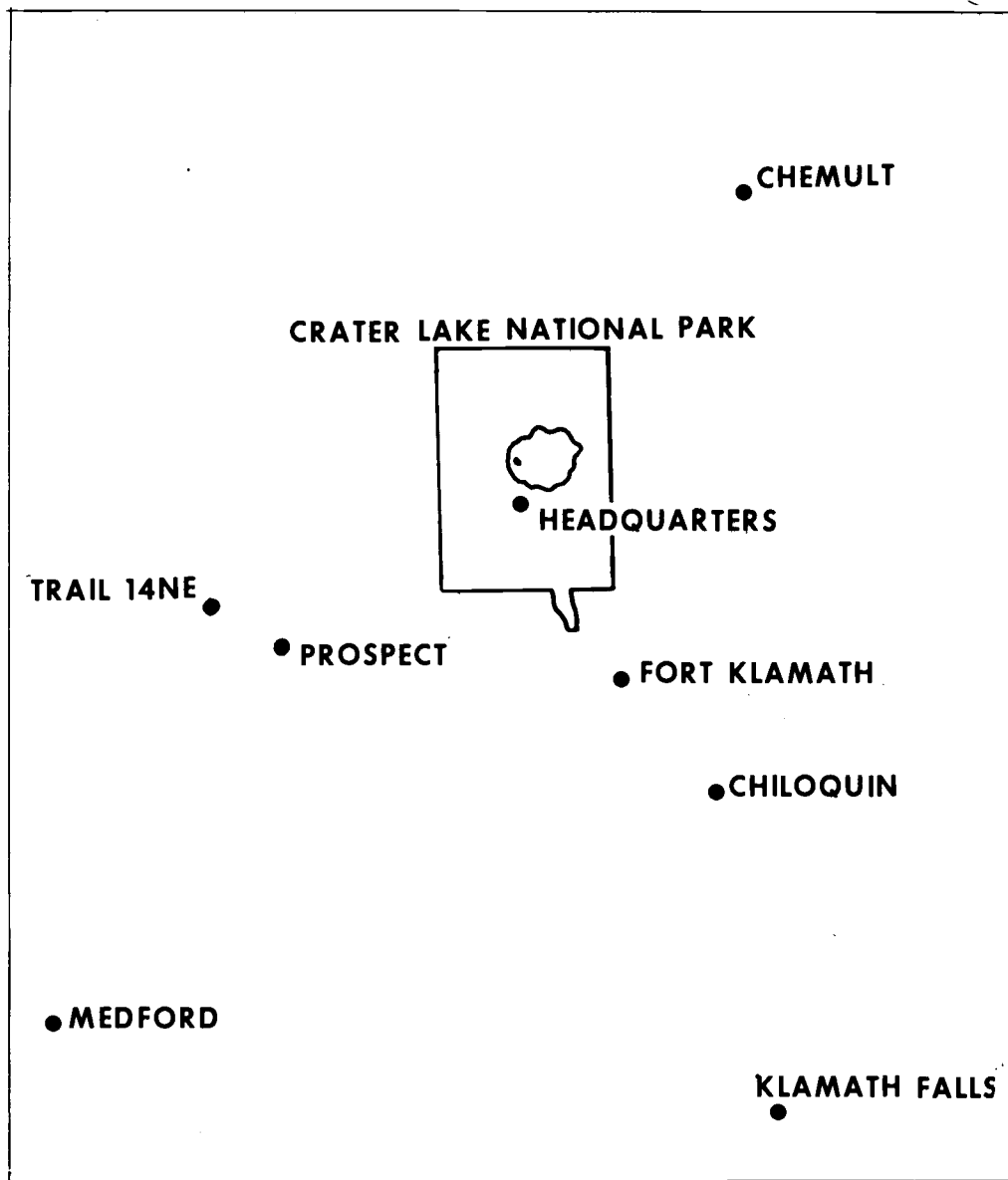


Figure 8

each of the eight recording stations. The general characteristics of the temperature, precipitation, and snowfall will now be discussed for the National Park.

Temperature

At all elevations within the National Park, and for any month of the year, freezing temperatures occur. The greatest frequency of freezing temperatures occurs in the lower eastern portion of the Park (NPS, 1976). The normal situation is for temperature to increase with a decrease in elevation. The greater frequency of freezing temperatures is unique to the environmental conditions of the eastern portion of the park. Two primary environmental conditions account for the large number of freezing temperatures in this region:

- (1) the formation of stagnant pools of dense cold air produced by air drainage and continued by the tendency of cloud layers to form over these pools of dense, cold air and to prevent the normal flow of radiant energy during daytime hours;
- (2) the invasion of Arctic air from the northeast, being cold and dense, forces the warmer air of the region to rise over the Arctic air (Sternes, 1963).

The conditions that prevail in the Park which produce cold temperatures in the eastern region of the Park occur in times of light or non-existent winds. The main movement of

air for the creation of these stagnant pools is primarily through air drainage.

Table 7 also shows the average annual, average January, and average July air temperatures for the Park. During the summer and winter, the temperature of the Panhandle, located along the southern Park border, is ten or more degrees Fahrenheit warmer than the temperature at the rim (Sterns, 1963). This is partly due to elevation differences. Temperature differences would also be expected between areas of different vegetation densities. Areas such as the Pumice Desert or the sparsely vegetated meadows along the northeast part of the rim vicinity should show higher surface air temperatures due to the high reflecting pumice soil. In areas where dense stands of tree species occur, surface temperatures should be lower. This is due to the fact that large amounts of solar radiation is reflected from the dense crown canopy and very little radiation penetrates the crown canopy to the ground surface. The amount of solar radiation arriving at the ground level is quite different in lodgepole pine stands as compared to Mountain Hemlock stands, partly due to crown density differences.

Precipitation

The large precipitation variation which occurs within Crater Lake National Park is primarily due to the variation in topography, the orographic precipitation effect, and the

rainshadow effect. The precipitation which falls within the Park (Table 7) falls predominately during the winter season with only 6 percent of the annual precipitation falling between June and August (NPS, 1970). Soils throughout the Park therefore become very dry during the summer months, and vegetation stress can be observed in late summer. The risk of forest fires is greatest at this time because of the dry fire fuel conditions and the increased visitor use.

Snow

Most of the precipitation which falls in the Park does so in the form of snow (Table 7). At Park headquarters, it is common to have 150 inches (381.0 cm) of snow on the ground. Between the years 1924 and 1961, snowfalls in the Park began by September 29 fifty percent of the time with yearly averages being greater than 550 inches (1397.0 cm), 50 percent of the time (Sternes, 1963).

The snowpack accumulation and ablation rates within Crater Lake National Park and vicinity are quite important for Park and regional resource management. Regionally, for example, the amount of water available in the snowpack influences water availability during the summer season in the Klamath River basin and the Rogue River basin for crop and timber growth. Within the Park, snowfall depths, rates of occurrence, ablation rates, and water content of the snow affect moisture availability for vegetation growth and

regeneration, besides affecting the potential hazard of forest fire fuels and the timing of potential fire hazards.

Vegetation

The vegetation of Crater Lake National Park is quite varied in both composition and in areal coverage throughout the Park. This section is intended to only provide an introduction to the vegetation of the Park, with a more rigorous treatment of the distribution of the vegetation within the Park forthcoming.

The tree species and dominant brush types which occur within Crater Lake National Park are presented in Table 8. This table lists the scientific as well as the common name for each of the tree species which occur in the Park. The major tree species found in the Park listed in Table 8 will be discussed as to their general location, and the presence of other tree species and brush types which occur in association.

Lodgepole pine is the dominant tree species found in the middle elevations within the Park between the lower elevation ponderosa pine and the higher elevation mountain hemlock. Two representative stands of lodgepole pine can be seen along highway 62. One site can be observed while entering the Park from the west, and the other site can be seen along the north entrance to the Park adjacent to the Pumice Desert. The Pumice Desert sample is poorer stocked

Major Tree Species and Common Brush Types
of Crater Lake National Park

Common Name	Scientific Name
Lodgepole Pine	<u>Pinus contorta</u> var. <u>latifolia</u>
Ponderosa Pine	<u>Pinus ponderosa</u>
Sugar Pine	<u>Pinus lambertiana</u>
Western White Pine	<u>Pinus monticola</u>
Whitebark Pine	<u>Pinus albicaulis</u>
Engelmann Spruce	<u>Picea engelmannii</u>
Western Hemlock	<u>Tsuga heterophylla</u>
Mountain Hemlock	<u>Tsuga mertensiana</u>
Douglas-Fir	<u>Pseudotsuga menziesii</u>
Pacific Silver Fir	<u>Abies amabilis</u>
White Fir	<u>Abies concolor</u>
Subalpine Fir	<u>Abies lasiocarpa</u>
Shasta Red Fir	<u>Abies magnifica shastensis</u>
Noble Fir	<u>Abies procera</u>
Incense Cedar	<u>Calocedrus decurrens</u>
Pacific Yew	<u>Taxus brevifolia</u>
Pacific Willow	<u>Salix lasiandra abramsii</u>
Quaking Aspen	<u>Populus tremuloides</u>
Black Cottonwood	<u>Populus trichocarpa</u>
Sitka Alder	<u>Alnus sinuata</u>
Thinleaf alder	<u>Alnus tenuifolia</u>
Oregon White Oak	<u>Quercus garryana</u>
Greenleaf Manzanita	<u>Arctostaphylos patula</u>
Snowbrush Ceanothus	<u>Ceanothus velutinus</u>
Oregon Boxwood	<u>Pachistima myrsinites</u>
Swamp Huckleberry	<u>Vaccinium occidentale</u>
Broom Huckleberry	<u>Vaccinium scoparium</u>
Pinemat Manzanita	<u>Arctostaphylos nevadensis</u>
Pacific Serviceberry	<u>Amelanchier florida</u>

Table 8

Table 8 (continued)

Common Name	Scientific Name
Saskatoon Serviceberry	<u>Amelanchier alnifolia</u>
Western Common Chokecherry	<u>Prunus virginiana demissa</u>
Rubber Rabbitbrush	<u>Chrysothamnus nauseosus</u>
Sharpleaf Snowberry	<u>Symphoricarpos acutus</u>
Antelope Bitterbrush	<u>Purshia tridentata</u>
Baldhip Rose	<u>Rosa gymnocarpa</u>
Oregongrape	<u>Mahonia nervosa</u>
Wax Currant	<u>Ribes cereum</u>
Partridgefoot	<u>Luetkea pectinata</u>
Sticky Currant	<u>Ribes viscosissimum</u>
Deerbrush Ceanothus	<u>Ceanothus integerrimus</u>
Bitter Cherry	<u>Prunus emarginata</u>
Common Snowberry	<u>Symphoricarpos albus</u> <u>laevigatus</u>
Sierra Evergreen Chinkapin	<u>Castanopsis sempervirens</u>
Newberry's Knotweed	<u>Polygonum newberryi</u>
Silvery Eriogonum	<u>Eriogonum ovalifolium</u>
Geyers' Everlasting	<u>Antennaria geyeri</u>
Dwarf Monkey Flower	<u>Mimulus nanus</u>
Silvery Ragwort	<u>Senecio canus</u>
Anderson Lupine	<u>Lupinus andersoni</u>
Golden Chinkapin	<u>Castanopsis chrysophylla</u>

Table 8

lodgepole pine than the sample along the west highway entrance to the Park.

Ecologically, the lodgepole pine stands can be grouped into two categories: Sub-climax stands and transitional stands (Fowells, 1965). Subclimax stands of lodgepole pine can exist because of isolation of the lodgepole pine from other tree species which possess the seed supplies to replace the lodgepole pine. These circumstances may develop due to the advent of fire. Both fire and the relationship between soil and water help maintain the conditions favorable for the continued occurrence of lodgepole pine. Lodgepole pine may also exist as a transitional species. In these stands, other species may become more dominant due to greater amounts of reproduction; limited extent of pure lodgepole pine stands surrounded by climax species; and by the occurrence of a mixed stand with lodgepole pine not being the climax species (Fowells, 1965).

The major tree species that are associated with lodgepole pine in the National Park are subalpine fir, shasta red fir, whitebark pine, ponderosa pine, western white pine, and in very limited areas, mountain hemlock. The dominant brush species which occur in association with lodgepole pine include: Oregon boxwood, swamp huckleberry, broom huckleberry, pinemat manzanita, pacific serviceberry, and saskatoon serviceberry.

Ponderosa pine within the Park occurs primarily in the southern panhandle and in the southeast and northeast corners of the Park. In the southern panhandle of the Park, the ponderosa pine is mixed with dense stands of white fir. In the southeast corner of the Park, white fir, sugar pine, and shasta red fir occur with the ponderosa pine. In the northeast portions of the Park, ponderosa pine occurs as a large, singularly occurring species near Sharp Peak, and mixed with shasta red fir, white fir, and lodgepole pine further toward the corner of the Park. In the area north of and surrounding Sharp Peak, only the large, sparsely stocked ponderosa pine are evident. Ponderosa pine regeneration is not readily apparent. The same general lack of ponderosa pine regeneration characterizes the other areas mentioned. Species associated with ponderosa pine in the Park are sugar pine, white fir, shasta red fir, and some incense-cedar, and varying amounts of lodgepole pine. These ponderosa pine associated species are establishing regeneration within the Park, while the ponderosa pine is experiencing difficulty in establishing good regeneration.

Within the National Park, wildfires have been quickly suppressed in order to preserve the existing vegetation of the Park. This fire suppression tactic has prevented the occurrence of natural processes and conditions. Fire introduced to the ponderosa pine area may simulate natural processes and conditions such as the reduction of the litter

layer; the decrease of plant competition; and the development of a seedbed which is more conducive to ponderosa pine regeneration.

The brush species which occur in areas of ponderosa pine include: western common chokecherry, big sagebrush, rubber rabbitbrush, snowberry ceanothus, sharpleaf snowberry, saskatoon serviceberry, antelope bitterbrush, baldhip rose, Oregon grape, pinemat manzanita and greenleaf manzanita.

Mountain hemlock is the dominant tree species which occurs in the upper elevations of the Park. Two examples within the Park where mountain hemlock occur are the general vicinity between the Park headquarters and the caldera rim, and the vicinity of Grouse Mountain. Mountain hemlock occurs within the Park in two distinct settings: one as a continuous, dense forest cover, and the other as a mosaic of forested patches and tree groups interspersed with shrubby or herbaceous plant communities. The associated tree species vary locally with gradients in temperature, moisture, and accumulation and duration of snow (Brooke et al., 1970; Franklin, 1966). Apparently, regeneration of mountain hemlock develops after the old growth stands begin to break up, since significant amounts of mountain hemlock regeneration does not occur under closed forest canopies (Franklin and Dyrness, 1973).

The associated tree species which occur with mountain hemlock within the Park include subalpine fir, shasta red fir, ponderosa pine, noble fir, whitebark pine, and varying amounts of lodgepole pine and western white pine. Some of the more dominant brush types which occur in the understory of mountain hemlock stands include wax currant, partridge-foot, pinemat manzanita, and huckleberry.

White fir occurs in association with two major species in two general regions within the Park. White fir is mixed with ponderosa pine in the panhandle and in the southeast corner of the Park. Douglas-fir occurs in heavy association with white fir in the Red Blanket Creek area, located in the southwest corner of the Park.

White fir is usually a good competitor with associated species. In the early stages of growth, white fir is easily injured by fire. Older white fir with its thicker bark is more resistant to fire-caused injury (Baker, 1942). The zone in which white fir occurs generally experiences lower temperatures, less plant moisture stress, and less soil drought than adjacent zones (Waring, 1969). Incense cedar may be a climax associate of white fir in areas where species are at or near the moisture extreme of white fir. Douglas-fir or incense cedar or both appear to be climax associates in areas at or near the dry extremes, while white fir appears to be the sole climax species on moister habitats (Franklin and Dyrness, 1973).

Tree types which exist in association with white fir within the borders of Crater Lake National Park are ponderosa pine, Douglas-fir, shasta red fir, sugar pine, incense cedar, and lodgepole pine. The major brush species found as part of the understory is sticky currant, pinemat manzanita, greenleaf manzanita, deerbrush ceanothus, and snowbrush ceanothus.

Shasta red fir is an abundant tree species which occurs throughout the upper reaches of the Park. Evidence suggests that extensive interbreeding has occurred between shasta red fir and noble fir. The result of this interbreeding is that individual trees within the Park can be assigned to one species or the other species with great difficulty or not at all.

There are numerous areas within the Park where distinctive stands of shasta red fir can be observed. One particular location is along highway 62 near Castle Creek. Another area of shasta red fir is found along highway 62 between the Mazama campgrounds and Park headquarters. Shasta red fir commonly will invade the area occupied by intermingled patches of lodgepole pine. Reproduction of shasta red fir is generally present within the understory of shasta red fir (Oosting and Billings, 1943).

Tree species which occur with the shasta red fir in the National Park include, mountain hemlock, subalpine fir, ponderosa pine, sugar pine, noble fir, whitebark pine,

Douglas-fir, and small amounts of western white pine. The dominant brush types which occur as understory and in openings of shasta red fir stands are pinemat manzanita, bitter cherry, common snowberry, sierra evergreen chinkapin, and sticky currant.

The remaining tree species which appear in the Park (Table 8) occur in more restricted areas and do not constitute dominant tree species (based upon areal extent) of Crater Lake National Park. These remaining tree species will be grouped according to their association of occurrence and will be discussed in regard to their general distribution within the Park.

Oregon white oak and Pacific willow are found in the southwest corner of the Park in or near Red Blanket Creek canyon. The oaks are found in dry openings on the south facing wall of Red Blanket Creek. The willow can be found in the moist Red Blanket Creek Canyon. Thinleaf alder, quaking aspen, and Pacific yew are generally found at low levels within the Park such as the moist areas within the southern panhandle vicinity near and along Annie and Sun Creeks. Black cottonwood and Sitka alder also occur in moist areas such as adjacent to creeks and streams. These two species are known to occur on the west inner caldera wall of Crater Lake. Sugar pine and incense cedar both occur in association with ponderosa pine in the southern reaches of the Park, near Annie and Sun Creeks. Whitebark

pine and western white pine often occur with lodgepole pine within the Park. Whitebark pine can be seen on Cloudcap and on the slopes of Mount Scott. Western white pine can be particularly observed in the area of the Pinnacles, especially north of the Pinnacles. In the southwest corner of the Park, in Red Blanket Creek Canyon, and on south facing slopes on the west side of the Park, Douglas-fir and white fir occur. Engelmann spruce can also be found along Red Blanket Creek Canyon. Subalpine fir, generally mixed with other conifers, also occurs along streams, in deep canyons, in wet meadows, and along the margins of bogs. A cluster of subalpine fir can be observed along Munson Creek just south of the Park employees' residences near Park headquarters. The occurrence of Pacific silver fir is meager within the Park. The occurrence of only one Pacific silver fir has been authenticated.

In a forthcoming chapter, the distribution of the tree species throughout the entire National Park will be presented and discussed by way of surface cover type maps. This general discussion of the dominant and the less dominant tree species of the Park was intended only to provide an introduction to the tree species distribution and variations within the Park.

III. DATA ACQUISITION

Sampling Strategy and Parameters

In utilizing aerial photography and LANDSAT digital tapes and images for tree species mapping, one of the primary concerns is "ground truth" within the study area. "Ground truth" is information obtained on surface features to aid in the interpretation of aerial photography and remotely-sensed data. "Ground truth" is the only reliable means of determining the performance of the aerial photography and LANDSAT sensors for their use in forest cover type mapping, because it provides a standard by which the remotely sensed data can be compared.

A concern in "ground truth" preparation is the pre-determination of the vegetation parameters which will be measured in the field. The number and location of "ground truth" sample sites which will be required in order to provide the desired mapping information is a further consideration.

Information retrieved by the sensors on-board LANDSAT and the camera systems on-board the U-2 aircraft is obtained from reflected solar radiation. Such factors as vegetation type, surface area, object density, slope angle, and slope aspect all affect the amount of radiation reflected from a ground object. The parameters that influence

the spectral reflectance of ground objects which are recorded on LANDSAT digital tapes and U-2 aerial photography emulsion are the parameters which should be measured and/or observed at each "ground truth" site.

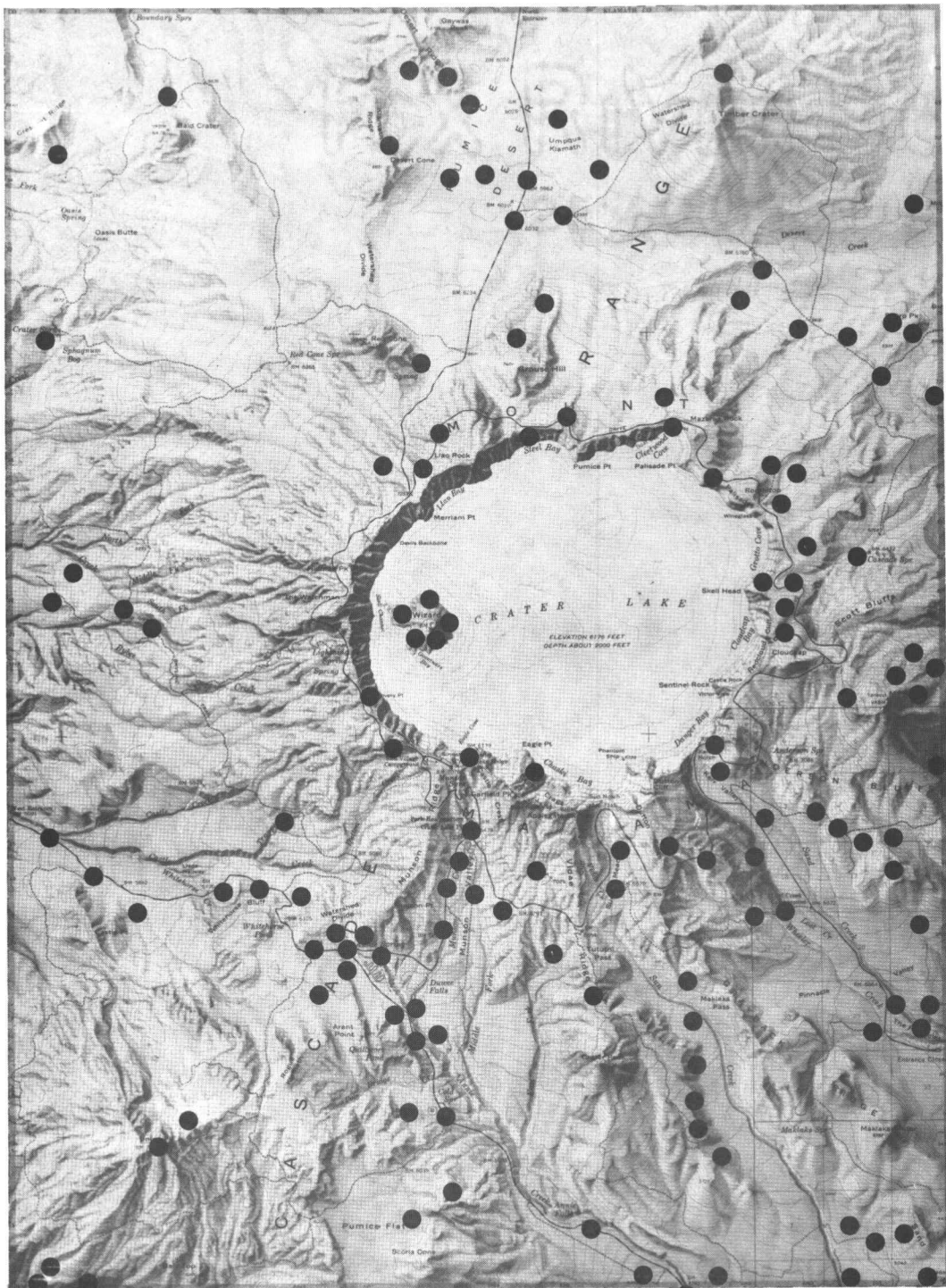
The surface cover type parameters which have been measured and/or observed for forest cover type mapping include:

- Tree species or brush type;
- Percentage of tree species in mix;
- Distribution of tree species in mix;
- Tree height, single or multiple layered canopy;
- Crown size;
- Crown density;
- Diameter-breast-high (DBH);
- Slope angle;
- Slope aspect;
- Tree species branching characteristics;
- Sample site understory;
- Time of year of sampling;
- Vegetation vigor;
- Moisture characteristics of the site (swampy, pumice);
- Sample site near landmark location and identifiable on LANDSAT and aerial photography data.

In order to determine where to sample in Crater Lake National Park, color infrared aerial photography, generalized vegetation maps, topographic maps, and a constructed

slope map of the Park were utilized to permit sampling of at least the major slope aspects, slope angles, and the main forest cover types. A number of the same sample types have been "ground truthed" because of the variability of reflectivity of forest cover types. The location of all sample sites "ground truthed" within the National Park appear in Figure 9.

The determination of the size of the sampling unit is a basic consideration when doing "ground truth" work for aerial photography data and especially when utilizing LANDSAT digital data. The scale and emulsion type of the aerial photography which will be employed during analysis should be determined prior to "ground truth" activities. If the scale of the aerial photography is small, the size of the "ground truth" area must be sufficiently large to be located and studied on the photography. If color infrared aerial photography will be used during analysis, the "ground truth" parameters and activities should be geared to complement and exploit this type of aerial photography. Color infrared photography provides good discrimination of various vegetation types. Easily separable vegetation types such as deciduous from coniferous tree types can be minimally "ground truthed." More time must be devoted to vegetation types which are more difficult to separate on the aerial photography such as conifer tree species.



“Ground Truth” Sample Site
Within Crater Lake National Park



Figure 9

"Ground truth" considerations for LANDSAT data are even more exacting. The vegetation composition, terrain variation, and the relative location of landscape components within the sample unit must be determined. These factors, in addition to the above-mentioned "ground truth" parameters, must be evaluated since all these factors influence reflectance values which are recorded by the LANDSAT sensors. All of these reflectance factors are important because the LANDSAT resolution unit of 1.118 acres (.452 ha) is an integrated spectral response of all the surface phenomena which occur within that 1.118 acres (.452 ha) pixel area. Each pixel also overlaps its adjacent pixel by 75.46 feet (23 m). These LANDSAT characteristics cause problems in analyzing the reflectance value of a particular vegetation type after it has been located and "ground truthed" in the field.

A 25 to 30 cluster pixel group (approximately 30 acres or 13.6 ha) supplies an area sufficiently large to be located on LANDSAT products and to be field checked. Numerous scattered and/or adjacent pixel groups can be "ground truthed" within the same vegetation type to increase the size of the total sampled area of one vegetation type. In areas such as Crater Lake National Park, where motorized travel and trail access is a restriction to "ground truth" activities, small sample units are preferable because one trail may provide access to the entire site.

The actual field measurements were accomplished through the use of the Abney and the Brunton compasses. The Brunton compass was used to measure slope angle, slope aspect, and tree height. The Abney compass was also used to obtain tree heights. Aerial photographs were used in the field to verify sampling locations. Numerous 100 x 100 foot (30.48 x 30.48 m) subsample plots were marked with flagging tape to facilitate estimates of crown density, percentage of species mix, and distribution of tree species in mix. All of these estimates were then verified by photointerpretation measurements on 1:7,400 scale color infrared aerial photography. Crown size measurements were also completed on the aerial photography. Terrestrial photographs were made of all sample sites, with a six-foot scaler in the photograph in order to provide dimensions.

"Ground truth" is essential in any aerial photography and/or remote sensing study. As the desired level of detail sought from the aerial photography and/or remotely sensed data is increased, so must the amount and quality of the "ground truth" be increased. Prudent preparation of "ground truth" activities and the accurate measurement and/or observation of sampling parameters underpins the quality of results.

Aerial Photography Acquisition

Color infrared aerial photography from 3 July 1974 and 10 August 1976 flown by a NASA U-2 aircraft over Crater Lake National Park has been utilized in this research. Both dates of photography were taken by NASA at the request of the Environmental Remote Sensing Applications Laboratory (ERSAL), located on the Oregon State University campus. Natural color aerial photography was taken from a light aircraft at a low altitude by Dr. James F. Lahey on 1 July, 15 July, 26 July, 12 August 1974, and 2 July, 1 August 1976. The color infrared photography, however, has provided the bulk of the information required for surface cover type identification and subsequent mapping within the Park.

The initial scales of the 1974 and 1976 color infrared aerial photography, as photographed by NASA, are approximately 1:122,000 (1 in = 1.93 mi and 1 cm = 1.22 km) and 1:30,500 (1 in = 0.48 mi and 1 cm = .304 km). The 1:122,000 scale photography provides complete coverage of the Park for 1974 and 1976. The 1:30,500 scale photography provides partial coverage of the Park for the same years. Complete coverage of the Park at the scale of 1:30,500 is achieved by combining the area covered by the 1974 and 1976 flights.

Enlargements of the color infrared photographs for 1974 and 1976 have been obtained for the Park from the EROS Data Center in Sioux Falls, South Dakota. By enlarging the

1:122,000 scale photography to the scale of 1:30,500, complete coverage of the Park is obtained for the years 1974 and 1976 at the 1:30,500 scale. This enables the determination of several surface cover type patterns, as well as the determination of slope angle, and slope aspect, where stereoscopic vision permits. Also, the 1974 photography was flown with a large amount of snow on the ground; 1976 was a very light snowfall year with little snow remaining on the ground at the time of photography. The analysis of these two different snowfall years aids in surface cover type identification due to the manner in which certain surface cover types are modified by the snowfall or snowmelt patterns. Enlargements of the 1:30,500 scale photography to approximately 1:7,600 (1 in = 617 ft and 1 cm = 74.04 m) have been employed for selected areas throughout the Park. The location of "ground truth" sites determines where the 1:7,600 scale photography will be utilized, so that the ground truth areas and the large scale photography will coincide in coverage. With these enlargements, detailed determination has been made, not only of the tree species areal extent, but also details concerning crown characteristics, some branching characteristics, brush and grassfield patterns, and snow patterns. The information extracted from the varying scales of the color infrared aerial photography has aided in the delineation of surface cover types in the

Park, besides laying the foundation for surface cover type identification through use of LANDSAT data.

LANDSAT Data Acquisition

The sun-synchronous, near polar orbiting satellite (LANDSAT) has also been employed in this study. On-board the satellite is a multi-spectral scanner (MSS) which senses reflective properties of the earth surface, and records the data on digital tapes. These digital tapes have been utilized for surface cover type location and analysis within the National Park. The dates of the digital tapes utilized are: 06 January 1973, 30 June 1974, 23 August 1974, and 10 September 1974. The variety of dates provides coverage of the Park at approximately the solstices and equinox which allows for variation in earth-sun geometry in the interpretation of LANDSAT MSS data for surface cover type analysis.

The 10 September 1974 LANDSAT digital tapes have been the prime analysis tool for the surface cover type mapping of the National Park. The tapes were utilized primarily because of their absence of bad scan lines; the medium to relatively high sun angle during this time of the year within the Park; the cloud-free conditions over the Park at the time of the LANDSAT pass; and the absence of snow on the ground within the Park.

The 10 September 1974 LANDSAT digital tapes and especially the 06 January 1973 tapes provide good variation in sun angle due to earth-sun geometry. The 10 September tapes are just prior to the autumnal equinox, while the 06 January tapes are just after the time of the winter solstice. The use of these two varying, low to high sun angle tapes aid in landform identification, surface cover type differentiation, and slope estimation. A short discussion on the use of the low sun angle digital tape for surface cover type differentiation will be presented in Chapter VI which deals with data extraction techniques.

The 30 June 1974 and the 23 August 1974 tapes provide good contrast due to the snow-covered and snow-free conditions which they respectively present. These two tapes provide information as to the occurrence of openings in the tree canopy; ephemeral drainage patterns within the Park which aid in understanding the phenological changes of certain surface cover types induced by moisture availability; and an indication of the possible tree and brush species which may occur in association with these high elevation moist conditions. The use of LANDSAT data to monitor the Park throughout the seasons of the year is a multi-temporal approach to data analysis and can be used as a general data enhancement technique.

IV. RECONNAISSANCE TECHNIQUES

To effectively utilize LANDSAT data and aerial photography in surface cover type identification and mapping, an understanding of the scanning and imaging systems, instrumentation and products of LANDSAT and the U-2 aircraft is important. Such information aids in determining the limitations, capabilities, and difficulties involved in applying LANDSAT data and aerial photography to surface cover type analysis.

LANDSAT Satellite

The Earth Resources Technology Satellite Program was designed and sponsored by the National Aeronautics and Space Administration (NASA) in an effort to utilize the information gained through space programs and to direct this information to the efficient monitoring and management of earth resources. NASA, in response to this general objective, launched an experimental satellite (ERTS-1) on 23 July 1972 into a circular, near polar orbit around the earth. In January, 1975, another satellite (ERTS-2) was launched. Near the time period of the second satellite launching, the Earth Resources Technology Satellite Program was redesignated as the LANDSAT program in order to emphasize the prime area of satellite monitoring. The two orbiting satellites were renamed LANDSAT-1 and LANDSAT-2.

Parameters and Earth Coverage

The LANDSAT satellites are sun-synchronous, near polar, circular orbiting satellites. The satellites orbit the earth at an altitude of 570 miles and require 103 minutes to make one complete orbit of the earth. Each satellite completes 14 earth orbits per day. Figure 10 depicts a typical LANDSAT ground trace of an orbital revolution. Each LANDSAT satellite provides repetitive coverage every 18 days over the same ground area. The repetitive image centers are maintained within 20 miles (32.18 km) of successive satellite passes (NASA, 1976). The satellites provide repeat coverage of ground points at the same local time each day.

The launching of LANDSAT-2 was timed so that its orbit would follow the orbit of LANDSAT-1 with a delay of nine days. Since the launch of LANDSAT-2, the timing of the repetitive coverage when combined with LANDSAT-1 has been changed to six days between the orbit of LANDSAT-1 and LANDSAT-2 over the same ground area, and 12 days between the pass of LANDSAT-2 and LANDSAT-1. The general orbital parameters of LANDSAT are presented in Table 9.

Instrumentation

On-board LANDSAT-1 and LANDSAT-2 are multispectral scanners (MSS). The MSS is a line scanner that uses an oscillating mirror to continuously scan perpendicular to the path of travel of the spacecraft (Figure 11). Figure 11

LANDSAT Ground Coverage Pattern

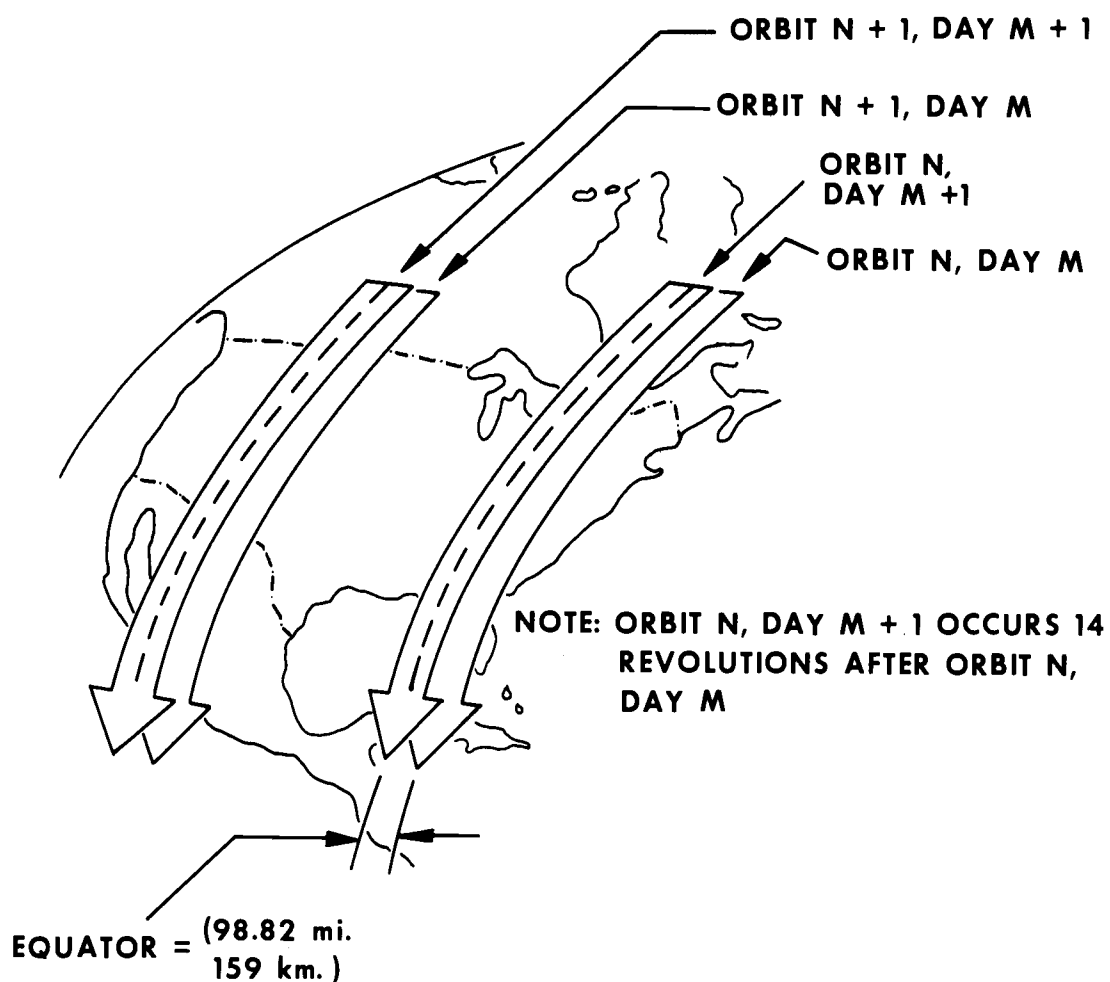


Figure 10. Adapted from Data Users Handbook (NASA, 1976).

LANDSAT Orbit Parameters
(September 1976)

Orbit parameter	LANDSAT spacecraft	
	1	2
Semi-major axis	4527.93 miles (7285.438 km)	4528.11 miles (7285.730 km)
Inclination (degrees)	98.906	99.015
Period (min)	103.143	103.149
Eccentricity	.001070	.001392
Time at descending node	8:50 A.M.	9:20 A.M.
Coverage cycle duration	18 days	18 days
Distance between adjacent ground tracks at equator	98.82 miles (159.38 km)	98.82 miles (159.38 km)

Table 9. Adapted from the Data Users Handbook (1976).

Schematic Diagram of the LANDSAT MSS Scanning Arrangement

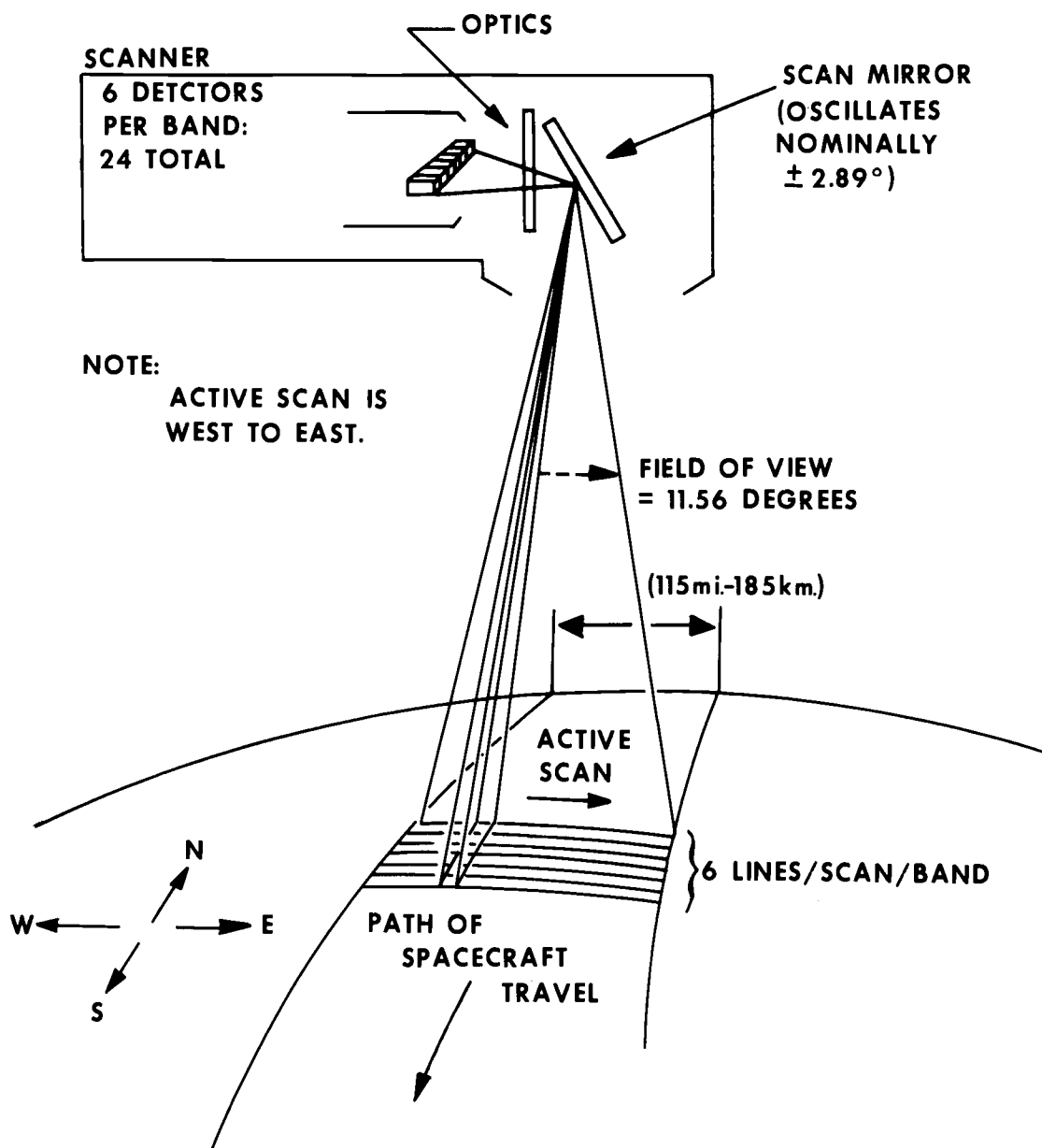


Figure 11. Adapted from the Data Users Handbook (NASA, (1976)).

also shows that the effective crosstrack field of view is 11.56 degrees with the scanning mirror oscillating at ± 2.89 degrees about its normal position. Six lines were scanned simultaneously for each sweep of the mirror. The motion of the spacecraft from roughly north-northeast to south-southwest provides for the along-track progression of the scan lines. The MSS scans cross track swaths of 115 miles (185 km) wide normal to the direction of the satellite pass (Figure 12). The 115-mile-wide (185 km) swath or LANDSAT scene is composed of 2,340 scan lines. Each scan line covers the width of the scene and is comprised of between 3,000 and 3,450 pixels of video data (Figure 13)(Thomas, 1975). The direction of the scan is shown in Figure 14. The scanning mirror operates in a scan and scan-retrace cycle. The active scan is in a west-east direction (Figure 14).

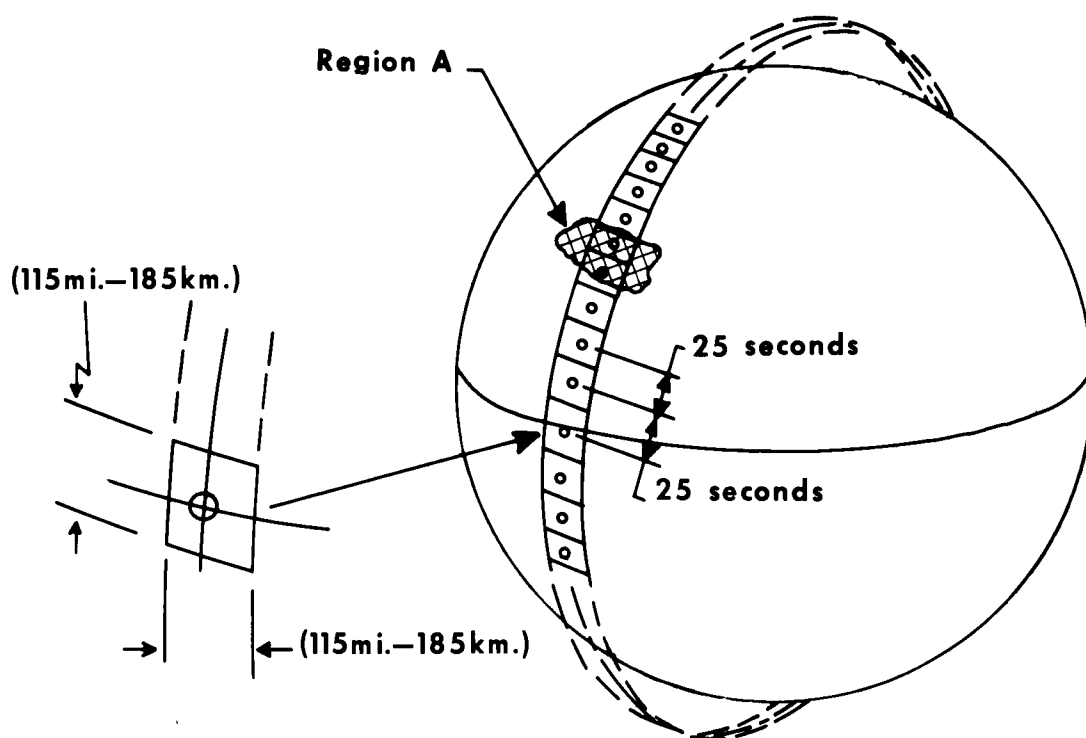
On the satellites, the MSS utilizes six detectors per band. Photo-multipliers are used in bands 4, 5, and 6. Band 7 utilizes silicon photodiodes to sense in the near infrared (GSFC,* 1976). The sensors of all four bands are exposed to a rotating variable density wedge optical filter illuminated by on-board calibration lamps on every other mirror retrace. The calibration data are used to perform radiometric corrections to the MSS detectors.

The MSS, while sensing the earth in the scanning format, senses reflected solar radiation in four bands of the

*Data Users Handbook.

LANDSAT Tracking Scheme

Frame shot within ± 2 seconds on equator,
other frames spaced at 25 seconds



In-Track Picture Scheduling.

Figure 12. Adapted from the Data Users Handbook (NASA, 1976).

LANDSAT MSS System

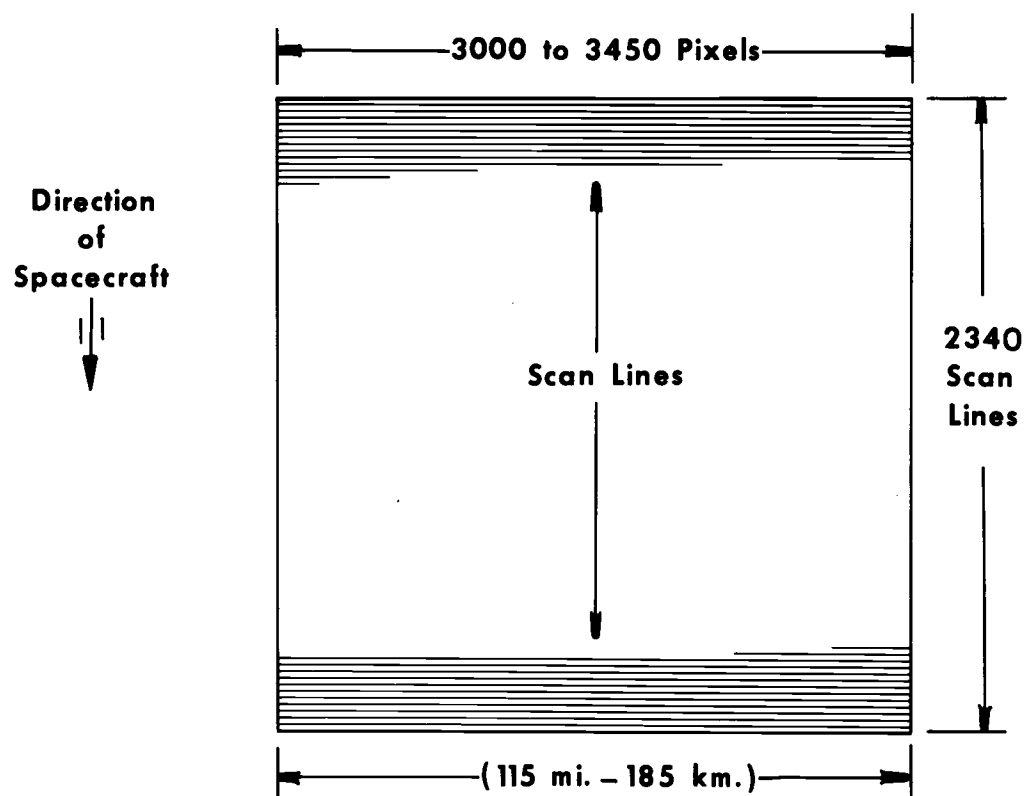


Figure 13. Components of a completed ground scene as represented on the MSS CCT. Adapted from Thomas (1975).

Ground Scan Pattern for a single MSS Detector

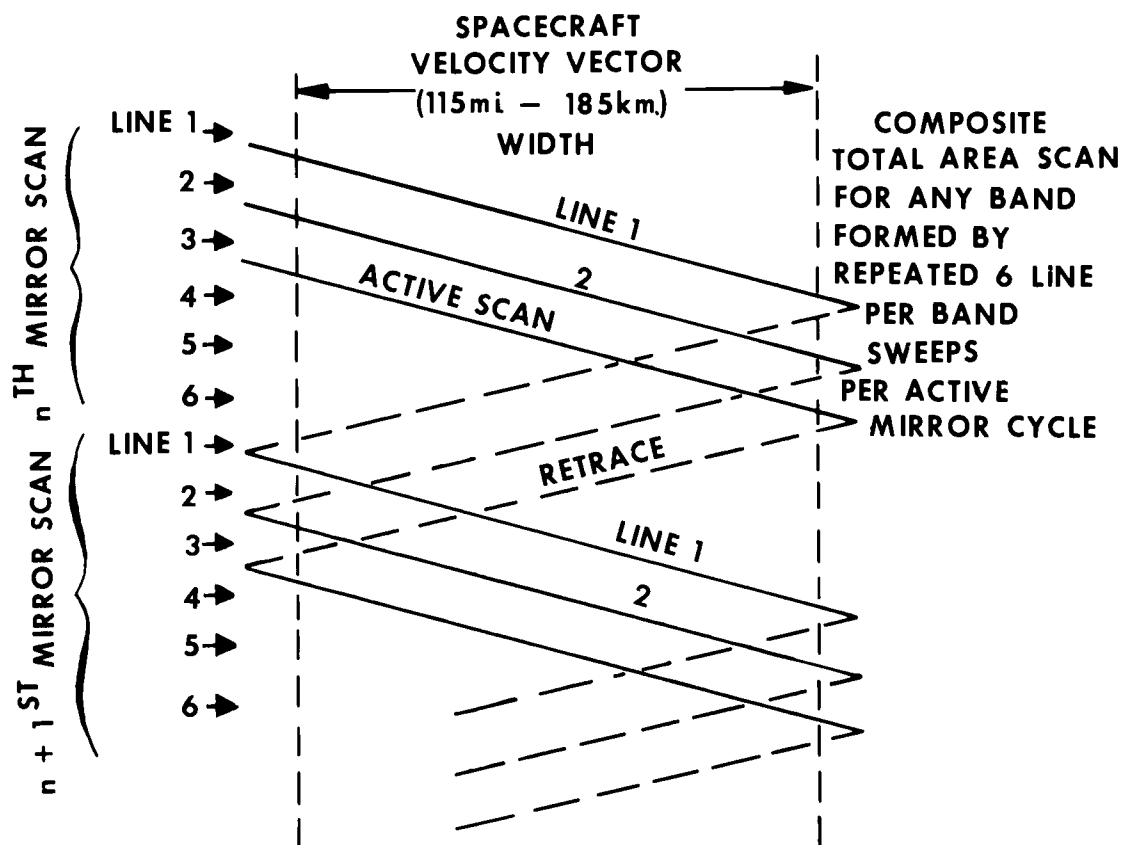


Figure 14. Adapted from the Data Users Handbook (NASA, 1976).

electromagnetic spectrum. The wavelengths sensed by the MSS are in four bands between 0.5 and 1.1 micrometers. Band 4 corresponds to wavelengths between 0.5 and 0.6 micrometers; band 5 between 0.6 and 0.7 micrometers; band 6 between 0.7 and 0.8 micrometers; and band 7 to wavelengths between 0.8 and 1.1 micrometers. The MSS senses through the visible wavelengths and into the near infrared and thus senses different attributes of the same object.

The multispectral system of data acquisition is based upon the assumption that every ground object reflects a distinctive amount of radiant energy and thus provides a unique means of identification through the establishment of a spectral signature. Ground objects reflect solar radiation over a broad spectrum, but generally at some particular frequency there is a maximum amount of radiant energy which is reflected. In sensing the earth in discrete bands or wavelengths of the electromagnetic spectrum (multispectral scanning), the opportunity for recognizing that the sensed object is distinct from all other background objects because of its unique spectral signature is greatly enhanced. A method of comparing spectral responses in bands is by having the sensed data recorded in the form of digital tapes in order to facilitate comparisons through quantitative techniques.

The MSS detectors sense different levels of radiance or reflectance caused by differing amounts of solar

radiation being reflected from surface features and by variable atmospheric attenuation. The level of radiance sensed by the detectors is rated on a scale from 0 to 127 for bands 4, 5 and 6, and from 0 to 63 for band 7. On these scales, zero is minimum radiance while 127 and 63 are the maximum levels of radiance. For processing purposes, LANDSAT data are often stretched to a scale of 0 to 256 for all four bands. This is accomplished by multiplying the reflectance values recorded in bands 4, 5 and 6 by two and band 7 by a factor of four. Units of 1.118 acres (.452 ha) are sensed individually by each of the band sensors, and a reflectance value for each band is assigned to that particular 1.118 acre (.452 ha) unit. These four reflectance values (one for each band) provide a spectral signature for the surface cover types which were sensed in that 1.118 acre (.452 ha) area. This 1.118 acre (.452 ha) area is the resolution unit or picture element (pixel) of the MSS system. The pixel value recorded at the LANDSAT sensors is a reflectance value which is obtained from the integration of radiance values from all of the surface cover types which occur within that pixel area.

The pixel area measures 259 x 259 feet (79 x 79 meters); however, the active advance or area of new information of each pixel area is approximately 259 x 184 feet (79 x 56 meters). Nearly 75.5 feet (23 meters) of every pixel area is overlapped with its adjacent pixel and therefore the

reflectance value for the pixel area as registered by the sensors is integrated by the surface cover types of the newly scanned information and further by the overlapped information. The actual shape of the pixel is a curved lined parallelogram and not a square which is used for computing purposes.

As described in Chapter III under sampling parameters and strategy, there are many factors which are capable of influencing the reflectance value of a pixel area. In mountainous terrain, such as within Crater Lake National Park, surface cover typing through use of LANDSAT data becomes very complex. The slope angle and slope aspect tends to alter the spectral responses of tree and brush types (Hoffer, et al., 1974). The analysis of pixel cluster values aids in determining how much slope angle and which slope aspects are required to effectively alter the spectral reflectance (Bonner, 1975). An understanding of the degree that various landscape components (i.e. vegetation types, bare ground, water, etc.) contribute to the total integrated pixel and pixel cluster reflectance values may lead to improved surface cover type differentiation in especially steep terrain, such as within Crater Lake National Park (Kan, et al., 1975; Smedes, et al., 1975). These considerations will be investigated in the forthcoming chapter dealing with pixel value analysis.

LANDSAT Computer Compatible Tapes

The computer compatible tapes (CCT's) are a final product of the multispectral scanner (MSS) on-board LANDSAT. The MSS CCT'S are composed of four groups of data: identification data, annotation data, video data, and special image annotation tape data. The identification data contain a combination of binary and Extended Binary Coded Decimal Interchange Code (EBCDIC) information which is utilized to identify the video data on the CCT's (GSFC, 1976). The annotation information contains binary and EBCDIC data which provide additional information concerning the LANDSAT scene including scene format center, nadir and sun elevation, and tick mark location information which links the digitized LANDSAT scene with the latitude and longitude earth coordinates. The video data contain LANDSAT scene information which has been digitized so that differing levels of gray comprising the video image are represented by a reflectance value. The special image annotation tape information are written in a separate file following the information on the fourth tape of the CCT set.

Data from the four spectral bands are combined on the CCT through a process called interleaving whereby bytes of data from each band are interspersed by twos to produce an eight-byte "group" (Figure 15) (GSFC, 1976). The "group" is the smallest element of interleaved data.

Interleaving of LANDSAT Data

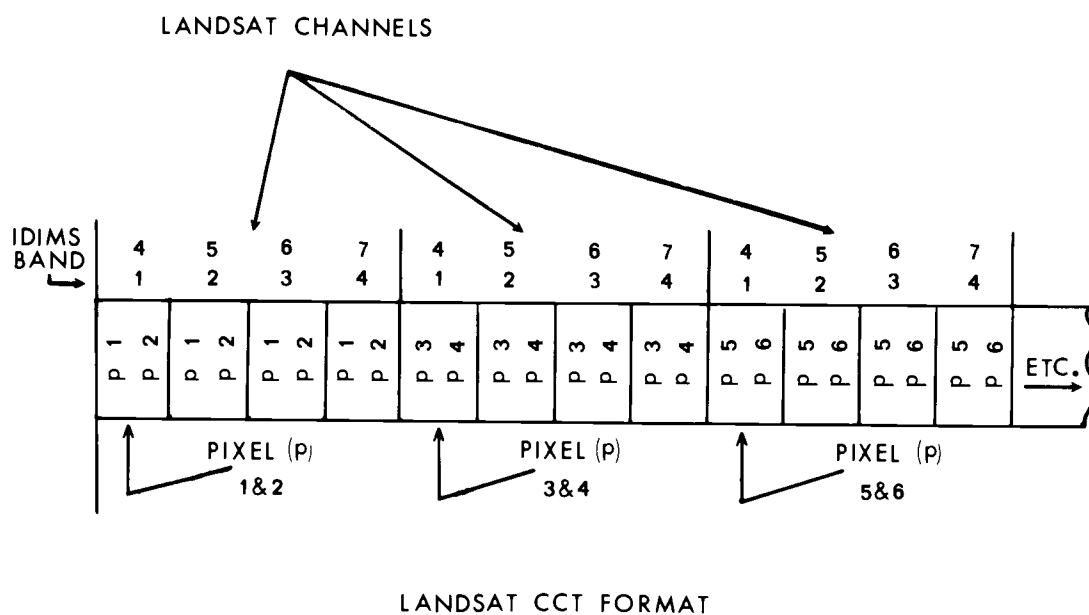
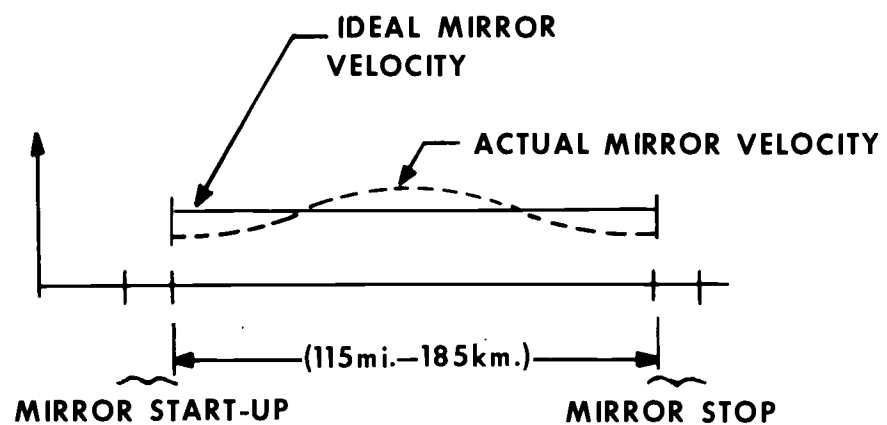


Figure 15. Adapted from Thomas (1975).

During the MSS scan of the ground, the pixel data corresponding to 259 x 259 ft (79 x 79 m) would have a constant overlap with adjacent pixels of 75.5 ft (23 m), if the scanning mirror of the MSS was constant. The actual mirror scanning velocity, however, is not constant; therefore, the active advance or area of new information of each pixel area varies slightly from the 259 x 75.5 ft (79 x 56 m) area. A graphic representation of the mirror velocity versus time is shown in Figure 16. The graph reveals a near cosine curve during the mirror active scan. Since the mirror scanning velocity is not constant with time, the amount of pixel overlap between pixels also is not constant with time. Figure 17 shows the variable pixel overlap. Figure 18 shows the relationship between the distance covered on the ground and the scan of the MSS mirror for a constant scanning mirror velocity and for a variable scanning mirror velocity. The straight line in the graph shows a constant scanning mirror velocity versus the ground distance covered. The curved line represents the actual ground distance covered with a variable velocity scanning mirror of the MSS LANDSAT satellite. The difference between the straight line and the curved line reflects the necessary corrections which must be made between the location of points on the CCT's and the same points' location on the ground (Thomas, 1975).

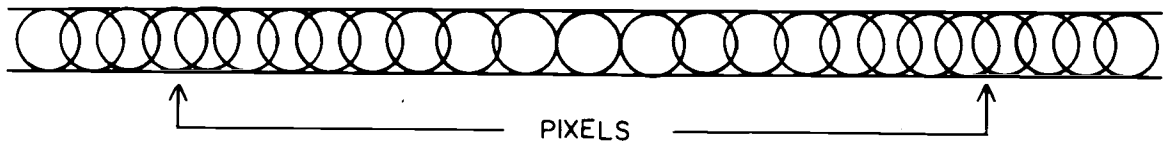
Comparison of the Constant Mirror Velocity and the Variable Mirror Velocity of LANDSAT



NOTE:
NOT DRAWN TO SCALE

Figure 16. Adapted from Thomas (1975).

Integration and Variable Overlapping of Pixels Corresponding to a Variable Mirror Velocity

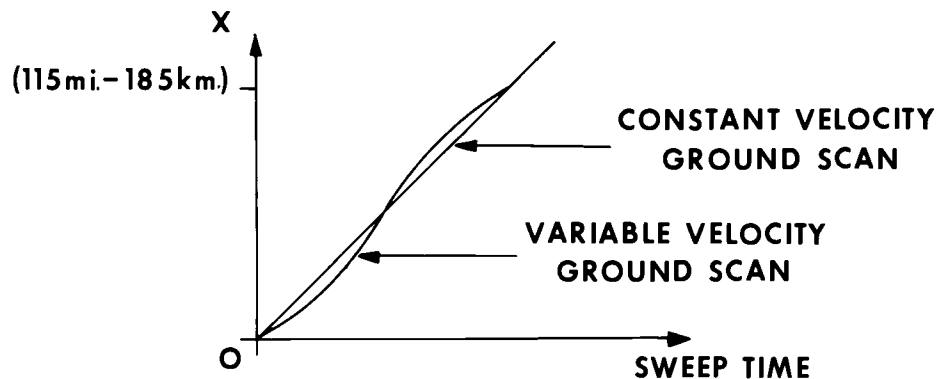


NOTE:

1. Pixels are represented by circles for ease of illustration
2. Not drawn to scale.

Figure 17. Adapted from Thomas (1975).

Comparison of Distance Covered on the Ground for a Constant Mirror Velocity and a Variable Mirror Velocity



NOTE:

1. X = THE EASTERLY SCAN OF THE GROUND
2. NOT DRAWN TO SCALE

Figure 18. Adapted from Thomas (1975).

LANDSAT Products

The reflectance values sensed by the MSS system of the LANDSAT satellites are converted into photographic and computer products by the image processing facility at the Goddard Space Flight Center in Greenbelt, Maryland.

Third- and fourth-generation products are available to the public in the form of film positives, negatives, and prints. The scales of the available photographic products are 1:3,369,000, 1:1,000,000, 1:500,000, and 1:250,000. The photographic products initially are processed from the LANDSAT digital tapes into black and white photographic products. One black and white image is produced for each band. Four black and white images are available for each LANDSAT scene, and false color composite products can be produced from the four black and white images. The false color composite combines the photographic data acquired by the four band LANDSAT MSS sensors into a single photographic image.

Computer compatible, magnetic, digital tapes are also available as LANDSAT products. The digital tapes may be requested as either 7-track or 9-track. The data on the 7-track tapes are formatted in 800 bits per inch (bpi), and the 9-track tapes are formatted in 800 bpi and 1,600 bpi. A bit is the smallest element of binary computer-intelligible data.

LANDSAT products possess an error in the registration of data bytes with the corresponding ground area covered caused by the variable velocity of the LANDSAT scanning mirror. The maximum accumulated error for each scan line is approximately 1,312 ft (400 m) (i.e., approximately five pixels) (Thomas, 1975). Figure 19 shows the error across the 115 mile (185 km) LANDSAT scene. The maximum positive error occurs at 28.75 miles (46.24 km); at 57.50 miles (92.50 km), the error is zero, and at 86.25 miles (138.75 km), the maximum negative error occurs.

LANDSAT Surface Cover Type
Differentiation Potential

The use of LANDSAT digital tapes and images for surface cover type differentiation and mapping has several distinct advantages over ground surveying: (1) the vantage point of observation; (2) LANDSAT's repetitive coverage over the same ground area at the same local time; and (3) its discriminatory capability between different types of surface cover types due to LANDSAT's sensing wavelengths extending through the visible and into the near infrared.

Various spectral bands of the LANDSAT MSS are considered to be appropriate for the detection of certain surface cover types. A LANDSAT digitally constructed image for each of the four MSS bands will now be presented. These images show various examples of the optimum band for the investigation of surface cover types within Crater Lake

Ground Registration Error Due to Variable Mirror Velocity

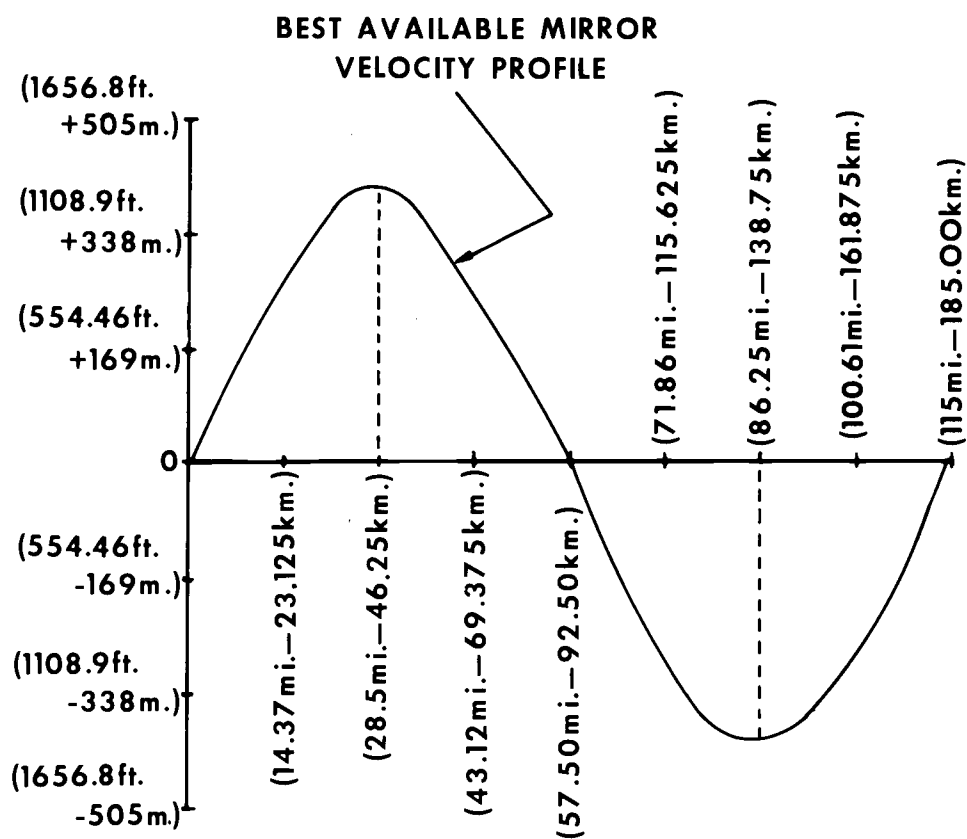


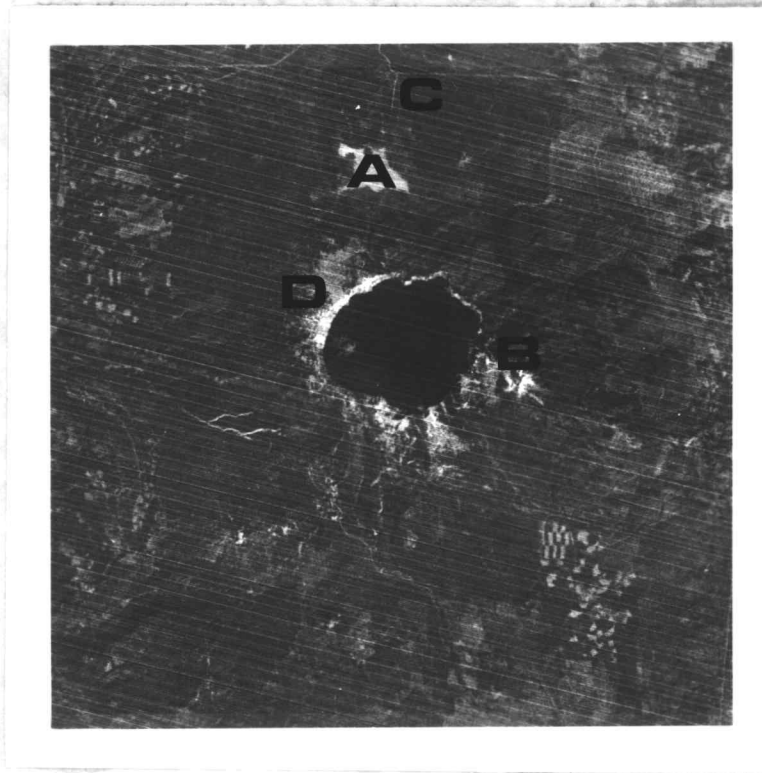
Figure 19. Mirror velocity profile for the active MSS mirror scan. Adapted from Thomas (1975).

National Park. The 10 September 1974 LANDSAT images (ID No. 1779-18171) will be employed because most of the processing involved in this research has been accomplished with the 10 September 1974 LANDSAT data.

Figure 20 shows a LANDSAT image formed when wavelengths between 0.5 and 0.6 micrometers are detected by the band 4 sensors on-board LANDSAT. Certain surface cover types on the image are highlighted while other surface features cannot be easily delineated. Examples of surface cover types which are well delineated on band 4 and which are labelled on Figure 20 include: the distinction between pumice, in the pumice desert, and snow on the summit of Mt. Scott; the identification of roads through the Park and north of the Park; and the difference in vegetation growth between the Pumice Desert and the pumice-grassfield complex northwest of Crater Lake.

Figure 21 is an image of band 5 (0.6 to 0.7 micrometers) of the MSS, 10 September 1974. Band 5 can effectively detect vegetation differences such as those east of the Pumice Desert. In that area, mountain hemlock and shasta red fir communities can be readily separated from the lodgepole pine stands. Openings in the tree canopy can also be easily detected in band 5, in addition to the land-water boundaries; topography changes; landform features; pumice areas; and roads. These surface cover types are identified on Figure 21.

LANDSAT Image of Band 4



- | | |
|----------------------|------------------------------|
| A. Pumice Desert | C. Roads |
| B. Snow on Mt. Scott | D. Pumice-Grassfield Complex |

Figure 20. LANDSAT image of the 10 September 1974 pass over Crater Lake National Park.

LANDSAT Image of Band 5



- | | |
|--|-----------------------|
| A. Mountain Hemlock and Shasta Red fir | E. Topography Changes |
| B. Lodgepole Pine | F. Landform Features |
| C. Openings in Tree Canopy | G. Pumice Areas |
| D. Land-Water Boundaries | H. Roads |

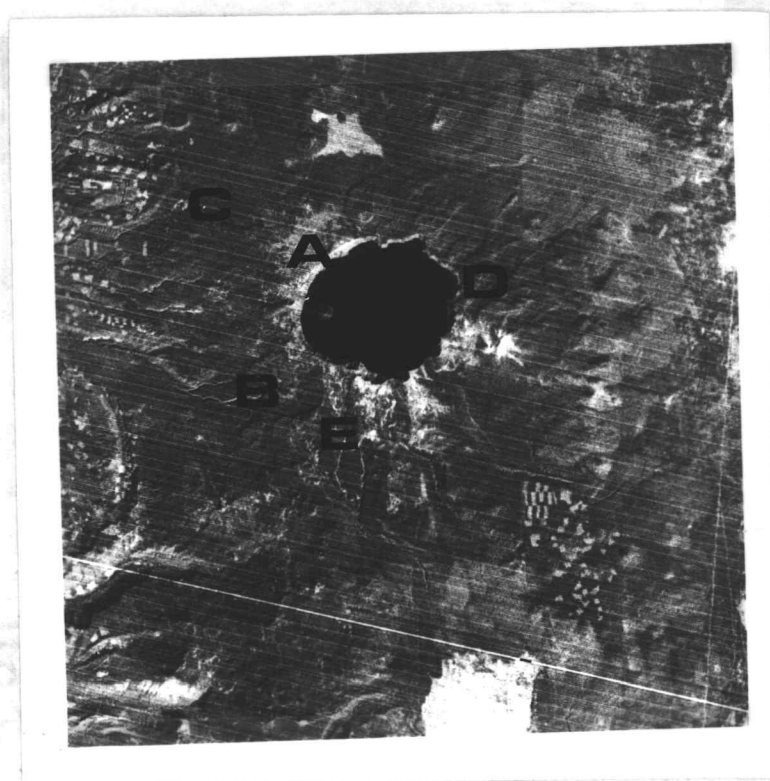
Figure 21. LANDSAT image of the 10 September 1974 pass over Crater Lake National Park.

Band 6 (0.7 to 0.8 micrometers), 10 September 1974 presented in Figure 22 can best be used in sensing surface water (Crater Lake), geologic features (Castle Creek), marsh and bogs (Sphagnum Bog), igneous rock (cinder cones), and creeks (Munson Creek). These various surface cover types are located on Figure 22.

Figure 23 shows a LANDSAT image of band 7 (0.8 to 1.1 micrometers), 10 September 1974. Surface cover types such as tectonic features (Sharp Peaks and Grouse Mountain); geologic features (caldera rim); wetlands (Sphagnum Bog); surface water (Crater Lake); and vegetation differences can be well delineated through the use of band 7. The above mentioned surface cover types are shown in Figure 23.

It is apparent from a visual inspection of bands 4, 5, 6 and 7 that the multispectral capability of the LANDSAT satellite is a distinct advantage in surface cover type identification and delineation. Since the Park is heavily vegetated by predominately coniferous species, band 5 and band 7 are most appropriate to this research. Band 4 and band 6 are important but of less use as compared to the other two bands. When all four bands of LANDSAT are used collectively and simultaneously through a color composite or a four band digital system, the discriminatory capability of LANDSAT for surface cover types is greatly enhanced (Figure 24).

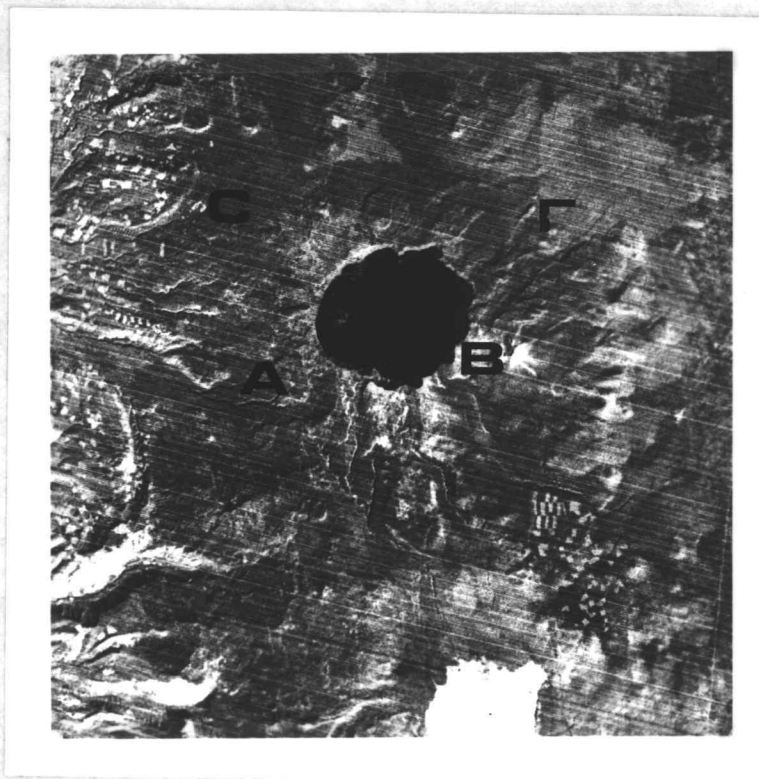
LANDSAT Image of Band 6



- A. Crater Lake
- B. Castle Creek
- C. Sphagnum Bog
- D. Igneous Rocks
- E. Munson Creek

Figure 22. LANDSAT image of the 10 September 1974 pass over Crater Lake National Park.

LANDSAT Image of Band 7



A. Tectonic Features

D. Crater Lake

B. Caldera Rim

E. Sharp Peaks

C. Sphagnum Bog

D

Figure 23. LANDSAT image of the 10 September 1974 pass over Crater Lake National Park.

LANDSAT Color Composite of
Bands 4, 5, 6, and 7



Figure 24. LANDSAT image of the 10 September 1974 pass
over Crater Lake National Park.

Aerial Photography

The aerial photography utilized during this research was color infrared aerial photography flown by a NASA U-2 high altitude aircraft based at NASA/Ames Research Center, Moffet Field, California. The U-2 aircraft conventionally flies at an altitude of 65,000 feet and is capable of operating multiple camera systems simultaneously. The film formats and emulsion that can be utilized are 9 x 9 inch and 9 x 18 inch color infrared.

Instrumentation

The U-2 aircraft employed two different camera systems to obtain the two initial film formats and scales utilized in this research. The RC-10 camera system provided the 1:122,000 average scale photographs at the 9 x 9 inch (22.86 x 22.86 cm) film format, while the HR-732 camera system provided the 1:30,500 average scale photographs at the 9 x 18 inch (22.86 x 45.72 cm) film format. Each 9 x 9 inch (22.86 x 22.86 cm) photograph covers approximately 18 x 18 miles (29 x 29 km) on the ground, and each 9 x 18 inch (22.86 x 45.72 cm) photograph covers approximately 4.5 x 9 miles (7.25 x 14.50 km) on the ground.

Unlike natural color photography, color infrared film emulsions are sensitive to green, red, and infrared. A wratten 12 yellow filter is used on the camera to filter out blue, since all film layers are blue sensitive. During

reversal processing, a yellow positive image records in the green sensitive layer, and positive images of magenta and cyan appear in the red and infrared sensitive layers, respectively (Kodak, 1972). Figure 25 illustrates the various steps of color formation with color infrared film and lists the wavelengths to which the U-2 color infrared photographic emulsions are sensitive. A comparison of the wavelengths sensed by the LANDSAT MSS system (0.5 to 1.1 micrometers) with the wavelengths sensed by the U-2 color infrared photography (0.5 to 0.9 micrometers) reflects a mutual compatibility of data between both methods of information acquisition, since both systems sense through the visible and into the near infrared portion of the electromagnetic spectrum.

Color Infrared Aerial Photography Surface Cover Type Differentiation Potential

The use of color infrared aerial photography for surface cover type differentiation and mapping maintains similar advantages over ground surveying as cited in the section dealing with LANDSAT surface cover type differentiation potential. These advantages include the expansion of detecting wavelengths through the visible and into the near infrared; and the vantage point of earth observation. Aerial photography data and LANDSAT data differ in five major ways: (1) LANDSAT system provides repetitive coverage over the same ground area every six and twelve days, while aerial photography missions are flown for specific reasons

Color Formation with Color Infrared Film

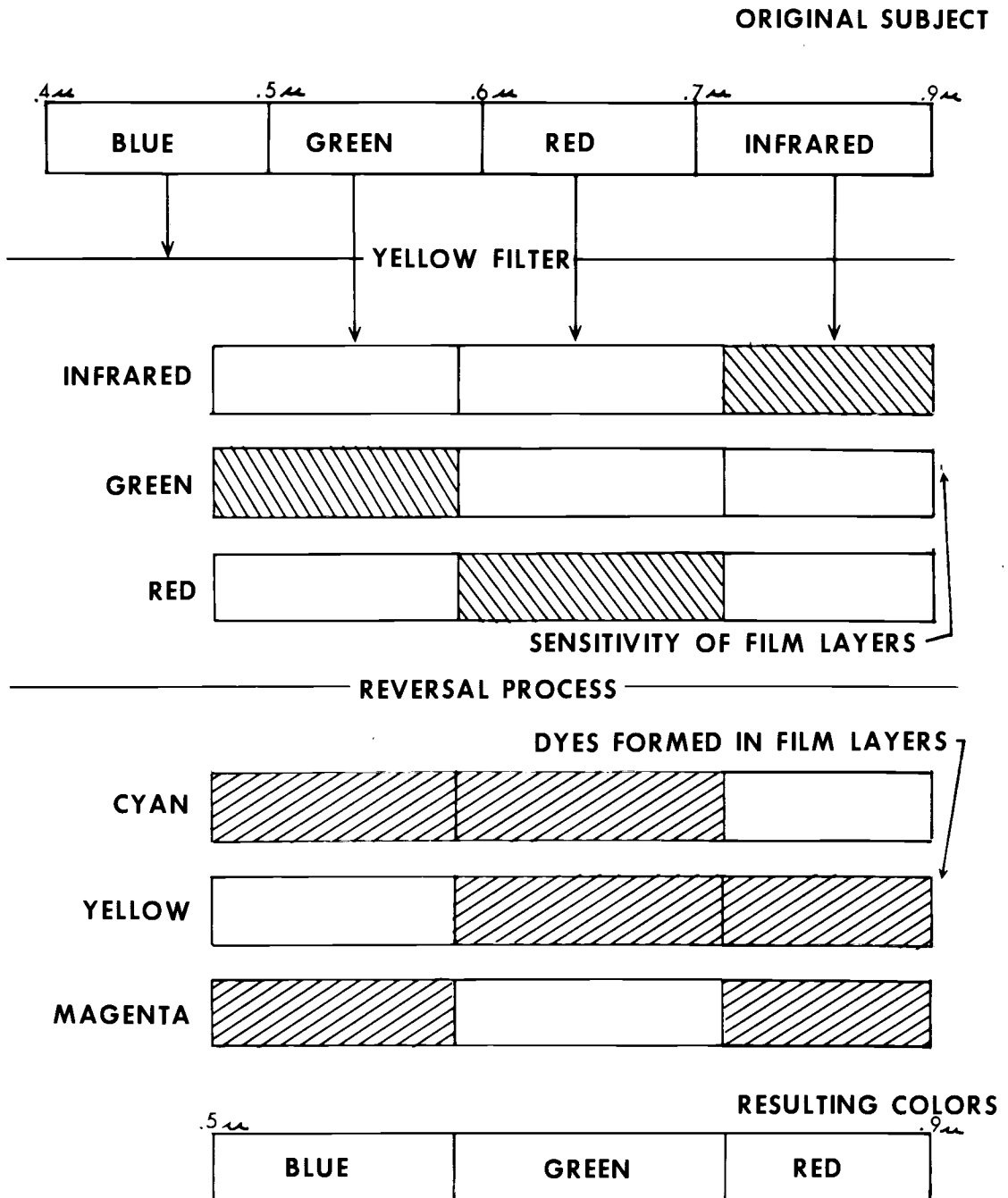


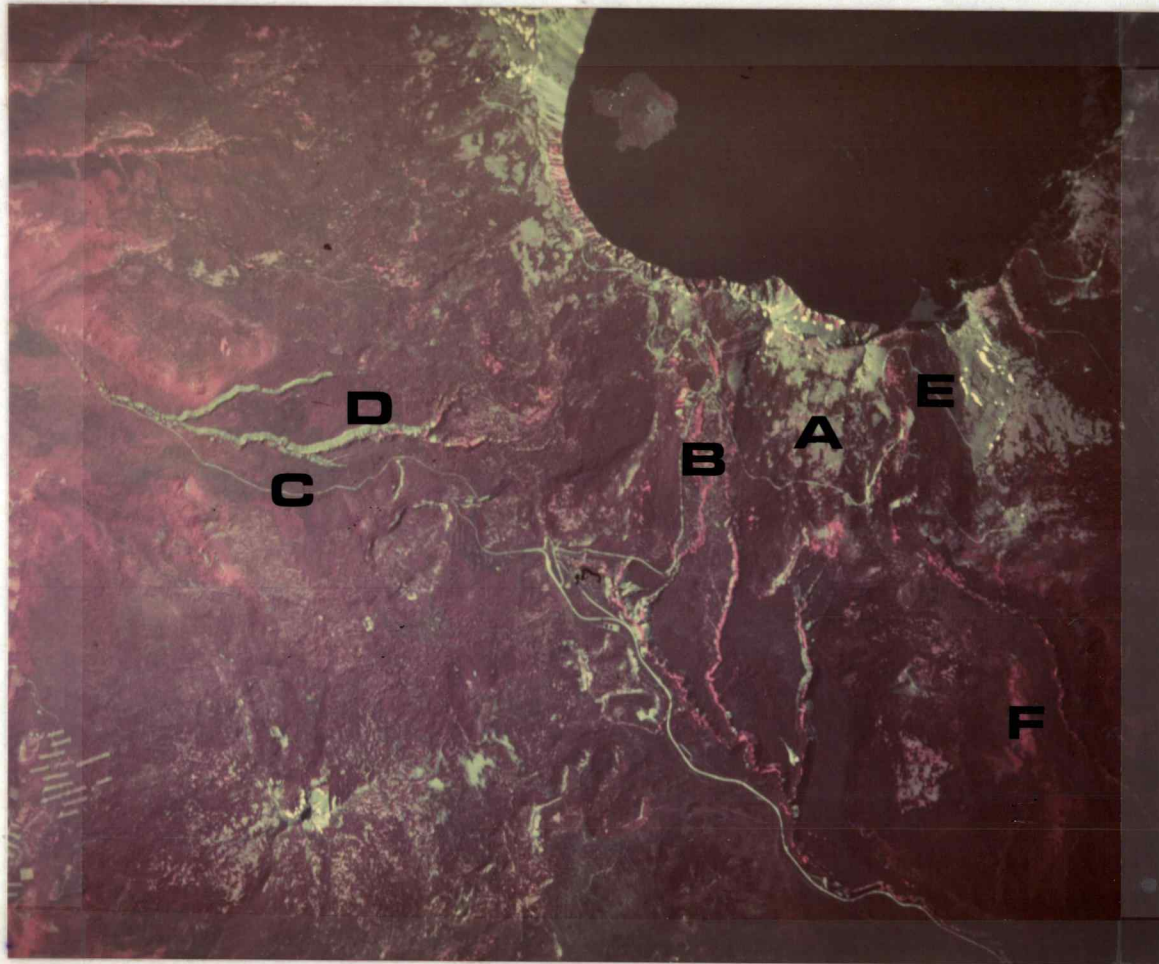
Figure 25. Adapted from Kodak M-28 (1972).

and at specific requests; (2) the NASA U-2 aircraft produces larger scale imagery than LANDSAT, approximately 1:30,000 and 1:130,000; (3) NASA U-2 photography has greater resolution (approximately 7.0 feet (2.0 m) on 1:30,000 scale photography) than LANDSAT; (4) NASA U-2 photography is less affected by atmospheric attenuation of the reflected signal than LANDSAT because of a lower operating altitude; (5) LANDSAT data is in a digital format and is computer compatible. The U-2 aerial photography is generally visually interpreted by textures, tones, and hues, unless a densitometer or a related piece of equipment is utilized to quantify the photographic data. The quantified photographic data must be reformatted for computer compatibility.

The following discussion will describe the potential for surface cover type separation by citing examples on a color infrared photograph covering the southern portion of Crater Lake National Park.

The primary advantage of aerial photography as compared to LANDSAT data is the increased scale and resolution of the photography. Figure 26 is an example of color infrared aerial photography, which has been reduced for presentation purposes. Particular examples of surface cover type mapping on color infrared aerial photography are labelled on Figure 26. The examples include: the recognition of small clusters of trees; the identification of creeks and drainages; the vegetation distinction between lodgepole

Color Infrared Photograph of the Southern Portion
of Crater Lake National Park



- A. Small tree clusters
- B. Creeks and drainages
- C. Lodgepole pine
- D. Shasta red fir
- E. Mountain hemlock
- F. Brush

Figure 26

pine and shasta red fir and mountain hemlock; and the difference between brush types and tree types.

Most of the surface cover types recognized by the four bands of LANDSAT can be equally well recognized on the color infrared aerial photography due to the similarity in wavelength detection. Some features, however, which can be delineated in band 7 of LANDSAT cannot be as well delineated on aerial photography due to wavelength differences. This difference in wavelengths can be compensated for by the aerial photography through the increased scale and resolution of the photography versus LANDSAT. LANDSAT, however, can partially mitigate the image scale and resolution shortcoming by providing multitemporal data which aids in surface cover type identification and delineation that aerial photography generally does not provide. There exist relative advantages and disadvantages in both types of data; but when both color infrared aerial photography and LANDSAT data are used in conjunction with each other, cover type mapping becomes more efficient.

V. CLASSIFICATION PROBLEMS AND LIMITATIONS

Within Crater Lake National Park, geologic activity, soil conditions, climate, and vegetation influence the spectral reflectivity of surface cover types. One should appreciate to what degree the spectral reflectivity of surface cover types are affected by environmental factors particularly when analyzing and mapping surface cover types in mountainous terrain. One should also appreciate the implications, limitations, and problems of utilizing a system such as LANDSAT for surface cover type mapping, and one should further appreciate the effect of atmospheric attenuation on remotely sensed data.

This chapter deals with the three above mentioned concerns, beginning with how certain environmental factors influence spectral reflectance values detected by LANDSAT. The use of U-2 color infrared aerial photography requires similar considerations as those employed when LANDSAT data are utilized; therefore, aerial photography will not be mentioned separately.

Environmental Factors and Spectral Reflectivity

Computer processing of LANDSAT data demonstrated that certain environmental factors influenced the spectral reflectivity of specific surface cover types. These environmental factors caused the spectral reflectance values

recorded by LANDSAT to be quite different for some extremely similar surface cover types. The phenomenon of spectral reflectivity being affected by environmental factors is well known; but unless this phenomenon is appreciated and dealt with, surface cover type mapping by use of LANDSAT data loses some of its effectiveness. Misclassification of data can result, for example, by selecting training areas for a specific surface cover type which do not account for the variation in the spectral reflectance values found in some extremely similar surface cover types.

Some environmental factors which influence spectral reflectivity of surface cover types studies within Crater Lake National Park include: surface cover type; crown size; crown density; slope angle; and slope aspect. Other factors influence the spectral reflectivity of surface cover types, but these five factors are most important and appropriate to the analysis and mapping of surface cover types found within Crater Lake National Park. The Park is primarily composed of coniferous type tree species with varied slope angles and slope aspects.

To fully appreciate the effect of each of the five environmental factors in modifying the spectral reflectance value, all factors were divided into subclasses in order to investigate, for example, which slope class was most effective in causing a change in the reflectance value in each of the four LANDSAT bands.

The surface cover type class was divided into ten subclasses which included: ponderosa pine, large, with scattered shasta red fir (coded PP); shasta red fir and scattered mountain hemlock (SRF-MH); mountain hemlock and scattered shasta red fir (MH-SRF); lodgepole pine, poorly stocked (LP, poor); lodgepole pine, densely stocked (LP, dense); white fir with scattered ponderosa pine and shasta red fir (WF); pumice and bare rock (Pumice); ponderosa pine and white fir mix (PP-WF); brush (Brush); marsh and moist grass and deciduous (Marsh). The slope angle class (coded S) was divided into seven subclasses: 0 to 5 percent; 6 to 15 percent; 16 to 30 percent; 31 to 45 percent; 46 to 60 percent; 61 to 75 percent; and greater than 75 percent. The slope aspect class (coded by actual direction) was comprised of the eight points of the compass: north, northeast, east, southeast, south, southwest, west, and northwest facing slopes. Crown size (diameter) (coded FT) was divided into five subclasses which included: 5 to 13 feet (1.53 to 3.98 m); 14 to 20 feet (4.28 to 6.12 m); 21 to 27 feet (6.42 to 8.26 m); 28 to 34 feet (8.56 to 10.40 m); and greater than 34 feet (10.40 m). The crown density class (coded C) was also divided into five subclasses which included: 0 to 10 percent; 11 to 30 percent; 31 to 50 percent; 51 to 70 percent; and 71 to 90 percent.

The surface cover type class was divided into 10 subclasses because they represent the major surface cover

types found within the Park based upon areal extent. The slope class was divided into seven subclasses because the extent of each slope class was mapped prior and during the field work and because most slopes classes are characteristic of certain surface cover types within the Park. Those slopes which are greater than 75 percent are generally clustered near the rim of the caldera and were also found to exhibit similar influence in the reflectance value. The eight slope aspect subclasses were chosen in order to analyze the major slope directions. The crown size and crown density subclasses were chosen due to field work measurements throughout the Park which indicated the average and extreme crown sizes and crown densities.

A statistical approach was designed to analyze how the 35 subclass variables influenced a change in the mean spectral reflectance value for each of the four LANDSAT bands, and which variables were statistically related through correlation. The mean reflectance values per LANDSAT band were generated from the 10 September 1974 LANDSAT digital tape classification statistics for Crater Lake National Park. The statistical approach consisted of a multiple regression analysis of all 35 independent variables regressed against the mean reflectance value (dependent variable) per LANDSAT band. A multiple regression analysis of each class of subclass variables (ten surface cover types, seven slope angles, eight slope aspects, five crown sizes, and five crown densities) was also regressed

individually against the mean reflectance value per LANDSAT band. The regression analyses were generated through use of the Statistical Interactive Programming System (SIPS) at the Oregon State University campus. An analysis of variance table (ANOVA) also through SIPS, was generated for each regression, in addition to T-values for each variable in the regressions. A correlation coefficient was also obtained for each variable correlated with every variable for all four LANDSAT bands.

The significance level employed to test the regression analyses with the F-test was .05. A .05 significance level was also utilized to test the importance or validity of each variable in the regressions (similar to the backstep regression) tested by the T-test. One hundred eighty-two samples used in this statistical study were selected from "ground truth" sample sites. The strategy of selecting "ground truth" sample sites was discussed in Chapter III. The surface cover type, slope angle, slope aspect, crown size, and crown density information was obtained for each of the 182 samples and recorded into one of the appropriate subclasses. Chapter VI presents and discusses the classification statistics.

Dummy variables were employed in this study because nominal-scale variables were used in the regression analyses. A nominal variable is a variable which is not assumed to have an order and unit of measurement. A set of dummy

variables were "created" by treating each subclass of a nominal variable class as a separate variable and assigning arbitrary scores for all cases depending upon their "presence" or "absence" in each of the categories (Nie, et al., 1975). For example, if for sample one, the surface cover type was shasta red fir and scattered mountain hemlock, a "1" was placed within the appropriate surface cover type subclass signifying "presence," and a "0" was placed within all other surface cover type subclasses signifying "absence." This procedure was used to input data for the generation of all regressions, analysis of variance tables, and correlations of all four LANDSAT bands. Because dummy variables were exclusively utilized, one variable per class (surface cover type, slope angle, slope aspect, crown size, crown density) was deleted from the regression model for the regression of all the variables combined ("full regression"), and for the five specific class regressions ("partial regression"), per four bands. This deletion results from the fact that a regression is solved by inverting the data matrix. An inverse of the matrix can be achieved when linear independence occurs. Linear independence exists when no column in the matrix can be written as a linear combination of any other column in the matrix. A variable for each class regression was deleted so that no column in the matrix is a combination of all other matrix columns. This same characteristic of dummy variable regressions

precludes the use of the backstep regression analysis to arrive at the variables which most contribute to the regression model. In all regressions ("partial" and "full"), marsh surface cover type; greater than 75 percent slope angle; southwest slope aspect; greater than 34 feet (10.40 m) crown size; and 71 to 90 percent crown density were deleted from the regressions.

In the regressions of the five specific classes ("partial regressions"), degree and direction of reflectance value change from the mean reflectance value caused by each of the above-mentioned deleted variables were obtained by summing the beta values of each variable in the respective "partial" regression. This procedure cannot be used for the regression of all variables ("full regression") because the sum of the beta values within the regression represents the degree that all five deleted variables differ from the mean reflectance value. Their individual differences are undistinguishable.

In Table 10, the "full regression" model, ANOVA, and T-values for 30 independent variables (one variable deleted for each of the five classes) for bands 4, 5, 6, and 7 is presented. By referring to the beta-values in the regressions, the degree and direction that each variable differs from the mean reflectance values can be determined. From the R squared term in the ANOVA of the "full regression" for each band (Table 10), one can observe that 72.75 percent

Regression Analysis
(Bands 4, 5, 6, and 7)

BAND 4

Beta values	= 1.8326E+01	SRF	+3.0740E-01	PP
	-7.8195E-01	LPP00R	-2.4841E-01	MH-SRF
	-1.8389E+00	WF	-1.6402E+00	LPDENS
	-2.1032E+00	PP-WF	+9.8333E+00	PUMICE
	-1.7061E+00	SC-5	-8.3497E-01	BRUSH
	-3.2930E-01	S16-30	-1.4534E+00	S6-15
	-2.3012E+00	S46-60	-1.4002E+00	S31-45
	-3.3638E-01	NORTH	-1.1029E+00	S61-75
	-4.3074E-01	EAST	+7.6726E+01	SOUTH
	+1.3994E-01	NE	-6.0554E-01	WEST
	-1.3859E-01	SE	-1.6276E+00	NW
	+1.2129E+00	FT5-13	+1.1811E+00	FT21-27
	+6.3975E-01	FT28-34	+2.9754E-01	CO-10
	-4.0178E-01	C11-30	+5.1205E-01	C31-50
	+1.1777E+00	C51-70	-4.1647E-02	
	-9.2747E-01			

ENTERING F VALUE: 13.4393
DEGREES OF FREEDOM: 30, 151

+AVTABLE

ANALYSIS OF VARIANCE TABLE

SOURCE	DF	SUM OF SQUARES	MEAN SQUARE
TOTAL	181	3.89373603E 03	2.15123537E 01
REGRESSION	30	2.83279218E 03	9.44264061E 01
RESIDUAL	151	1.06094384E 03	7.02611817E 00

R SQUARED = .72752548

+TVALUES

VARIABLE	S.E. OF REGR. COEF	T
CONSTANT	3.98626390E-01	4.59718418E 01
PP	8.78491353E-01	3.49926956E-01
SRF	6.05325619E-01	-1.29178907E 00
MH-SRF	6.97991876E-01	-3.55388119E-01
LPP00R	1.16619800E 00	-1.57678794E 00
LPDENS	7.83296192E-01	-2.09396224E 00
WF	7.55620389E-01	-2.76705494E 00
PUMICE	7.37039836E-01	1.33416795E 01
PP-WF	1.03228654E 00	-1.65270935E 00
BRUSH	1.15369247E 00	-7.23737070E-01
SC-5	4.96429779E-01	-6.71441892E-01
S6-15	4.95648430E-01	-2.93214105E 00
S16-30	5.07427238E-01	-3.94383016E 00
S31-45	6.78747223E-01	-2.06279056E 00
S46-60	6.421522115E-01	-5.2333132E-01
S61-75	8.15999169E-01	-1.35163892E-01
NORTH	5.70392396E-01	-7.01338639E-01
SOUTH	5.018945433E-01	1.52875749E 00
EAST	6.02870395E-01	3.31639057E-01
WEST	5.92874459E-01	-1.19324011E 00
NE	5.38678305E-01	-3.68650861E-01
NW	8.24455483E-01	-1.97419069E 00
SE	5.020944092E-01	2.41351228E 00
FT5-13	7.44026068E-01	1.53744141E 00
FT14-20	6.57026249E-01	1.04981037E 00
FT21-27	5.69451838E-01	5.84046540E-01
FT28-34	5.44443282E-01	-7.37965076E-01
CO-10	9.27021727E-01	5.52364156E-01
C11-30	8.51262519E-01	1.383350784E 00
C31-50	5.15959436E-01	-8.07302362E-02
C51-70	4.52807595E-01	-2.0427235E 00

Table 10. Band 4

BAND 5 = 1.4003E+01

	+9.1958E-01	PP
	-1.4965E+00	SRF
	-2.2659E+00	LPP00R
Beta	-3.5863E+00	WF
values	-2.4726E+00	PP-WF
	-5.5380E-01	S0-5
	-2.7570E+00	S16-30
	-3.9500E-01	S46-60
	-5.3115E-01	NORTH
	+2.9266E-01	EAST
	-6.5125E-01	NE
	+1.4882E+00	SE
	+9.2252E-01	FT14-20
	-8.1746E-01	FT21-27
	+1.7920E+00	CO-10
	-1.2514E+00	C31-50

ENTERING F VALUE: 12.8374
 DEGREES OF FREEDOM: 30, 151

*AVTABLE

ANALYSIS OF VARIANCE TABLE

SOURCE	DF	SUM OF SQUARES	MEAN SQUARE
TOTAL	181	8.73611439E 03	4.82658253E 01
REGRESSION	30	6.27557136E 03	2.09185712E 02
RESIDUAL	151	2.46054302E 03	1.62949869E 01

R SQUARED = .71834812

*TVALUES

VARIABLE	S.E. OF REGR.	COEF	T
CONSTANT	6.16378843E-01		2.28634925E 01
PP	1.33539629E-00		6.88615944E-01
SRF	9.11973106E-01		-1.64097052E 00
MH-SRF	1.03736636E+00		-5.61784042E-01
LPP00R	1.68896024E+00		-1.34157084E 00
LPDENS	1.21133914E+00		-2.04220507E 00
WF	1.16455752E+00		-3.01123614E 00
PUMICE	1.17071079E+00		1.27285302E 01
PP-WF	1.57906615E+00		-1.56587943E 00
BRUSH	1.75374943E+00		-9.19283492E-01
S0-5	7.47390569E-01		-7.40972230E-01
S6-15	7.51127019E-01		-2.87498268E 00
S16-30	7.81313734E-01		-3.52865426E 00
S31-45	1.03660921E+00		-1.83877468E 00
S46-60	9.76949191E-01		-4.04318776E-01
S61-75	1.24267613E+00		-1.13545268E 00
NORTH	8.69995344E-01		-6.68218503E-01
SOUTH	7.86535634E-01		2.38642904E 00
EAST	9.18797319E-01		3.18524542E-01
WEST	8.87120266E-01		-1.37313441E 00
NE	8.10238583E-01		-7.94948235E-01
NW	1.25535229E+00		-1.71579816E 00
SE	7.57643819E-01		1.85872110E 00
FT5-13	1.13754666E+00		1.93629263E 00
FT14-20	1.02235533E+00		9.02343530E-01
FT21-27	7.86946874E-01		4.74854843E-01
FT28-34	8.39252043E-01		-9.74035365E-01
CO-10	1.47076506E+00		3.87949557E-01
C11-30	1.26396271E+00		1.41779675E 00
C31-50	7.75091122E-01		2.35598624E-01
C51-70	6.89798654E-01		-1.81412312E 00

Table 10 (continued), Band 5

BAND 6 = 2.3526E+01		+1.4004E+00	PP
	-3.3609E+00	-2.9486E+00	MH-SRF
	-1.3511E+00	-4.5047E+00	LPOENS
	-3.1546E+00	+1.1737E+01	PUMICE
	-2.4105E+00	+4.8125E+00	BRUSH
Beta	-2.6633E-01	-2.2807E+00	S6-15
values	-1.3224E+00	-1.3711E+00	S31-45
	-1.2335E+00	-3.6542E-02	S46-50
	-2.3989E+00	+2.1052E+00	S61-75
	+1.1102E+00	-1.5619E+00	NORTH
	+7.7013E-01	-2.5909E+00	EAST
	+2.7115E+00	+9.0519E-01	WEST
	+1.1415E+00	+1.0070E+00	NW
	-3.7780E-01	+6.2158E-01	SE
	+1.0128E+00	-2.0347E-01	FT5-13
	-9.0713E-01	-2.0347E-01	FT14-20
			FT21-27
			FT28-34
			C0-10
			C11-30
			C31-50
			C51-70

ENTERING F VALUE: 12.3826
 DEGREES OF FREEDOM: 30, 151

+AVTABLE

ANALYSIS OF VARIANCE TABLE

SOURCE	DF	SUM OF SQUARES	MEAN SQUARE
TOTAL	181	7.86830819E 03	4.34713160E 01
REGRESSION	30	5.59431159E 03	1.86477053E 02
RESIDUAL	151	2.27399661E 03	1.50595802E 01

R SQUARED = .71099294

+TVALUES

VARIABLE	S.E. OF REGR.	COEF	T
CONSTANT	5.87262527E-01	4.00612948E 01	
PP	8.30891053E-01	1.64544753E 00	
SRF	8.70533583E-01	-3.86022090E 00	
MH-SRF	9.73410496E-01	-3.02910093E 00	
LPPCCR	1.59856624E 00	-8.45182687E-01	
LPOENS	1.15557656E 00	-3.99819027E 00	
WF	1.11555331E 00	-2.82784298E 00	
PUMICE	1.10691436E 00	1.06043336E 01	
PP-WF	1.52121285E 00	-1.54458724E 00	
BRUSH	1.62971162E 00	2.95297706E 00	
S0-5	7.18124738E-01	-3.70857379E-01	
S6-15	7.20295460E-01	-3.16633919E 00	
S16-30	7.63561732E-01	-1.73579149E 00	
S31-45	9.94896417E-01	-1.37817134E 00	
S46-50	9.37896931E-01	-1.31730573E 00	
S61-75	1.19081126E 00	-3.06869589E-02	
NORTH	8.38916643E-01	-3.57459285E 00	
SOUTH	7.48426024E-01	2.81285024E 00	
EAST	8.78533357E-01	1.26367133E 00	
WEST	8.53305230E-01	-1.80701742E 00	
NE	7.93394384E-01	-9.83065117E-01	
NW	1.20647734E 00	-2.14747015E 00	
SE	7.29011695E-01	3.71941985E 00	
FT5-13	1.07856737E 00	8.39252381E-01	
FT14-20	9.94468902E-01	1.14785997E 00	
FT21-27	7.25050027E-01	1.38936168E 00	
FT28-34	7.37674834E-01	-5.12695612E-01	
C0-10	1.40379303E 00	4.42748340E-01	
C11-30	1.21569268E 00	8.33994170E-01	
C31-50	7.33572588E-01	-2.77363409E-01	
C51-70	6.63527068E-01	-1.36714029E 00	

Table 10 (continued). Band 6

BAND 7 =

Beta values	2.4917E+01		+1.2833E-01	PP
	-5.6576E+00	SRF	-5.3644E+00	MH-SRF
	+2.1537E+00	LPPPOOR	-3.5161E+00	LPOENS
	-4.1307E+00	WF	+5.8388E+00	PUMICE
	-2.5000E+00	PP-WF	+9.1222E+00	BRUSH
	+2.3223E-01	SO-5	-2.2946E+00	S6-15
	-1.5130E-01	S16-30	-3.5004E-01	S31-45
	+4.7963E-02	S46-60	+9.0331E-01	S61-75
	-4.2357E+00	NORTH	+2.2251E+00	SOUTH
	+2.1526E+00	EAST	-2.1900E+00	WEST
	+1.0788E-01	NE	-2.2306E+00	NW
	+2.3397E-00	SE	-1.3735E+00	FT5-13
	-5.2868E-01	FT14-20	+1.2949E+00	FT21-27
	+1.2497E+00	FT28-34	+2.2967E-01	CO-10
	-8.0604E-01	C11-30	-2.3358E-01	C31-50
	-3.1166E-01	C51-70		

ENTERING F VALUE: 6.7848
 DEGREES OF FREEDOM: 30, 151

+AVTABLE

ANALYSIS OF VARIANCE TABLE

SOURCE	DF	SUM OF SQUARES	MEAN SQUARE
TOTAL	181	8.24935413E 03	4.55725422E 01
REGRESSION	30	4.73595676E 03	1.57865225E 02
RESIDUAL	151	3.51339737E 03	2.32675322E 01

R SQUARED = .57410031

+TVALUES

VARIABLE	S.E. OF REGP. COEF	T
CONSTANT	7.36539220E-01	3.34233469E 01
PP	1.59572608E 00	8.04239225E-02
SRF	1.08975830E 00	-5.19164639E 00
MH-SRF	1.23959643E 00	-4.322786437E 00
LPPPOOR	2.01821570E 00	1.06711733E 00
LPOENS	1.44744444E 00	-2.42838724E 00
WF	1.39152208E 00	-2.96836691E 00
PUMICE	1.39833822E 00	-4.16815494E 00
PP-WF	1.88689824E 00	-1.32063646E 00
BRUSH	2.09563574E 00	4.35310393E 00
SO-5	8.93091108E-01	-2.60027716E-01
S6-15	8.97955966E-01	-3.59549880E-01
S16-30	9.33627451E-01	-1.62254431E-01
S31-45	1.23469167E 00	-2.83871529E-01
S46-60	1.16740119E 00	4.10855934E-01
S61-75	1.43493844E 00	6.00316584E-01
NORTH	1.03949715E 00	-4.07432957E 00
SOUTH	9.39867344E-01	2.36750719E 00
EAST	1.09791288E 00	1.96159162E 00
WEST	1.06086051E 00	-2.06592555E-01
NE	9.78945585E-01	1.10107430E-01
NW	1.58007777E 00	-1.48697443E 00
SE	9.05342174E-01	-2.58443460E 00
FT5-13	1.35942614E 00	-1.00103492E 00
FT14-20	1.22165905E 00	-4.32752405E-01
FT21-27	9.40405542E-01	1.37270284E 00
FT28-34	1.00286059E 00	1.24609553E 00
CO-10	1.75748432E 00	-1.14068085E-01
C11-30	1.51036607E 00	-3.33972053E-01
C31-50	9.27267213E-01	-3.65814950E-01
C51-70	8.24271905E-01	-3.78093403E-01

Table 10 (continued). Band 7

of the variation found in the reflectance values is explained by the "full regression" for band 4. The regression for band 5 explains 71.83 percent; band 6 explains 71.10 percent; and band 7 explains 57.41 percent of the variation found in the reflectance values by the "full regressions." All four "full regressions" are significant at the .05 level, based on F-test results. T-values are also shown in Table 10. The T-values show how close the beta values of the independent variables in the "full regressions" are to zero, and therefore how important each variable is in the regression model. The level of significance is also .05. The significant variables (most important to explaining regression) for bands 4, 5, 6, and 7 are marked by asterisks in Table 11 and were determined by significant T-values.

Table 11 lists the ranking of surface cover types, slope angles, slope aspects, crown sizes, and crown densities as to the degree and direction of mean reflectance value change due to each variable, for bands 4, 5, 6, and 7. Negative beta values indicate that the respective variable produces a change in the mean reflectance value in the negative direction in the amount of the beta value. An inspection of the ranking of the surface cover type beta values for bands 4, 5, 6, and 7 in Table 11 shows that pumice and ponderosa pine, large, with scattered shasta red fir consistently influence a positive impact upon the mean reflectance

Ranking of Variables for "Full Regression"
(Bands 4, 5, 6, and 7)

Surface Cover Types

Band 4		Band 5	
<u>Beta Values</u>		<u>Beta Values</u>	
-2.1032	WF*	-3.5068	WF*
-1.8388	LP, poor	-2.5223	LP, dense*
-1.7061	PP-WF	-2.4726	PP-WF
-1.6402	LP, dense*	-2.2659	LP, poor
-.8350	Brush	-1.6122	Brush
-.7820	SRF-MH	-1.4965	SRF-MH
-.2484	MH-SRF	-.5828	MH-SRF
+.3074	PP	+.9196	PP
+9.8333	Pumice*	+14.8950	Pumice*

Band 6		Band 7	
<u>Beta Values</u>		<u>Beta Values</u>	
-4.5047	LP, dense*	-5.6576	SRF-MH*
-3.3605	SRF-MH*	-5.3648	MH-SRF*
-3.1546	WF*	-4.1307	WF*
-2.9486	MH-SRF*	-3.5151	LP, dense*
-2.4105	PP-WF	-2.5090	PP-WF
-1.3511	LP, poor	+.12833	PP
+1.4004	PP	+2.1537	LP, poor
+4.8125	Brush*	+5.8285	Pumice*
+11.7370	Pumice*	+9.1225	Brush*

Slope Angle

Band 4		Band 5	
<u>Beta Values</u>		<u>Beta Values</u>	
-2.0012	16-30%*	-2.7570	16-30%*
-1.4534	6-15%*	-2.1595	6-15%*
-1.4002	31-45%*	-1.9061	31-45%
-1.1028	61-75%	-1.4110	61-75%
-.3364	46-60%	-.5538	0- 5%
-.3293	0- 5%	-.3950	46-60%

Band 6		Band 7	
<u>Beta Values</u>		<u>Beta Values</u>	
-2.2806	6-15%*	-2.2946	6-15%*
-1.3711	31-45%	-.35064	31-45%
-1.3254	16-30%	-.15130	16-30%
-1.2355	46-60%	+.047963	46-60%
-.2663	0- 5%	+.23223	0- 5%
-.0365	61-75%	+.90331	61-75%

Table 11

Table 11 (continued)

Slope Aspect

Band 4		Band 5	
<u>Beta Values</u>		<u>Beta Values</u>	
-1.6276	NW*	-2.1539	NW*
-.6955	W	-1.2181	W
-.4000	N	-.6513	NE
-.1986	NE	-.5814	N
+.1999	E	+.2927	E
+.7673	S	+1.4082	SE
+1.2128	SE*	+1.8141	S*

Band 6		Band 7	
<u>Beta Values</u>		<u>Beta Values</u>	
-2.9988	N*	-4.2357	N*
-2.5909	NW*	-2.2306	NW
-1.5419	W	-2.1900	W*
-.7701	NE	+.10788	NE
+1.1102	E	+2.1526	E*
+2.1052	S*	+2.2251	S*
+2.7115	SE*	+2.3397	SE*

Crown Size

Band 4		Band 5	
<u>Beta Values</u>		<u>Beta Values</u>	
-.4018	28-34 ft	-.8175	28-34 ft
+.2975	21-27 ft	+.3731	21-27 ft
+.6898	14-20 ft	+.9225	14-20 ft
+1.1811	5-13 ft	+2.0891	5-13 ft

Band 6		Band 7	
<u>Beta Values</u>		<u>Beta Values</u>	
-.3779	28-34 ft	-1.3737	5-13 ft
+.9052	5-13 ft	-.52868	14-20 ft
+1.0070	21-27 ft	+1.2497	28-34 ft
+1.1415	14-20 ft	+1.2909	21-27 ft

Crown Density

Band 4		Band 5	
<u>Beta Values</u>		<u>Beta Values</u>	
-.9275	51-70%*	-1.2514	51-70%
-.0416	31-50%	+.1828	31-50%
+.5121	0-10%	+.5706	0-10%
+1.1777	11-30%	+1.7920	11-30%

Table 11 (continued)

Crown Density (continued)

Band 6		Band 7	
<u>Beta Values</u>		<u>Beta Values</u>	
-.9071	51-70%	-.80604	11-30%
-.2035	31-50%	-.31166	51-70%
+.6216	0-10%	-.28358	31-50%
+1.0128	11-30%	+.22967	0-10%

Table 11

for bands 4, 5, 6, and 7, and that white fir with scattered ponderosa pine and shasta red fir, lodgepole pine, dense, and shasta red fir with scattered mountain hemlock have a negative effect on the mean reflectance for all four bands.

The ranking of surface cover types by LANDSAT bands shows inconsistencies in the placement of numerous surface cover types. This occurs because each LANDSAT band senses different attributes of the same surface cover type, and this therefore, would be expressed by different reflectance values.

Slope angle, crown size, and crown density ranking of beta values for each band are a function of the surface cover type. White fir within the Park, for example, are very large with crown diameters of generally 28 to 34 feet (8.56 to 10.4 m) and crown densities varying between 51 and 90 percent. White fir, within the Park, generally occur on 0 to 5 percent slope angles (Panhandle area) or on 16 to 30 percent slope angles in the southwest corner of the Park (Red Blanket Creek area). To appreciate how the rankings of the various slope angles, crown sizes, and crown density subclasses show a difference in reflectance values from the mean, one must understand the characteristics of the surface cover types and some of the interrelationships between environmental parameters. In general, however, the larger the crown size and crown density, the greater is the negative change in reflectance values from the mean value per band.

Slope aspect beta values for all four bands show the effect of an early morning (approximately 9:30 a.m.) sun when the satellite passed over Crater Lake National Park on 10 September 1974. The north and northwest directions show the most negative change from the mean reflectance. The northeast and east show intermediate effects, with south and southeast showing the greatest positive difference from the mean reflectance values per band.

Slope angles are often associated with surface cover types within the National Park. On extremely steep slopes (61 to 75 percent and to a lesser degree 46 to 60 percent), pumice and bare rock or a slight conifer-pumice and bare rock mix occurs. On level areas (0 to 5 percent), lodge-pole pine is the dominant surface cover type. When reflectance from steep slope areas are sensed by LANDSAT, the high reflecting pumice and bare rock on the steep slopes tend to buffer the potential large negative beta values caused by shadowing effects and reduce the difference in reflectance values from the mean. From the data, slope angles between 6 and 45 percent have the greatest negative difference from the mean reflectance with slope class 31 to 45 percent showing the most consistency in all four bands. Slope angles greater than 75 percent were deleted, as mentioned earlier. The five individual class regressions per band show a finer relationship with changes in the mean reflectance values than the "full regression" because the

"full regression" reflects the influence of all subclass variables.

When all subclass variables in each "full regression" are ranked as to the degree and direction of difference from the mean reflectance value per band, surface cover types, slope aspects, and slope angles are, in general, most responsible for the greatest positive and negative changes in reflectance values from the mean for all four LANDSAT bands.

Regressions for the five classes (surface cover type, slope angle, slope aspect, crown size, and crown density) for band 4 are presented in Table 12. The R squared term in the ANOVA shows the percent variation in the reflectance values explained by each regression. The R squared terms range from 60.27 percent for the surface cover type regression to 2.93 percent for the slope aspect regression. The slope aspect regression is not significant at the .05 level. All other regressions in band 4 are significant at the .05 level.

Table 13 shows the ranking of subclasses per class for band 4 as to the difference of each variable from the mean reflectance, in addition to the significant variables in the regression based on the T-values. The T-values show which variables best describe the variation in reflectance values for each class and are denoted by an asterisk.

In the crown density beta value ranking, subclass 71 to 90 percent shows a large positive change in the

Regression Analysis
(Band 4)

BAND 4 = 1.7844E+01 -8.1471E-01 PP
 Beta -1.8349E+00 SRF -1.7996E+00 MH-SRF
 +1.2023E-01 LPP00R -1.0412E+00 LPDENS
 values -2.6113E+00 WF +1.0405E+01 PUMICE
 -2.0868E+00 PP-WF -6.0137E-02 BRUSH

+AVTABLE

ANALYSIS OF VARIANCE TABLE

SOURCE	DF	SUM OF SQUARES	MEAN SQUARE
TOTAL	181	3.89373603E 03	2.15123537E 01
REGRESSION	9	2.34663973E 03	2.60737748E 02
RESIDUAL	172	1.54709630E 03	8.99474592E 00

R SQUARED = .60267047

+TVALUES

VARIABLE	S.E. OF REGR. COEF	T
CONSTANT	2.54140242E-01	7.00555615E 01
PP	7.86199776E-01	-1.03625899E 00
SRF	5.19739813E-01	-3.52987773E 00
MH-SRF	5.08947481E-01	-3.53667250E 00
LPP00R	8.15007356E-01	1.47519289E-01
LPDENS	6.25834549E-01	-1.66371451E 00
WF	7.37771675E-01	-3.53940221E 00
PUMICE	6.81435059E-01	1.52669175E 01
PP-WF	1.04525510E 00	-1.99644518E 00
BRUSH	9.81866519E-01	-6.12989348E-02

BAND 4 = 1.9117E+01 -1.1079E+00 S0-5
 Beta -2.5357E+00 S6-15 -2.0279E+00 S16-30
 -3.3757E+00 S31-45 +2.5146E-02 S46-60
 values -1.5461E+00 S61-75

+AVTABLE

ANALYSIS OF VARIANCE TABLE

SOURCE	DF	SUM OF SQUARES	MEAN SQUARE
TOTAL	181	3.89373603E 03	2.15123537E 01
REGRESSION	6	7.81857297E 02	1.30309550E 02
RESIDUAL	175	3.11187873E 03	1.77821642E 01

R SQUARED = .20079874

+TVALUES

VARIABLE	S.E. OF REGR. COEF	T
CONSTANT	4.37299805E-01	4.37159113E 01
S0-5	6.56416733E-01	-1.64780410E 00
S6-15	6.83631246E-01	-3.70909774E 00
S16-30	7.59029934E-01	-2.87165819E 00
S31-45	9.32510823E-01	-3.60269065E 00
S46-60	9.27218168E-01	2.71196193E-02
S61-75	1.16013667E 00	-1.33264503E 00

Table 12. Band 4

BAND 4 = 1.7465E+01 +4.4419E-01 NORTH
 Beta +6.3131E-01 SOUTH -1.5536E-01 EAST
 -1.5159E+01 WEST -2.5656E-01 NE
 values -3.4736E-01 NW +1.2255E+00 SE

+AVTABLE

ANALYSIS OF VARIANCE TABLE

SOURCE	DF	SUM OF SQUARES	MEAN SQUARE
TOTAL	181	3.89373603E 03	2.15123537E 01
REGRESSION	7	1.13990976E 02	1.62844252E 01
RESIDUAL	174	3.77974505E 03	2.17226727E 01

R SQUARED = .02927548

+TVALUES

VARIABLE	S.E. OF REGR. COEF	T
CONSTANT	3.67362867E-01	4.75425171E 01
NORTH	9.35682177E-01	4.74723252E-01
SOUTH	8.23421091E-01	-7.66693134E-01
EAST	9.54340199E-01	-1.62783248E-01
WEST	9.74451447E-01	-1.55599860E-00
NE	8.86924832E-01	-2.89263937E-01
NW	1.32821532E 00	-2.61520776E-01
SE	7.74881488E-01	1.58153446E 00

BAND 4 = 1.8191E+01 +6.8489E-01 FT5-13
 Beta +2.1674E-01 FT14-20 -1.1474E+00 FT21-27
 values -1.7982E+00 FT28-34

+AVTABLE

ANALYSIS OF VARIANCE TABLE

SOURCE	DF	SUM OF SQUARES	MEAN SQUARE
TOTAL	181	3.89373603E 03	2.15123537E 01
REGRESSION	4	2.02421773E 02	5.06054433E 01
RESIDUAL	177	3.69131425E 03	2.08548828E 01

R SQUARED = .05198652

+TVALUES

VARIABLE	S.E. OF REGR. COEF	T
CONSTANT	4.16936815E-01	4.36295291E 01
FT5-13	8.21728741E-01	8.33476913E-01
FT14-20	8.21728741E-01	2.63765616E-01
FT21-27	6.66771482E-01	-1.72079072E 00
FT28-34	8.33429559E-01	-2.83106876E 00

Table 12 (continued). Band 4

BAND 4 = 1.8933E+01 +5.1761E+00 C0-10
 Beta +1.2812E+00 C11-30 -1.4066E+00 C31-50
 values -2.7905E+00 C51-70
 +AVTABLE

ANALYSIS OF VARIANCE TABLE

SOURCE	DF	SUM OF SQUARES	MEAN SQUARE
TOTAL	181	3.89371603E 03	2.15123537E 01
REGRESSION	4	7.35741179E 02	1.83935295E 02
RESIDUAL	177	3.15799485E 03	1.78417788E 01

R SQUARED = .18895507

+TVALUES

VARIABLE	S.E. OF REGR. COEF	T
CONSTANT	3.79326453E-01	4.99119860E 01
C0-10	1.09964962E-00	4.71135117E 00
C11-30	8.96704965E-01	1.43842975E 00
C31-50	6.39437899E-01	-2.19981253E 00
C51-70	5.61422699E-01	-4.97048396E 00

Table 12 (continued). Band 4

Ranking of Subclass Variables per Class
Regression (Band 4)

<u>Surface Cover Type</u>		<u>Slope Angle</u>	
<u>Beta Values</u>		<u>Beta Values</u>	
-2.6113	WF*	-10.7682	>75%*
-2.0868	PP-WF*	-3.5757	31-45%*
-1.8348	SRF-MH*	-2.5357	6-15%*
-1.7996	MH-SRF*	-2.0279	16-30%*
-1.0412	LP, dense	-1.5461	61-75%
-.81471	PP	-1.1079	0- 5%
-.0602	Brush	+.0251	46-60%
+.1202	LP, poor		
+.2766	Marsh*		
+10.4050	Pumice*		
<u>Crown Size</u>		<u>Crown Density</u>	
<u>Beta Values</u>		<u>Beta Values</u>	
-2.0440	>34 ft*	-2.7905	51-70%*
-1.7982	28-34 ft*	-1.4066	31-50%*
-1.1474	21-27 ft	+1.2812	11-30%
+.2167	14-20 ft	+2.2602	71-90%*
+.6849	5-13 ft	+5.1761	0-10%*

Note: Slope aspect regression not significant at .05 level.

*Significant T-values.

Table 13

reflectance value from the mean because brush fields or manzanita and ceanothus were described as having a brush crown density of 71 to 90 percent. In the low density (0 to 10 percent) subclass, pumice fields were categorized.

Table 14 is formatted similar to Table 12, but shows band 5 values. The R squared values range from 59.76 percent for the surface cover type class to 2.60 percent for the slope aspect class which, as in band 4, is not significant at the .05 level. All other regressions in band 5 are significant at the .05 level. Table 15 is formatted similar to Table 13, but shows the ranking of band 5 beta values.

Table 16 is also formatted similar to Table 12, but shows band 6 beta values. The R squared values range from 56.70 percent for the surface cover type class to 5.95 percent for the crown size class. All class regressions are significant at the .05 level. Table 17 is formatted similar to Table 13, but shows the ranking of band 6 beta values.

Table 18 which shows the regression analyses is similar to Table 12, but for band 7. The R squared values range from 44.01 percent for the surface cover type class to 2.59 percent for the slope angle class which is not significant at the .05 level. All other regressions are significant at the .05 level. Table 19 is formatted similar to Table 13, but shows the ranking of band 7 beta values.

Regression Analysis
(Band 5)

BAND 5 = 1.3305E+01 -9.7281E-01 PP
 -2.8862E+00 SRF -2.7370E+00 MH-SRF
 Beta +5.5335E-01 LPDOR -1.4670E+00 LPDENS
 values -4.2854E+00 WF +1.5799E+01 PUMICE
 -3.4068E+00 PP-WF -3.1261E-01 BRUSH

+AVTABLE

ANALYSIS OF VARIANCE TABLE

SOURCE	DF	SUM OF SQUARES	MEAN SQUARE
TOTAL	181	8.73611438E 03	4.82658253E 01
REGRESSION	9	5.22069855E 03	5.80077616E 02
RESIDUAL	172	3.51541583E 03	2.04394641E 01

R SQUARED = .59759961

+TVALUES

VARIABLE	S.E. OF REGR. COEF	T
CONSTANT	3.83699550E-01	3.46758676E 01
PP	1.18531725E-00	-8.20714535E-01
SRF	7.75508502E-01	-3.72172052E 00
MH-SRF	7.59939997E-01	-3.60154342E 00
LPDOR	1.18531725E 00	4.65834301E-01
LPDENS	9.62202422E-01	-1.52464754E 00
WF	1.11232941E 00	-3.85297857E 00
PUMICE	1.05310751E 00	1.50022697E 01
PP-WF	1.57576959E 00	-2.15820200E 00
BRUSH	1.48822693E-00	-2.11193848E-01

BAND 5 = 1.512AE+01 -1.4761E+00 S0-5
 Beta -3.7026E+00 S6-15 -3.3498E+00 S16-30
 values -5.3639E+00 S31-45 +2.0341E-01 S46-60
 -1.8654E+00 S61-75

+AVTABLE

ANALYSIS OF VARIANCE TABLE

SOURCE	DF	SUM OF SQUARES	MEAN SQUARE
TOTAL	181	8.73611438E 03	4.82658253E 01
REGRESSION	6	1.71000756E 03	2.85001260E 02
RESIDUAL	175	7.02610682E 03	4.01491818E 01

R SQUARED = .19574006

+TVALUES

VARIABLE	S.E. OF REGR. COEF	T
CONSTANT	6.57342657E-01	2.30133264E 01
S0-5	9.91765551E-01	-1.48835610E 00
S6-15	1.01467103E 00	-3.64910273E 00
S16-30	1.15251305E 00	-2.98654891E-01
S31-45	1.49146637E 00	-3.59639493E 00
S46-60	1.39336534E 00	-1.45987416E-01
S61-75	1.74332698E 00	-1.07026431E 00

Table 14. Band 5

BAND 5 = 1.2726E+01 +7.7216E-01 NORTH
 Beta +1.2543E+00 SOUTH -8.4115E-02 EAST
 -2.3470E+00 WEST -4.3562E-01 NE
 values -2.7302E-01 NW +1.2669E+00 SE

+AVTABLE

ANALYSIS OF VARIANCE TABLE

SOURCE	DF	SUM OF SQUARES	MEAN SQUARE
TOTAL	181	8.73611438E 03	4.82658253E 01
REGRESSION	7	2.27575697E 02	3.25108138E 01
RESIDUAL	174	8.50853868E 03	4.88996476E 01

R SQUARED = .02604999

+TVALUES

VARIABLE	S.E. OF REGR. COEF	T
CONSTANT	5.53206980E-01	2.30007579E 01
NORTH	1.40469211E 00	5.49701907E-01
SOUTH	1.27119569E 00	9.86457181E-01
EAST	1.43266970E 00	-5.87121543E-02
WEST	1.46212715E 00	-1.60444102E 00
NE	1.33158399E 00	-3.27144132E-01
NW	1.99338909E 00	-1.36962668E-01
SE	1.12749772E 00	1.12361633E 00

BAND 5 = 1.3976E+01 +1.1030E+00 FT5-13
 Beta +1.9719E-01 FT14-20 -1.9469E+00 FT21-27
 -3.0225E+00 FT28-34

values

+AVTABLE

ANALYSIS OF VARIANCE TABLE

SOURCE	DF	SUM OF SQUARES	MEAN SQUARE
TOTAL	181	8.73611438E 03	4.82658253E 01
REGRESSION	4	5.95939750E 02	1.38984938E 02
RESIDUAL	177	8.18017463E 03	4.62156758E 01

R SQUARED = .06363696

+TVALUES

VARIABLE	S.E. OF REGR. COEF	T
CONSTANT	6.46090289E-01	2.16322964E 01
FT5-13	1.23927281E 00	8.90023717E-01
FT14-20	1.25579681E 00	1.57023673E-01
FT21-27	1.00462979E 00	-1.93794877E 00
FT28-34	1.02212210E 00	-2.95704609E 00

Table 14 (Continued). Band 5

Band 5 = 1.5066E+01 +8.3187E+00 C0-10
 Beta +2.0138E+00 C11-30 -2.0949E+00 C31-50
 values -4.3733E+00 C51-70

+AVTABLE

ANALYSIS OF VARIANCE TABLE

SOURCE	DF	SUM OF SQUARES	MEAN SQUARE
TOTAL	191	8.73611438E 03	4.82658253E 01
REGRESSION	4	1.77478024E 03	4.43695059E 02
RESIDUAL	177	6.96133414E 03	3.93295714E 01

R SQUARED = .20315442

+TVALUES

VARIABLE	S.F. OF REGR. COEF	T
CONSTANT	5.75773870E-01	2.62885781E 01
C0-10	1.70380141E 00	4.86817517E 00
C11-30	1.32864385E 00	1.51564696E 00
C31-50	6.56770331E-01	-2.18958477E 00
C51-70	8.38650395E-01	-5.21464899E 00

Table 14 (continued). Band 5

Ranking of Subclass Variables per Class
Regression (Band 5)

<u>Surface Cover Type</u>		<u>Slope Angle</u>	
<u>Beta Values</u>		<u>Beta Values</u>	
-4.2858	WF*	-15.5548	>75%*
-3.4008	PP-WF*	-5.3639	31-45%
-2.8862	SRF-MH*	-3.7026	6-15%
-2.7370	MH-SRF*	-3.3498	16-30%*
-1.4670	LP, dense	-1.8658	61-75%
-.9728	PP	-1.4761	0- 5%
-.3126	Brush	+.2034	46-60%
+.2901	Marsh		
+.5534	LP, poor		
+15.7990	Pumice*		
<u>Crown Size</u>		<u>Crown Density</u>	
<u>Beta Values</u>		<u>Beta Values</u>	
-3.6692	>34 ft*	-4.3733	51-70%
-3.0225	28-34 ft*	-2.0949	31-50%*
-1.9469	21-27 ft	+2.0138	11-30%
+.1972	14-20 ft	+3.8643	71-90%
+1.1030	5-13 ft	+8.3187	0-10%

Note: Slope aspect regression not significant at the .05 level.

*Significant T-values.

Table 15

Regression Analysis
(Band 6)

BAND 6	=	2.3383E+01		+7.8658E-01	PP
Beta		-3.8234E+00	SRF	-5.0867E+00	MH-SRF
		-1.1016E-01	LPP00R	-4.4219E+00	LPDFNS
values		-3.0013E+00	WF	+1.1935E+01	PUNICE
		-1.0373E+00	PP-WF	+5.5632E+00	BRUSH

+AVTABLE

ANALYSIS OF VARIANCE TABLE

SOURCE	DF	SUM OF SQUARES	MEAN SQUARE
TOTAL	181	7.86830819E 03	4.34713160E 01
REGRESSION	9	4.46160493E 03	4.95733881E 02
RESIDUAL	172	3.40670326E 03	1.98064143E 01

R SQUARED = .56703485

+TVALUES

VARIABLE	S.E. OF REGR. COEF	T
CONSTANT	3.77639598E-01	6.19200097E 01
PP	8.14963684E-01	8.67012869E-01
SRF	7.61987429E-01	-5.01765704E 00
MH-SRF	7.54849196E-01	-6.73872483E 00
LPP00R	1.16194374E 00	-9.48109355E-02
LPDFNS	9.44494177E-01	-4.68176391E 00
WF	1.09044413E 00	-2.75132399E 00
PUNICE	1.03316029E 00	1.15518807E 01
PP-WF	1.53964461E 00	-1.19333032E 00
BRUSH	1.44754227E 00	3.84318537E 00

BAND 6	=	2.3611E+01		-8.1647E-01	S0-5
Beta		-2.6438E+00	S6-15	-1.4055E+00	S16-30
		-4.2102E+00	S31-45	-4.7358E-01	S46-60
values		-1.8615E+00	S61-75		

+AVTABLE

ANALYSIS OF VARIANCE TABLE

SOURCE	DF	SUM OF SQUARES	MEAN SQUARE
TOTAL	181	7.86830819E 03	4.34713160E 01
REGRESSION	6	8.71051306E 02	1.45175218E 02
RESIDUAL	175	6.99725689E 03	3.99843251E 01

R SQUARED = .11070376

+TVALUES

VARIABLE	S.E. OF REGR. COEF	T
CONSTANT	6.55991610E-01	3.59933550E 01
S0-5	9.39727350E-01	-8.24944447E-01
S6-15	1.01258871E 00	-2.61090168E 00
S16-30	1.15014445E 00	-1.22204975E 00
S31-45	1.48840166E 00	-2.82868542E 00
S46-60	1.39050175E 00	-3.40578749E-01
S61-75	1.73974416E 00	-9.55003283E-01

Table 16. Band 6

~~BAND 6 = 2.4231E+01~~ ~~+8.4352E+00 C0-10~~
~~Beta +6.9463E-01 C11-30~~ ~~-2.7355E+00 C31-50~~
~~values -4.0862E+00 C51-70~~
~~+AVTABLE~~

ANALYSIS OF VARIANCE TABLE

SOURCE	DF	SUM OF SQUARES	MEAN SQUARE
TOTAL	181	7.96830819E 03	4.34713160E 01
REGRESSION	4	1.48351945E 03	3.70879863E 02
RESIDUAL	177	6.39478874E 03	3.60722528E 01

R SQUARED = .18854364

+TVALUES

VARIABLE	S.E. OF REGR. COEF	T
CONSTANT	5.51415510E-01	4.39431992E 01
C0-10	1.63650983E 00	5.15436134E 00
C11-30	1.27243500E 00	5.38050299E-01
C31-50	6.16293752E-01	-2.98538895E 00
C51-70	8.03170931E-01	-5.08755956E 00

Table 16 (continued). Band 6

Ranking of Subclass Variables per Class
Regression (Band 6)

<u>Surface Cover Type</u>		<u>Slope Angle</u>	
<u>Beta Values</u>		<u>Beta Values</u>	
-5.0867	MH-SRF*	-11.2111	>75%*
-4.4219	LP, dense*	-4.2102	31-45%*
-3.8234	SRF-MH*	-2.6438	6-15%*
-3.0013	WF*	-1.6615	61-75%
-1.8373	PP-WF	-1.4055	16-30%
-.1102	LP, poor	-.8165	0- 5%
-.0760	Marsh	-.47358	46-60%
+.7066	PP		
+5.5532	Brush*		
+11.9350	Pumice*		
<u>Crown Size</u>		<u>Crown Density</u>	
<u>Beta Values</u>		<u>Beta Values</u>	
-2.2824	>34 ft*	-4.0862	51-70%*
-2.2579	28-34 ft*	-2.7355	31-50%*
-1.7589	21-27 ft	+.6846	11-30%
-.4603	14-20 ft	+2.2981	71-90%*
+2.1947	5-13 ft	+8.4352	0-10%*
<u>Slope Aspect</u>			
<u>Beta Values</u>			
-2.8103	West*		
-2.5088	N*		
-2.2523	NW		
-.9770	SW		
-.2757	NE		
+1.1512	E		
+2.1629	S		
+3.5560	SE*		

*Significant T-values.

Table 17

Regression Analysis
(Band 7)

BAND 7 = 2.5285E+01 +5.6563E-01 PP
 Beta -4.4399E+00 SRF -6.2717E+00 MH-SRF
 values -1.6591E-01 LPPCOR -5.3575E+00 LPDENS
 -2.0777E+00 WF +5.5454E+00 PUMTCE
 -1.4085E-01 PP-WF +9.1749E+00 BRUSH

+AVTABLE

ANALYSIS OF VARIANCE TABLE

SOURCE	DF	SUM OF SQUARES	MEAN SQUARE
TOTAL	181	8.24935413E 03	4.55765422E 01
REGRESSION	9	3.63070257E 03	4.03411396E 02
RESIDUAL	172	4.61865156E 03	2.68526254E 01

R SQUARED = .4411962

+TVALUES

VARIABLE	S.E. OF REGR. COEF	T
CONSTANT	4.39805381E-01	5.74916528E 01
PP	1.35463870E 00	4.16321992E-01
SRF	8.89985946E-01	-6.99474716E 00
MH-SRF	8.71060963E-01	-7.20008982E 00
LPPCOR	1.35863030E 00	-1.22113044E-01
LPDENS	1.10239888E-00	-4.85767036E-00
WF	1.27497796E 00	-1.62967987E 00
PUMTCE	1.20709641E 00	4.59404089E 00
PP-WF	1.80618389E 00	-7.79934904E-02
BRUSH	1.69667066E 00	5.40756790E 00

BAND 7 = 2.3796E+01 +5.1221E-01 S0-5
 Beta -1.1500E+01 S6-15 -1.5312E-01 S16-30
 values -2.1644E+01 S31-45 +7.0323E-01 S46-60
 -1.2717E+01 S61-75

+AVTABLE

ANALYSIS OF VARIANCE TABLE

SOURCE	DF	SUM OF SQUARES	MEAN SQUARE
TOTAL	181	8.24935413E 03	4.55765422E 01
REGRESSION	6	2.13291630E 02	3.55469383E 01
RESIDUAL	175	8.03607250E 03	4.59204143E 01

R SQUARED = .02585434

+TVALUES

VARIABLE	S.E. OF REGR. COEF	T
CONSTANT	7.03001577E-01	3.38434934E 01
S0-5	1.06085364E 00	4.82923247E-01
S6-15	1.08515009E 00	-1.05975869E 00
S16-30	1.23256662E 00	-1.24230396E-01
S31-45	1.54506417E 00	-1.35691880E 00
S46-60	1.49014851E 00	4.71917023E-01
S61-75	1.86441849E 00	-6.82090310E-01

Table 18. Band 7

BAND 7 = 2.2809E+01 -4.2904E+00 NORTH
 Beta +2.7052E+00 SOUTH +1.7728E+00 EAST
 values -3.0106E+00 WEST +8.9694E-01 NE
 -3.5471E+00 NW +4.0599E+00 SE

+AVTABLE

ANALYSIS OF VARIANCE TABLE

SOURCE	DF	SUM OF SQUARES	MEAN SQUARE
TOTAL	181	8.24935413E 03	4.55765422E 01
REGRESSION	7	1.57946238E 03	2.25637483E 02
RESIDUAL	174	6.66989175E 03	3.83327112E 01

R SQUARED = .19146497

+TVALUES

VARIABLE	S.E. OF REGR. COEF	T
CONSTANT	4.89871704E-01	4.65612973E 01
NORTH	1.24369259E 00	-3.44974773E 00
SOUTH	1.12549599E 00	2.40358156E 00
EAST	1.26846391E 00	-1.39763084E 00
WEST	1.29518445E 00	-2.32446316E 00
NE	1.17396379E 00	-7.60784982E-01
NW	1.76491576E 00	-2.00976281E 00
SE	9.95268880E-01	4.06692525E 00

BAND 4-5 = 2.3836E+01 +3.4941E+00 FT5-13
 Beta -8.5632E-01 FT14-20 -1.6915E+00 FT21-27
 values -9.3695E-01 FT28-34

+AVTABLE

ANALYSIS OF VARIANCE TABLE

SOURCE	DF	SUM OF SQUARES	MEAN SQUARE
TOTAL	181	8.24935413E 03	4.55765422E 01
REGRESSION	4	5.19475637E 02	1.29868909E 02
RESIDUAL	177	7.72987849E 03	4.35716299E 01

R SQUARED = .06297167

+TVALUES

VARIABLE	S.E. OF REGR. COEF	T
CONSTANT	6.28055802E-01	3.79519301E 01
FT5-13	1.20468073E 00	2.99040744E 00
FT14-20	1.22074350E 00	-7.01473980E-01
FT21-27	9.76587363E-01	-1.73206237E 00
FT28-34	9.93591405E-01	-9.42997109E-01

Table 18 (continued). Band 7

BAND 7 = 2.5106E+01
 Beta -L.0389E-01 C11-70 +6.6383E+00 C0-10
 values -3.2598E+00 C51-70 -2.6655E+00 C31-50
 +AVTABLE

ANALYSIS OF VARIANCE TABLE

SOURCE	DF	SUM OF SQUARES	MEAN SQUARE
TOTAL	181	8.24935413E 03	4.55765422E 01
REGRESSION	4	9.63120035E 02	2.40780009E 02
RESIDUAL	177	7.28623409E 03	4.11651644E 01

R SQUARED = .11675096

+TVALUES

VARIABLE	S.E. OF REGR. COEFF	T
CONSTANT	5.39056933E-01	4.26201710E 01
C0-10	1.74822333E 00	3.79747525E 00
C11-70	1.35929557E 00	-2.97132441E -01
C31-50	9.78842955E-01	-2.7434953E 00
C51-70	8.57994001E-01	-3.79932345E 00

Table 18 (continued). Band 7

Ranking of Subclass Variables per Class
Regression (Band 7)

<u>Surface Cover Type</u>		<u>Slope Aspect</u>	
<u>Beta Values</u>		<u>Beta Values</u>	
-6.2717	MH-SRF*	-4.2904	North*
-5.3575	LP, dense*	-3.5471	NW*
-4.4399	SRF-MH*	-3.0106	W*
-3.1677	Marsh*	+ .8969	NE
-2.0778	WF	+1.4133	SW
-.16591	LP, poor	+1.7728	E
-.14085	PP-WF	+2.7052	S*
+ .56563	PP	+4.0599	SE*
+5.5454	Pumice*		
+9.1749	Brush*		
 <u>Crown Size</u>		 <u>Crown Density</u>	
<u>Beta Values</u>		<u>Beta Values</u>	
-1.6915	21-27 ft	-3.2598	51-70%*
-.9370	28-34 ft	-2.6855	31-50%*
-.8563	14-20 ft	-.4039	11-30%
+ .0093	>34 ft	+ .2896	71-90%
+3.4941	5-13 ft*	+6.6388	0-10%*

Note: Slope angle is not significant at the .05 level.
*Significant T-values.

Table 19

Table 20 presents a correlation of the 35 subclass variables against each other at the .05 significance level. The "+" and "-" sign indicate a positive or negative correlation between two variables in that particular band, respectively, and the "blank" indicates no correlation of the two variables at the .05 significance level. From Table 20, it is possible to determine which slope angles, slope aspects, crown sizes, and crown densities per band are characteristic of various surface cover types within the 182 sample sites investigated within the Park, and also which environmental factors are related and in which direction.

Data from Tables 12 through 20 reveal which surface cover types, slope angles, slope aspects, crown sizes, and crown densities found within Crater Lake National Park are responsible for altering the reflectance values recorded by LANDSAT from the mean reflectance value per band. These types of data are useful in helping to guide field work for remote sensing studies into areas that possess environmental factors which are capable of altering the spectral reflectance of surface cover types recorded by LANDSAT. Supervised classifications, for example, which select training areas on which to classify the entire study area could make use of these types of data in selecting appropriate training areas. For example, a mountain hemlock stand on 0 to 5 percent slope may appear quite

Correlation of Surface Cover Types and Parameters

	LANDSAT Bands					LANDSAT Bands			
	4	5	6	7		4	5	6	7
PP, Marsh	+				LP poor, C. D., 11-30%	+	+	+	+
PP, Slope 6-15%	+	+		+	LP poor, C. D. 51-70%	-	-	-	-
PP, Southeast	+				LP dense, Slope 0-5%	+	+	+	+
SRF-MH, MH-SRF	-	-	-	-	LP dense, C. S. 14-20'	+	+	+	+
SRF-MH, LP dense	-	-	-	-	LP dense, C. S. 21-27'	-	-	-	-
SRF-MH, WF	-	-		-	LP dense, C. S. 28-34'	-	-	-	-
SRF-MH, Pumice	-	-	-	-	LP dense, C. D. 31-50%	+	+	+	+
SRF-MH, Marsh	-				LP dense, C. D. 71-90%	-	-	-	-
SRF-MH, Slope 61-75%	+	+	+	+	WF, C. D. 71-90%	+	-	+	+
SRF-MH, East	+	+	+	+	Pumice, Slope >75%	+	+	+	+
SRF-MH, Northeast	-	-	-	-	Pumice, C. S. 21-27'	-	-	-	-
SRF-MH, C. S. 5-13'	-	-	-	-	Pumice, C. S. 28-34'	-	-	-	-
SRF-MH, C. S. 28-34'	+	+	+	+	Pumice, C. D. 0-10%	+	+	+	+
SRF-MH, C. S. >34'	+				Pumice, C. D. 31-50%	-	-	-	-
MH-SRF, LP dense	-	-	-	-	Pumice, C. D. 51-70%	-	-	-	-
MH-SRF, WF	-	-	-	-	Pumice, C. D. 71-90%	-			
MH-SRF, Pumice	-	-	-	-	PP-WF, Southeast	+	+	+	+
MH-SRF, Marsh	-	-	-	-	Brush, C. S. 5-13'	+	+	+	+
MH-SRF, Slope 0-5%	-	-	-	-	Brush, C. D. 0-10%	+	+	+	+
MH-SRF, Slope 16-30%	+	+	+	+	Brush, C. D. 71-90%	-	-	+	+
MH-SRF, Slope 31-45%	+	+	+	+	Marsh, C. S. 5-13'	+	+	+	+
MH-SRF, North	+	+	+	+	Marsh, C. S. 21-27'	-	-	-	-
MH-SRF, Southeast	-	-	-	-	Marsh, C. D. 0-10%	+	+	+	+
MH-SRF, C. S. 5-13'	-	-	-	-	Slope 0-5%, Slope 6-15%	-	-	-	-
MH-SRF, C. S. 21-27'	+	+	+	+	Slope 0-5%, Slope 16-30%	-	-	-	-
MH-SRF, C. D. 11-30%	-	-	-	-	Slope 0-5%, Slope 31-45%	-	-	-	-
MH-SRF, C. D. 51-70%	+	+	+	+	Slope 0-5%, Slope 46-60%	-	-	-	-
LP, poor, Slope	+	+	+	+	Slope 0-5%, Slope 61-75%	-	-	-	-
LP poor, C. S. 5-13'	+	+	+	+					
LP poor, C. S. 14-20'	+	+	+	+					
LP poor, C. S. 28-34'	-	-	-	-					

Table 20 (continued)

	LANDSAT Bands					LANDSAT Bands			
	4	5	6	7		4	5	6	7
Slope 0-5%, East	-	-	-	-	East, C. D. 31-50%	+	-	+	+
Slope 0-5%, C. S. 14-20'	+	+	+	+	West, Southeast	-	-	-	-
Slope 0-5%, C. S. 21-27'	-	-	-	-	Northeast, Southeast	-	-	-	-
Slope 6-15%, Slope 16-30%	-	-	-	-	Northwest, C.D. 0-10%	+	+	+	+
Slope 6-15%, Slope 31-45%	-	-	-	-	Southeast, Southwest	-	-	-	-
Slope 6-15%, Slope 46-60%	-	-	-	-	C. S. 5-13', C. S. 14-20'	-	-	-	-
Slope 6-15%, Slope 61-75%	-	-	-	-	C. S. 5-13', C. S. 21-27'	-	-	-	-
Slope 6-15%, West	-	-	-	-	C. S. 5-13', C. S. 28-34'	-	-	-	-
Slope 16-30%, Slope 31-45%	-	-	-	-	C. S. 5-13', C. D. 11-30%	+	+	+	+
Slope 16-30%, Slope 46-60%	-	-	-	-	C. S. 5-13', C. D. 51-70%	-	-	-	-
Slope 16-30%, C. D. 71-90%	+	+	+	+	C. S. 14-20', C. S. 21-27'	-	-	-	-
Slope 31-45%, C. D. 51-70%	+	+	+	+	C. S. 14-20', C. S. 28-34'	-	-	-	-
Slope 61-75%, C. D. 31-50%	+	+	+	+	C. S. 14-20', C. D. 11-30%	+	+	+	+
Slope >75%, C. S. >34'	+	+	+	+	C. S. 14-20', C. D. 31-50%	+	+	+	+
North, South	-	-	-	-	C. S. 14-20', C. D. 71-90%	-	-	-	-
North, Northeast	-	-	-	-	C. S. 21-27', C. S. 28-34'	-	-	-	-
North, Southeast	-	-	-	-	C. S. 21-27', C. D. 0-10%	-	-	-	-
South, East	-	-	-	-	C. S. 21-27', C. D. 71-90%	+	+	+	+
South, West	-	-	-	-	C. S. 28-34', C. D. 11-30%	-	-	-	-
South, Northeast	-	-	-	-	C. S. 28-34', C. D. 51-70%	+	+	+	+
South, Southeast	-	-	-	-	C.S. >34', C. D. 71-90%	+	-	-	-
South, Southwest	-	-	-	-					
East, Northeast	-	-	-	-					
East, Southeast	-	-	-	-					

Table 20 (continued)

	LANDSAT Bands					LANDSAT Bands			
	4	5	6	7		4	5	6	7
C. D. 0-10%, C. D. 51-70%	-	-	-	-	C. D. 51-70%	-	-	-	-
C. D. 11-30%, C. D. 31-50%	-	-	-	-	C. D. 71-90%	-	-		
C. D. 11-30%, C. D. 51-70%	-	-	-	-	PP, Northeast		+		+
C. D. 31-50%, C. D. 51-70%	-	-	-	-	PP, C. S. 28-34'		+		+
C. D. 31-50%, C. D. 71-90%	-	-	-	-	PP, C. D. 31-50%		+		+
C. D. 51-70%, C. D. 71-90%	-	-	-	-	Slope 6-15%, C. D. 0-10%		+	+	+
SRF-MH	-	-	-	-	Slope 16-30%, C. S. >34'		+		
MH-SRF	-	-	-	-	LP dense			-	-
WF	-	-	-	-	North			-	-
Pumice	+	+	+	+	West			-	-
Slope >75%	-	-	-	-	Southeast			+	+
C. S. 21-27'	-	-	-	-	PP, C. S. >34'			+	
C. S. 28-34'	+	-	-	-	Slope 31-45%, C. S. >34'			+	+
C. D. 0-10%	+	+	+	+	Marsh				+
					Northwest				+
					Brush				+

Key

PP - Ponderosa pine

SRF - Shasta red fir

MH - Mountain hemlock

LP - Lodgepole pine

WF - White fir

C. S. - Crown size (feet)

C. D. - Crown density (%)

Slope 0-5% - Slope angle (%)

North - Slope aspect

PP, Marsh - Ponderosa pine correlated with Marsh

+ - Positive correlation

- - Negative correlation

(Blank) - Significant correlation at .05 does not exist

Table 20

different spectrally from a mountain hemlock stand on a 31 to 45 percent slope. Training areas which only train on the 0 to 5 percent slope mountain hemlock stand and not on the 31 to 45 percent slope stand runs the risk of misclassifying the steeper sloped mountain hemlock stand. In steeply sloped areas or in other areas where environmental factors exert a large influence on the reflectance value, more ground work should be focused to determine if a training area for mountain hemlock, steeply sloped, would be helpful in order to alleviate the chance for misclassification. Areas within a study area could also be delineated as areas of potential misclassification, due to the influence of certain environmental factors (slope angle, slope aspect, etc.), and those areas could be classified with new training areas which represent a particular surface cover type under reflectance value altering conditions.

LANDSAT Classification and Pixel Problems

The application of LANDSAT digital data to surface cover type identification and mapping has limitations and problems inherent to the LANDSAT system, which should be appreciated by LANDSAT investigators and LANDSAT data users. Through this appreciation, in addition to knowledge as to the functioning of LANDSAT, data investigators and users can effectively apply LANDSAT data to appropriate earth

resources problems and expect results at an appropriate level of detail.

The general functioning of LANDSAT has been described in Chapter IV. Some limitations and problems of LANDSAT data will be described in the following discussion.

Spectral Reflectance Properties

The main problem involved in detecting spectral reflectance of surface cover types by LANDSAT is ascertaining the effect of environmental factors on the spectral reflectance, as described in the previous section. In general, the intensity and degree of polarization of the spectral reflectance of surface cover types is strongly dependent on the angle of incidence of incoming solar radiation; azimuth and elevation angles at which the surface cover types are viewed; wavelength of the radiation; and the physical state of the surface cover type itself (Coulson, Bouricius, and Gray, 1965).

Pixel Integration

Surface cover types as detected by LANDSAT are generally small in size in comparison to the ground resolution of the pixel area (1.118 acres, .452 ha). Because of this size differential, it is common to have numerous surface cover types being sensed within the pixel unit area. The spectral reflectance of a mixture of surface cover types

within the pixel is not representative of the individual component surface cover types which composed the pixel mixture (Smedes, Hulstrom, and Ranson, 1975) (Figure 27). It is thus important to select training areas which represent these surface cover type mixtures and not just train on homogeneous areas. If one neglects to sample the mixture pixels, misclassified or unclassified pixels may result causing an underestimation of area covered per surface cover type (Horwitz, et al., 1971).

Pixel mixtures may be observed in boundary pixels occurring between adjacent surface cover types, and also in pixel clusters which are composed of many different surface cover types. In areas of boundary pixels, the likelihood of misclassifications or nonclassification increases only along the interface between the two surface cover types. In areas of mixtures within pixel clusters, misclassification or unclassification can result throughout the entire surface cover type cluster if the mixture pixels were not trained on for generation of classification statistics (Heller, et al., 1974).

In addition to being concerned with obtaining training statistics for areas of surface cover type mixtures, one must also be concerned with obtaining statistics for surface cover type mixtures which have density differences or some other difference which alters the spectral reflectance of similar surface cover types.

Spectral Reflectance of Two Pixel Component Surface Cover Types

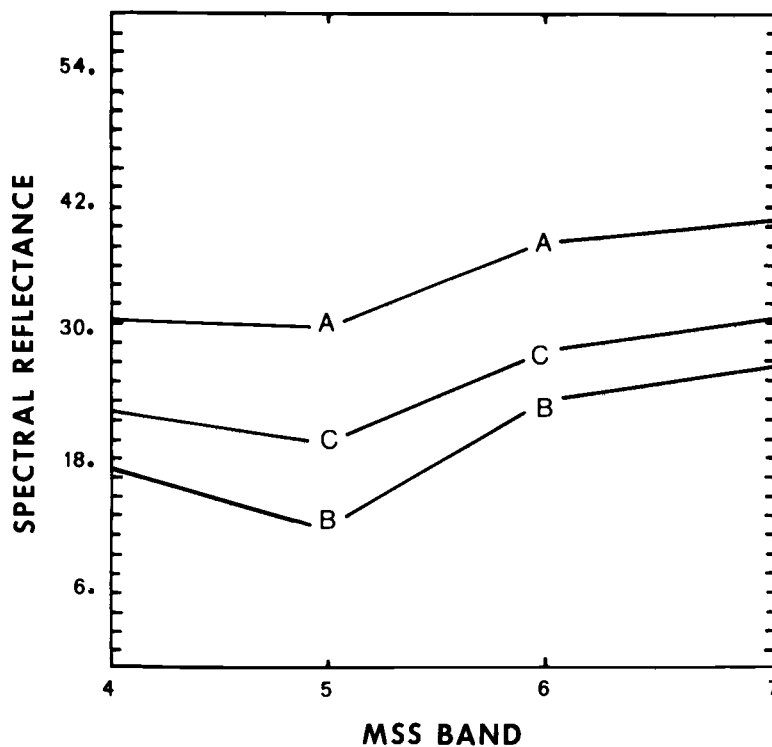


Figure 27. "C" is the mixture of surface cover types "A" and "B." By obtaining the reflectance of "A" and/or "B," "C" is not necessarily obtained. Adapted from Smedes, Hielstrom, and Ranson, 1975.

To obtain "good" training statistics, one must further evaluate how well the training statistics actually represent the spectral reflectance throughout the study area for a "good" classification (Kalensky, 1974).

LANDSAT Scanner Readjustment

As the LANDSAT multispectral scanner senses reflected solar radiation from surface cover types, there exists a time lag between the time the satellite resolution unit moves into a different surface cover type and the time the reflectance value of the different surface cover type is recorded. There is a transition period between the scanned and scanning surface cover type known as the boundary pixel. The boundary pixels are areas which are scanned during the readjustment period from the scanning of one surface cover type to another. Figure 28 shows the scanning process of LANDSAT and the readjustment between differing surface cover types (boundary pixels).

Through the classification of surface cover types within Crater Lake National Park, the extent of boundary pixels on the classification seems to be a function of reflectance value differences between the adjacent surface cover types. If, for example, the LANDSAT scanners were sensing a low reflecting water body and then sensing a high reflecting pumice soil, the extent of the boundary or readjustment pixels would be greater than if two similar

Functioning of the MSS in Sensing Different Surface Cover Types

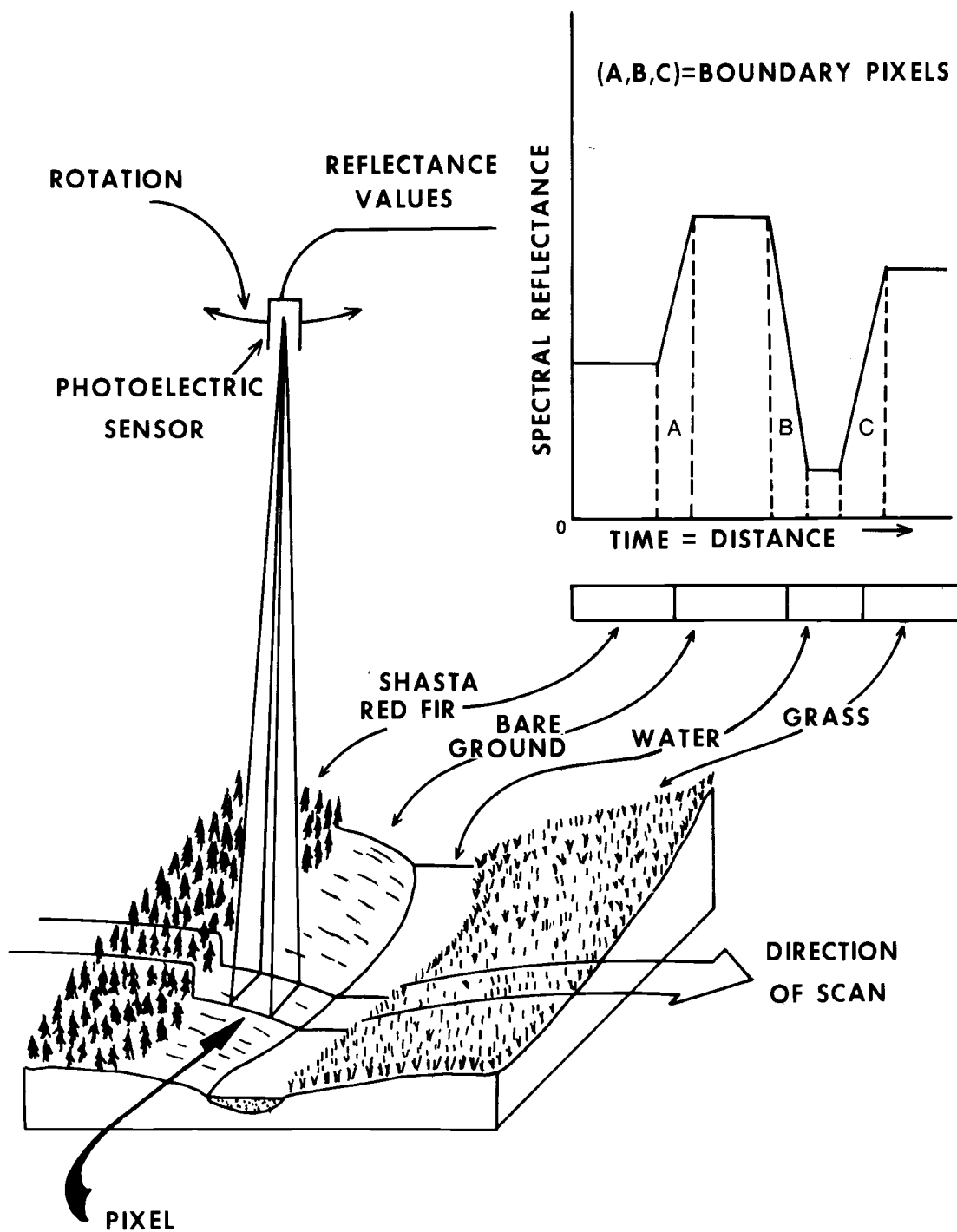


Figure 28. Adapted from Grabau, 1976.

coniferous tree species with similar reflectances were successively scanned. Between two largely differing surface cover types, there exist boundary pixels which show gradations of pixel readjustment from low to high reflectance value pixels. The extent of the readjustment pixel gradations is a function of the difference between the successively scanned surface cover types. Figure 29 shows the boundary pixel effect with only one pixel readjustment from one surface cover type to another.

Extremes in surface cover type reflectance values tend to increase or decrease adjacent pixel values along the scan line primarily due to the overlap between pixels, described in Chapter IV (Evans, 1974). This increased or decreased pixel value of the adjacent pixel tends to give a false representation of what surface cover type is actually being detected within that pixel. Classification problems can arise depending upon the degree of pixel value increase or decrease.

Loss of Boundary and Size Definition

A problem of LANDSAT digital data interpretation is the change in the nature, position, size, and shape of surface cover types as mapped by LANDSAT. Figure 30 shows the loss of boundary resolution caused by the increase or decrease in the reflectance value because of sensor readjustment between different surface cover types. In the upper

Changes in Reflectance Values for Differing and Adjacent Surface Cover Types

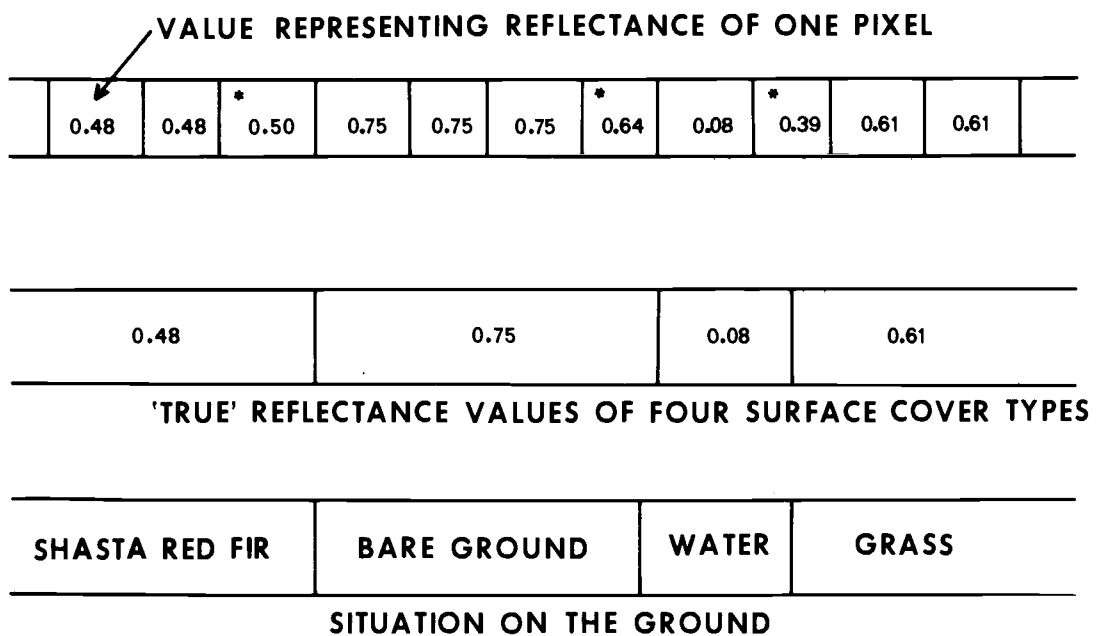
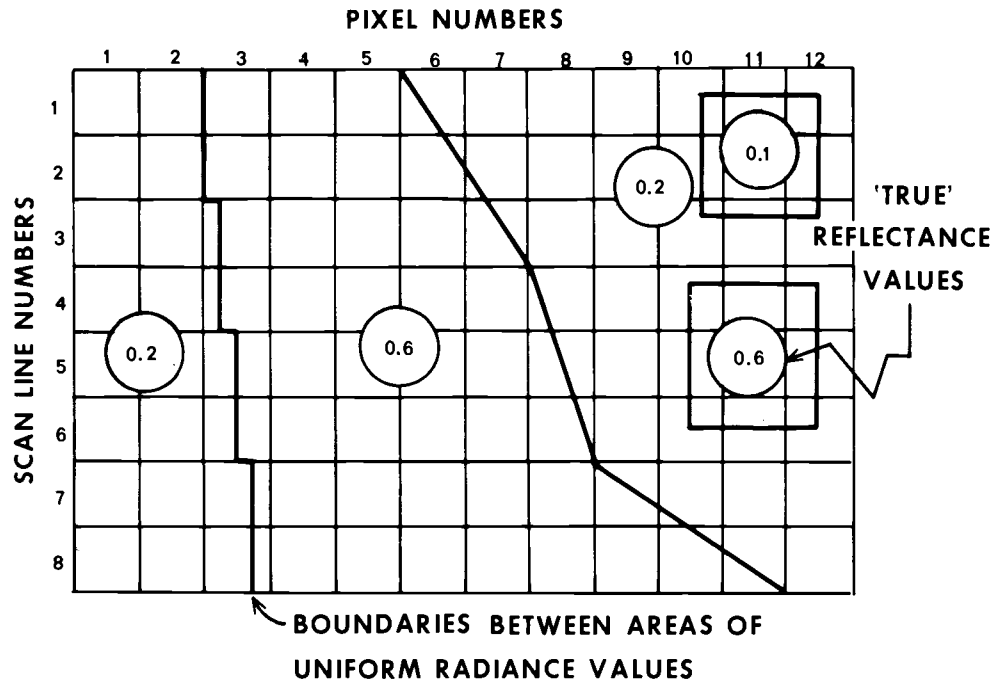


Figure 29. The boundary pixels do not show the same reflectance as do the four surface cover types. Adapted from Grabau, 1976 (* = boundary pixel).

Loss of Pixel Boundary and Size Definition



	PIXELS											
	1	2	3	4	5	6	7	8	9	10	11	12
1	0.2	0.2	0.6	0.6	0.6	0.39	0.2	0.2	0.2	0.19	0.18	0.18
2	0.2	0.2	0.6	0.6	0.6	0.57	0.23	0.2	0.2	0.18	0.10	0.18
3	0.2	0.2	0.5	0.6	0.6	0.6	0.47	0.2	0.2	0.19	0.18	0.18
4	0.2	0.2	0.5	0.6	0.6	0.6	0.6	0.27	0.2	0.30	0.40	0.30
5	0.2	0.2	0.4	0.6	0.6	0.6	0.6	0.4	0.2	0.4	0.6	0.4
6	0.2	0.2	0.4	0.6	0.6	0.6	0.6	0.53	0.2	0.35	0.45	0.35
7	0.2	0.2	0.35	0.6	0.6	0.6	0.6	0.6	0.47	0.23	0.2	0.2
8	0.2	0.2	0.3	0.6	0.6	0.6	0.6	0.6	0.6	0.57	0.53	0.2

Figure 30. Values in pixels indicate reflectance values. Adapted from Grabau, 1976.

portion of Figure 30, the 0.1, 0.2, and 0.6 pixel values indicate three different surface cover types, with the lines indicating boundaries. In the lower portion of Figure 30, the shaded pixels indicate the positions of boundary reflectance values. One can observe that the boundary (mixture) pixels have reflectance values different from the three surface cover types (0.1, 0.2, and 0.6). The boundary change between surface cover types is quite prominent. Figure 30 also shows the loss of size definition caused by boundary pixels. The lower portion of Figure 30 also shows the loss of surface cover type size due to pixel overlap boundaries denoted by the shaded pixels, and reflectance value differences.

In order for the classification of surface cover types to be accurate and inclusive of boundary and mixture pixels, pixels representative of this kind of data should be a part of the training statistics. If they are not part of the training statistics, the classification statistics may be required to be "loose" in order to classify, with existing training statistics (no post processing available), the boundary pixels. This may lead to misclassification of surface cover types due to surface cover type spectral similarity. If the statistics are kept "tight" in order to classify the major portions of surface cover types, generally exclusive of boundary pixels, changes in the shape and area of the surface cover type can result.

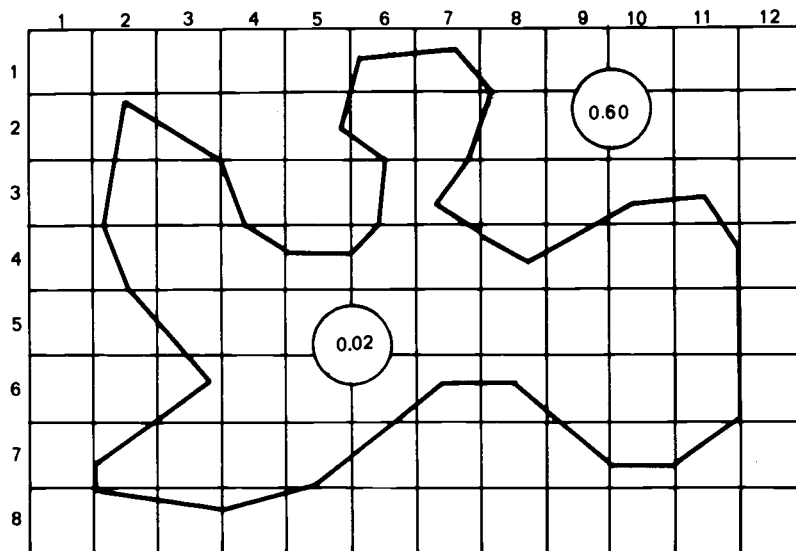
Figure 31 shows a loss of surface cover type shape and size due to boundary and mixture pixels. In the top portion of Figure 31, the map boundaries of a surface cover type with a reflectance value of 0.02 are drawn. The surface cover type is surrounded by another surface cover type with a reflectance value of 0.60. The lower portion of Figure 31 shows the loss of surface cover type size and shape when classified by using relatively "tight" statistics.

Pixel to Ground Registration

In utilizing interpreted LANDSAT data for surface cover type analysis by land managers, the fact that along a LANDSAT scan line of 115 miles (185 km), there exists a maximum error in the registration of pixels versus ground area coverage of approximately five pixels should be appreciated (Thomas, 1975 and discussed in Chapter IV). The amount of the registration error depends upon the location of the study area within the scene. This error would make the locating of very small pixel clusters on the ground very difficult with the difficulty being further compounded by the LANDSAT data problems described earlier in this section.

When LANDSAT pixel clusters are compared to map coordinates, the difference between a pixel grid and a Cartesian map coordinate system should be realized. A pixel grid defines the position of pixels in terms of an area of 1.118

Shape and Size Changes of Surface Cover Types



'TRUE' AREA = 38.5 UNITS (1 PIXEL = 1 UNIT OF AREA)

a. MAP OF SURFACE COVER TYPE

	1	2	3	4	5	6	7	8	9	10	11	12
1	0.60	0.60	0.60	0.60	0.60	0.26	0.26	0.59	0.60	0.60	0.60	0.60
2	0.60	0.34	0.43	0.60	0.57	0.26	0.26	0.57	0.60	0.60	0.60	0.60
3	0.60	0.18	0.22	0.50	0.60	0.31	0.30	0.60	0.59	0.43	0.47	0.60
4	0.60	0.24	0.22	0.29	0.25	0.27	0.24	0.27	0.11	0.22	0.13	0.60
5	0.60	0.53	0.29	0.22	0.22	0.22	0.22	0.22	0.22	0.22	0.22	0.60
6	0.60	0.60	0.29	0.22	0.22	0.22	0.33	0.31	0.22	0.22	0.22	0.60
7	0.60	0.21	0.22	0.22	0.50	0.60	0.60	0.60	0.46	0.22	0.43	0.60
8	0.60	0.56	0.47	0.48	0.59	0.60	0.60	0.60	0.60	0.60	0.60	0.60


 = CLASSIFIED SURFACE COVER TYPE = 28 UNITS (RADIANCE ≤ 0.15) b. PIXEL CHARACTERIZATION OF SURFACE COVER TYPE USING REFLECTANCE VALUE CUTOFF VALUE OF 0.15 ('TIGHT STATISTICS')

Figure 31. Adapted from Grabau, 1976.

acres (0.452 ha), and with respect to its neighboring pixel areas. The Cartesian coordinate system defines the position of a point, and not an area. One can designate the corner of a pixel or the center of a pixel, but not the entire area within a pixel with Cartesian coordinates (Grabau, 1976).

Atmospheric Attenuation of LANDSAT and Aerial Photography Data

Both NASA U-2 high flight color infrared aerial photography and LANDSAT sensors detect reflected solar radiation in the visible and near infrared wavelengths of the electromagnetic spectrum. Solar radiation incident upon and reflected from the earth and detected by the LANDSAT and U-2 sensors encounters atmospheric attenuation of the solar beam to and from ground objects. As solar radiation penetrates the earth's atmosphere, the solar beam is subjected to denser atmospheric layers which cause the beam to be scattered, absorbed, and refracted in all directions due to the increased presence of solid, liquid, and gas molecules. Besides affecting the direction of incident and reflected solar radiation, the atmosphere affects the speed and frequency of radiation, the intensity of radiation, and also the radiation's spectral distribution (Nunnally, 1973).

In the visible and near infrared wavelengths which LANDSAT and the U-2 aircraft systems detect, scattering is the chief cause of the reduction of solar radiation through

atmospheric effects (Fraser, 1975). Through scattering, wavelengths of radiation are deflected into directions of random travel by contact with atmospheric particles. This scattering is called Mie scattering and the responsible atmospheric particles include water vapor, dust, and smoke particles. Another type of scattering, Rayleigh scattering, is largely due to molecules and other very small particles. Essentially, all molecular scattering is accounted for by nitrogen and oxygen in the atmosphere. Below the visible wavelengths (0.4 to 0.7 micrometers), gaseous attenuation is dominant but particulate attenuation becomes much greater in the visible and near infrared (Wolf, 1974). The Rayleigh effect states that scattering is inversely proportional to the fourth power of the wavelength. Therefore, scattering increases rapidly as wavelength decreases.

Once radiant energy has penetrated the atmosphere and becomes incident on the earth's surface, the amount of energy reflected back to the sensor will primarily determine the image color or tonal qualities. Factors influencing the amount of energy reflected back to the sensor include the wavelength, intensity and angle of incident energy, thickness of the atmosphere, surface roughness of the imaging object, orientation of the object, the object's absorption characteristics with respect to wavelength, and the back scattering, absorption, and refraction of energy from the object back through the atmosphere and to the sensor (Fraser, 1975).

It is important to appreciate that satellite and aerial photography reflectance data are susceptible to atmospheric effects which alter reflectance values, because through this realization, a practical method of correcting satellite and aerial photography radiance data can be developed and applied (Dana, 1975).

The effect of environmental factors and spectral reflectance properties; the implications of pixel integration, LANDSAT scanner readjustments, loss of boundary and size definition, and pixel to ground registration; and the effect of atmospheric attenuation on remotely sensed data should be ascertained in order to classify LANDSAT data and to evaluate classified data. Chapter VI will present data extraction techniques used to classify LANDSAT data and also evaluated classification output.

VI. DATA EXTRACTION TECHNIQUES FOR LANDSAT AND NASA U-2 AERIAL PHOTOGRAPHY

LANDSAT digital data and NASA U-2 aerial photography has been employed in this research to identify and delineate surface cover types within Crater Lake National Park.

LANDSAT and NASA U-2 data were acquired and subjected to various data extraction techniques in order to effectively manipulate the raw information. The following discussion will present the data extraction techniques used to analyze LANDSAT digital data, and the NASA U-2 aerial photography, and the products generated from the extracted information.

LANDSAT

LANDSAT digital data were analyzed through the computer facilities on the Oregon State University campus and at the EROS Data Center at Sioux Falls, South Dakota. The bulk of the computer analysis of LANDSAT was achieved at the EROS Data Center; however, important preliminary LANDSAT data analysis was achieved through use of the Oregon State University computer facilities. Table 21 provides a summary of LANDSAT data extraction techniques employed.

Oregon State University Computer System

A grayscale analysis was the initial technique employed to analyze the LANDSAT data at Oregon State

Summary of LANDSAT Data Extraction Techniques

Institution	Technique	Function	Output Product
Oregon State University	Grayscale analysis	Grouping of reflectance values and density slice (contrast stretching)	Alphanumeric map of Crater Lake National Park
	Selection of points for training sets (10 September 1974 and 06 January 1973 LANDSAT tapes).	Plots of pixel frequency versus reflectance intensity for four LANDSAT bands and plots of mean reflectance versus LANDSAT bands.	Graphs of the 10 September 1974 and 06 January 1973 LANDSAT data.
EROS Data Center	LANDSAT tape reformatting.	LANDSAT scene divided in four strips.	Computer tape file.
	Study area definition on LANDSAT tapes.	Establishment of 512X512 pixel study area.	Computer tape file.
	Geometric corrections.	Register latitude and longitude to scan line and pixel ("register")	Computer tape file and hard copy of statistics.
	Control point selection and digitizing.	Crater Lake National Park boundaries delineated on LANDSAT tape.	Hard copy statistical output and computer tape file.
	Stratification mask generation.	Zeroing out unwanted portion of original 512X512 pixel study area to only the boundaries of the park.	Computer tape file.
	Training set selection.	Control clustering, spectral relationship plot ("TSSELECT").	Computer tape file, hard copy statistics and graphs, and CRT display.

Table 21

Table 21 (continued)

Institution	Technique	Function	Output Product
EROS Data Center (continued)	Training set statistics.	Training set statistics input to IDIMS and clusters generated ("ISOCLS"). Maximum standard deviation determined ("STDMAX"). Determination of if and where additional training areas required ("CLASFY"), and quality of generated classes (distinctiveness) (59 generated classes).	Computer tape file and hard copy of mean reflectance per band and covariance matrix of generated class, also distance between clusters and weighted divergence.
	Classification	Application of training statistics to the entire study area ("CLASIFY"), 59 generated classes.	Alphanumeric printout of 512X512 pixel study area, and only area of Park. Scale of 512X512 pixel area printout--approximately 1:25,000, each symbol equals one pixel. Park area printout -- approximately 1:62,500, each symbol equals five pixels
	Combining of classes.	Generated 59 classes combined to 12 classes for the Park.	Color coded map of the Park (optronix's product), scale approximately 1:250,000.

Table 21

University. A grayscale is a grouping of reflectance values, through determination and placement of threshold values, and assignment of symbols to discern similar band reflectance clustering. Denser symbols are generally chosen to represent low reflectance values. The less dense the symbol, the higher are the reflectance values of that cluster.

On the grayscale, the ground truth sample site (refer to Chapter III) were located and delineated by means of the geography department's Zoom Transfer Scope. Transferring of sample sites from the Crater Lake topographic map to the grayscale provided an indication of the relative reflectance values of known surface cover types and an appreciation of the influence of known environmental factors such as slope angle, slope aspect, crown size, and crown density on the reflectance value of various surface cover types. A density slice was performed to determine if the setting of threshold values in the grayscale caused a grouping of reflectance values which relayed a false sense of relative reflectance between different surface cover types. A density slice is a process of rejecting unwanted portions of the grayscale while simultaneously expanding into the full grayscale range the remaining portions within which tone distinction among surface cover types can best be made. A further objective of the density slice was to evaluate how many different coniferous tree species could be

differentiated. This technique aided, for example, in confirming that two major lodgepole pine classes could be separated. The grayscale, besides providing a synoptic view of the study area in a digital format, provided insight into the subtleties of surface cover type differences which could be detected by the LANDSAT system.

To further investigate the discriminatory capability of LANDSAT, especially between coniferous tree species, a computer function ("selpt")¹ was employed to determine and analyze the reflectance values for selected areas within the Park. The ground truth sample sites which were located on the grayscale provided the areas for analysis through "selpt." Ground truth areas provide control over which surface cover types are to be statistically analyzed and which environmental factors are influencing the reflectance value, and to what relative degree. The statistics supplied for each selected area through "selpt" included: the mean reflectance per band; the standard deviation per band; the total number of pixels sampled; the distance from the mean of each pixel reflectance value per band; and the scan line and pixel number of each statistical unit in the selected analysis area.

The "selpt" function was utilized to analyze the 10 September 1974 and 06 January 1973 LANDSAT digital tapes. Through the use of "selpt," the possible differentiation of

¹Selection of points for training sets.

certain coniferous tree species by LANDSAT was confirmed. Comparison of the statistics obtained for the same ground truth sample sites on the 10 September 1974 and on the 06 January 1973 digital tapes reveals the importance of using multitemporal LANDSAT scenes in surface cover type differentiation (Figure 32). In Figure 32, reflectance intensity statistics for LANDSAT bands 4, 5, 6, and 7 have been plotted against pixel frequency for sites representing lodgepole pine, poorly stocked, lodgepole pine, densely stocked, mountain hemlock, a combination of lodgepole pine, densely stocked and mountain hemlock, and a combination of shasta red fir and mountain hemlock (see Table 8 for scientific names). The standard deviation (after "selpt") for each of the four LANDSAT bands are listed for each surface cover type described in Figure 32 for the LANDSAT dates of 10 September 1974 and 06 January 1973. The mean reflectance for each surface cover type was also plotted against each band for 10 September 1974 and 06 January 1973, and appears in Figure 32A.

The reflectance intensity data plotted against pixel frequency in Figure 32 and the mean reflectance data plotted against LANDSAT bands in Figure 32A shows that the 10 September 1974 LANDSAT digital tapes are superior to the 06 January 1973 LANDSAT digital tape for surface cover type analysis within Crater Lake National Park due to the discrimination of surface cover types shown by reflectance

Spectral Reflectance

10 SEPT. 74

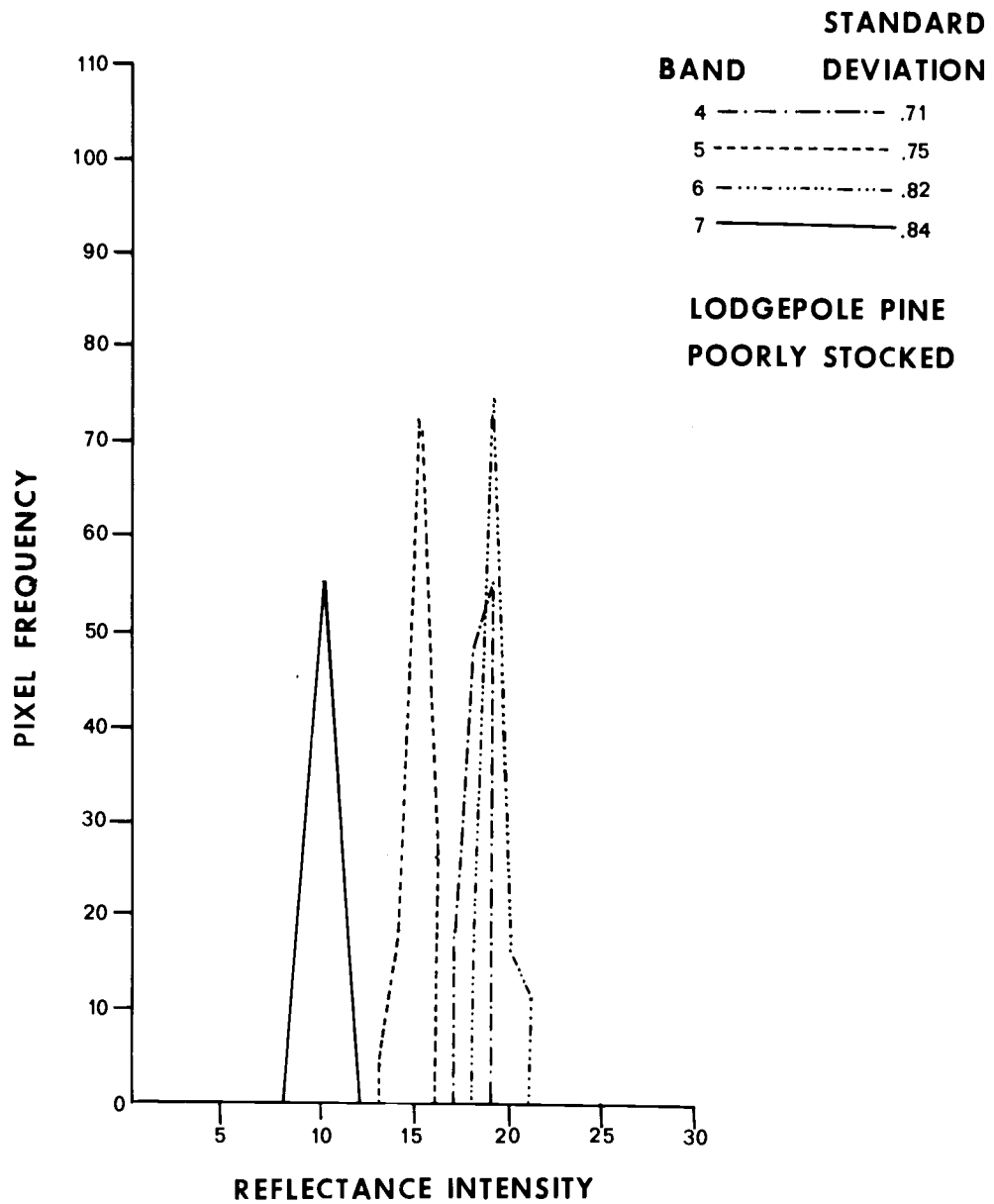


Figure 32

Spectral Reflectance

06 JAN. 73

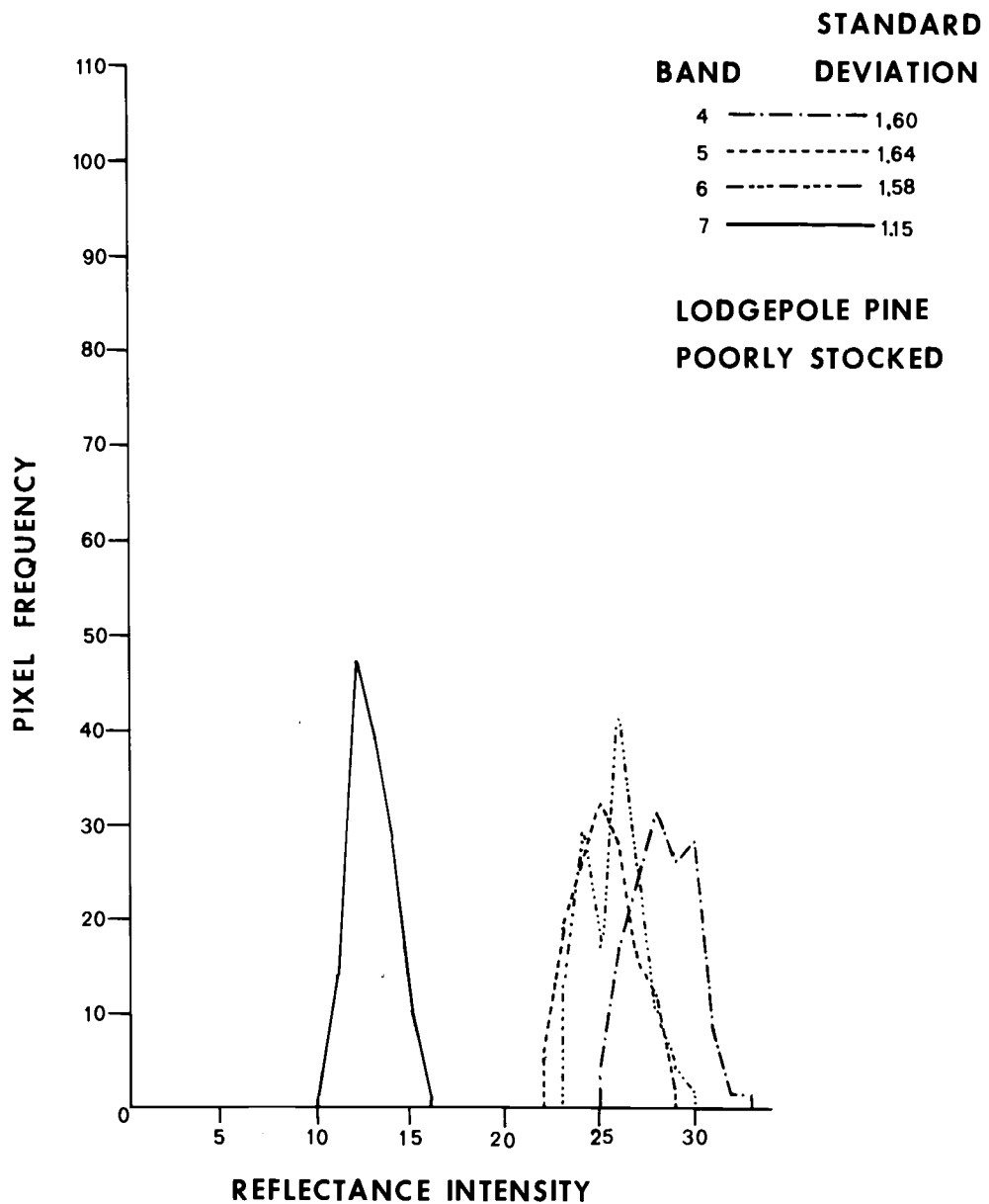


Figure 32 (continued)

Spectral Reflectance

10 SEPT. 74

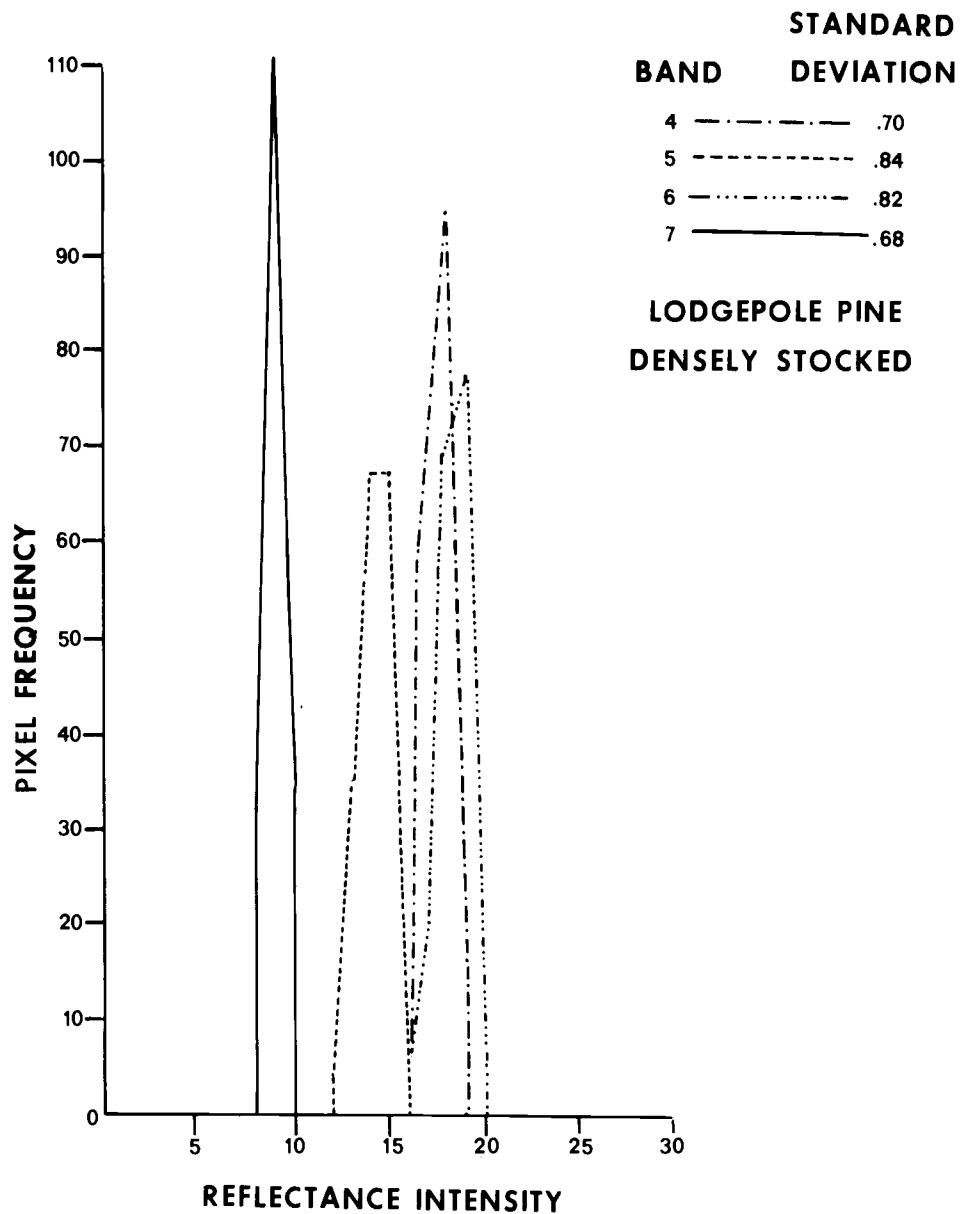


Figure 32 (continued)

Spectral Reflectance

06 JAN. 73

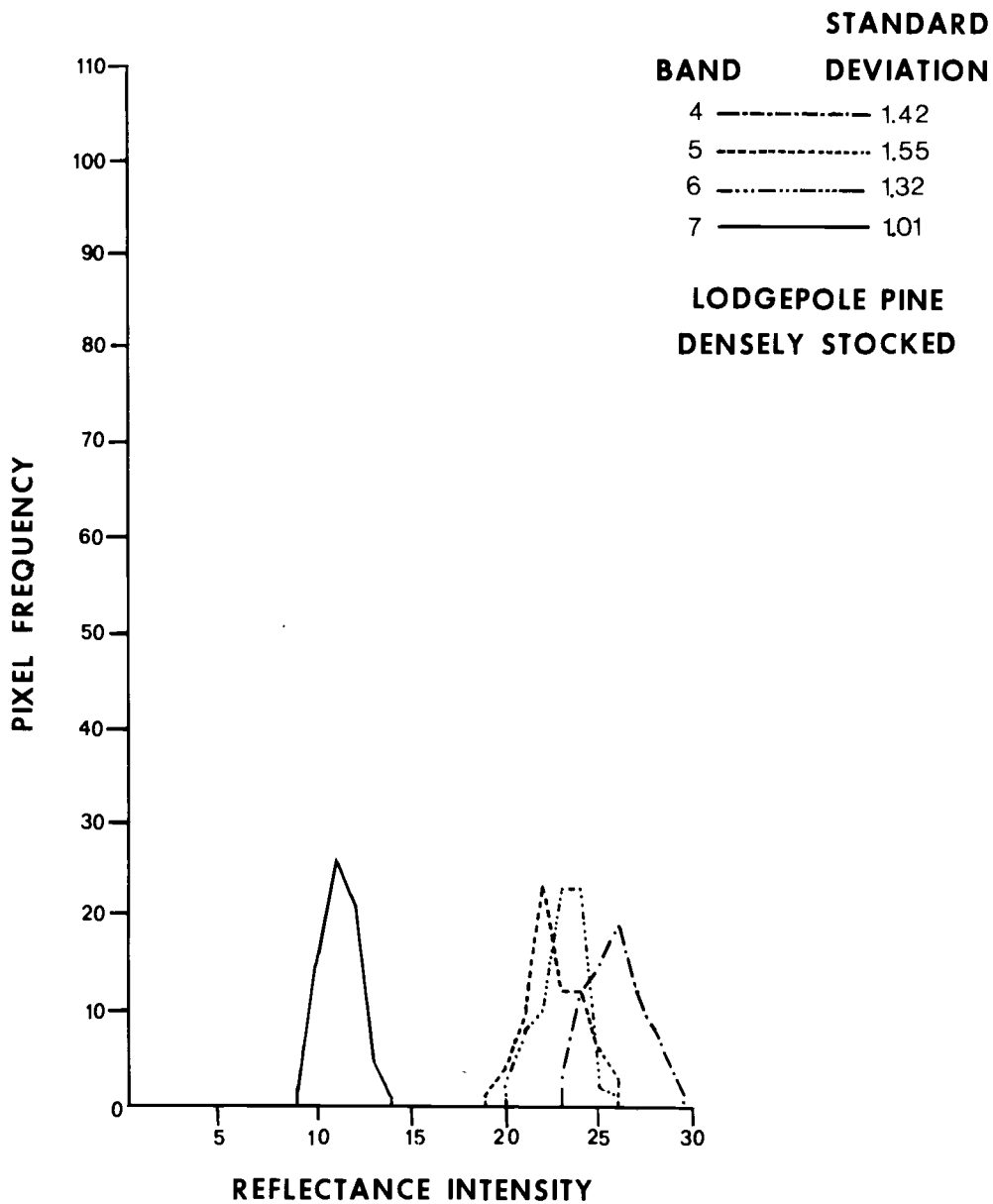


Figure 32 (continued)

Spectral Reflectance

10 SEPT. 74

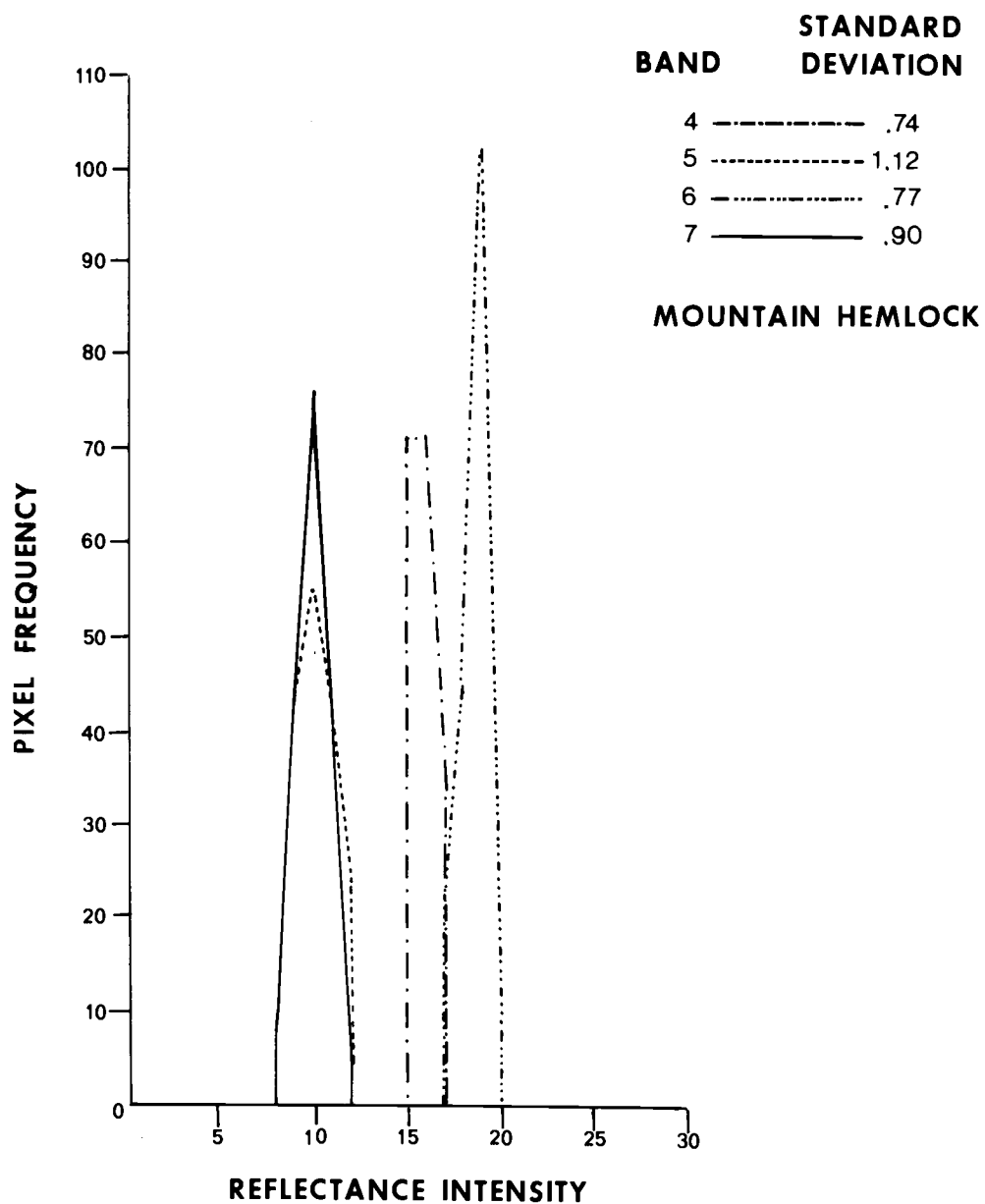


Figure 32 (continued)

Spectral Reflectance

06 JAN. 73

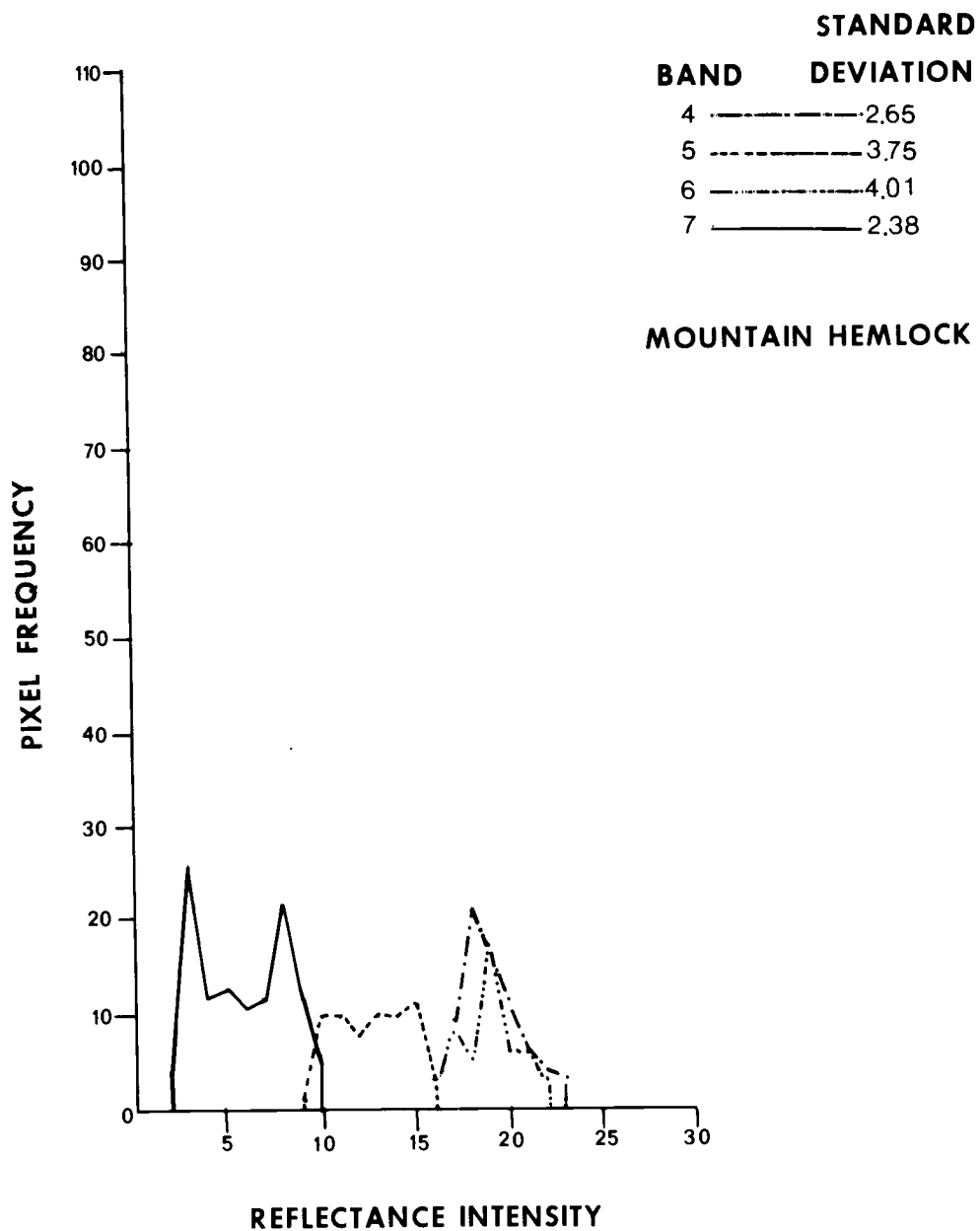


Figure 32 (continued)

Spectral Reflectance

10 SEPT. 74

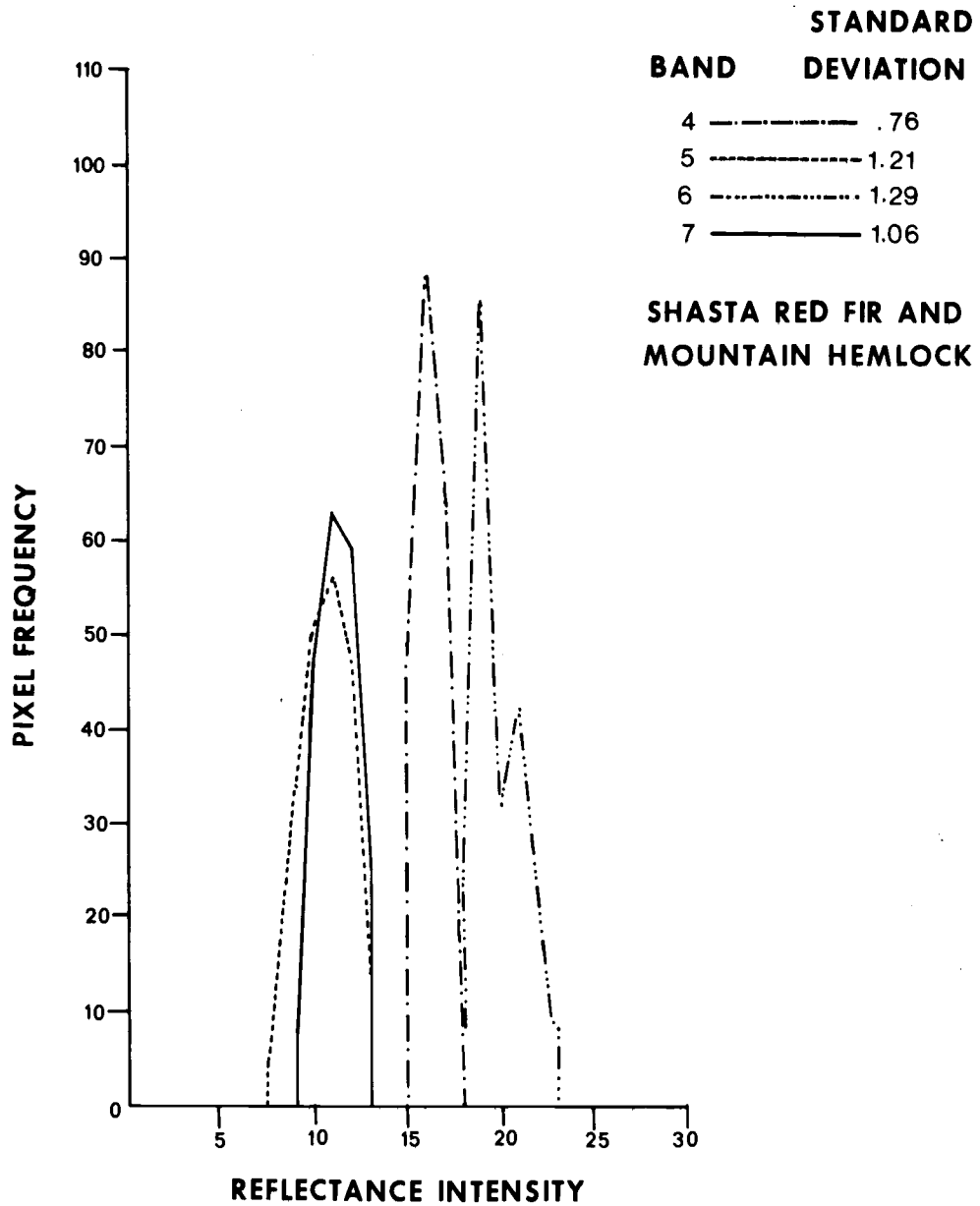


Figure 32 (continued)

Spectral Reflectance

06 JAN. 73

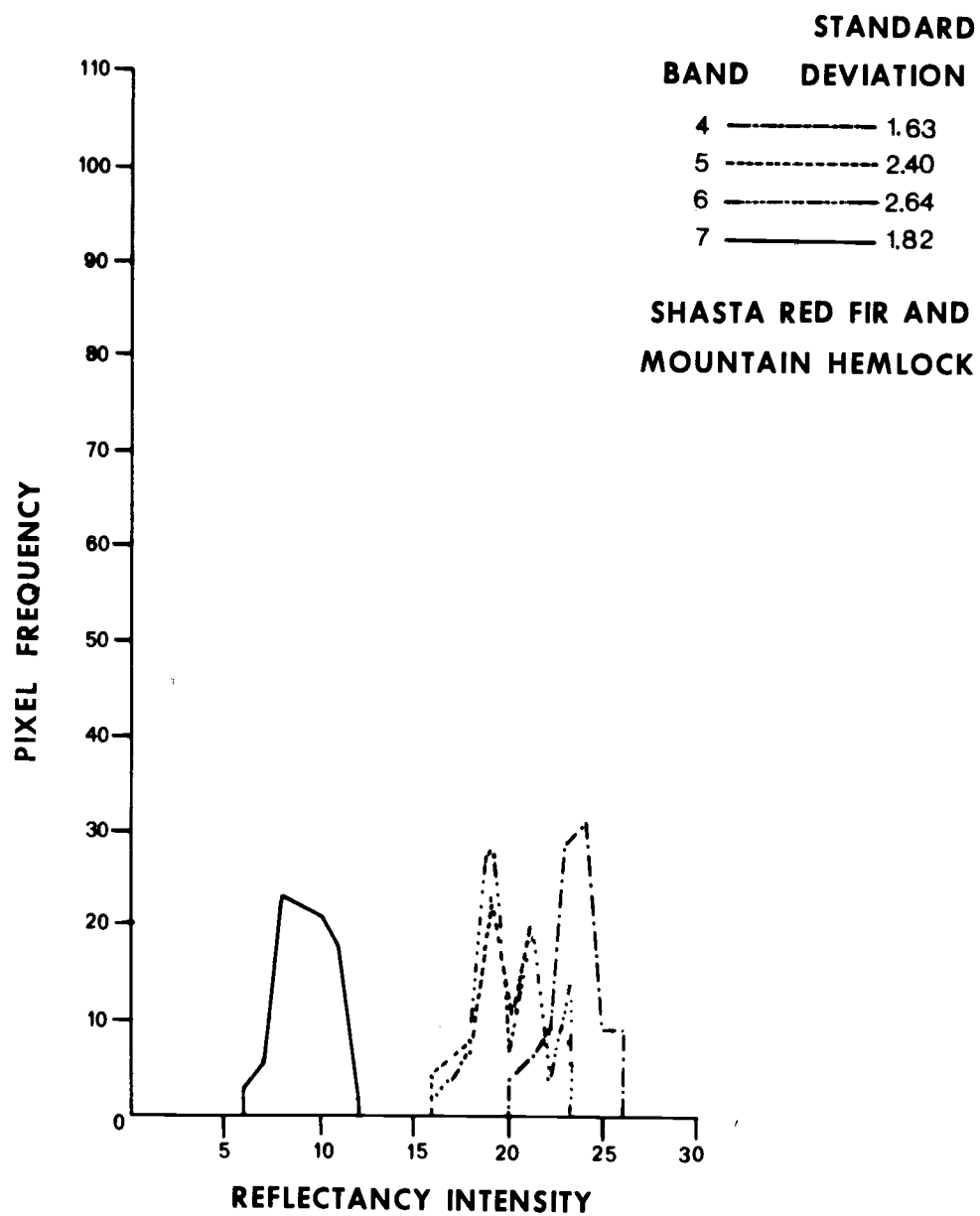


Figure 32 (continued)

Spectral Reflectance

10 SEPT. 74

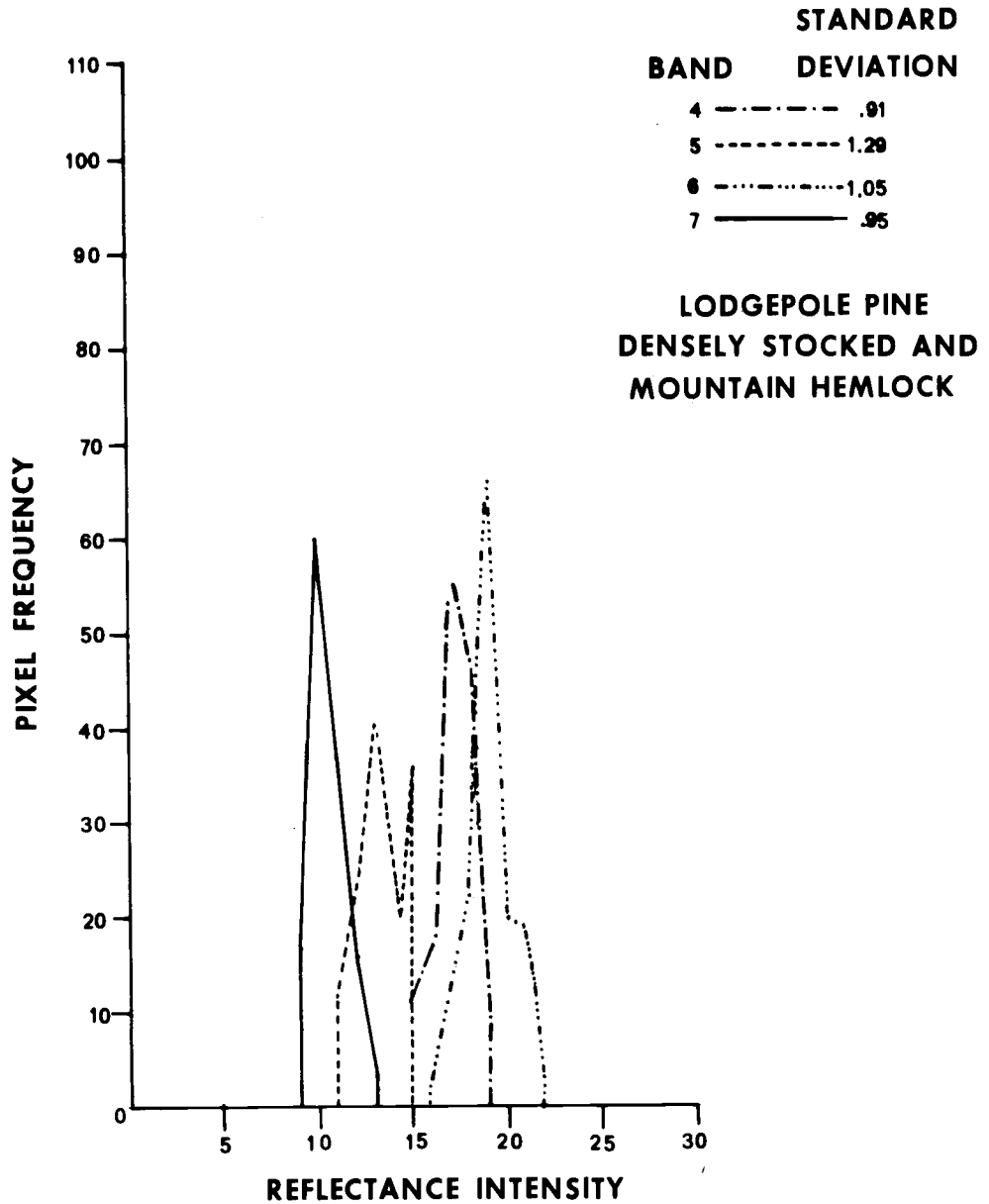


Figure 32 (continued)

Spectral Reflectance

06 JAN. 73

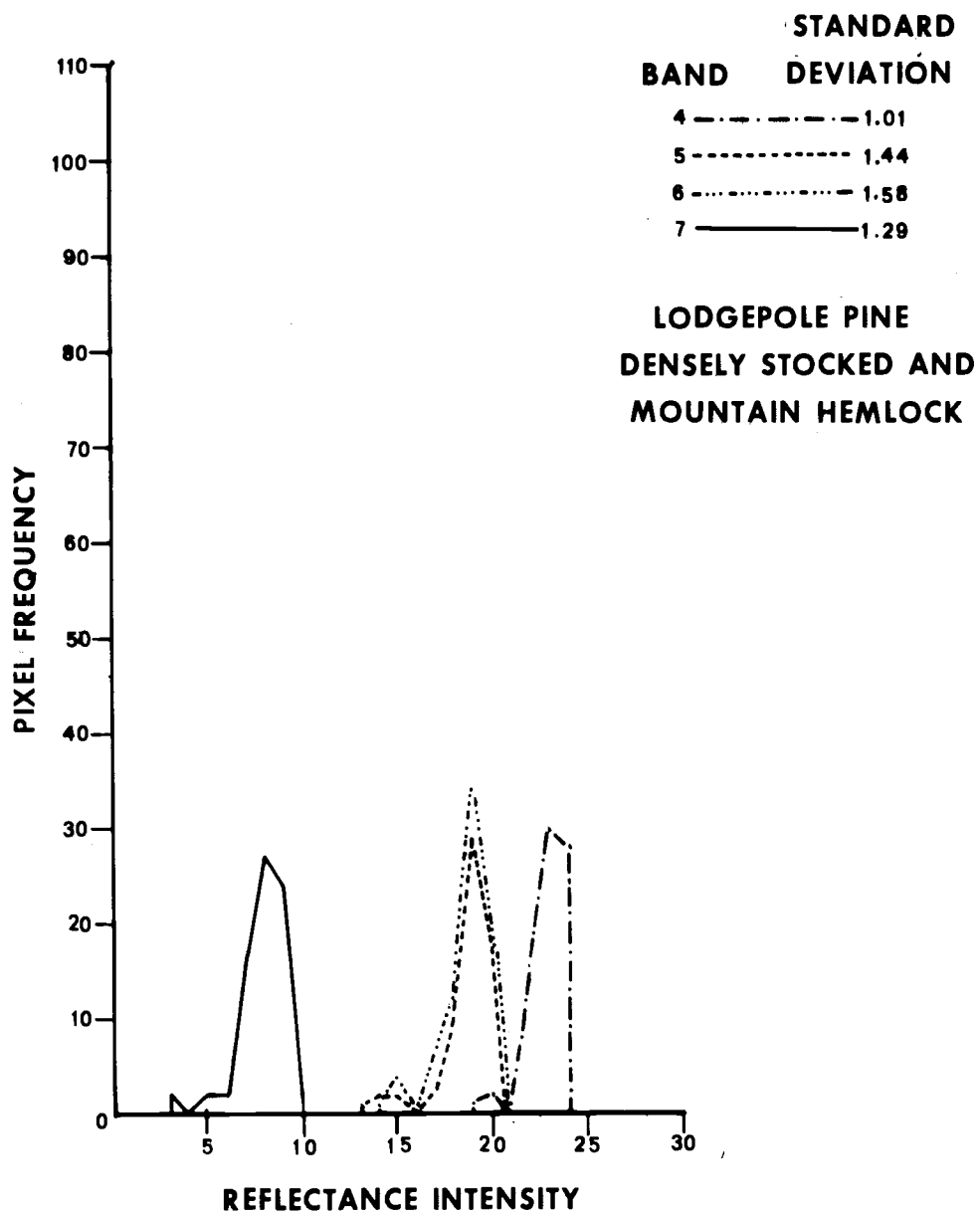


Figure 32 (continued)

Reflectance Values

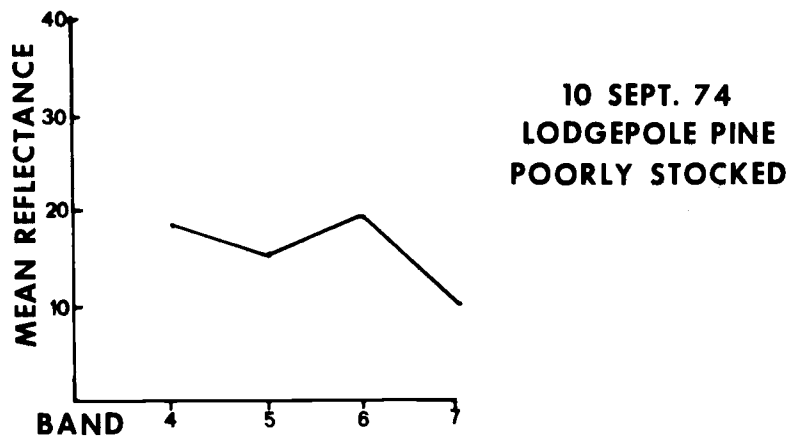


Figure 32A

Reflectance Values

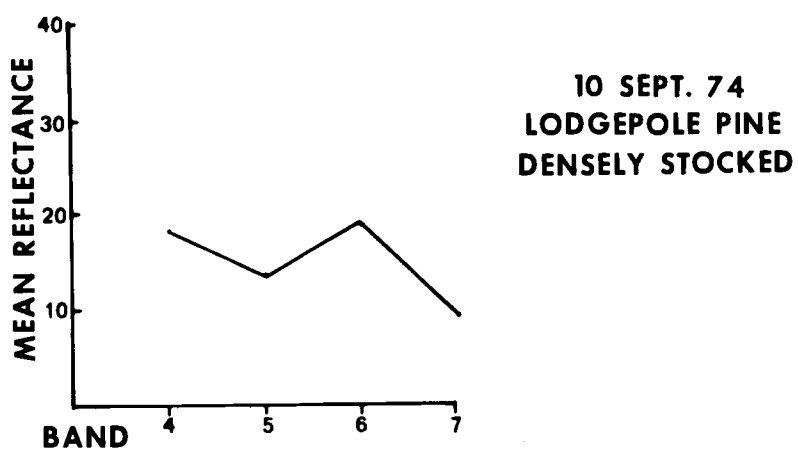


Figure 32A (continued)

Reflectance Values

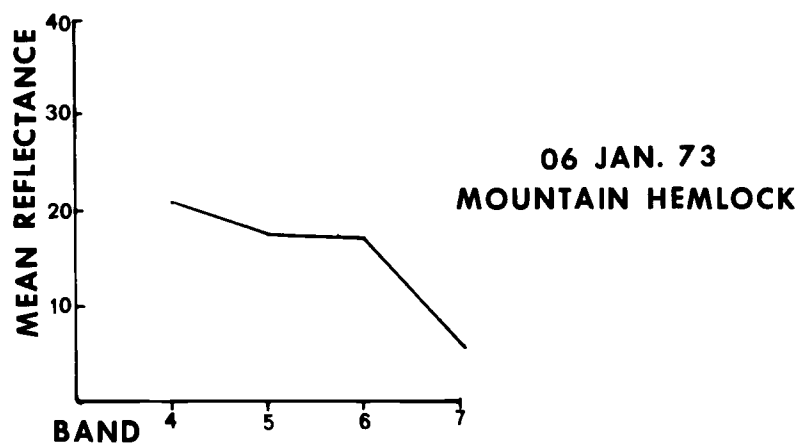
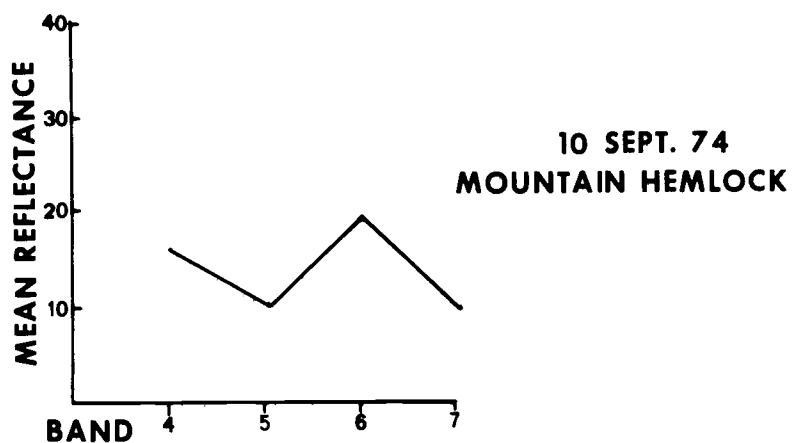
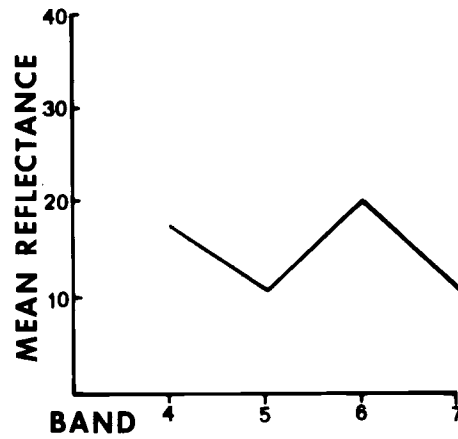
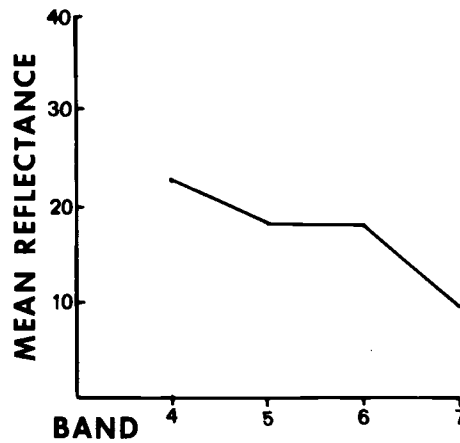


Figure 32A (continued)

Reflectance Values



**10 SEPT. 74
SHASTA RED FIR
and
MOUNTAIN HEMLOCK**



**06 JAN. 73
SHASTA RED FIR
and
MOUNTAIN HEMLOCK**

Figure 32A (continued)

Reflectance Values

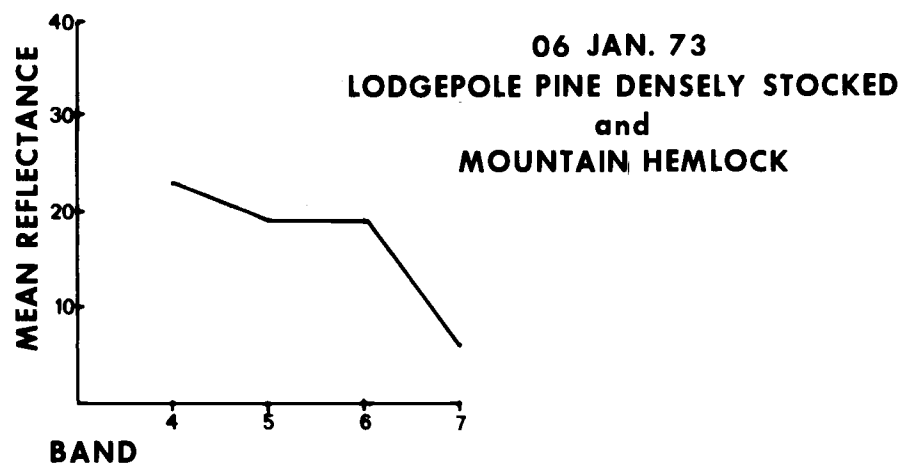
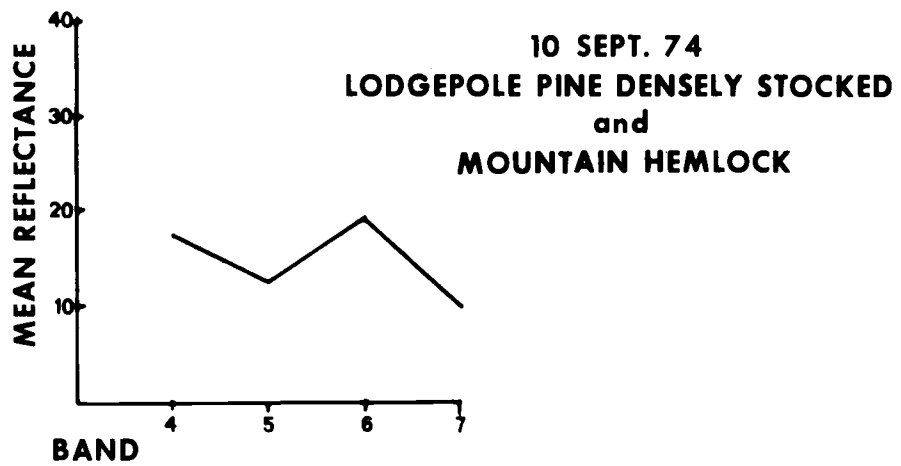


Figure 32A (continued)

value differences between bands. As will be described in a forthcoming discussion, LANDSAT bands 5 and 7 are most useful of the four LANDSAT bands in differentiating between coniferous tree species, which constitute the major surface cover types within the Park. The reflectance values for bands 5 and 7, in Figure 32, for a combination of shasta red fir and mountain hemlock, and a combination of lodgepole pine, densely stocked and mountain hemlock are better differentiated from one another on the 06 January 1973 LANDSAT digital tape than on the 10 September 1974 LANDSAT tape. This better separation of the reflectance values in bands 5 and 7 for the 06 January 1973 LANDSAT tapes indicates that for various surface cover types, identification and separation can best be achieved by using low sun angle digital tapes. Low sun angle LANDSAT tapes have also been employed for a more precise outlining of openings in the forest canopy resulting from the occurrence of natural glades, and rock and pumice outcrops.

Also in Figure 32A the mean reflectance values per band for the two different dates (06 January 1973 and 10 September 1974) also change relative positions and alter reflectance value intensities for the same sites primarily due to changes in sun angle and vegetation growth periods (Williams, 1976).

The 06 January 1973 and the 10 September 1974 LANDSAT tapes, when used in conjunction seem to provide a more

explicit distinction between many surface cover types. The use of digital tape combinations which make use of changes in sun angle can lead to improved surface cover type separation and improved classification accuracy (Kalensky, 1974).

EROS Data Center

Processing of LANDSAT digital tapes was achieved through use of the Interactive Digital Image Manipulation System (IDIMS) and the Tektronix digitizing system at the EROS Data Center. The 10 September 1974 LANDSAT tape was the only tape analyzed for surface cover type differentiation within Crater Lake National Park due to equipment operating time restrictions. The following discussion will provide a summary of the LANDSAT data processing functions that were employed at EROS, and the strategy behind the implementation of various processing techniques.

Tape Reformatting

LANDSAT digital tape reformatting must first be accomplished prior to any analysis on IDIMS. Each LANDSAT scene contains 2,340 scan lines of data and 3,264 pixels along a line in four separate spectral bands (Figure 15). In the tape reformatting function at EROS, the data are divided into four strips of 816 pixels wide. Each strip is kept separate, and utilized in that arrangement (Figure 33).

IDIMS Transfer Tape Format

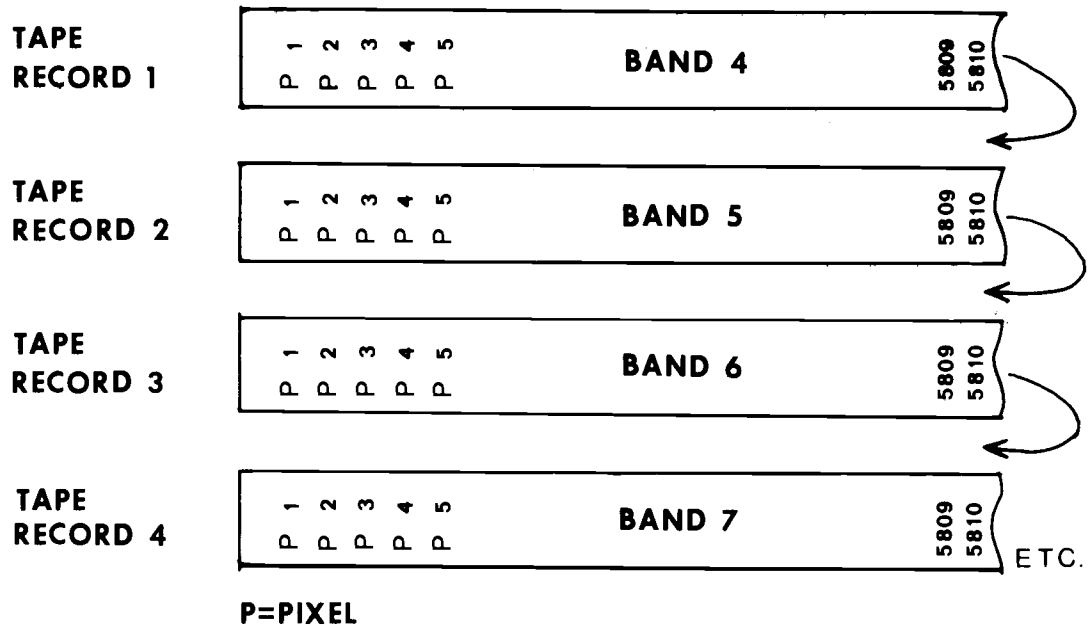


Figure 33

Study Area Definition

The initial step in the computer processing and analysis of LANDSAT digital tapes was to define the area which was to be investigated in order to acquire proper LANDSAT tapes and to locate the study area on the digital tapes. The size of the study area was 512 x 512 pixels, which was the maximum size capable of being presented on the IDIMS cathode ray tube (CRT) at one time and at the desired magnification. The size of the study area was chosen purposely larger than needed to be confident that the entire National Park would be presented on the CRT and to allow for good control point selection. Unwanted portions of the 512 x 512 pixel study area were later masked out.

Geometric Corrections

LANDSAT data has inherent distortions caused by earth rotation and satellite motion. IDIMS has functions available which correct these types of distortions.

As the satellite revolves around the earth, the earth is rotating under the satellite. This earth rotation causes a successive displacement of scan lines to the west while an image is being scanned. This distortion is called skew and requires correction. Another distortion is involved with the pass of the satellite not being true north-south (approximately east 10° north) to coincide with lines of longitude. The LANDSAT image is rotated west of north,

the degrees depending upon the latitude when the image was taken. A further distortion of the LANDSAT data is caused by the ground distance which is covered by one pixel. The average distance is 183 x 259 feet (56 x 79 meters). In digitizing the satellite data, more samples are chosen along a scan line than are chosen from scan line to scan line. This results in the pixel being rectangular and not square. The correction utilized is called squaring and results in the size of the pixel being 259 x 259 feet (79 x 79 meters). These corrections are completed by the "register" function on the IDIMS at EROS.

Control Point Selection and Digitizing

Most digitizing on the IDIMS at EROS is performed using the Geographic Entry System (GES) with the HP 3000 computer. The GES system has the capability of using any map as long as the map has tick marks for latitude and longitude for registering the map within the LANDSAT scene. The only connection between the delineation from the map and the LANDSAT data is through the set of control points which are digitized.

In selecting control points, the color composite image of the 10 September 1974 Crater Lake LANDSAT image (512 x 512 pixels) was displayed on the IDIMS CRT terminal. Significant landmarks (river junctions or mountain peaks -- landmarks which could be located on the map and the IDIMS

display) were visually interpreted from the display. U-2 color infrared aerial photography, a topographic map of Crater Lake National Park, ground truth information, and LANDSAT images were used to locate landmarks for control point selection. These interpreted landmarks on IDIMS were paired with the same landmarks on the Crater Lake topographic map. These points were labelled on the map and on IDIMS with identifying symbols. The basis for selecting control points was to have the points distributed uniformly throughout the National Park; to have the corners of the Park boundaries selected for control points; and to be able to locate the same points found on the map on the LANDSAT color composite displayed on IDIMS. Figure 34 shows the location of the selected control points used throughout the Park.

The LANDSAT coordinates for the same points located on the topographic map were located on the IDIMS display of the color composite representation of the Park by means of the locator-trackball. The scan line and pixel number was obtained for each point located on the display. Using the GES software, the control points located on the CRT terminal and on the topographic map were digitized by use of the Tektronix digitizing system (Table 22). The coordinates for the two sets of points were read by a program that performed a least squares fit on IDIMS and generated coefficients for a first, second, and third order

Control Point Location

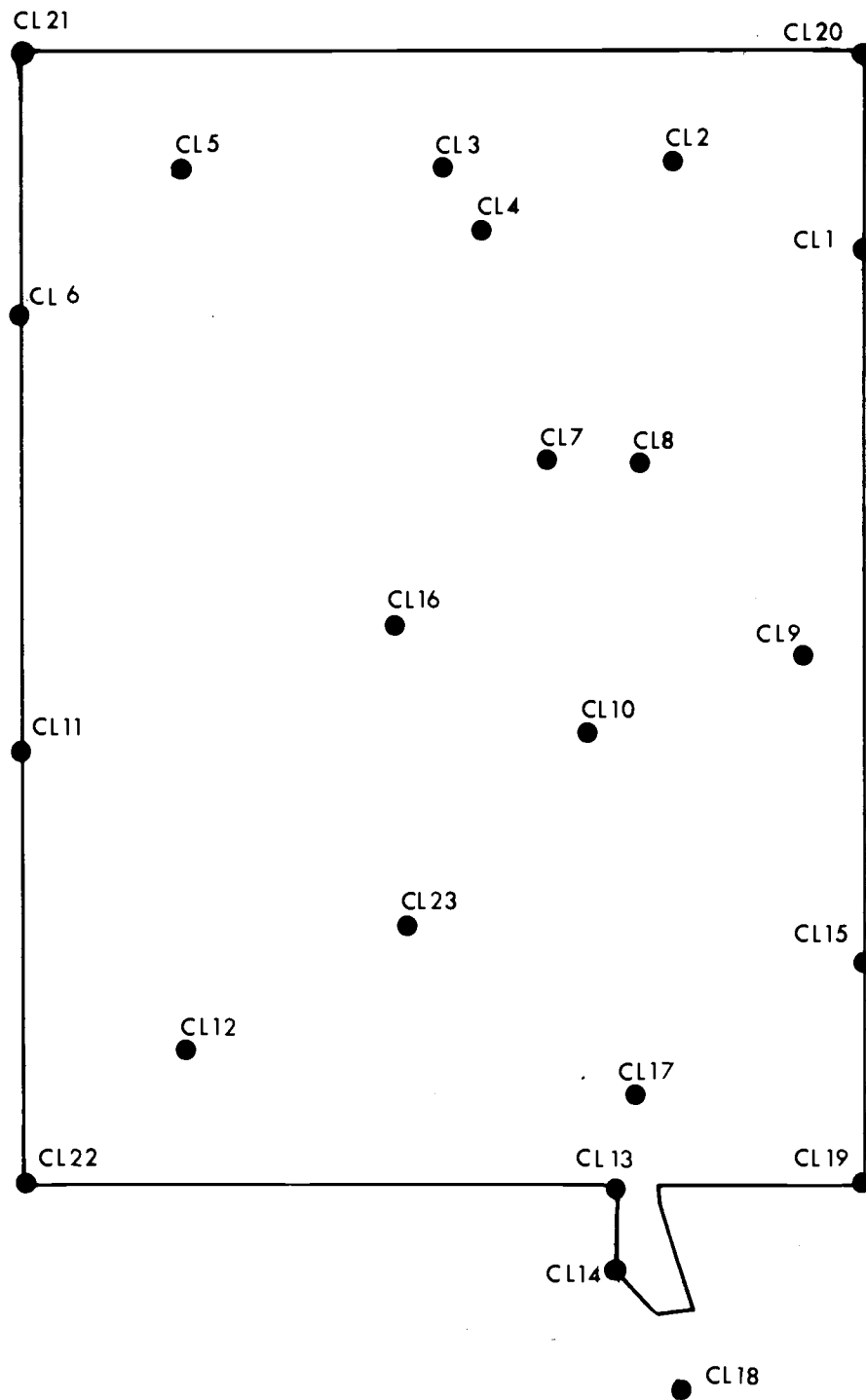


Figure 34

Control Point List for Overlay of
Crater Lake National Park

1 CONTROL POINT LIST FOR OVERLAY CPNPS

NUMBER	IDENT	COORDINATES		LAT (TOT SECS) LON			
29	CL1	43	1' 18" N	121	59' 54" W	154878	-439195
30	CL2	43	2' 39" N	122	3' 45" W	154959	-439426
31	CL3	43	2' 44" N	122	8' 8" W	154964	-439689
32	CL4	43	1' 38" N	122	7' 16" W	154898	-439637
33	CL5	43	2' 33" N	122	13' 6" W	154953	-439987
34	CL6	42	59' 49" N	122	15' 13" W	154789	-440114
35	CL7	42	58' 26" N	122	6' 11" W	154706	-439572
36	CL8	42	58' 23" N	122	4' 26" W	154703	-439467
37	CL9	42	55' 23" N	122	0' 53" W	154525	-439254
38	CL10	42	54' 34" N	122	3' 21" W	154474	-439522
39	CL11	42	53' 44" N	122	13' 2" W	154424	-440103
40	CL12	42	49' 54" N	122	13' 17" W	154194	-439998
41	CL13	42	48' 44" N	122	4' 38" W	154084	-439479
42	CL14	42	46' 49" N	122	4' 37" W	154009	-439478
43	CL15	42	51' 6" N	121	39' 51" W	154266	-439192
44	CL16	42	56' 22" N	122	8' 59" W	154562	-439740
45	CL17	42	48' 43" N	122	4' 9" W	154085	-439450
46	CL18	42	44' 47" N	122	3' 21" W	153887	-439402
47	CL19	42	48' 43" N	121	39' 50" W	154085	-439191
48	CL20	43	4' 33" N	121	39' 53" W	155043	-439194
49	CL21	43	4' 33" N	122	15' 52" W	155043	-440153
50	CL22	42	48' 43" N	122	15' 53" W	154085	-440154
51	CL23	42	51' 43" N	122	8' 57" W	154305	-439738

Table 22

transformation (Table 23). These transformation equations converted digitized units of the map (latitude and longitude) to LANDSAT units (scan line and pixel). The transformation also corrected for X and Y direction displacement between the points on the map and the same points on the displaced digital image. After the first order transformation was performed (Table 23), the average error between the location of the control points on the topographic map and on the IDIMS display screen was 0.808156 pixels. This error was reduced to 0.787204 pixels by employing a second order transformation and was further reduced to 0.534385 pixels after third order transformation was utilized. Table 23 shows a reduction of control points from 23 to 14 after employing the first, second, and third order transformations. Some points easily located on the topographic map were difficult to precisely locate on the IDIMS screen and were therefore dropped when transformation statistics were generated. The digitized data were overlaid on the final LANDSAT classification in order to mask out all parts of the 512 x 512 pixel area where summary statistics were not wanted.

Stratification Mask Generation

Stratification as used by IDIMS is the process of extracting and summarizing data within irregularly shaped regions on a digital image. Data were stratified and

First, Second, and Third Order Transformations
of Control Points

Point	TX	TY	RX	RY
<u>First Order</u>				
1 CL1	390	108	-1.1	-.7
2 CL3	189	105	1.0	.2
3 CL4	219	127	1.2	.1
4 CL5	76	128	-1.4	.3
5 CL6	51	197	.6	-.5
6 CL7	272	195	-1.8	.2
7 CL8	312	190	.5	-.1
8 CL9	420	244	.4	.4
9 CL12	182	414	.5	-.9
10 CL13	396	424	.6	1.4
11 CL15	480	337	-.2	-1.1
12 CL16	228	260	-1.0	.5
13 CL18	456	492	-.3	-.1
14 CL20	366	45	.9	.1
Residual Means = .808156, .467354				
<u>Second Order</u>				
1 CL1	390	107	-1.3	-.3
2 CL3	189	105	.9	-.3
3 CL4	219	127	1.2	-.3
4 CL5	76	128	-1.3	.3
5 CL6	51	197	.8	.1
6 CL7	272	195	-1.6	-.2
7 CL8	311	190	.6	-.3
8 CL9	419	243	.7	.7
9 CL12	183	413	.1	-.4
10 CL13	396	424	.6	1.1
11 CL15	480	337	.2	-.7
12 CL16	228	260	-.8	.3
13 CL18	457	492	-.5	-.4
14 CL20	367	45	.4	.4
Residual Means = .787204, .420799				
<u>Third Order</u>				
1 CL1	389	107	-.3	.1
2 CL3	189	105	.8	-.4
3 CL4	219	127	1.2	-.3
4 CL5	76	128	-1.0	.4
5 CL6	52	197	.3	-.1
6 CL7	272	195	-1.6	-.1
7 CL8	312	191	.2	-.5
8 CL9	419	243	.6	.7
9 CL12	183	413	.3	-.4
10 CL13	398	424	-.6	.6

Table 23

Table 23 (continued)

Point	TX	TY	RX	RY
<u>Third Order</u> (continued)				
11 CL15	480	337	.2	-.7
12 CL16	227	259	.0	.6
13 CL18	456	492	.2	-.1
14 CL20	367	45	-.2	.2
Residual Means = .534385, .367832				

Table 23

summaries generated for Crater Lake National Park from a LANDSAT classification by delineation of clusters on the IDIMS display. The image mask generated was the area of Crater Lake National Park, which was part of the original 512 x 512 pixel study area. The initial step in mask generation was to build a pre-mask file which was scanned and built into a final mask file. This final mask file was a byte image that contains only two gray levels, zero and one. Within the 512 x 512 pixel study area displayed on IDIMS, all lines digitized in GES appeared as a one. The remainder of the image which did not appear in the GES appeared as zero and therefore was masked out.

Training Set Selection

The concept of training set selection is to generate a set of statistics that represent the spectral response of a particular surface cover type. A set of algorithms have been developed that generate statistical records by analyzing a subset of LANDSAT data within the study area. The information in the statistical record consists of the mean value of the gray level data from each band, and a covariance matrix, which is a measure of the size and shape of the cluster of points used to generate the statistics (Figure 35). Training sets are small sets of data used to "train" a classification algorithm. Based upon the spectral response for a small training area, the classifier

Training Set Statistics

CLASS 3: WATER

MSS Band	4	5	6	7
Mean Reflectance	12.98	4.27	2.10	2.01
Covariance Matrix	.56			
	.08	.49		
	.03	.07	.25	
	.00	-.00	-.00	.02

Note: The shape, location, and size of Class 3 is determined by obtaining a positive or negative correlation and the mean reflectance between two selected bands, for example, bands 4 and 5.

$$\begin{aligned}
 \text{Correlation} &= \frac{\text{covariance of bands 4 and 5}}{(\sqrt{\text{Variance band 4}}) (\sqrt{\text{Variance band 5}})} \\
 &= \frac{.08}{(\sqrt{.56}) (\sqrt{.49})} \\
 &= \frac{.08}{.5238319} \\
 &= +0.1527207
 \end{aligned}$$

The positive correlation determines the direction (slope) of the class plot, the class means determine the mid-point of the class, and the magnitude of the correlation and the standard deviation (the square root of the variance) determines the size of the class represented by a circle or an ellipse. As the correlation increases between bands, the ellipse tightens; as the correlation decreases, the ellipse approaches a circle.

Figure 35. Mean reflectance and covariance matrix for the four LANDSAT bands for class 3. Class 3 is a water class.

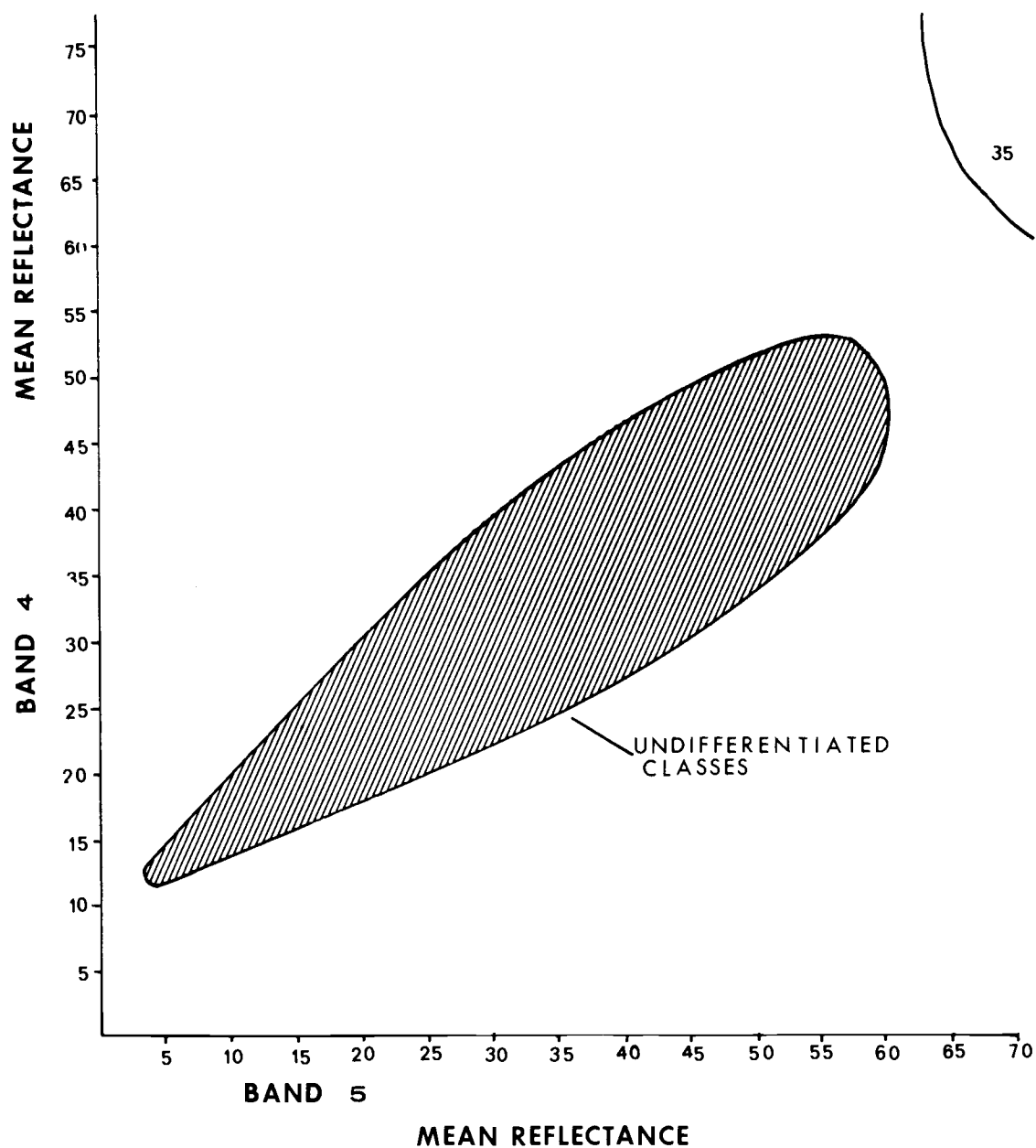
(in this case, the maximum likelihood classifier²) attempts to group all similar surface cover types on a pixel by pixel basis. Three different training set selection techniques can be employed: the unsupervised clustering technique, the supervised clustering technique, and the controlled clustering technique. The controlled clustering technique is a combination of the unsupervised and supervised technique and was the approach utilized in this research for training set selection. The controlled clustering technique requires that after the study areas have been satisfactorily classified, the user determines what surface cover type each class or group of classes represents on the ground.

Spectral Relationship Plot

A spectral relationship plot of two LANDSAT MSS bands is an analysis technique used to determine which combination of LANDSAT bands best distinguishes one training set class from another (Figure 36). The standard deviation, covariance, and mean reflectance of each band determines the location and shape of each class cluster shown in Figure 36. Figure 36 shows the change in class location

²The maximum likelihood classifier is a scheme which first divides the four spectral reflectance values for a pixel (one reflectance value for each band) into a number of distinct regions; each region corresponds to a known class. The likelihood of the pixel belonging to each of the possible classes is calculated. The pixel is assigned to the class with the maximum likelihood value.

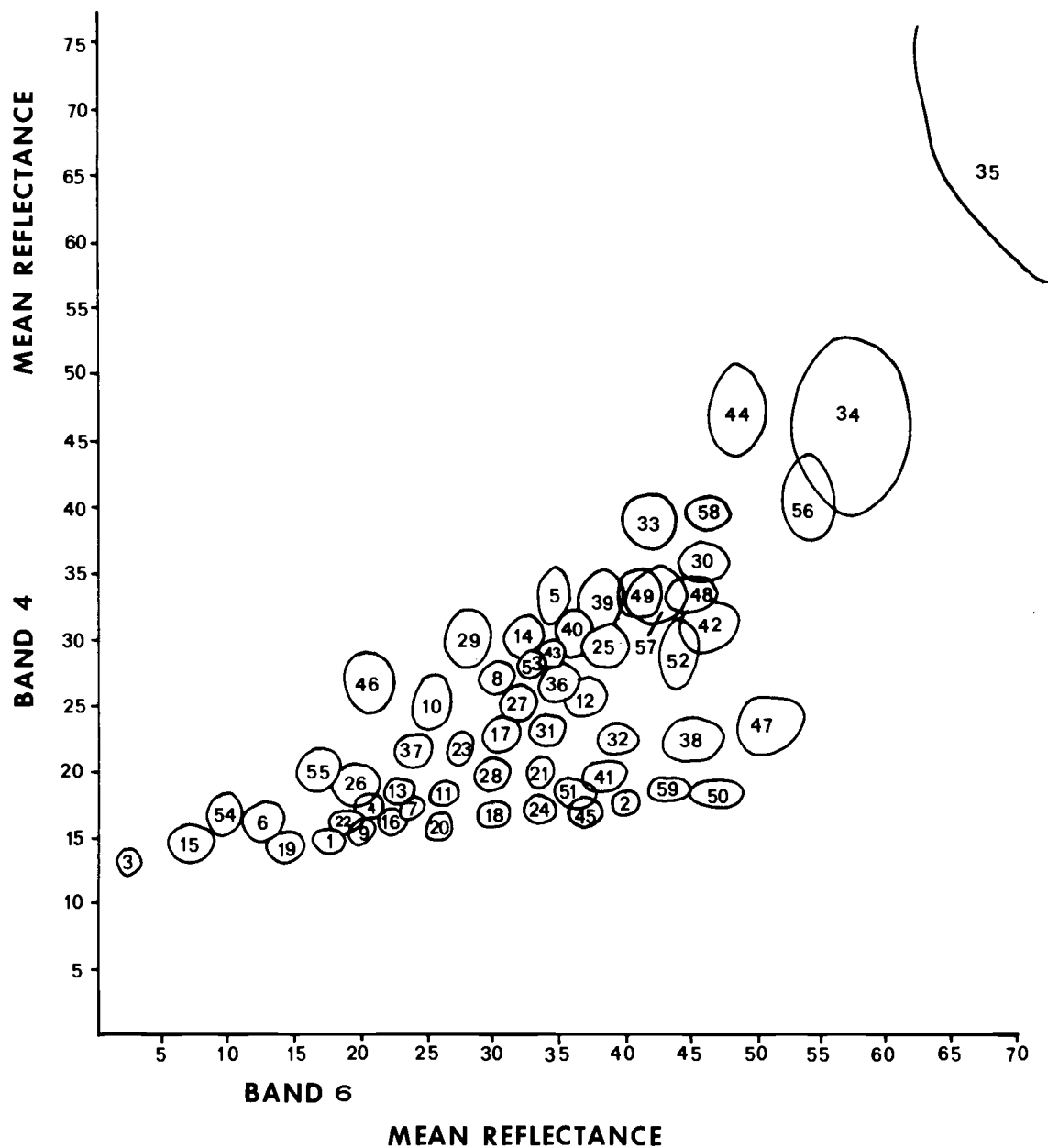
Spectral Reflectance Plotting



10 SEPT. 74

Figure 36

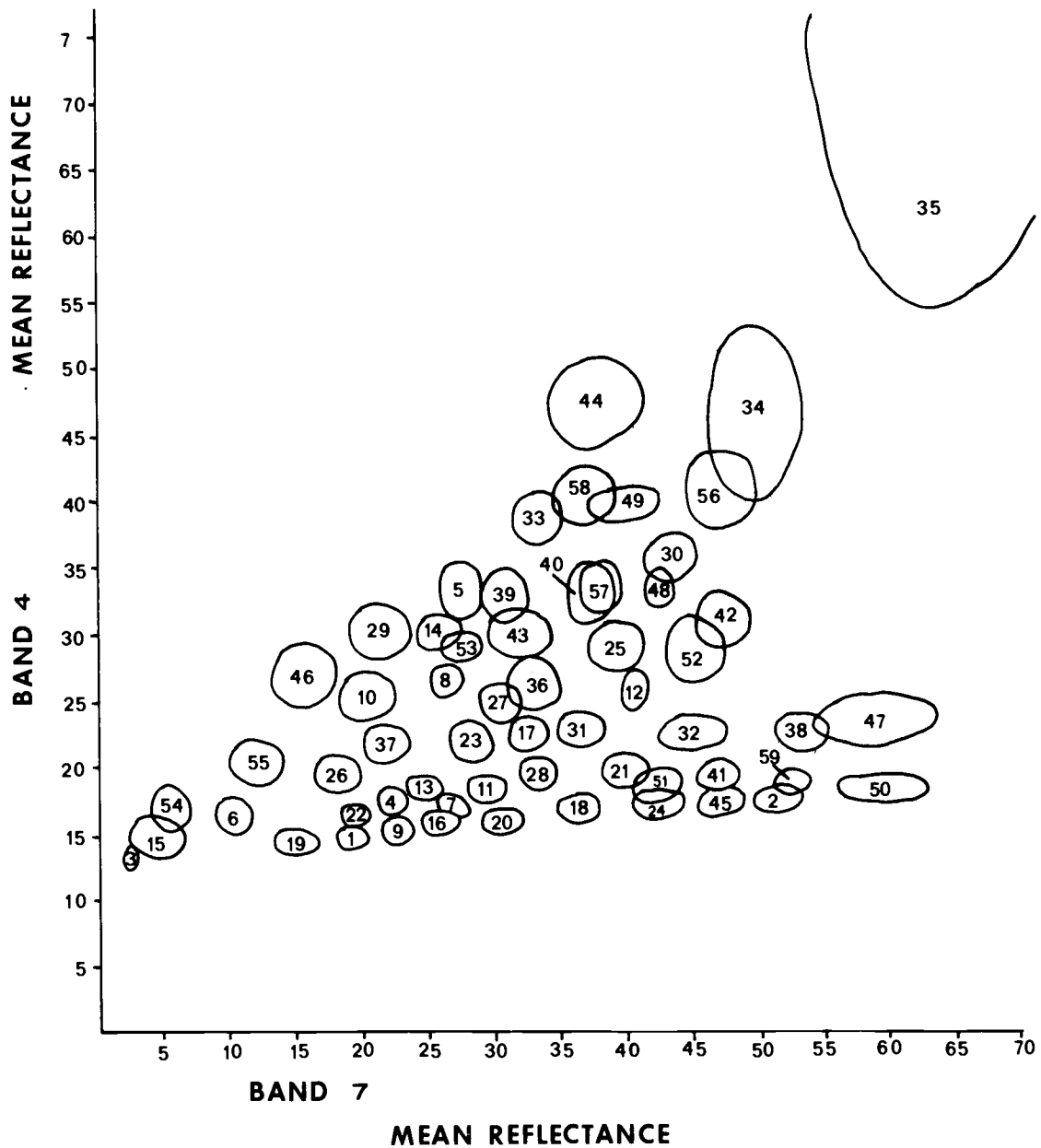
Spectral Reflectance Plotting



10 SEPT. 74

Figure 36 (continued)

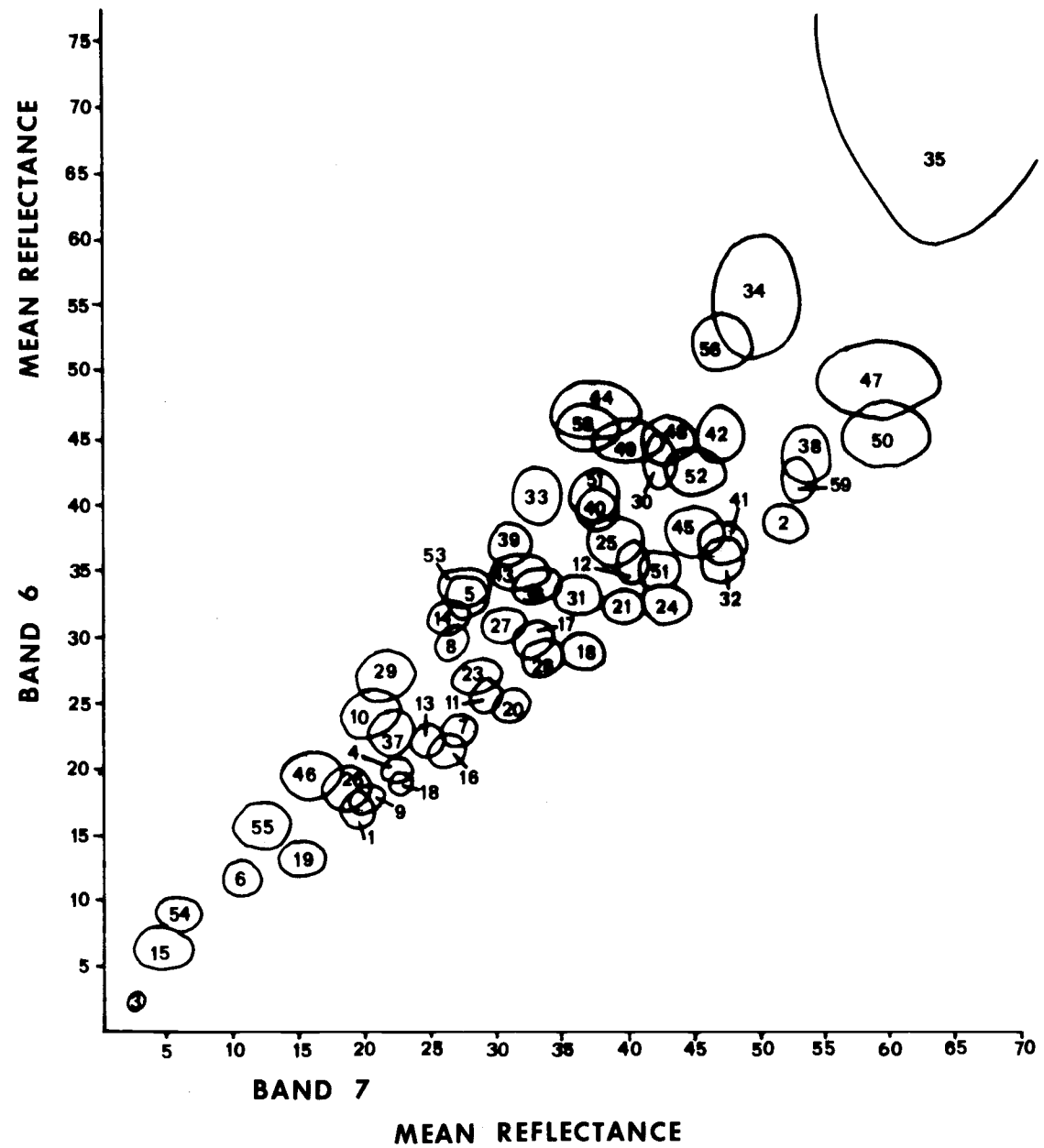
Spectral Reflectance Plotting



10 SEPT. 74

Figure 36 (continued)

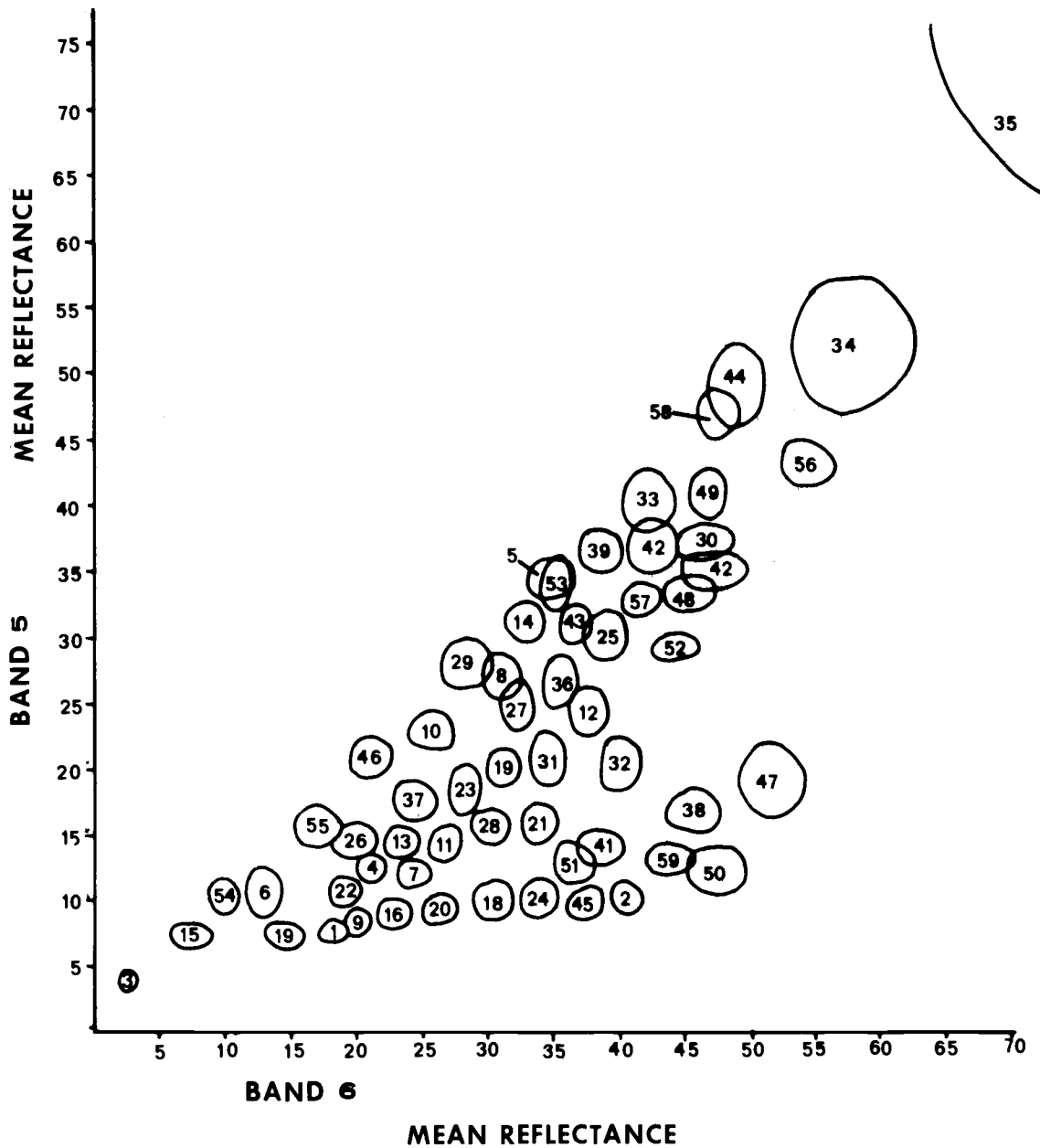
Spectral Reflectance Plotting



10 SEPT. 74

Figure 36 (continued)

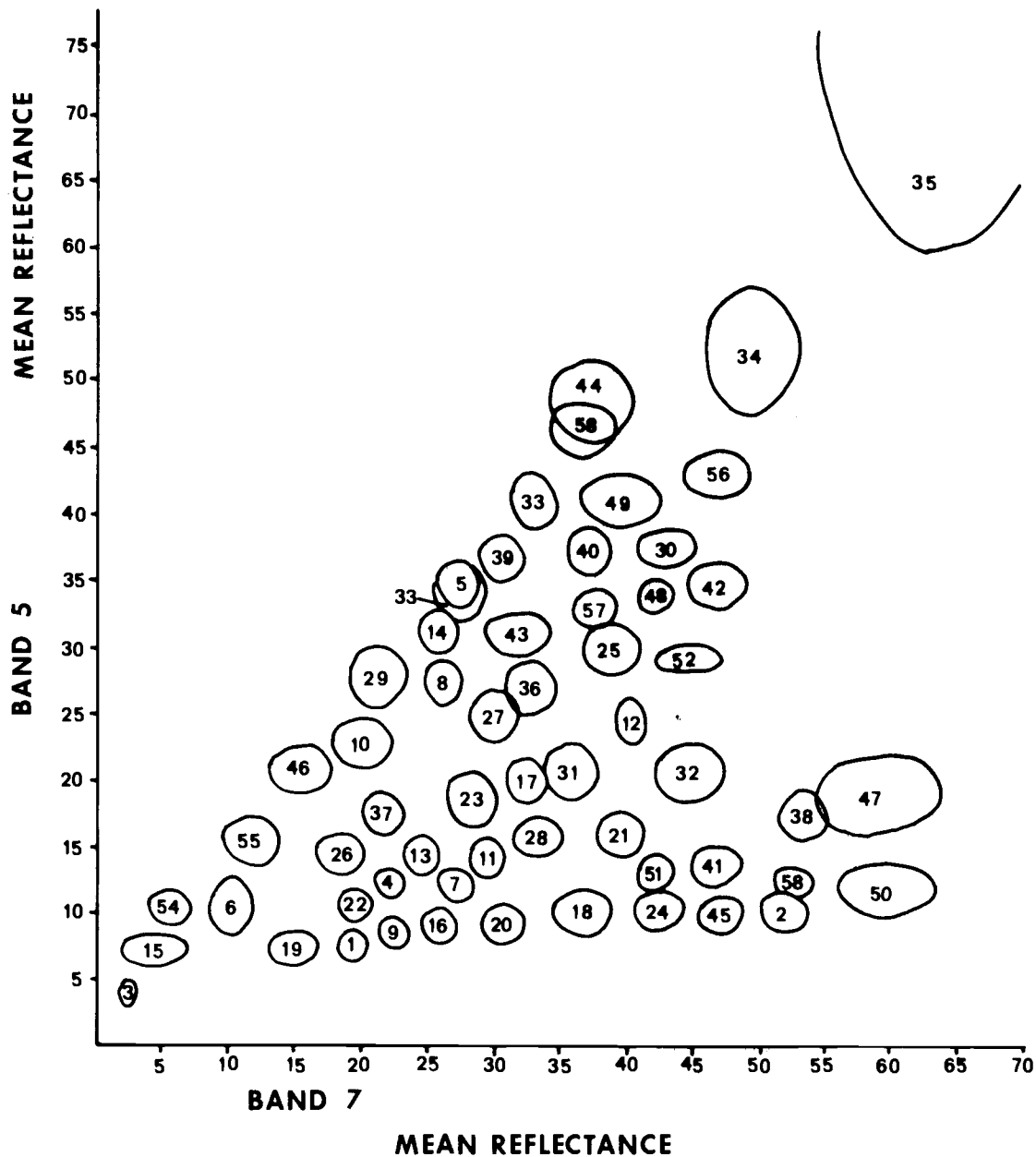
Spectral Reflectance Plotting



10 SEPT. 74

Figure 36 (continued)

Spectral Reflectance Plotting



10 SEPT. 74

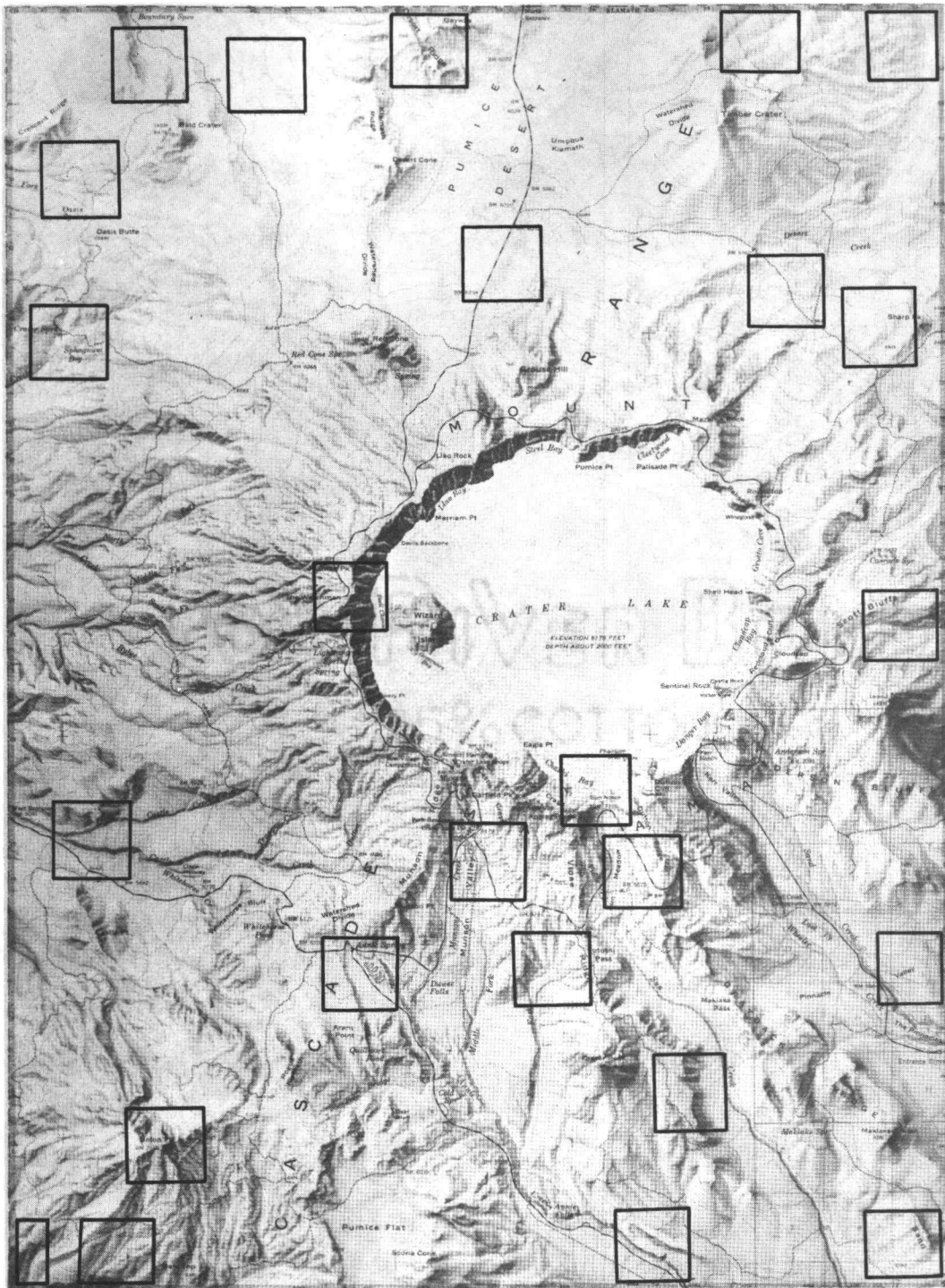
Figure 36 (continued)

and shape of the 59 generated LANDSAT training set classes through the spectral relationship plotting of bands 4 and 5, 4 and 6, 4 and 7, 5 and 6, 5 and 7, and 6 and 7. The graph produced through the plotting of bands 4 and 5 shows the 59 classes clustered so densely that most classes are unintelligible as to class location, size, and shape. The separation of spectral classes, representing various surface cover types within Crater Lake National Park, would be quite futile when employing only bands 4 and 5 because of the class overlap. Plotting of bands 4 and 6 produced better class separation, but numerous classes were still overlapped. The unoverlapped classes were densely clustered showing large spectral similarity between classes. Bands 4 and 7 show a greater dispersion of classes, but numerous classes were still partially combined. Bands 6 and 7 show the overlapping of various classes and the overall dense clustering of the 59 classes, similar to bands 4 and 5. Bands 5 and 6, and 5 and 7 show the best separation between the 59 classes with bands 5 and 7 providing the best class separation for all LANDSAT band combinations. Class pairs 44 and 58, 38 and 47, and 5 and 53 were still partially combined when bands 5 and 7 were plotted. By utilizing bands 4 and 7 for class pairs 44 and 58, and 5 and 58, and bands 5 and 6 for class pair 38 and 47, separation of all 59 classes was achieved. Class separation showing uniqueness of spectral reflectance is imperative to

obtain, prior to applying the training set class statistics to the entire study area, in order to achieve a "good fit" classification for the existing surface cover types within the Park.

Training Set Statistics

As a separate and parallel process with the strata mask generation, a set of training set statistics was generated by using the controlled clustering procedure on IDIMS. By using the IDIMS function "TSSelect," areas on the IDIMS display screen were chosen for potential training set candidates by outlining the area by means of a track-ball. The size of these outlined areas were 32 x 32 pixels. The size was chosen to be 32 x 32 pixels in order to have proper magnification on the IDIMS screen. These 32 x 32 pixel blocks are called Intensive Study Areas (ISA). The strategy in the placement of these ISA throughout Crater Lake National Park was to tap as much spectral variation in surface cover types within the Park as possible. The placement of 25 ISA was accomplished through use of ground truth information, photointerpretation of 1:122,000, 1:30,500, and 1:7,600 color infrared aerial photography, photointerpretation of terrestrial photography, and photointerpretation of a LANDSAT color composite displayed on the IDIMS CRT terminal. Figure 37 shows the placement of the ISA within the National Park.



Distribution of Intensive Study Areas
Within Crater Lake National Park



Figure 37

The method of locating and delineating the 25 ISA was to move the trackball of IDIMS to the desired area on the CRT screen. The trackball was placed in the upper left corner of the desired 32 x 32 pixel block area. The location of the trackball (scan line and pixel) was input to the computer. The complete 32 x 32 pixel block area was then drawn on the IDIMS screen. Once all ISA were chosen and delineated, the individual ISA were enlarged ten times. The trackball was then utilized to outline distinct surface cover type varieties within the enlarged ISA and to discard unwanted areas within the ISA. Areas were discarded because of surface cover type duplication or because only a portion of the surface cover type within the ISA was needed to secure satisfactory statistics. Training set statistics were then obtained from all the outlined areas within the ISA. The data from the 25 ISA were then input to an IDIMS function called "ISOCLS" of which the most significant function is its maximum standard deviation (STDMAX). This function calculated the mean value and standard deviation of naturally occurring clusters for all the input pixels. "STDMAX" then selected cluster center points at the mean value plus and minus one standard deviation. The computer function looked at each pixel again and reassigned pixels to the nearest cluster center. If the standard deviation of a cluster group was greater than "STDMAX," the cluster was split by adding and subtracting one standard deviation

to the mean and forming two new cluster centers. Once again, all pixels were reassigned to the clusters they were nearest to and the process continued until the standard deviation of each cluster was less than 2.20, the standard deviation employed in this study.

The clusters or classes formed in "ISOCLS" were grouped into naturally occurring clusters, as previously mentioned. The "ISOCLS" algorithm in IDIMS, which is an iterative algorithm, used a combination of distance measurements plus statistical parameters to help distinguish between classes. This type of procedure was used to train the maximum likelihood classifier (MLC) of IDIMS. The MLC was used to determine the statistical parameters which characterize the class. The MLC consisted of evaluating a probability density function for each pixel and assigning the pixel to the class for which the probability of occurrence was a maximum. Chi-square values were generated by the MLC function "CLASFY" to determine if and where additional training statistics should be generated. Classification accuracy can be greatly impaired if the training statistics do not effectively define a class (Kalensky, 1974). No additional training statistics were needed to be generated. Table 24 shows statistics for the 59 clusters or classes which were generated by the above-mentioned procedure. The statistics include the mean reflectance value per LANDSAT band per class, and a

Class Statistics (59)

CLASS	LABEL	TYPE	COMMENT	MEANS	MATRIX
1	TREE		CRATER LAKE NAT. PARK VEGETATION	14.36	7.79 16.81 17.76
				.64	
				.11	.66
				.02	.15 1.51
2	TREE		CRATER LAKE NAT. PARK VEGETATION	17.00	10.17 37.38 47.92
				.92	
				.75	1.64
				-.08	.19 1.65
				-.33	.01 .03 3.15
3	TREE		CRATER LAKE NAT. PARK VEGETATION	12.98	4.27 2.10 2.01
				.56	
				.08	.49
				.03	.07 .25
				.00	-.00 -.00 .92
4	TREE		CRATER LAKE NAT. PARK VEGETATION	16.73	12.16 19.34 20.42
				.69	
				.37	1.26
				-.03	-.07 .87
				-.14	-.16 .17 1.29
5	TREE		CRATER LAKE NAT. PARK VEGETATION	31.98	33.02 32.40 25.46
				4.08	
				.15	3.50
				-.46	-.16 1.43
				-.89	-.46 .04 2.92
6	TREE		CRATER LAKE NAT. PARK VEGETATION	15.89	10.51 11.67 9.23
				2.19	
				2.30	4.34
				.92	1.37 1.82
				.22	.36 1.12 1.99
7	TREE		CRATER LAKE NAT. PARK VEGETATION	16.72	11.80 22.42 24.95
				.56	
				.22	1.11
				.03	-.15 1.18
				.01	-.09 .24 1.56
8	TREE		CRATER LAKE NAT. PARK VEGETATION	25.80	26.37 28.57 24.07
				1.31	

Table 24

Table 24 (continued)

			.35	1.24		
			-.12	-.11	1.29	
			-.21	-.37	.30	1.77
17	LABEL:	TREE				
	TYPE:					
	SUB-TYPE:					
	COMMENT:	CRATER LAKE NAT. PARK VEGETATION				
	MEANS:	21.99	19.67	28.74	30.09	
	MATRIX:					
			1.43			
			-.32	2.14		
			-.14	.64	1.51	
			.22	-.30	.29	2.40
18	LABEL:	TREE				
	TYPE:					
	SUB-TYPE:					
	COMMENT:	CRATER LAKE NAT. PARK VEGETATION				
	MEANS:	16.37	10.12	28.05	33.68	
	MATRIX:					
			.86			
			.78	1.99		
			.29	.52	2.13	
			-.11	-.19	1.06	2.99
19	LABEL:	TREE				
	TYPE:					
	SUB-TYPE:					
	COMMENT:	CRATER LAKE NAT. PARK VEGETATION				
	MEANS:	14.10	7.52	13.19	13.77	
	MATRIX:					
			.97			
			.98	1.13		
			.38	.51	1.53	
			.46	.22	.99	2.82
20	LABEL:	TREE				
	TYPE:					
	SUB-TYPE:					
	COMMENT:	CRATER LAKE NAT. PARK VEGETATION				
	MEANS:	15.54	9.21	24.33	28.36	
	MATRIX:					
			.74			
			.57	1.66		
			.23	.22	1.27	
			-.06	-.07	.70	2.23
21	LABEL:	TREE				
	TYPE:					
	SUB-TYPE:					
	COMMENT:	CRATER LAKE NAT. PARK VEGETATION				
	MEANS:	19.48	15.66	31.34	36.61	
	MATRIX:					
			1.36			
			.64	2.23		
			.49	.04	1.31	
			.40	-.07	.32	2.83
22	LABEL:	TREE				
	TYPE:					
	SUB-TYPE:					
	COMMENT:	CRATER LAKE NAT. PARK VEGETATION				
	MEANS:	15.83	10.61	17.48	18.09	
	MATRIX:					
			.45			
			.19	1.00		
			.02	.04	.99	
			-.04	-.08	.28	1.34
23	LABEL:	TREE				
	TYPE:					
	SUB-TYPE:					
	COMMENT:	CRATER LAKE NAT. PARK VEGETATION				
	MEANS:	21.16	18.16	25.90	26.05	
	MATRIX:					
			1.95			
			1.34	3.38		
			.43	.41	1.47	
			-.55	-.93	-.01	2.62
24	LABEL:	TREE				
	TYPE:					
	SUB-TYPE:					
	COMMENT:	CRATER LAKE NAT. PARK VEGETATION				

Table 24 (continued)

	MEANS:	16.53	10.01	31.35	39.32
	MATRIX:				
		.89			
		-.65	1.91		
		-.11	-.00	1.26	
		-.23	-.15	.15	3.68
25	LABEL:	TREE			
	TYPE:				
	SUB-TYPE:				
	COMMENT:	CRATER LAKE NAT PARK VEGETATION			
	MEANS:	28.10	29.18	36.03	36.05
	MATRIX:				
		2.71			
		-.25	3.38		
		-.34	.10	2.64	
		-.21	.94	.38	3.89
26	LABEL:	TREE			
	TYPE:				
	SUB-TYPE:				
	COMMENT:	CRATER LAKE NAT PARK VEGETATION			
	MEANS:	18.77	14.45	19.30	16.86
	MATRIX:				
		1.72			
		.89	1.44		
		.77	.60	2.30	
		-.27	.11	1.18	2.72
27	LABEL:	TREE			
	TYPE:				
	SUB-TYPE:				
	COMMENT:	CRATER LAKE NAT PARK VEGETATION			
	MEANS:	23.99	24.11	29.89	28.01
	MATRIX:				
		1.45			
		.45	2.80		
		-.03	-.04	1.32	
		-.23	-.10	.45	2.66
28	LABEL:	TREE			
	TYPE:				
	SUB-TYPE:				
	COMMENT:	CRATER LAKE NAT PARK VEGETATION			
	MEANS:	18.97	15.48	27.77	30.77
	MATRIX:				
		1.41			
		.39	1.35		
		.14	.40	1.78	
		.08	-.04	.65	2.59
29	LABEL:	TREE			
	TYPE:				
	SUB-TYPE:				
	COMMENT:	CRATER LAKE NAT PARK VEGETATION			
	MEANS:	29.10	27.19	26.31	19.68
	MATRIX:				
		3.64			
		.40	3.25		
		.28	.81	3.28	
		-.60	-.10	1.62	4.28
30	LABEL:	TREE			
	TYPE:				
	SUB-TYPE:				
	COMMENT:	CRATER LAKE NAT PARK VEGETATION			
	MEANS:	34.47	36.18	43.00	40.00
	MATRIX:				
		2.25			
		-.20	1.72		
		.47	.12	3.77	
		.06	-.47	1.76	3.88
31	LABEL:	TREE			
	TYPE:				
	SUB-TYPE:				
	COMMENT:	CRATER LAKE NAT PARK VEGETATION			
	MEANS:	22.19	20.29	31.92	33.39
	MATRIX:				
		1.14			
		.95	3.80		
		.03	.38	1.74	
		.08	-.31	.12	3.25
32	LABEL:	TREE			

Table 24 (continued)

		TYPE:					
		SUB-TYPE:					
		COMMENT:	CRATER LAKE NAT PARK VEGETATION				
		MEANS:	22.00	20.00	36.81	41.63	
		MATRIX:					
			1.25				
			-.06	4.63			
			.69	.38	2.03		
			.75	-.87	1.30	6.11	
33		LABEL:	TREE				
		TYPE:					
		SUB-TYPE:					
		COMMENT:	CRATER LAKE NAT PARK VEGETATION				
		MEANS:	37.25	39.36	39.25	30.58	
		MATRIX:					
			3.69				
			.85	4.34			
			-.17	1.94	3.97		
			.10	-.04	.91	3.24	
34		LABEL:	TREE				
		TYPE:					
		SUB-TYPE:					
		COMMENT:	CRATER LAKE NAT PARK VEGETATION				
		MEANS:	44.35	50.15	53.50	45.90	
		MATRIX:					
			38.93				
			23.05	23.53			
			11.18	15.88	19.15		
			-7.26	1.72	8.35	11.79	
35		LABEL:	TREE				
		TYPE:					
		SUB-TYPE:					
		COMMENT:	CRATER LAKE NAT PARK VEGETATION				
		MEANS:	72.43	80.00	75.14	59.14	
		MATRIX:					
			404.82				
			446.71	521.14			
			314.37	387.29	290.41		
			154.94	177.71	154.12	20.12	
36		LABEL:	TREE				
		TYPE:					
		SUB-TYPE:					
		COMMENT:	CRATER LAKE NAT PARK VEGETATION				
		MEANS:	25.56	25.92	32.80	30.52	
		MATRIX:					
			2.44				
			-.12	3.09			
			-.49	-.13	1.57		
			.40	-.91	-.09	3.35	
37		LABEL:	TREE				
		TYPE:					
		SUB-TYPE:					
		COMMENT:	CRATER LAKE NAT PARK VEGETATION				
		MEANS:	20.92	17.41	22.41	20.02	
		MATRIX:					
			1.44				
			.78	2.12			
			.15	.54	2.20		
			-.12	.03	1.07	2.84	
38		LABEL:	TREE				
		TYPE:					
		SUB-TYPE:					
		COMMENT:	CRATER LAKE NAT PARK VEGETATION				
		MEANS:	21.56	16.62	42.25	49.50	
		MATRIX:					
			2.12				
			1.77	2.73			
			-.27	.53	3.81		
			-1.34	-1.06	.00	3.25	
39		LABEL:	TREE				
		TYPE:					
		SUB-TYPE:					
		COMMENT:	CRATER LAKE NAT PARK VEGETATION				
		MEANS:	31.07	35.22	35.65	28.55	
		MATRIX:					
			3.46				
			.25	2.17			
			-.08	-.11	2.55		

Table 24 (continued)

40			.92	-.28	.30	2.87	
	LABEL:	TREE					
	TYPE:						
	SUB-TYPE:						
	COMMENT:	CRATER LAKE NAT. PARK VEGETATION					
	MEANS:	31.82	35.94	39.41	34.35		
	MATRIX:						
		4.03					
		-.72	3.11				
		-1.22	.61	3.65			
41		-.05	-.74	1.44	2.35		
	LABEL:	TREE					
	TYPE:						
	SUB-TYPE:						
	COMMENT:	CRATER LAKE NAT. PARK VEGETATION					
	MEANS:	18.86	13.74	35.79	43.48		
	MATRIX:						
		.93					
		.53	1.72				
		-.13	-.03	2.41			
42		.07	.34	.60	2.68		
	LABEL:	TREE					
	TYPE:						
	SUB-TYPE:						
	COMMENT:	CRATER LAKE NAT. PARK VEGETATION					
	MEANS:	29.92	33.92	43.62	43.54		
	MATRIX:						
		4.38					
		1.53	2.23				
		1.82	.13	5.01			
43		.27	.58	1.98	3.79		
	LABEL:	TREE					
	TYPE:						
	SUB-TYPE:						
	COMMENT:	CRATER LAKE NAT. PARK VEGETATION					
	MEANS:	29.09	30.28	33.78	29.46		
	MATRIX:						
		2.53					
		.88	2.13				
		-.18	.15	1.62			
44		.60	.30	.40	4.58		
	LABEL:	TREE					
	TYPE:						
	SUB-TYPE:						
	COMMENT:	CRATER LAKE NAT. PARK VEGETATION					
	MEANS:	45.38	46.85	45.46	34.77		
	MATRIX:						
		9.78					
		-.32	9.52				
		-.02	1.76	4.40			
45		-3.76	4.58	5.11	9.87		
	LABEL:	TREE					
	TYPE:						
	SUB-TYPE:						
	COMMENT:	CRATER LAKE NAT. PARK VEGETATION					
	MEANS:	16.65	9.87	34.65	43.50		
	MATRIX:						
		.98					
		.66	1.44				
		.35	.39	1.85			
46		-.18	-.05	-.34	2.42		
	LABEL:	TREE					
	TYPE:						
	SUB-TYPE:						
	COMMENT:	CRATER LAKE NAT. PARK VEGETATION					
	MEANS:	25.81	20.62	19.25	14.31		
	MATRIX:						
		4.78					
		.99	2.23				
		-.77	.78	2.44			
47		-.07	.74	2.17	5.34		
	LABEL:	TREE					
	TYPE:						
	SUB-TYPE:						
	COMMENT:	CRATER LAKE NAT. PARK VEGETATION					
	MEANS:	22.42	18.21	47.89	54.68		
	MATRIX:						
		3.40					
		3.54	7.22				

Table 24 (continued)

48	LABEL:	-1.22	-1.61	5.99	20.32
	TYPE:	-4.45	-7.67	8.28	
	SUB-TYPE:	TREE			
	COMMENT:	CRATER LAKE NAT. PARK VEGETATION			
	MEANS:	32.19	32.56	41.87	39.19
	MATRIX:				
		1.78			
		.11	1.62		
		.52	.88	4.11	
49	LABEL:	15	-60	.15	1.15
	TYPE:	TREE			
	SUB-TYPE:				
	COMMENT:	CRATER LAKE NAT. PARK VEGETATION			
	MEANS:	38.09	39.68	43.32	36.82
	MATRIX:				
		1.36			
		.71	2.94		
		.38	.97	2.03	
50	LABEL:	-89	.03	.69	7.79
	TYPE:	TREE			
	SUB-TYPE:				
	COMMENT:	CRATER LAKE NAT. PARK VEGETATION			
	MEANS:	18.00	12.20	44.00	55.10
	MATRIX:				
		.80			
		1.30	3.36		
		.30	.70	4.60	
51	LABEL:	.60	1.98	4.40	11.29
	TYPE:	TREE			
	SUB-TYPE:				
	COMMENT:	CRATER LAKE NAT. PARK VEGETATION			
	MEANS:	17.84	12.84	33.84	38.98
	MATRIX:				
		.61			
		.58	2.20		
		.05	.03	2.41	
52	LABEL:	.46	.50	.08	2.16
	TYPE:	TREE			
	SUB-TYPE:				
	COMMENT:	CRATER LAKE NAT. PARK VEGETATION			
	MEANS:	28.00	28.47	41.33	41.53
	MATRIX:				
		5.47			
		-1.27	1.05		
		.27	.78	2.49	
53	LABEL:	1.20	.55	2.49	5.18
	TYPE:	TREE			
	SUB-TYPE:				
	COMMENT:	CRATER LAKE NAT. PARK VEGETATION			
	MEANS:	28.07	33.37	32.15	25.40
	MATRIX:				
		.76			
		.47	1.82		
		.31	.29	1.99	
54	LABEL:	13	-.03	.81	1.93
	TYPE:	TREE			
	SUB-TYPE:				
	COMMENT:	CRATER LAKE NAT. PARK VEGETATION			
	MEANS:	16.28	10.40	9.02	4.95
	MATRIX:				
		2.60			
		1.36	1.69		
		.04	.47	1.37	
55	LABEL:	-71	.02	.93	2.20
	TYPE:	TREE			
	SUB-TYPE:				
	COMMENT:	CRATER LAKE NAT. PARK VEGETATION			
	MEANS:	19.57	15.43	15.62	10.90

Table 24 (continued)

	MATRIX:				
		2.72			
		1.47	2.44		
		-.02	.83	2.71	
		-.47	-.20	2.30	3.61
56	LABEL:	TREE			
	TYPE:				
	SUB-TYPE:				
	COMMENT:	CRATER LAKE NAT PARK VEGETATION			
	MEANS:	39.17	41.42	50.42	43.50
	MATRIX:				
		7.47			
		2.93	2.41		
		4.10	1.24	3.74	
		-.42	-.79	1.04	5.42
57	LABEL:	TREE			
	TYPE:				
	SUB-TYPE:				
	COMMENT:	CRATER LAKE NAT PARK VEGETATION			
	MEANS:	31.93	31.40	38.53	34.80
	MATRIX:				
		3.00			
		.29	1.44		
		-1.23	-.35	2.25	
		-1.08	-1.19	.64	2.16
58	LABEL:	TREE			
	TYPE:				
	SUB-TYPE:				
	COMMENT:	CRATER LAKE NAT PARK VEGETATION			
	MEANS:	38.92	44.88	44.40	34.08
	MATRIX:				
		4.07			
		-.81	2.99		
		-.73	-.79	2.40	
		-.23	.57	1.81	5.59
59	LABEL:	TREE			
	TYPE:				
	SUB-TYPE:				
	COMMENT:	CRATER LAKE NAT PARK VEGETATION			
	MEANS:	18.36	12.82	40.64	48.73
	MATRIX:				
		.41			
		.16	1.06		
		.13	-.43	2.59	
		.10	.68	.45	1.45

covariance matrix of all four MSS bands per class. The mean value per band for each class, together with the covariance matrix, defines the shape of the class which provides an indication of class quality or uniqueness (Figure 35). Distances between clusters for the 59 classes appear in Appendix I. Distance between clusters is the euclidean distance measured in space between classes generated through the function "ISOCLS." This measure indicates distance between clusters or classes with a large value indicating greater distinction between classes and a small value indicating statistical relatedness between classes. These distance between cluster statistics in Appendix I also aid in evaluating the quality of the 59 classes. In Appendix I, the distance between classes number from 1 to 60 and not 1 to 59 because class three was deleted due to an error in computing which resulted in a standard deviation and mean reflectance for band 7 being equal to zero. In Appendix I, the weighted divergence of class pairs for all 59 classes is also presented. Weighted divergence is a saturated transformed divergence measure based on the covariance. Weighted divergence is also a measure of the statistical distance between classes. The weighted divergence statistics in Appendix I were used to determine if any class pairs should be combined due to statistical relatedness or if the 59 classes were statistically separate and unique. A weighted divergence value of 2,000

represents no statistical relatedness between class pairs and, therefore, a "good" statistical distinction exists. A weighted divergence value of 1,000 or less represents a class pair which is statistically related and should be combined. A review of Appendix I shows that all 59 classes are statistically "good" for training set statistics.

Classification

Classification is the process of assigning each of the pixels of a LANDSAT scene study area to a class based upon the set of input statistics generated by training set selection and cluster formation (Swain, 1972). An inference is made in a classification that the training set classes adequately represent the reflectance values found throughout the entire study area. "CLASFY," as previously mentioned, does alleviate this concern.

The entire 512 x 512 pixel study area on IDIMS was classified by the maximum likelihood classifier. Appendix II shows the distribution of the 59 classes throughout the 512 x 512 pixel area, with a symbol representing each class. Each symbol represents a LANDSAT pixel area of 1.118 acres (0.452 ha).

In addition to representing the distribution of the 59 classes throughout the 512 x 512 pixel study area in an alphanumeric format through IDIMS, a graylevel representation of the 59 classes was presented on the IDIMS CRT

screen. It was extremely difficult if not impossible to visually appreciate 59 different levels of gray throughout the study area. It can also be very confusing to study the distribution of 59 classes on the alphanumeric printout in Appendix II. For presentation purposes, classes were grouped according to their statistical and spatial relatedness and displayed on IDIMS with a different color representing a different class or group of classes. These two class analysis parameters (statistical and spatial) are inefficient and ineffective for combining classes when used independently, but when both a statistical and spatial analysis of each class is completed, the process of combining classes becomes more efficient and effective (Kirvida, 1973).

Reflectance statistics were generated and available in hard copy for examination. Since LANDSAT bands 5 and 7, through spectral relationship plots, were shown to best discriminate between surface cover types within Crater Lake National Park, they were heavily relied upon in combining classes. The spatial parameter for class analysis was available through use of the IDIMS CRT display. As described in Chapter V, there are various factors which influence reflectance values as detected by LANDSAT. Such factors include slope angle, slope aspect, surface cover type, crown density, and crown size. If, for example, the reflectance values of two identical surface cover types are

obtained with the only difference between the two surface cover types being slope angle and slope aspect, the obtained reflectance values may be sufficiently different as to indicate the occurrence of two extremely different surface cover types. If classes are combined solely on the basis of reflectance statistics, the accuracy of the combined classes in depicting surface cover types can expectedly be low. If ground truth and photointerpretation in the study area has been extensive, the process of displaying a class or group of classes on the IDIMS CRT screen, studying its spatial organization and reflectance statistics in order to combine classes into similar surface cover types, can be very effective and accurate. Each class was displayed on IDIMS individually, in a bright color to appreciate very small pixel clusters. Classes were combined into the same color to further study spatial similarity of classes within the study area.

The IDIMS computer has available 30 different colors for display. Approximately 12 colors, however, can be adequately distinguished on the IDIMS screen. Therefore, prior to the combining of classes, the 12 most important classes for the classification purposes of this research were listed and studied. Since coniferous tree species differentiation is a major concern within this study, the classes which represented different coniferous tree types were not combined. Numerous pumice classes were combined,

since only one pumice class was desired to be mapped and presented on IDIMS. The result of combining various combinations of the 59 classes was the production of a 12-class color coded surface cover type map displayed on IDIMS for the 512 x 512 pixel area. Figure 38 is a photographic reproduction of the 12-class color coded map which has been statistically masked in order to show only the area color coded within Crater Lake National Park. A description of the surface cover type represented by which color is also shown in Figure 38. The color coded photograph was reproduced from an Optronix system film positive produced at the EROS Data Center. The Optronix product was constructed from the 12-class color coding done on the IDIMS computer. Figure 39 shows which of the 59 classes were combined, together with the mean reflectance values per band for each class. An examination of Figure 39 shows how important the spatial parameter was in combining classes because reflectance values of many classes which were combined are not spectrally similar in all four LANDSAT MSS bands due primarily to environmental factors modifying the reflectance and variation within forest communities. Figure 40 (in pocket) is an alphanumeric printout of the 59 classes, which has been masked to show only the area within Crater Lake National Park, at a scale of 1:62,500. Each symbol equals approximately seven acres (2.83 ha). A key of the surface cover types represented by each class is shown as

Color Coded Map of Crater
Lake National Park



Figure 38

Key to Figure 38

Symbol	Color	Surface Cover Type and Percent Coverage
-	Sand	Ponderosa pine, large, densely stocked and/or shasta red fir, large, moderately stocked (3.54%).
+	Medium Blue	Ponderosa pine, large, poorly stocked and/or shasta red fir, large, poorly stocked (5.79%).
%	Yellow	Ponderosa pine (65%) and white fir (35%) (1.95%).
⌋	Green	White fir (75%) and shasta red fir and/or ponderosa pine (6.71%).
\$	Peach	Mountain hemlock (80%) and shasta red fir (20%) (17.60%).
⌘	Brown	Shasta red fir (80%) and mountain hemlock (20%) (10.27%).
#	Black	Water (8.46%).
.	Blue-green	Pumice fields, rock outcrops, and bare soil (8.35%).
1	Dark green	Lodgepole pine (80%), densely stocked with scattered amounts of related pines, firs, and hemlock (14.16%).
0	Purple	Lodgepole pine (80%), poorly stocked with scattered amounts of related pines, firs, and hemlock (19.22%).
*	Dark Gray	Shadow and boundary pixels of land-water interface; scattered deciduous and brush associated with steep moist areas (1.03%).
^	Red	Scattered tree and light brush on pumice underlying canopy openings (2.92%).

Figure 38

Combining of Classes of Color Designation

Class Color	Mean Reflectance per LANDSAT Band				Class
	Band 4	Band 5	Band 6	Band 7	
Green	15.34	08.90	21.02	23.95	16
Red	24.64	23.82	34.64	37.32	12
	21.99	19.67	28.74	30.09	17
	16.53	10.01	31.35	39.32	24
	18.97	15.48	27.77	30.77	28
	22.19	20.29	31.92	33.39	31
Sand	17.87	13.90	24.70	27.32	11
Brown	14.82	08.43	18.59	20.77	09
	14.10	07.52	13.19	13.77	19
Black	12.98	04.27	02.10	02.01	03
	14.07	07.20	06.56	04.02	15
Medblue	16.72	11.80	22.42	24.95	07
Yellow	16.37	10.12	28.05	33.69	18
	15.54	09.21	24.35	28.36	20
Peach	14.36	07.79	16.61	17.76	01
Purple	16.73	12.16	19.34	20.42	04
	24.64	23.82	34.64	37.32	13
	18.77	14.45	18.30	16.86	26
Dkgreen	15.83	10.61	17.48	18.09	22
Dkgray	17.00	10.17	37.38	47.92	02
	15.89	10.51	11.67	09.29	06
	19.48	15.66	31.34	36.61	21
	18.86	13.74	35.79	43.48	41
	16.65	09.81	34.65	43.50	45
	25.81	20.62	19.25	14.31	46
	18.00	12.20	44.00	55.10	50
	16.28	10.40	09.02	04.95	54
	19.57	15.43	15.62	10.90	55
Bluegreen	31.98	33.02	32.40	25.46	05
	25.80	26.37	28.57	24.27	08
	24.41	22.19	23.70	18.68	10
	29.08	30.21	30.44	24.06	14
	21.16	18.16	25.90	26.05	23
	28.10	29.18	36.03	36.05	25
	23.99	24.11	29.89	28.01	27

Figure 39

Figure 39 (continued)

Class Color	Mean Reflectance per LANDSAT Band				Class
	Band 4	Band 5	Band 6	Band 7	
Bluegreen (continued)					
	29.10	27.19	26.31	19.68	29
	34.47	36.18	43.00	40.00	30
	22.00	20.00	36.81	41.63	32
	37.25	39.36	39.25	30.58	33
	44.35	50.15	53.50	45.90	34
	72.43	80.00	75.14	59.14	35
	25.56	25.92	32.80	30.52	36
	20.92	17.41	22.41	20.02	37
	21.56	16.62	42.25	49.50	38
	31.67	35.22	35.65	28.55	39
	31.82	35.94	39.41	34.35	40
	29.92	33.92	43.62	43.54	42
	29.09	30.28	33.78	29.46	43
	45.38	46.85	45.46	34.77	44
	22.42	18.21	47.89	54.68	47
	32.19	32.56	41.87	39.19	48
	38.09	39.68	43.32	36.82	49
	17.84	12.84	33.84	38.98	51
	28.00	28.47	41.33	41.53	52
	28.07	33.37	32.15	25.40	53
	39.16	41.42	50.42	43.50	56
	31.93	31.40	38.53	34.80	57
	38.92	44.88	44.40	34.08	58
	18.36	12.82	40.64	48.73	59

Figure 39

part of Figure 40 in the text (page 213). Correlation of surface cover types with spatial and spectral LANDSAT data is difficult due to the integrated and overlapped pixel area and the spatial and spectral variation of forest cover types (Sayn-Wittgenstein and Kalensky, 1974). The generation of Figure 40 was accomplished by resampling the data used to generate the alphanumeric printout appearing in Appendix II. The initial scale of the alphanumeric printout in Appendix II of the 512 x 512 pixel study area of Crater Lake National Park and vicinity was approximately 1:25,000 prior to reduction for presentation purposes, with each symbol being equivalent to 1.118 acres (0.452 ha). The 1:62,500 scale in alphanumeric printout of Crater Lake National Park (Figure 40, in pocket) was accomplished without combining classes, from the 1:25,000 scale printout, represented by symbols, but by a resampling scheme based on the nearest neighbor function from the 1:25,000 scale printout. A transformation algorithm was employed that determined which data point to extract from the 1:25,000 scale alphanumeric printout to be printed on the 1:62,500 scale product. The transformation algorithm, for example, scans the desired scale output product (1:62,500) and scans the 1:25,000 printout for data point 10, 20 (scan line 10, pixel 20), which appears on the 1:62,500 product. Since the transformation algorithm is resampling data points (represented by class symbols) from a pool of more data

Key to Figure 40. (in pocket)

Class number	Class symbol	Surface cover types of the generated 59 spectral classes
1	1	Mountain hemlock (80%) with scattered shasta red fir (20%).
2	2	Wax currant, newberry's knotweed, sticky currant on a pumice soil.
3	3	Water.
4	4	Lodgepole pine poorly stocked with 5-10% western white pine. Most dense of the three poorly stocked lodgepole pine classes. Large amount of downed materials on a pumice soil.
5	5	Pumice, dense with slight cover of newberry's knotweed, silvery ragwort, geyer's everlasting, and grass types. Scattered sandy drywash areas are intermixed.
6	6	Bare rock and basalt outcrops on steep slopes and in heavily shadowed areas. Sparse, small groups of trees occur which include western white pine, shasta red fir, and mountain hemlock.
7	7	Ponderosa pine, large and poorly stocked. Understory includes a sparse cover of green-leaf manzanita, pinemat manzanita, and wax currant on dry, often sandy pumice.
8	8	Pumice with scattered dry-wash areas (sandy pumice) and scattered denser pumice drainage areas. A few scattered lodgepole pine occur which are invading the pumicefield. Existing cover includes newberry's knotweed, silvery eriogonum, and Anderson lupine.
9	9	Shasta red fir (80%) with scattered mountain hemlock (20%).
10	A	Pumice, densely drained with small and sparse lodgepole pine clusters. Existing vegetation is similar to class 5.
11	B	Ponderosa pine and shasta red fir. Medium stocked. Understory vegetation includes a sparse cover of pinemat manzanita, and a

Figure 40 (continued)

Class number	Class symbol	Surface cover types of the generated 59 spectral classes
		small amount of snowbrush ceanothus on pumice.
12	C	Sparse newberry's knotweed and dwarf monkey flower on a pumice soil.
13	D	Lodgepole pine, poorly stocked. Least stocked of any of the three poorly stocked lodgepole pine areas. Large amount of downed materials.
14	E	Pumice, similar to class 5, but less sandy drywash areas.
15	F	Water.
16	G	White fir with scattered amounts of ponderosa pine, shasta red fir, and a very small amount of Douglas-fir. Shasta red fir is the dominant secondary species in all areas of this class except in the southern panhandle, where ponderosa pine dominates.
17	H	Medium to high density of newberry's knotweed, silvery eriogonum, geyer's everlasting, silvery ragwort, and Anderson lupine on pumice field with some very small clumps of invading lodgepole pine.
18	I	Relatively dense and moist sitka alder and swamp huckleberry with scattered amounts of shasta red fir and subalpine fir.
19	J	Shasta red fir (60%) and mountain hemlock (40%), dense stocking and generally occurring on steep slopes.
20	K	Low to medium density shasta red fir, white fir and/or ponderosa pine with snowbrush ceanothus and greenleaf manzanita on pumice soil.
21	L	Similar to class 18 but less moist and a greater density of brush.
22	M	Lodgepole pine, densely stocked.

Figure 40 (continued)

Class number	Class symbol	Surface cover types of the generated 59 spectra classes
23	N	Dense grass and herbaceous plants on a scattered pumice soil.
24	O	Similar to class 18, but less moist and no scattered shasta red fir, and very little subalpine fir.
25	P	Pumice and bare rock.
26	Q	Lodgepole pine, poorly stocked with a small amount of western white pine. Intermediate density of the three poorly stocked lodgepole pine classes. Large amount of downed materials.
27	R	Similar to class 17, but less vegetation and more drained pumice.
28	S	Scattered mountain hemlock on a mix of dense and sandy pumice.
29	T	Pumice, very dense due to drainage near the outer periphery of the pumice desert.
30	U	Extremely sandy pumice, large drywash areas in pumice desert.
31	V	Similar to class 28, but denser pumice, less sandy pumice, and more newberry's knotweed, etc., similar to class 17.
32	W	Sparse brush on pumice soil, generally south facing. Brush includes snowbrush ceanothus.
33	X	Sandy pumice drywash with intermixed drained dense pumice.
34	Y	Similar to class 30, but also trace of snow and bare rock.
35	Z	Bare rock and possibly a trace of snow on south facing slopes.
36	@	Similar to class 17, but more drywash sandy pumice.

Figure 40 (continued)

Class number	Class symbol	Surface cover types of the generated 59 spectra classes
37	\	Lodgepole pine-pumice desert interface. Small amount of lodgepole pine, very poorly stocked. Class is mainly a very dense drained pumice.
38	-	Brush, such as snowbrush ceanothus, green-leaf manzanita, pinemat manzanita, and wax currant on pumice soil.
39	*	Pumice and bare rock.
40	+	Similar to class 33.
41	⊗	Similar to class 38, but large and more numerous clusters of mountain hemlock.
42	=	Pumice and bare rock mix on a generally south facing slope.
43	.	Similar to class 5, but greater amount and extent of drywashes.
44	<	Very sandy pumice and south facing barerock slopes.
45	>	Shasta red fir and mountain hemlock, very low density, on pumice slopes.
46	[Sitka alder, and black cottonwood on the north facing slope of the caldera, near the water edge.
47]	Similar to class 38, but more bare rock or pumice.
48	!	Bare rock with a few scattered mountain hemlock.
49	%	Similar to class 33.
50	#	Brush and grasses on a pumice surface or rock outcrop, also scattered shasta red fir and mountain hemlock.
51	:	Similar to class 38, but denser brush.

Figure 40 (continued)

Class number	Class symbol	Surface cover types of the generated 59 spectra classes
52	;	Mottled appearance of pumice, bare rock, sandy pumice, and very sparse mountain hemlock.
53	,	Similar to class 43.
54	Ⓐ	Shadows and shadow-water interface.
55	Ⓑ	Steep sloped rock outcrops near the caldera rim, with scattered mountain hemlock, generally on a north facing slope.
56	Ⓒ	Bare rock.
57	Ⓓ	Bare rock, similar to class 56, but with aspect changes.
58	Ⓔ	Bare rock, similar to class 56, but with aspect changes.
59	Ⓕ	Similar to class 50, but with a few more scattered shasta red fir and mountain hemlock.

Figure 40
(map in pocket)

points (each symbol equals 1.118 acres (0.452 ha); scale of the printout 1:25,000) to an output product of less data points (each symbol equals 7.0 acres (2.83 ha); scale of the printout equals 1:62,500), the transformation algorithm cannot locate a data point for location 10, 20, but finds a number of points which are clustered around data point location 10, 20. By utilizing the nearest neighbor function, the transformation algorithm determines which data point in the cluster will be selected to represent location 10, 20 on the 1:62,500 alphanumeric printout. Figure 41 (in pocket) is an alphanumeric printout of the 12 classes color coded and generalized for presentation purposes. Each symbol also equals approximately seven acres (2.83 ha). This printout is also only for Crater Lake National Park; the remainder of the 512 x 512 pixel area has been masked out. The summary statistics for the 59 classes and the 12 classes within the Park are shown in Table 25. The summary data includes the symbol used in the alphanumeric printout for each of the 12 classes (Figure 41); the colors used to code the distribution of the 12 generalized classes throughout the Park (Figure 38); the pixel count for each of the 59 classes and the individual and total count for each of the 12 classes; the percent area covered by each of the 59 classes and the individual and total percent area covered for each of the 12 classes; the acreage covered within the Park for each of the 59 classes and the

Summary Data

Symbol	Color	Pixel count	% area	Class	Computed acreage/ha*	
}	Green		<u>9,580</u>	<u>6.708</u>	16	<u>10,710.44</u>
		Total	9,580	6.708		10,710.44 (4,331.0 ha)
^	Red		351	0.246	12	392.42 (158.68 ha)
			1,261	0.883	17	1,409.80 (570.07 ha)
			142	0.099	24	158.76 (64.20 ha)
			1,697	1.188	28	1,897.25 (767.19 ha)
			727	0.509	31	812.79 (328.67 ha)
	Total	<u>4,178</u>	<u>2.922</u>		<u>4,671.02</u> (1,888.81 ha)	
-	Sand		<u>5,057</u>	<u>3.541</u>	11	<u>5,653.73</u> (2,286.18 ha)
		Total	5,057	3.541		5,653.73 (2,286.18 ha)
&	Brown		21,790	15.257	9	24,361.22 (9,850.88 ha)
			3,342	2.340	19	3,736.36 (1,510.86 ha)
		Total	<u>25,132</u>	<u>17.597</u>		<u>28,097.58</u> (11,361.74 ha)
#	Black		2,467	1.727	3	2,758.11 (1,115.29 ha)
			9,621	6.736	15	10,756.28 (4,349.49 ha)
		Total	<u>12,088</u>	<u>8.463</u>		<u>13,514.39</u> (5,464.78 ha)
+	Medblue		<u>8,269</u>	<u>5.790</u>	7	<u>9,244.74</u> (3,738.27 ha)
		Total	8,269	5.790		9,244.74 (3,738.27 ha)

Table 25

Table 25 (continued)

Symbol	Color	Pixel count	% area	Class	Computed acreage/ha*
%	Yellow	771	0.540	18	861.98 (348.56 ha)
		2,016	1.412	20	2,253.89 (911.40 ha)
		<u>2,787</u>	<u>1.952</u>		<u>3,115.87</u> (1,259.96 ha)
Total					
\$	Peach	14,667	10.270	1	16,397.71 (6,630.70 ha)
		<u>14,667</u>	<u>10.270</u>		<u>16,397.71</u> (6,630.70 ha)
Total					
O	Purple	17,564	12.298	4	19,636.55 (7,940.38 ha)
		6,888	4.823	13	7,700.78 (3,113.94 ha)
		2,990	2.094	26	3,342.82 (1,351.73 ha)
		<u>27,442</u>	<u>19.215</u>		<u>30,680.15</u> (12,406.04 ha)
Total					
1	DkGreen	20,223	14.160	22	22,609.32 (9,142.47 ha)
		<u>20,223</u>	<u>14.160</u>		<u>22,609.32</u> (9,142.47 ha)
Total					
*	DkGray	19	0.013	2	21.24 (8.59 ha)
		528	0.370	6	590.30 (238.70 ha)
		323	0.226	21	361.11 (146.02 ha)
		74	0.052	41	82.73 (33.45 ha)
		40	0.028	45	44.72 (18.08 ha)
		82	0.057	46	91.68 (37.07 ha)
		8	0.006	50	8.94 (3.62 ha)

Table 25 (continued)

Symbol	Color	Pixel count	% area	Class	Computed acreage/ha*
	DkGray (continued)				
		186	0.130	54	207.95 (84.09 ha)
		204	0.143	55	228.07 (92.22 ha)
	Total	<u>1,464</u>	<u>1.025</u>		<u>1,636.74</u> (661.84 ha)
	Bluegreen	341	0.239	5	381.24 (154.16 ha)
		1,090	0.763	8	1,218.62 (492.77 ha)
		412	0.288	10	460.62 (186.26 ha)
		673	0.471	14	752.41 (304.25 ha)
		2,720	1.905	23	3,040.96 (1,229.66 ha)
		457	0.320	25	510.93 (206.60 ha)
		1,079	0.756	27	1,206.32 (487.80 ha)
		208	0.146	29	232.54 (94.03 ha)
		103	0.072	30	115.15 (46.56 ha)
		111	0.078	32	124.10 (50.18 ha)
		168	0.118	33	187.82 (75.95 ha)
		115	0.081	34	128.57 (51.99 ha)
		60	0.042	35	67.10 (27.13 ha)
		973	0.681	36	1,087.81 (439.87 ha)
		1,272	0.891	37	1,422.10 (575.05 ha)

Table 25 (continued)

Symbol	Color	Pixel count	% area	Class	Computed acreage/ha*
Bluegreen (continued)					
		20	0.014	38	22.36 (9.04 ha)
		216	0.151	39	241.49 (97.65 ha)
		156	0.109	40	174.41 (70.53 ha)
		101	0.071	42	112.92 (45.66 ha)
		481	0.337	43	537.76 (217.45 ha)
		69	0.048	44	77.14 (31.19 ha)
		49	0.034	47	54.78 (22.15 ha)
		102	0.071	48	114.04 (46.11 ha)
		106	0.074	49	118.51 (47.92 ha)
		107	0.075	51	119.63 (48.37 ha)
		138	0.097	52	154.28 (62.39 ha)
		339	0.237	53	379.00 (153.26 ha)
		35	0.025	56	39.13 (15.82 ha)
		128	0.090	57	143.10 (57.86 ha)
		83	0.058	58	92.79 (37.52 ha)
		12	0.008	59	13.42 5.43 ha)
		<u>11,944</u>	<u>8.350</u>		<u>13,331.05</u> <u>(5,390.64 ha)</u>
					<u>159,663.00</u> <u>(64,562.47 ha)</u>

*Pixel count x 1.118 acres).

individual and total acreage for each of the 12 classes; and the total acreage for the entire Crater Lake National Park.

The surface cover type maps of Crater Lake National Park (Figures 38, 40, and 41) produced through use of LANDSAT digital tapes, provides an appreciation of the distribution of dominant surface cover types, especially tree species, within the Park. Small percentage mixtures of tree species within more dominant tree species stands, for example, do not have a particular mapping class assigned to them because of their limited areal extent, which made the obtaining and isolating of reflectance value statistics for that tree type extremely difficult. Through "ground truth" activities, photointerpretation, and plant association information, some minor species (based on areal extent), such as western white pine, have been combined with dominant species in the listing of which surface cover types are represented by which spectral classes. A similar procedure was employed in assigning understory surface cover types to particular classes. In some cases, however, minor surface cover types were readily defined by LANDSAT.

LANDSAT Classification Accuracy

The LANDSAT classification of the surface cover types within Crater Lake National Park was compared to "ground truth" data and to the NASA U-2 aerial photography map

constructed for the National Park in order to determine the percent accuracy of the LANDSAT classification. The percent accuracy measurement denotes the degree in which actual ground conditions (surface cover types) were recognized and mapped through use of LANDSAT data. The accuracy measurement is a measure of the number of pixels that were correctly classified within a particular surface cover type classification delineation. The LANDSAT classification which was evaluated as to the percent accuracy was the 59-class classification of the National Park. The 12-class classification of the Park was highly generalized for presentation purposes, and hence was not so evaluated.

The approach utilized to measure the percent accuracy of the classification was to stratify the classification by major surface cover type and to conduct a random sample of pixel clusters within the stratified surface cover type. A failure of a pixel to represent the actual ground conditions was recorded as a "no" or as a misclassification. The size of the pixel cluster was 5 x 5 pixels. Pixel cluster size was chosen in order that the same size pixel cluster could be used for all the major surface cover types even in those areas which were four to seven pixels wide. The 5 x 5 pixel cluster is also the cluster size employed by the EROS Data Center to test LANDSAT classification accuracies. The random location of the pixel clusters per stratified surface cover type was achieved through use of a

random number table and a pixel cluster grid which was overlaid on the LANDSAT classification. The number of pixel clusters sampled was 5 percent of the total stratified surface cover type area. The sampling size of 5 percent is large enough to obtain appropriate classification accuracy measurements (Williams, 1976). Pixel counts and acreage summaries per class were given in Chapter VI.

In order to show which major surface cover types were the easiest and most difficult to classify, a classification accuracy measurement was completed for lodgepole pine, poorly stocked; lodgepole pine, densely stocked; mountain hemlock with scattered shasta red fir; shasta red fir with scattered mountain hemlock; white fir with scattered ponderosa pine and shasta red fir; ponderosa pine and white fir with scattered shasta red fir; pumice and bare rock with a slight herbaceous cover; water; ponderosa pine, large, medium to poorly stocked; brush; and marsh vegetation. An overall classification measurement was achieved by averaging the 12 individual surface cover type accuracy measurements. Table 26 shows the percent accuracy measurement for each surface cover type and for the entire classification.

The accuracy measurements for the 12 individual surface cover types, which appear in Table 26, reflect relatively high accuracy measurements. In six cases out of the 12 surface cover types tested for accuracy, three pairs of

Classification Accuracy Test

Surface cover type	Percent accuracy	Combined surface cover types	Percent accuracy		
Lodgepole pine, poorly stocked	93	Lodgepole pine	96		
Lodgepole pine, densely stocked	94				
Mountain hemlock with scattered shasta red fir	89	Ponderosa pine, white fir, and shasta red fir either PP or WF	89		
Shasta red fir with scattered mountain hemlock	91				
White fir with scattered ponderosa pine and shasta red fir	86				
Ponderosa pine and white fir with scattered shasta red fir	84				
Pumice with a slight herbaceous cover and bare rock	96	Ponderosa pine, large, poorly and medium stocked	96		
Water	98				
Ponderosa pine, large, poorly stocked	86				
Ponderosa pine, large, medium stocked	87				
Brush	91				
Marsh vegetation	93				
	Average accuracy				Average accuracy
	91				93

Table 26

surface cover types were related causing a reduction in the level of accuracy for each surface cover type per related pair. In measuring the accuracy level for lodgepole pine, poorly stocked and lodgepole pine, densely stocked, most of the pixels which were wrongly assigned to the lodgepole pine, poorly stocked classes belonged to the lodgepole pine, densely stocked classes. The same occurred for misclassified pixels of the lodgepole pine, densely stocked classes. Since the error (even though small) for the lodgepole pine classes occurred due to the relatedness between two similar lodgepole pine classes, an accuracy measurement for lodgepole pine was obtained irregardless of stocking. The value as shown in Table 26 is 96 percent. The two surface cover types which showed the lowest accuracy were the white fir with scattered ponderosa pine and shasta red fir and the ponderosa pine and white fir with scattered shasta red fir. These two surface cover types differ only in the degree of white fir occurrence, from 65 to 35 percent. If these two surface cover types were combined, the level of accuracy would increase to 90 percent. The crown density factor is the main cause in pixels of one surface cover type being classified as the other surface cover type.

The ponderosa pine, large, poor and medium stocked surface cover types are also related causing pixels of one surface cover type to be classified as the other surface

cover type. When only a ponderosa pine, large, poor to medium stocked is tested for accuracy, the level of accuracy also increases.

The mountain hemlock with scattered shasta red fir surface cover type has been misclassified mostly due to crown density differences and slope angle differences. In some areas of steep slopes resulting in partial shadows, mountain hemlock was classified as lodgepole pine, densely stocked. The slope aspect determined which surface cover type mountain hemlock was to be misclassified. Mountain hemlock was most frequently misclassified as shasta red fir. White fir on relatively steep south facing slopes were occasionally misclassified as shasta red fir or mountain hemlock, depending upon the crown density of the white fir and the understory reflectance.

The pumice and bare rock with a slight herbaceous cover and the water surface cover types experienced misclassified pixels due to the shadowing problem caused by the Crater Lake caldera and the surrounding cinder cones and peaks. The water classes also showed misclassification due to pixel boundary problems, discussed in Chapter V. The brush and marsh surface cover types showed misclassification between each other in areas of dry marsh vegetation and boundaries between the two surface cover types.

The accuracy measurements of the 12 surface cover types as shown in Table 26 average to 91 percent. When

the three pairs of related surface cover types were combined, the accuracy level increased to 93 percent. This increase in the level of accuracy shows that, as the level of detail increases, the level of accuracy decreases.

It should be appreciated when evaluating accuracy measurements that extremely high accuracy levels can be expected with quite general LANDSAT mapping classes. For example, within the USGS professional paper 964 (A Land Use and Land Cover Classification System for Use with Remote Sensor Data), the level I forest mapping class is "forest lands." The level II forest mapping class consists of "deciduous, evergreen, and mixed." When variations in coniferous tree species represent the LANDSAT mapping classes, the level of detail is much greater so the level of the percent accuracy would be expectedly lower.

Another factor which can tend to inflate accuracy measurements is to use only training areas in which to conduct accuracy evaluations. Since the training areas were used to generate the statistical classes, one would expect that they would be highly accurate when classified. No measurement, however, would still be made as to the success or failure of the classification throughout the remainder of the study area.

The accuracy measurements of the LANDSAT classification of surface cover types within Crater Lake National Park evaluate a classification of surface cover types

with spectral subtleties and not through use of only training areas.

Misclassification Problem

When employing LANDSAT digital tapes to identify and map surface cover types, one must face the possibility of misclassifying pixels. This can occur either due to training areas not representing a particular surface cover type or because of environmental factors which have modified the spectral reflectance of the pixel resulting in that pixel being assigned to an inappropriate class.

Figure 42 shows a two-class example of training areas not representing surface cover types resulting in misclassified or unclassified pixels. By rejecting a very small percentage of the pixels belonging to the training classes, it is possible to reject a relatively large number of pixels not belonging to any of the training areas (Swain, 1972).

Figure 43 shows a two-class example of pixels being assigned to inappropriate classes. In Figure 43a, two classes are statistically related within the areas of low probability of occurrence. The maximum likelihood decision rule must determine which pixels in the overlapped areas belong to which class. The decision rules can only minimize and not eliminate the probability of misclassification. In Figures 43a and b, it can be seen that the probability

Classification Error

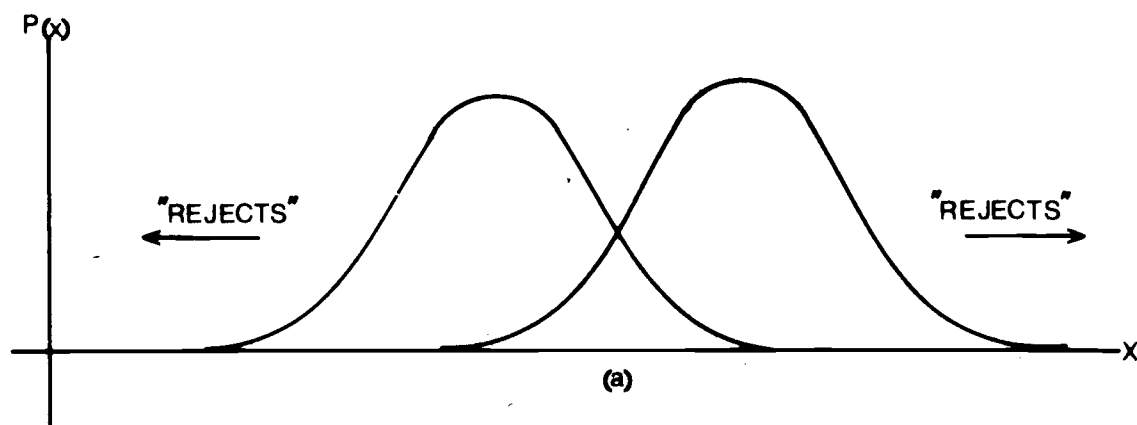


Figure 42. Two-class example. Adapted from Swain (1972).

Classification Error

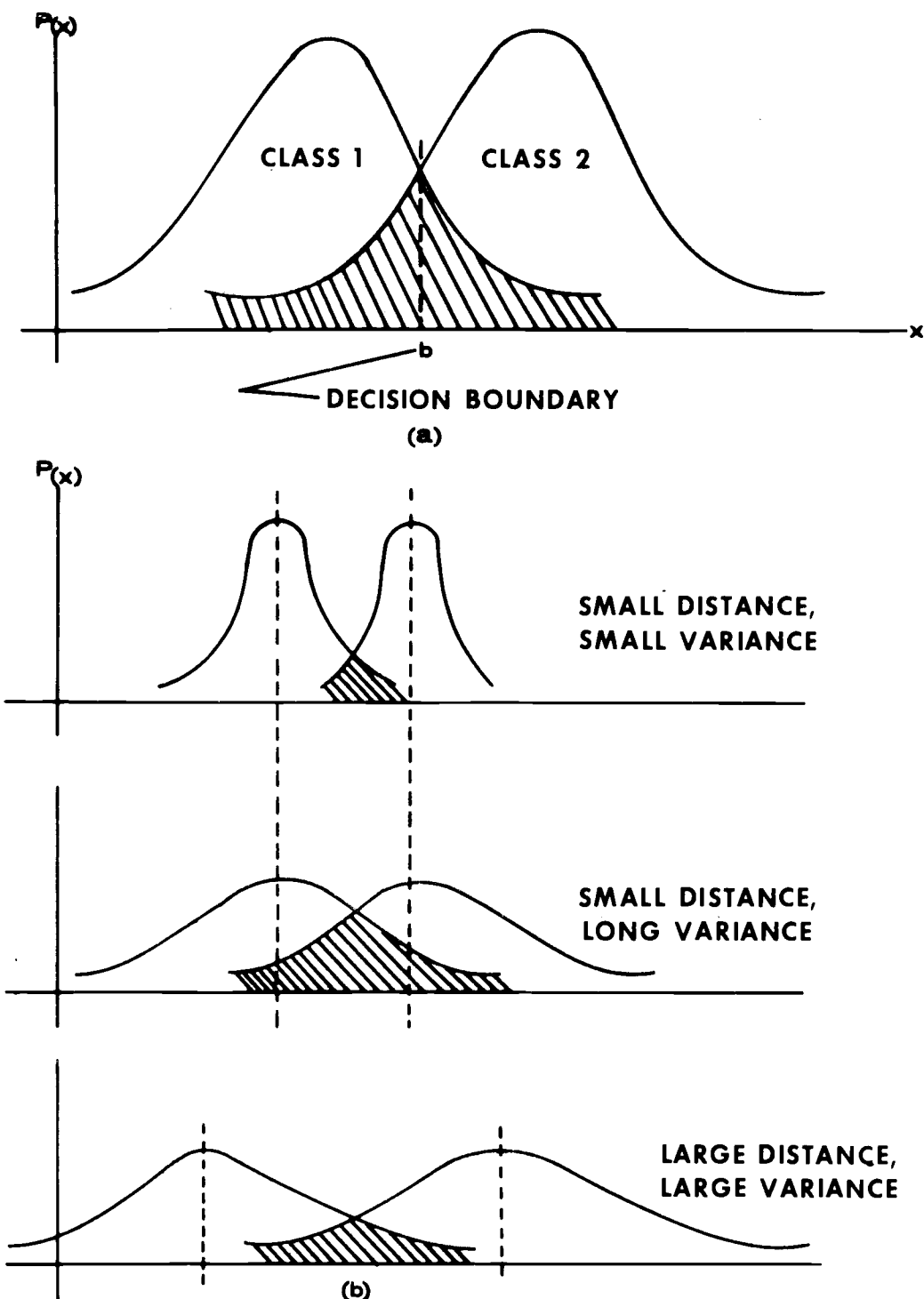


Figure 43. Classification error depends on distance between means and on variance. Adapted from Swain, 1972.

of misclassifying a pixel is a function of the "normalized distance" between the classes (Swain, 1972). The error of misclassification depends upon the distance between the means and the variance of each class. The greater the distance between classes, the smaller is the probability of error.

NASA U-2 Aerial Photography

NASA U-2 color infrared aerial photography was utilized to map the surface cover types within Crater Lake National Park. Detailed mapping and analysis of surface cover types in the Park requires the differentiation of brushfields, non-vegetated areas, water areas, and variations in coniferous tree species. Color infrared aerial photography was employed because it provides significantly more information on surface cover types, especially forest surface cover types, than do other types of aerial photography (Lauer, 1968 and Colwell, 1969).

NASA U-2 color infrared photography employs multi-wavelength aerial photography which exploits differences in spectral signatures due to tone and hue differences of surface cover types as photographed in various portions of the electromagnetic spectrum, through the visible and into the near infrared wavelengths. The false color rendition of the National Park's surface cover types on the color infrared photography provided large contrasts and small

subtleties in hues and tones between different surface cover types, which permitted surface cover type differentiation and mapping.

The primary difficulty in mapping the surface cover types within Crater Lake National Park was the identification and differentiation of coniferous tree species. A list of the coniferous tree species, as well as the deciduous tree species, which occur within the Park, are shown in Table 8. Various techniques, such as photographic scale, ecological and plant geography information, photographic interpretation parameters, stereoscopic vision, recognition of hues associated with different surface cover types on the photography, and "ground truth" were all utilized to aid in separating and mapping surface cover types within the Park. The following discussion will describe the techniques listed above which were utilized to identify and map surface cover types within the Park.

Photographic Scale

Photographic scale largely determines the degree that surface cover types can be recognized on aerial photography (Sayn-Wittgenstein, 1961). The scale of the NASA U-2 color infrared aerial photography employed for surface cover type mapping was 1:30,500. Through use of an Old Delft scanning stereoscope with 1.5 to 4.5 magnification, the general level of plant discrimination was increased from the recognition

of broad vegetation types to the identification of individual large trees and large shrub clusters. The stereoscope, in addition to providing insight into topographical variations to identify surface cover types, also provided insight into relative tree heights, slope aspects, and slope angles which added in explaining surface cover type zonation for species identification.

Ecology and Plant Geography Information

An appreciation of the ecological, silvicultural, and geographical knowledge of various tree species and brush types within the Park was of great importance in the identification of surface cover types on aerial photography. Many surface cover types are characteristic of a particular habitat. In general, physiography and related features are very important to the identification of tree species found in an area (Sayn-Wittgenstein, 1960). For example, white-bark pine occurs in rocky, exposed areas such as near the rim of the caldera, the summit of Wizard Island, and on the steep slopes of Mount Scott. Familiarity with the more easily recognizable common surface cover types occurring in an area can provide insight into other more difficult to identify surface cover types through existing plant association relationships. Snowbrush ceanothus and green-leaf manzanita, for example, are common brush types

occurring within the ponderosa pine forest in the southeast portion of the Park.

Even though the tree canopy often prohibits the observation of understory vegetation, inferences can be made as to general understory types due to tree cluster identification and ground work inspection which can relate understory with dominant tree types.

Photographic Interpretation Parameters

The main photographic interpretation parameters employed to identify and delineate surface cover types within Crater Lake National Park were size, shape, shadow, tone, hue, texture, pattern, site, association, and resolution (Estes and Simonett, 1975). Since color infrared aerial photography was utilized, tone, hue, and texture were the most employed interpretation parameters. Because the scale of the color infrared aerial photography was too small, even with stereoscopic magnification, for analysis of surface cover types by branching and crowning characteristics, tone, texture, and hue differences became very important. Tones, textures, and hues on the photographs are dependent upon many variables, such as altitude of the sun, length of exposure, method of printing and developing, atmospheric haze, and all the details of camera and lens construction. Differences in tone, texture, and hue are very useful in surface cover type identification, but a photographic key

based on tones, textures, and hues has the limitation that it can be used only for particular series of photographs for which it was constructed (Sayn-Wittgenstein, 1960). Because of this restriction in the employment of a photographic key for only these particular color infrared photographs, a listing of certain photographic parameters characteristic of the surface cover types within the Park will be presented rather than a photographic key (Table 27).

The more dominant colors which appear on the color infrared aerial photography (red, pink, white, yellow, orange, and brown) are all caused by relatively high reflectance levels in the visible and near infrared wavelengths to which the film emulsions are sensitive. Vegetation which appears blue, green, gray, or black indicates low reflectance of tree limbs, branches, soil and non-living ground cover exposed through openings in the vegetation cover or through nearly bare crowns (Knipling, 1969). The dark gray to black color generally represents shadows which form areas of extremely low reflectance and cause a dark mottled appearance on the photograph.

Crowning and branching characteristics of vegetation types are important in interpreting color infrared aerial photography, even if the photography is at too small a scale to identify the tree species by use of the crowning and branching characteristics. Crowning and branching

Photographic Parameters Characteristic of
Certain Surface Cover Types within the Park

1. Surface cover type:	lodgepole pine, densely stocked
2. Crown size:	small
3. Crown shape:	oval, small clumps
4. Shadow shape:	small, tapering to rounded to oval crown
5. Texture:	fine
6. Tone:	dark grayblue, small variation densely stocked
7. Hue:	grayblue
8. Pattern:	very lightly speckled from pumice
9. Association:	pumicefields, low elevation, western white pine, poorly stocked lodgepole pine
1. Surface cover type:	lodgepole pine, poorly stocked
2. Crown size:	small
3. Crown shape:	oval, small clumps
4. Shadow shape:	small, tapering to rounded to oval crown
5. Texture:	fine
6. Tone:	dark grayblue
7. Hue:	grayblue with whitegreen background intermixed
8. Pattern:	salt and pepper, heavily speckled from pumice and lodgepole pine
9. Association:	pumicefields, low elevation, western white pine, densely stocked lodgepole pine

Table 27

Table 27 (continued)

1. Surface cover type:	western white pine
2. Crown size:	small to medium
3. Crown shape:	scraggly long branches, wheel spokes
4. Shadow shape:	irregular branches, bent upward
5. Texture:	coarse
6. Tone:	medium to dark
7. Hue:	red purple
8. Pattern:	irregular occurrence, never pure stand
9. Association:	lodgepole pine, medium to high elevation, especially pinnacles area
1. Surface cover type:	subalpine fir
2. Crown size:	small
3. Crown shape:	dark center point of small crown
4. Shadow shape:	small, and tapering to crown top, church spire
5. Texture:	fine
6. Tone:	dark
7. Hue:	purple red
8. Pattern:	irregular occurrence, can have pure stands but small
9. Association:	marsh and bogs, along creek bottoms, often near deciduous

Table 27 (continued)

1. Surface cover type:	ponderosa pine
2. Crown size:	large
3. Crown shape:	round and full
4. Shadow shape:	full crown, branches only near crown, not much tapering
5. Texture:	coarse
6. Tone:	pinkish-white
7. Hue:	pink to light red
8. Pattern:	generally poorly to slightly medium stocked
9. Association:	white fir, shasta red fir, north-east and southeast portion of Park
1. Surface cover type:	white fir
2. Crown size:	medium to large
3. Crown shape:	small to medium starlike top
4. Shadow shape:	pointed crown, branches generally entire length to 3/4 length of tree
5. Texture:	fine
6. Tone:	dark
7. Hue:	grayblue
8. Pattern:	dense, large trees
9. Association:	ponderosa pine, panhandle, north-east, southwest and along western border

Table 27 (continued)

1. Surface cover type:	mountain hemlock
2. Crown size:	large
3. Crown shape:	starlike top
4. Shadow shape:	decreasing in size to tree top, pointed crown and curved leader
5. Texture:	medium to coarse
6. Tone:	dark
7. Hue:	deep purple red
8. Pattern:	rough and blotchy
9. Association:	medium and high elevation, shasta red fir
1. Surface cover type:	shasta red fir
2. Crown size:	large
3. Crown shape:	round
4. Shadow shape:	decreasing in size to crown top, multipronged crown top
5. Texture:	medium to coarse
6. Tone:	light to cream
7. Hue:	light red to pink
8. Pattern:	rough and blotchy
9. Association	medium and high elevation, moun- tain hemlock

Table 27 (continued).

1. Surface cover type:	brush
2. Crown size:	very small
3. Crown shape:	irregular
4. Shadow shape:	dense and irregular
5. Texture:	very fine
6. Tone:	bright
7. Hue:	pink to red
8. Pattern:	dense, low lying and absence of trees except in clumps
9. Association:	east, southeast, and south facing relatively steep slopes; most dominant occurs with ponderosa pine
1. Surface cover type:	marsh
2. Crown size:	not applicable (NA)
3. Crown shape:	NA
4. Shadow shape:	dense and irregular
5. Texture:	very fine
6. Tone:	light and dark, mottled
7. Hue:	pink and mix of blue-gray
8. Pattern:	low lying vegetation, dense and mottled due to the water
9. Association:	stream bottoms, subalpine fir and deciduous

Table 27 (continued)

1. Surface cover type:	deciduous
2. Crown size:	medium to large depending on the season
3. Crown shape:	irregular and cylindrical
4. Shadow shape:	dense and irregular
5. Texture:	rougher than conifers
6. Tone:	bright
7. Hue:	pink to red
8. Pattern:	occurs in clusters
9. Association:	along drainage channels, near marsh and water bodies
1. Surface cover type:	pumice and bare rock
2. Crown size:	NA
3. Crown shape:	NA
4. Shadow shape:	NA
5. Texture:	fine
6. Tone:	light to dark depending upon slope angle and slope aspect
7. Hue:	green
8. Pattern:	mottled
9. Association:	near the caldera, rim and in other high areas and in extremely flat areas

Table 27

characteristics can provide information to help explain the reflectance of a particular tree species recorded on the color infrared aerial photography. Much of the solar radiation incident on vegetation types is transmitted through the uppermost leaves or needles of a crown canopy and is reflected from lower branches, leaves, or needles and transmitted up through the upper leaves or needles to enhance the spectral reflectance recorded on the film emulsion (Allen and Richardson, 1968). Where green leaves or needles overlap and are clustered, the total infrared reflectance is higher and the resulting image color on the photography is a brighter red than compared to single or small clusters of leaves and needles (Knipling, 1969).

"Ground Truth" and Terrestrial Photography

"Ground truth" and terrestrial photography is the link between aerial photography, remote sensing, and surface cover type identification and analysis. Surface cover types which cannot be accurately identified through photo-interpretation, due to scale, shadowing, overstory, or similarities in spectral reflectance, can be identified by "ground truth" investigation. Once a surface cover type has been identified and delineated on the ground, its tone, texture, hue, shape, and organization as seen on the photograph can be appreciated and applied to other areas on the photograph for comparison and identification. The amount

and quality of "ground truth" must be increased as the need for more detailed information from the aerial photography is sought. The value of good "ground truth" cannot be overstated.

Surface Cover Type Map Generation

Through photointerpretation of the 1:30,500 average scale color infrared aerial photography, a surface cover type map of Crater Lake National Park was generated. Interpretation of the 1:30,500 scale color infrared aerial photographs was supplemented by use of an Old Delft scanning stereoscope which, in addition to providing stereoscopic vision, enlarged the scale of the photographs to approximately 1:20,333 and 1:6,778. The use of 4 time enlargements of the 1:30,500 scale photographs and two existing but quite poor surface cover type maps of the Park were also utilized.

The first known surface cover type map of Crater Lake National Park was produced in 1937 by the U. S. Branch of Forestry. This map was generally accurate as to the dominant surface cover type within a delineation but was imprecise as to combinations of surface cover types within a delineation and the boundaries between different surface cover types. The second surface cover type map of the Park was produced in 1946 also by the U. S. Forest Service, Mr. Mill, Director. This map was too general and imprecise as

to the dominant surface cover type within a delineation, the boundaries of the surface cover type, and the surface cover type combinations within a delineation. One point must be made, however, as to the two previous surface cover type maps of the Park and also the map which was compiled through use of color infrared aerial photography: maps may be extremely useful for the specific purpose intended; but when the map is used for other purposes, the effectiveness of the map may be greatly reduced. The surface cover type map of the Park constructed through use of color infrared aerial photographs was compiled with a design of showing the distribution of the dominant tree species within the Park as the major surface cover type. If this map is used to locate understory variations or extremely small clusters of trees, the effectiveness of the map would decrease. A map of the surface cover types within the Park is a tool to help solve certain problems of land managers. Different problems may require the use of additional or different tools.

The map of the surface cover types within the National Park compiled through use of the color infrared aerial photography delineated 17 major surface cover types. The symbols used on the map to represent the respective surface cover types include:

LP = lodgepole pine, poorly stocked

LD = lodgepole pine, densely stocked

- S = shasta red fir
 - M = mountain hemlock
 - W = western white pine
 - W' = white fir
 - S' = sugar pine
 - W'' = water
 - D = Douglas-fir
 - B' = whitebark pine
 - G = grass
 - D' = deciduous
 - A = subalpine fir
 - P = ponderosa pine
 - B = brush
 - l = marsh or moist grassfields
- "Blank" = pumice with slight herbaceous or scattered conifer cover and bare rock outcrops

Lodgepole pine, poorly stocked and lodgepole pine, densely stocked were separated on the basis of crown density differences caused by a large amount of downed and dying trees in the poorly stocked lodgepole pine. Poorly stocked lodgepole pine is represented by crown densities of under 40 percent. Densely stocked lodgepole pine is represented by crown densities greater than 40 percent and generally less than 60 percent. The brush class is characterized by such brush types as greenleaf manzanita, snowbrush ceanothus, pinemat manzanita, golden chiquapin, and

waxy currant. The pumice class is characterized by pure pumice and a pumice and light herbaceous mix. The herbaceous plants are represented by Newberry's knotweed, for example. The pumice class also may have small clumps of conifer tree species scattered throughout the pumice. The smallest surface cover type delineated was 1.0 acres. The marsh class represents moist grassfields and marsh either permanent or ephemeral if registered as marsh on either 3 July 1974 or 10 August 1976, the dates of the aerial photography. The marsh class is characterized by grasses, sedges, rushes, herbaceous plants, and low brush such as sitka alder.

Combinations of the above-mentioned surface cover types were also delineated. The first symbol in the surface cover type delineation represents the most dominant. The remaining symbols, if any, represent decreasing dominance with the last symbol representing the least dominant surface cover element. If a surface cover type delineation is composed of a surface cover type greater than 80 percent dominance, that delineation was recorded as "pure" by a single surface cover type designation. If two surface cover types are denoted within a delineation, the first surface cover type represents 65 to 80 percent of the area within the delineation, with the second surface cover type representing 20 to 35 percent of the area. If three or more surface cover types are represented within a map

delineation, the first surface cover type represents 55 to 65 percent of the area; the second represents 20 to 30 percent of the area; the third represents 5 to 15 percent of the area within the surface cover type delineation. If any delineation of lodgepole pine in which it was delineated as "pure" (greater than 80 percent of the area), or delineated as the dominant surface cover type in a two surface cover type combination, the poorly stocked or densely stocked lodgepole pine parameter was designated by the appropriate symbol following the "L." If lodgepole pine was the third or greater surface cover type in the delineation in terms of dominance, poorly or densely stocked lodgepole pine was not specified. For example, a delineation labelled SMLD represents shasta red fir, mountain hemlock, lodgepole pine, and Douglas-fir. Densely or poorly stocked lodgepole pine is not specified. Delineation LDSM represents lodgepole pine, densely stocked, shasta red fir, and mountain hemlock. Douglas-fir does not occur within the delineation.

The scale of the surface cover type map of Crater Lake National Park, which is presented in Figure 44 (in pocket) is 1:62,500, which is the same scale as the LANDSAT digital printouts shown in Chapter VI. A comparison of the maps constructed through the use of LANDSAT data and NASA U-2 aerial photography will be discussed in this chapter.

An inspection of Figure 44 shows that ponderosa pine, for example, is clustered in the northeast corner of the

Park and also in the southeast and eastern half of the Park "panhandle." In the ponderosa pine area in the southeast corner of the Park, brush is much more prevalent than in the ponderosa pine stands in the northeast corner of the Park. Lodgepole pine, poorly stocked is also shown, for example, to be clustered around the Pumice Desert and extending east to the Park boundary. A denser stocked lodgepole pine is shown to flank the poorly stocked lodgepole pine, generally in the upslope direction. Figure 44 (in pocket) also shows the close relationship between the occurrence of mountain hemlock and shasta red fir, lodgepole pine and western white pine, whitebark pine and mountain hemlock, ponderosa pine, white fir, and shasta red fir, Douglas-fir and white fir, brush types and south facing slopes, and subalpine fir and marsh and/or moist grassfields.

Comparison of LANDSAT Data and NASA U-2 Aerial Photography for Detailed Surface Cover Type Mapping

Comparisons of the surface cover type maps of Crater Lake National Park in Figures 40 and 44, constructed through use of LANDSAT digital tapes and NASA U-2 aerial photography show differing levels of mapping detail and quality due to the intrinsic characteristics of each mapping system. The LANDSAT and NASA U-2 aerial photography systems have been previously discussed. Some of the more

important interpretive characteristics of each system are shown in Table 28. The "+" symbol indicates the greater effect of a particular surface cover type detection parameter by LANDSAT or NASA U-2 photography. The "-" symbol indicates a lesser effect of a particular surface cover type detection parameter. In general, LANDSAT data can most effectively map dominant surface cover types and dominant mixtures of surface cover types over very large areas and on a repetitive basis.

The NASA U-2 aerial photography at the scale utilized in this study can most effectively map dominant and sub-dominant mixtures of surface cover types and details not mapped by LANDSAT due to the larger scale of the photography, and the greater resolution of the photography. The area covered by aerial photography for surface cover type mapping purposes is often quite smaller than that afforded by LANDSAT and also often does not afford repetitive coverage for map updates and seasonal change evaluation for surface cover type identification.

The techniques employed to extract data from NASA U-2 color infrared aerial photography and LANDSAT digital tapes for surface cover type identification and mapping within Crater Lake National Park have been examined within this chapter. Output products showing the areal extent of surface cover types within the Park have also been presented.

Comparison of LANDSAT and NASA U-2 Data

Surface cover type detection parameters	NASA U-2 photography	LANDSAT data
Greatest degree of detail detected in surface cover types	+	-
True size and shape of surface cover type delineation	+	-
Detection of dominant surface cover types	+	+
Greater resolution	+	-
Repetitive coverage (seasonal change)	-	+
Greater range of reflected infrared coverage (u)	-	+
More effective detection of surface cover type subtleties of dominant surface cover types	-	+
Detection of large surface cover type trends	+	+
Quantitative interpretive techniques without data reformatting	-	+
Reduced shadow effect (altitude)	-	+
Detection of slight surface cover type mixtures	+	-
Greater use of stereoscopic interpretation	+	-
Detection of dominant surface cover types over a large area	-	+

Table 28

The following chapter will summarize the major results of this research. Chapter VII will also cite the conclusions derived from this research and from the major results.

VII. SUMMARY AND CONCLUSIONS

Summary

This research has focused on the relationships between LANDSAT digital data, NASA U-2 color infrared aerial photography, and the identification and detailed mapping of surface cover types within Crater Lake National Park, Oregon. The identification and mapping of surface cover types within the National Park was achieved through "ground truth" activities; the application of suitable data reconnaissance techniques; the realization of LANDSAT data classification problems and the limitations of the NASA U-2 data; the employment of appropriate data extraction techniques and output products; and the recognition of the effectiveness of LANDSAT data and NASA U-2 color infrared aerial photography for detailed surface cover type mapping within a forested, mountainous environment.

"Ground Truth" Activities

Dynamic forces and/or conditions have in the past and do in the present affect the appearance and composition of surface cover types within the National Park. These forces and/or conditions which include geologic activity, soil conditions, climate, and vegetation, affect the spectral reflectance values of surface cover types as detected by

LANDSAT and by the NASA U-2 color infrared aerial photography.

General knowledge of surface characteristics are important in anticipating spectral reflectance variations and to guide "ground truth" activities. "Ground truth" should provide information as to surface cover type characteristics and particularly to those characteristics which greatly influence the spectral reflectance.

To effectively utilize LANDSAT and color infrared aerial photography which are based on spectral reflectance values, "ground truth" must be collected. The location of "ground truth" sample sites and the determination of sampling parameters was made in conjunction with those surface cover type factors which influence spectral reflectivity. The amount and quality of "ground truth" is related to the level of detail sought. Prudent preparation of "ground truth" activities and the accurate measurement and/or observation of sampling parameters underpins the quality of results. The 182 "ground truth" sample sites have proven sufficient for surface cover type identification and mapping by LANDSAT and NASA U-2 data.

Data Reconnaissance Techniques

The 10 September 1974 LANDSAT tape was the prime analysis tape employed. The 10 September 1974 tape used in conjunction with the 06 January 1973 tape provided good

contrasts in sun angle which aided in landform identification, surface cover type differentiation, and slope angle estimation. The 30 June 1974 and 23 August 1974 tapes provide good contrast due to the snow-covered and snow-free conditions which they respectively present. These two tapes provided information as to the occurrence of openings in the tree canopy: ephemeral drainage patterns within the Park which aided in understanding the phenological changes of certain surface cover types induced by moisture availability; and an indication of the possible tree and brush species which may occur in association with these high elevation moist conditions. Multi-season LANDSAT digital tapes which provide variation in sun angle provided more insight into surface cover type differentiation and identification than multiple tapes clustered around a single date. Precise outlining of openings in the forest canopy resulting from the occurrence of natural glades, and rock and pumice outcrops, for example, can also be effectively detected. Low sun angle, relatively snow-free LANDSAT digital tapes provided better discrimination between certain surface cover types than did medium to high sun angle tapes, due to greater separation of reflectance values between bands 5 and 7 on the lower sun angle scene. Use of all four LANDSAT bands collectively and simultaneously increased the discriminatory capability of LANDSAT for surface cover type identification and mapping.

The comparative analysis of NASA U-2 aircraft data of two different dates aided in surface cover type identification due to the manner that certain surface cover types were modified by the snowfall and snowmelt patterns. The 10 August 1974 aerial photography was most utilized because snow did not obstruct the viewing of surface cover types. NASA U-2 color infrared aerial photography was compatible with LANDSAT data due to the similarity of wavelengths sensed and the false-color representation of the surface cover types by both.

Data Problems and Limitations

Identification and mapping of surface cover types through analysis of spectral reflectance values was affected by reflectance values of surface cover types being influenced by environmental factors. The most dominant environmental factors within the Park include slope angle, slope aspect, and surface cover type, with crown size and crown density also being important factors. Misclassification or nonclassification of surface cover types can result by selecting training areas for a specific surface cover type which does not account for the modification in spectral reflectance values found in some extremely similar surface cover types. An analysis of variance of the regression analysis of all four individual LANDSAT bands for 30 variables representing classes of the five major

environmental factors (mentioned above) showed that a range between 72.75 and 57.41 percent of the variation found in the reflectance values of the surface cover types within Crater Lake National Park as recorded by LANDSAT were explained by the regression analysis. It was also shown that pumice and ponderosa pine, large, with scattered shasta red fir consistently produced a positive difference from the mean reflectance for bands 4, 5, 6, and 7 and that white fir with scattered ponderosa pine and shasta red fir, lodgepole pine, dense, and shasta red fir with scattered mountain hemlock produced a negative difference from the mean reflectance for all four LANDSAT bands. It was further shown that slope angle, slope aspect, crown size, and crown density beta value rankings for each band, which show relative impacts of reflectance value changes from the mean reflectance, are a function of the surface cover type. Inconsistencies in the placement of numerous environmental factor beta rankings for the four LANDSAT bands occur because each LANDSAT band senses different attributes of the same surface cover type. The individual class regressions (for the five major environmental factors) per band show a finer relationship between environmental factors and mean reflectance modification than the full regressions because the "full regressions" reflect the influence of all 30 environmental variables in the regression analyses while the

individual regressions are more specific to a particular environmental factor.

The problem of LANDSAT misclassification or nonclassification can be reduced by generating additional training statistics for surface cover types which occur in areas strongly affected by environmental factors (for example, steeply sloped areas). Attempting to classify surface cover types with training statistics which do not represent areas strongly affected by environmental factors can produce misclassification or nonclassification.

The pixel integration relationships with detail surface cover type mapping must also be appreciated. Surface cover types are generally small in size in comparison to the ground resolution of the pixel area. Because of this size differential, it is common to have numerous surface cover types being sensed within the pixel unit area. The spectral reflectance of a mixture of surface cover types within the pixel is not representative of the individual component surface cover types which composed the pixel mixture, hence, training areas should represent surface cover type mixtures and not just different homogeneous areas which comprise the pixel groups.

LANDSAT scanner readjustment between differing surface cover types determines the occurrence of boundary pixels. The number or extent of boundary pixels is determined by the reflectance value differences between the two adjacent

surface cover types. Gradations of pixel readjustment are seen within the boundary pixels. The extent of boundary pixels can produce a loss of surface cover type boundary and size definition.

Data Extraction Techniques

Techniques to analyze LANDSAT digital data were utilized at Oregon State University and at the EROS Data Center. The techniques employed at Oregon State University included a grayscale analysis, density slice, and selection of points for training areas. The analysis of the 10 September 1974 tape helped determine which surface cover types could be effectively differentiated. The comparative analysis of the 06 January 1973 tapes and the 10 September 1974 tapes for training area selection showed that some surface cover type could be better differentiated on the low sun angle 06 January 1973 tape than on the higher sun angle 10 September 1974 tape.

Generation of a grayscale from LANDSAT digital data and the locating of "ground truth" sample sites on the grayscale provided added appreciation of the relative reflectance values of known surface cover types and insight into the influence of known environmental factors on the spectral reflectance of known surface cover types.

A density slice aided in evaluating which subtle differences in surface cover type spectral reflectance values

LANDSAT could detect in order to determine possible and useful LANDSAT mapping classes. The density slice function also provided a more detailed view of the grayscale information by expanding into the full grayscale range a portion of the grayscale in order to detect relative spectral reflectance similarities of surface cover types which may be confusable during classification.

The data extraction techniques employed at the EROS Data Center consisted of LANDSAT digital tape reformatting, study area definition on the LANDSAT tapes, stratification mask generation, training set selection, spectral relationship plots, generation of classification statistics, and the use of the control clustering classification technique.

The strategy of selecting training areas, when employing the control clustering technique, is to tap as much spectral variation as possible throughout the study area. Prior to classifying the study area, the training statistics should be evaluated to determine if and where additional training statistics should be generated in order to alleviate the misclassified or nonclassified problem.

The mean reflectance per band; the distance between training classes; the weighted divergence between training classes; and a covariance matrix for each training class aided in determining the quality of the generated training classes. Quality is determined by statistical separation between classes.

The alphanumeric map of the distribution of the generated 59 classes for individual pixel areas throughout Crater Lake National Park was the most detailed LANDSAT output product developed. The 12-class alphanumeric map and the 12-class color coded Optronix's product of the Park have been generalized for presentation purposes from the 59 class alphanumeric map of the National Park. To generalize and combine data from 59 to 12 classes, statistical and spatial parameters of the classes must be collectively employed. Environmental factors can modify the spectral reflectance values of surface cover types to such a degree that similar surface cover types map appear unrelated, based upon mean reflectance values per LANDSAT bands. Information as to the spatial organization of surface cover types within the study area, denoted by spectral class distribution, can aid in reducing the spectral reflectance value problem in combining classes.

Increased scale and resolution of the NASA U-2 color infrared aerial photography as compared to LANDSAT provides greater mapping detail such as boundary and surface cover type size definition, percent mixtures of surface cover types within a delineation, identification of varied surface cover types within a 1.118 acre (.452 ha) area, and identification and mapping of most sub-dominant vegetation. Color infrared aerial photography also provides significantly more discriminatory power for surface cover types

than do other types of aerial photography. The identification and differentiation of coniferous tree species which have very subtle spectral reflectance differences are more effectively discriminated through the detecting of wavelengths of the photography, through the visible and into the near infrared.

An understanding of surface cover type crowning and branching characteristics provide information as to the expected relative spectral reflectance between related surface cover types as detected by LANDSAT and the NASA U-2 aircraft. If the scale of the photography is appropriate, identification of surface cover types through crowning and branching characteristics can be effectively utilized.

The Crater Lake National Park LANDSAT classification accuracy of the 59 class, individual pixel area map product, determined by the random location of pixel clusters stratified by surface cover type and achieved through use of a random number table, averages 91 percent. As related classes were combined, the accuracy level increased to 93 percent. The most difficult surface cover type to separate was ponderosa pine and white fir combinations. The least difficult surface cover type to separate and map was lodgepole pine.

Conclusions

The amount of "ground truth" is directly related to the level of LANDSAT and NASA U-2 aerial photography mapping detail sought.

Generating training statistics to represent areas strongly affected by environmental factors can reduce pixel misclassification or nonclassification. Two different surface cover types may be classified as the same surface cover type due to slope angle, slope aspect, crown size, crown density, or other related factors which are capable of influencing the spectral reflectance.

Appraisal of which environmental factors influence the reflectance value and to what relative degree can be determined by regression analysis, an investigation of beta values, and analysis of variance tables.

LANDSAT bands 5 and 7 of the four LANDSAT bands provide the greatest separation between forested surface cover types. The use of all four LANDSAT bands in surface cover type mapping is the most efficient approach.

An interactive computer system and a color display such as IDIMS provide invaluable flexibility in computer processing and classification of surface cover types with LANDSAT digital tapes.

The control clustering techniques of LANDSAT data analysis combines the advantages of the supervised and the unsupervised classification techniques. The control clustering technique reduces the problem of training areas not representing the variety of surface cover types within the study area by selecting training areas which sample as much spectral variation in the study areas as possible.

Low sun angle LANDSAT digital tapes provide better discrimination between some surface cover types than does medium to high sun angle LANDSAT tapes because various LANDSAT bands are better separated from one another. Those surface cover types which can be better differentiated on low sun angle LANDSAT digital tapes can be classified throughout the study area with low sun angle generated training statistics.

When combining LANDSAT classes, the spectral reflectance values and the spatial organization of the classes within the study area are equally important to obtain proper combinations of similar surface cover type classes.

Increased resolution of future LANDSAT systems will result in less boundary and size distortion of surface cover types and greater detail in surface cover type mapping. It will also result in greater computer processing time, difficulty, and cost.

The extent of boundary pixels between surface cover types is dictated by the spectral reflectance differences between the adjacent surface cover types.

Application of LANDSAT data to less mountainous terrain would reduce the shadow problem and improve classification accuracy.

Young tree species (approximately 0 to 25 years old) do not possess similar reflectances as do the more adult trees of the same species; training statistics must also be generated for the young tree species.

A change in LANDSAT's orbit pass from approximately 9:45 a.m. to 12:00 noon local time would reduce the shadowing problem in surface cover type mapping in forested, mountainous environments. Shadowing was the major cause of classification problems in this research.

LANDSAT data can effectively map surface cover types over a large area, detect subtle changes in spectral reflectances, and provide quick and accurate acreage summaries. NASA U-2 color infrared aerial photography provides more detail in surface cover type delineation than LANDSAT, has larger scale and better resolution than LANDSAT, but cannot detect the spectral reflectance subtleties of which LANDSAT is capable, primarily due to the application of quantitative versus qualitative analysis techniques

and the farther extension of wavelengths detected into the near infrared of LANDSAT.

BIBLIOGRAPHY

- Aldrich, R. C., et al. "Land use classification and forest disturbance monitoring," Evaluation of ERTS-1 Data for Forest and Rangeland Surveys, Pacific Southwest Forest and Range Experiment Station, Paper 112, (1975).
- Allen, W. A., Richardson, A. J. "Interaction of light with a plant canopy," Journal of Optics of the Society of America, Vol. 58 (1968), p. 1023-1028.
- Amidon, Elliot L. "Recording forest patterns from photographs and maps by computerized techniques," In Proceedings, Monitoring Forest Environment through Successive Sampling. (Syracuse, N.Y., June 24-26, 1974), State University New York, Syracuse, p. 119-132.
- Anderson, Hal E. "Fuels -- The source of the matter," Air Quality and Smoke from Urban and Forest Fires, Proceedings of the International Forest Fire Symposium, (1976), p. 318-321.
- Anderson, James R., et al. "A land use and land cover classification system for use with remote sensor data," USGS Professional Paper 964, (1976), p. 28.
- Applegate, Elmer I. "Plants of Crater Lake National Park (map)," Report to the National Park Officials at Crater Lake, (1938).
- Baker, Frederick S. "A revised tolerance table," Journal of Forestry, Vol. 47, (1949), p. 179-181.
- Beadle, N. C. "Soil temperatures during forest fires and their effect on the survival of vegetation," Journal of Ecology, Vol. 28, (1940), p. 180-192.
- Beaufait, William R., et al. "Inventory of slash fuels using 3P subsampling," USDA Forest Service General Technical Report INT-13, Intermountain Forest and Range Experiment Station, Ogden, Utah, (1974), 17p.
- Bentley, Jay R., Seegrict, D. W., and Blackman, D. A. "A technique for sampling low brush vegetation by crown volume classes," U.S. Forest Service Research Note PSW-215, (1970).
- Blank, Richard, Jr. Aeromagnetic and Gravity Surveys of the Crater Lake Region, Oregon, USGS, (1967), p. 42-52.

- Bonner, G. M. "A test of cluster sampling in forest inventories," Reprint from the Canadian Journal of Forest Research, Vol. 5, No. 2, (1975), p. 269-272.
- _____. "Estimation of ground canopy density from ground measurements," Journal of Forestry, (August, 1967), p. 45-89.
- _____. "A test of cluster sampling in forest inventories," Canadian Journal of Forest Research, Vol. 5, No. 2, (1975), p. 269-272.
- Brooke, Robert C. "The subalpine mountain hemlock zone," V. J. Krajina (Ed.), Ecology of Western North America, Vol. 2, (1970), p. 147-349.
- Buffo, John, Fritschen, Leo J., Murphy, James L. "Direct solar radiation on various slopes from 0 to 60 degrees north latitude," Pacific Northwest Forest and Range Experiment Station, USDA, Portland, Oregon, PNW-142, (1972), p. 74.
- Chapman, Peter, and Quade, Jack. "Ground truth/sensor correlation," Earth Resources Aircraft Program Status Review, Vol. II, (1969), p. 59-68.
- Clayton, James L. "Nutrient gains to adjacent ecosystems during a forest fire: An evaluation," Forest Science, Vol. 22, No. 2, (June, 1976), p. 162-166.
- Cochran, P. H. "Soil temperatures and natural forest regeneration in south-central Oregon," Forest Soils and Forest Land Management Proceedings of the Fourth North American Forest Soils Conference, USFS, (1975), 37-52.
- Coulson, Bouricuc, Gray. "Optical reflection properties of natural surfaces," Journal of Geophysical Research, Vol. 70, (1965), p. 4601-4611.
- Dana, Robert W. "Solar and atmospheric effects on satellite imagery derived from aircraft reflectance measurements," Pacific Southwest Forest and Range Experiment Station, Forest Service, USDA, (1975), p. 683-694.
- Debano, L. F., Rice, R. M. "Fire in vegetation management: Its effects on soil," American Society of Civil Engineers, Proceedings of the Symposium on Interdisciplinary Aspects of Watershed Management, Bozeman, Montana, (1970), p. 327-346.
- Dicken, Samuel N. The Cascade Mountains. University of Oregon Press, Eugene, Oregon, Chapter 7, p. 89-97.

- Dieterich, John H. "Prescribed burning in ponderosa pine--state of the art," Presented at Region 6, Eastside Prescribed Fire Workshop, Bend, Oregon, (May 3-7, 1976).
- Doverspike, G. E., Flynn, F. M., and Heller, R. T. "Microdensitometer applied to land use classification," Photogrammetric Engineering, Vol. 31, (1965), p. 294-306.
- Draper, N. R. and Smith, H. Applied Regression Analysis, John Wiley and Sons Publishing, (1966), 407 p.
- Driscoll, R. S., et al. "Microdensitometry to identify plant communities and components on color infrared aerial photos," Range Management Journal, Vol. 27, No. 1, (1974), p. 66-70.
- Driscoll, R. S., et al. "Range inventory -- Classification of plant communities," Evaluation of ERTS-1 Data for Forest and Rangeland Surveys, Pacific Southwest Forest and Range Experiment Station, paper 112, (1975).
- Dyrness, C. T. and Youngberg, C. T. "Soil-vegetation relationships in the central Oregon pumice region" First North American Forest Soils Conference Proceedings, (1958), p. 57-66.
- Eastman Kodak Company, "Applied infrared photography," Standard Book Number 0879850094, Manual Number 28, (1972), 89p.
- Erb, R., Bryan. "The ERTS-1 investigation, ERTS-1 forest analysis," Report for the NASA, LBJ Space Center, Houston, Texas, (July-June, 1973), p. 50, NASA Technical Memorandum--TM X-58119.
- Evans, William E. "Marking ERTS images with a small mirror reflector," Photogrammetric Engineering, (June, 1974), p. 665-671.
- Entzminger, Robert A. "Mosaic/photomontage: A new concept to help reclamation planning," Coal Mining and Processing, (June, 1976).
- Finch, William A. "Agriculture, forestry, land use, and mapping helped by ERTS," Journal of Environmental Sciences, (March-April, 1974), p. 23-42.
- Fowells, H. A. "The period of seasonal growth of ponderosa pine and associated species," Journal of Forestry, Vol. 39, (1941), p. 601-608.

- Fowells, H. A. "Silvics of forest trees of the United States," USDA Agricultural Handbook No. 271, Forest Service, Washington, D. C., (1965).
- Franklin, Jerry F. "Ecology and silviculture of the true fir-hemlock forest areas of the Pacific Northwest," U.S. Forest Service Research Paper PNW-22, (1965), 31p.
- _____. "Vegetation and soils in the subalpine forests of the southern Washington Cascade Range," (1966), 132 p. (unpublished doctoral dissertation on file at WSU, Pullman).
- Franklin, Jerry F. and Dyrness, C. T. "Natural vegetation of Oregon and Washington," Pacific Northwest Forest and Range Experiment Station, Forest Service, USDA, Portland, Oregon, General Technical Report PNW-8, (1973), p. 415.
- _____. "Vegetation of Oregon and Washington," USDA Forest Service Research Paper, PNW-80, (1969), 216p.
- Franklin, Jerry F. and Mitchell, Russell G. "Successional status of subalpine fir in the Cascade Range," USDA Forest Service, Pacific Northwest Forest and Range Experiment Station, Portland, Oregon, PNW-46, (1967), 16p.
- Gates and Tantraporn. "The reflectivity of deciduous trees and herbaceous plants in the infrared to 25 microns," Science, Vol. 115, (1952), p. 613-616.
- Gary, Howard L. "Crown structure and distribution of biomass in a lodgepole pine stand," USDA Forest Service Research Paper RM-165, (April, 1976), p. 19.
- Gialdini, Michael, et al. "The integration of manual and automatic image analysis techniques with supporting ground data in a multistage sampling framework for timber resource inventories: Three examples," Earth Observation Division Proceedings, NASA, Johnson Space Flight Center, Houston, Texas, (1975), p. 1377-1387.
- Gimbarzevsky, Philip. "Interpretation of remote sensing imagery in the evaluation of forest land," In Proceedings, Fourth North American Forest Soils Conference, (August, 1973), pp. 71-89.
- Goddard Space Flight Center. LANDSAT Data Users Handbook, National Aeronautics and Space Administration, Document No. 76SDS4258, (1976).

- Grabau, W. E. "Pixel problems," Mobility and Environmental Systems Laboratory, U. S. Army Engineers Waterways Experiment Station, Vicksburg, Mississippi, Miscellaneous Paper M-76-9, (1976), 38p.
- Gratowski, H. "Brush problems in southwest Oregon," U. S. Department of Agriculture, Forest Service, Pacific Northwest Forest and Range Experiment Station (un-numbered release), (1961), 53p.
- Haack, Paul M. "Evaluating color, infrared, and panchromatic aerial photos for the forest surveys of interior Alaska," Photogrammetric Engineering, Vol. 28, (1962), p. 592-598.
- Harward, M. E., Youngberg, C. T. "Soils from Mazama ash in Oregon: Identification, distribution, and properties," Pedology and Quaternary Research Symposium, University of Alberta, Edmonton, (1969), p. 163-177.
- Heller, R. C. "Evaluation of ERTS-1 data for forest and rangeland surveys," Pacific Southwest Forest and Range Experiment Station, USDA Forest Service Research paper PSW-112, (1975), 67p.
- Heller, R. C., Aldrich, R. C., Driscoll, R. S., Francis, R. E., and Weber, F. P. "Evaluation of ERTS-1 Data for Inventory of Forest and Range Land and Detection of Forest Stress, Final Technical Report to NASA," (1974), 218p.
- Heller, R. C., et al. "Identification of tree species on large scale panchromatic and color aerial photographs," Forest Service, USDA, Agricultural Handbook No. 261, (1964).
- Henderson, R. G., Thomas, G. S., and Nalepka, R. F. "Methods of extending signatures and training without ground information," Environmental Research Institute of Michigan, (1975), 91p.
- Hoffer, R., et al. "Use of computer-aided analysis techniques for cover type mapping in areas of mountainous terrain," Purdue University, Lafayette, Indiana, (1974), 15p.
- Horivitz, H. M., Nalepka, R. F., Hyde, P. D., and Morgenstern, J. P. "Estimating the proportions of objects within a single resolution element of a multispectral scanner," Proceedings of the Seventh International Symposium on Remote Sensing of the Environment, Ann Arbor, Michigan, (1971), p. 1307-1320.

- Jackson, M. T. and Faller, A. "Structural analysis and dynamics of the plant communities of Wizard Island, Crater Lake National Park," *Ecological Monographs*, Vol. 43, No. 4, (1973), p. 441-461.
- Kalensky, Z. "ERTS thematic map from multirate digital images," *Canadian Forest Management Institute*, (October, 1974), p. 767-785.
- Kan, E. P., Dillam, R. D. "Timber type separability in southeastern United States on LANDSAT-1 MSS data," *Proceedings of the Earth Observation Division, NASA, Johnson Space Flight Center, Houston, Texas, (1975)*, p. 135-156.
- Kan, E. P., Kalensky, Z., Wilson, D. A. "Spectral signatures of forest types," presented at the Third Canadian Symposium on Remote Sensing, Edmonton, Alberta, (September 22-24, 1975).
- Keenan, L., et al. "Making use of shadow enhancement," *Colorado School of Mines*, (1974), 20p.
- Kettig, Robert L. "Computer classification of remotely sensed multispectral image data by extraction and classification of homogeneous objects," *LARS, Purdue University, West Lafayette, Indiana, (1975)*, 184p.
- Kirvida, L. "Computerized interpretation of ERTS data for forest management," *Proceedings, Conference on Machine Processing of Remotely Sensed Data, Purdue University, (October, 1973)*.
- Knipling, E. B. "Leaf reflectance and image formation on color infrared film," *Remote Sensing in Ecology*, Chapter 7, (1969), p. 17-29.
- _____. "Physical and physiological basis for the reflectance of visible and near-infrared radiation from vegetation," *Remote Sensing of the Environment*, Vol. 1, (1970), p. 155-159.
- Lambeck, P. E. and Rice, D. P. "Signature extension using transformed cluster statistics and related techniques," *Environmental Research Institute of Michigan, Ann Arbor, Michigan, (May, 1976)*, 82p.
- Lauer, D. T. "Forest species identification and timber type delineation on multispectral photography: Annual progress report," *Remote Sensing Applications in Forestry for Earth Resources Survey Program, MASA, OSSA, by*

Forestry Remote Sensing Lab., University of California, Berkeley, California, (1968).

- Lawrence, Robert D., and Herzog, James H. "Computer classification of ERTS-1 digital data for information on geology and forestry," Oregon State University Department of Geology and Electrical and Computer Engineering, (1974).
- Lyons, R. J., et al. "Multispectral signatures in relation to ground control signatures using nested sampling approach," Stanford University, California, (1973), 20p.
- Malila, W. A., Hieber, R. H., and Sarno, J. E. "Analysis of multispectral signatures and investigation of multi-aspect remote sensing techniques," Environmental Research Institute of Michigan, (1974).
- Malila, William A., Hieber, Ross H., and Cicone, Richard C. "Studies of recognition with multitemporal sensor data," Environmental Research Institute of Michigan, Infrared and Optics Division, (1975), 99p.
- Malila, W. A., et al. "Correlation of ERTS MSS data and earth coordinate systems," Environmental Research Institute of Michigan, (1973), 15p.
- McBirney, A. R. "Compositional variations of the climatic eruptions of Mount Mazama," Oregon Department of Geology and Mineral Industries, Bulletin 62, (1968), p. 53-56.
- McCammon, B. P. "Snowpack influences on dead fuel moisture," Forest Science, (September, 1976), p. 323-328.
- McKee, Bates. "Cascadia -- The geologic evolution of the Pacific Northwest," The Cascade Volcanoes, McGraw-Hill Book Company, New York, Chapter 13, (1972), p. 194-217.
- McNeil, Robert C. "Vegetation and fire history of a ponderosa pine-white fir forest in Crater Lake National Park," Thesis (MS) Oregon State University, Botany Department, (1976).
- Minore, Don. "A classification of forest environment in the south Umpqua basin," USDA Forest Service Research Paper PNW-129, (1972).

- Moessner, K. E. "Training handbook -- Basic techniques in forest photo interpretation," Intermountain Forest and Range Experiment Station, USDA Forest Service, (1960).
- Mueller, Elizabeth Laura. "Introduction to the ecology of the pumice desert, Crater Lake National Park, Oregon," Thesis (MS) Purdue University, (1966).
- Mueller-Dombois, Dieter and Ellenberg, Heinz. Aims and Methods of Vegetation Ecology, John Wiley and Sons, New York, Ed. 1, (1974), p. 544.
- Muller, R. A. "Transmission components of solar radiation in pine stands in relation to climate and stand variables," USDA Forest Service Research Paper PSW-71, (1971).
- NASA Goddard Space Flight Center. "LANDSAT data users handbook," Document No. 76sd4258, Greenbelt, Maryland, (1976), p. 132.
- National Park Service. Department of the Interior, Draft for Crater Lake National Park -- Environmental Statement prepared by Denver Service Center, National Park Service, (1976 and 1970), p. 181.
- Nie, N. H., Hull, C. H., Jenkins, J. G., Steinbrenner, K., and Bent, D. B. Statistical Package for the Social Sciences, Second Ed., McGraw-Hill, New York, (1975), p. 673.
- Noble, Drake, Whallon. "Some preliminary observations on compositional variations within the pumice and scoria flow deposits of Mount Mazama," Oregon Department of Geology and Mineral Industries, Bulletin 65, (1969), p. 159-164.
- Norick, N. X. "Processing of ERTS computer-compatible tapes," Evaluation of ERTS-1 Data for Forest and Rangeland Surveys, Pacific Southwest Forest and Range Experiment Station, (1975).
- Nunnally, N. R. "Introduction to remote sensing: The physics of electromagnetic radiation," The Surveillant Science -- Remote Sensing of the Environment, Robert K. Holz, Ed., (1973), p. 18-27.
- Oosting, H. J. and Billings, W. D. "The red fir forest of the Sierra Nevadas," Ecological Monograph, Vol. 13, (1943), p. 260-274.

- Oregon's Long-Range Requirements for Water by State Water Resources Board (Klamath Drainage Basin), (1969), p. 100.
- Peet, F. G. "A primer on the use of digital LANDSAT data," Forest Management Institute, Canadian Forestry Service, (January, 1976), 21p.
- Poulton, Charles E. "Inventory and analysis of natural vegetation and related resources from space and high altitude photography," Report for the Earth Resources Survey Program, Office of Space Sciences and Applications, NASA, (September, 1972), 55p.
- Reeves, Robert G. Manual of Remote Sensing. Virginia (Falls Church), American Society of Photogrammetry, (1975), Vol. 1 and 2, p. 2144.
- Richardson, Wyman, and Gleason, James M. "Multispectral processing based on groups of resolution elements," Environmental Research Institute of Michigan, Infrared and Optics Division, (1975), 86p.
- Robinove, Charles J. "A radiometric interpretive legend for LANDSAT digital thematic maps," Photogrammetric Engineering and Remote Sensing, Vol. 43, No. 5, (May, 1977), p. 593-594.
- Sadowski, F. and Sarno, J. "Forest classification accuracy as influenced by multispectral scanner spatial resolution," Environmental Research Institute of Michigan, Ann Arbor, Michigan, (May, 1976), 130p.
- Sayn-Wittgenstein, L. "Recognition of tree species on air photographs by crown characteristics," Canadian Department of Forestry, Forest Research Branch, Technical Note No. 95, (1960), 55p.
- _____. "Phenological aids to species identification on air photographs," Canadian Department of Forestry, Forest Research Branch, Technical Note No. 104, (1961), 26p.
- Sayn-Wittgenstein, L. and Kalensky, Z. "Interpretation of forest patterns on ERTS-1/MSS images," Proceedings of the Second Canadian Symposium on Remote Sensing, Guelph, Ontario, Canada, (1974).
- Smedes, Harry W. "The mixture problem in computer mapping of terrain: Improved techniques for establishing spectral signatures, atmospheric path radiance, and transmittance," Proceedings of the NASA Earth Resources

- Survey Symposium, Houston, Texas, (June, 1975), 1099-1159.
- Smedes, Harry W. "Preprocessing of multispectral data and simulation of ERTS data channels to make computer terrain maps of a Yellowstone National Park test site," Third Annual Earth Resources Review, Sec. 10, (December, 1970).
- Smith, J. A., and Oliver, R. E. "Effects of changing canopy directional reflectance on feature selection," Applied Optics, (1974), p. 1597-1604.
- Snedecor, G. W. and Cochran, W. G. Statistical Methods, Iowa State University Press, Sixth Edition, Ames, Iowa, (1967), 593p.
- Sternes, G. L. Climate of Crater Lake National Park, Oregon. Crater Lake National History Association, (March, 1963), 12p.
- Storey, T. C., et al. "Crown characteristics of several coniferous tree species," United States Forest Service, Division of Fire Research, Interim Technical Report, AFSWP-416, (1955).
- Swain, Philip H. "Pattern recognition: A basis for remote sensing data analysis," Lars Information Note 111572, (1972), 4lp.
- Swanlund, G. D., et al. "Automatic photointerpretation for plant species and stress identification," Honeywell, Inc., (1973), 6p.
- Thomas, Valerie L. "Generation and physical characteristics of the LANDSAT 1 and 2 MSS computer compatible tapes," Goddard Space Flight Center, Greenbelt, Maryland, (November, 1975), p. 28.
- Thomson, F., et al. "Yellowstone National Park mapping from ERTS-1 computer compatible tapes," Environmental Research Institute of Michigan, (1974), 35p.
- Tordills, G. P., and Fandgrebe, D. "On pattern recognition," Lars Information Note 101866, Laboratory for Applications of Remote Sensing, Purdue University, (1966), 18p.
- Turner, Robert E. "Atmospheric effects in multispectral remote sensor data," Environmental Research Institute of Michigan, Infrared and Optics Division, (1975), 120p.

- Turner, Robert E. "Radiative transfer in real atmospheres," Environmental Research Institute of Michigan, Infrared and Optics Division, (1975), 107p.
- USDA Soil Conservation Service. "Soil interpretations for Oregon," OR-Soils-1, (12/1972).
- United States Geologic Survey, Department of the Interior. Topographic Map, "Crater Lake National Park and Vicinity, Oregon: Scale 1:62,500," (1956).
- Vincent, R. K., Thomas, G. S., and Nalepka, R. F. "Signature extension studies," Technical Report, Environmental Research Institute of Michigan to the LBJ Space Center, Houston, Texas, (1974), 49p.
- Waring, R. H. "Forest plants of the eastern Siskiyou: Their environmental and vegetational distribution," Northwest Science, Vol. 43, (1969), p. 1-17.
- Weber, F. D. et al. "Forest stress detection," Evaluation of ERTS-1 Data for Forest and Rangeland Surveys -- Pacific Southwest Forest and Range Experiment Station, (1975), paper 112.
- Wiegand, C. L., Gausman, H. W., Cuellar, J. A., Gerberman, A. H., Richardson, A. J. "Vegetation density as deduced from ERTS-1 MSS response," Third ERTS-1 Symposium, (1973), 93p.
- Williams, C. B., and Dyrness, C. T. "Some characteristics of forest floor and soils under true fir-hemlock stands in the Cascade Range," USDA Forest Service Research Paper PNW-37, (1967), 19p.
- Williams, Darrel L. "A canopy-related stratification of a southern pine forest using LANDSAT digital data," Goddard Space Flight Center, Greenbelt, Maryland, (August, 1976), 11p.
- Williams, Howel. Ancient Volcanoes of Oregon. Oregon University Press, Eugene, (1943), 68p.
- _____. Crater Lake -- The Story of its Origin. University of California Press, Berkeley, Los Angeles, and London, (1957 and 1972), p. 97.
- _____. The Geology of Crater Lake National Park, Oregon. Carnegie Institute, Washington, D. C., Publication 540, (1942), 162p.

- Williams, Howel, and Goles, Gordon. "Volume of the Mazama ash-fall and the origin of Crater Lake caldera," Oregon Department of Geology and Mineral Industries, Vol. 62, (1968), p. 37-41.
- Wolf, P. R. Elements of Photogrammetry. McGraw-Hill Publishers, New York, (1974), p. 562.
- Worley and Meyer. "Measurement of crown diameter and crown cover and their accuracy on 1:12,000 scale photographs," Photogrammetric Engineering, Vol. 19, (1955), p. 372-375.
- Wynd, F. L. "The flora of Crater Lake National Park," American Midland Natural, Vol. 17, No. 6, (1936), p. 881-949.
- Youngberg, C. T., and Dyrness, C. T. "Some physical and chemical properties of pumice soils in Oregon," Soil Science, Vol. 97, (1964), p. 391-399.
- Zobel, Donald B., et al. "Relationships of environment to composition, structure, and diversity of forest communities of the central western Cascades of Oregon," Ecological Monographs, Vol. 46, No. 2, (Spring, 1976), p. 135-156.
- _____. "Data users handbook," NASA Earth Resources Technology Program, (1972), 70p.
- _____. "A crown density scale for photo interpreters," Journal of Forestry, Vol. 47, No. 7, (1947), p. 569.
- _____. "Applied infrared photography," Kodak Manual M-28, (1972), 89p.
- _____. "The influence of soils and topography on the occurrence of lodgepole pine in Central Oregon," Northwest Science, Vol. 33, (1959), p. 111-120.
- _____. "Silvics of forest trees of the United States," United States Department of Agriculture Handbook No. 271, (1965), 762p.
- _____. "Silvicultural systems of the major forest types of the U.S.," USDA Forest Service, Agricultural Handbook No. 445, (1973), 114p.

APPENDICES

APPENDIX I

Cluster Analysis

DISTANCES BETWEEN CLUSTERS

	1	2	3	4	5	6	7	8	9	10	11	12	13	14	15
1	00														
2	27 86	00													
3	999 99	999 99	999 99												
4	46 33	104 40	999 99												
5	6 47	25 40	999 99	54 64											
6	28 51	22 72	999 99	69 49	22 62										
7	8 35	31 27	999 99	21 29	11 23	24 32									
8	9 63	19 90	999 99	63 41	4 89	21 42	00								
9	23 12	22 02	999 99	67 01	16 4	24 44	14 35	00							
10	3 56	26 68	999 99	56 02	4 28	26 6	20 11	15 6							
11	16 19	20 93	999 99	45 17	10 7	10 7	13 6	11 3	20 5	00					
12	28 71	17 21	999 99	68 59	17 33	10 17	13 38	11 3	12 4	14 26	00				
13	10 32	13 85	999 99	57 36	23 43	11 11	17 36	13 3	13 13	16 7	13 44	00			
14	26 51	21 14	999 99	68 74	21 8	3 12	23 33	10 3	13 13	25 93	13 8	16 49	00		
15	11 85	31 86	999 99	7 43	16 65	31 45	21 33	21 16	18 3	15 37	19 39	20 87	18 56	00	
16	0 66	20 76	999 99	58 16	13 82	11 45	26 16	10 55	26 34	16 76	13 20	6 55	33 47	18 82	31 17
17	19 25	15 25	999 99	72 82	13 67	17 12	26 56	7 76	16 83	16 92	7 76	6 93	20 80	6 14	23 40
18	14 94	10 62	999 99	73 62	12 10	19 04	19 52	7 57	15 81	12 88	13 34	5 89	8 05	9 68	10 27
19	4 11	27 79	999 99	28 87	9 09	28 01	4 02	12 19	23 61	7 47	15 99	14 82	12 32	9 59	19 56
20	10 92	16 26	999 99	60 42	8 31	21 03	16 72	4 04	16 61	8 43	12 88	4 55	28 47	12 04	27 73
21	20 86	9 42	999 99	83 75	16 96	14 78	24 12	11 11	16 58	18 33	12 88	8 76	16 63	7 06	21 22
22	3 82	27 27	999 99	47 16	9 34	26 01	16 52	12 77	12 16	18 72	12 57	10 74	6 86	12 59	15 08
23	14 55	17 05	999 99	81 90	3 46	26 01	16 52	12 77	20 6	12 18	13 33	4 21	26 60	5 75	25 38
24	19 99	16 86	999 99	83 85	17 47	19 62	24 39	12 77	19 9	12 18	13 33	10 25	11 83	5 75	10 46
25	28 29	16 52	999 99	80 60	22 17	19 4	26 69	12 77	19 9	12 18	13 33	10 25	11 83	5 75	10 46
26	7 95	23 00	999 99	38 74	3 87	18 7	26 7	12 77	13 3	26 7	12 18	16 25	11 3	10 94	8 07
27	8 7	17 54	999 99	36 23	16 24	16 7	26 7	12 77	13 3	19 66	16 11	8 66	20 54	4 77	17 45
28															6 29

1	2	3	4	5	6	7	8	9	10	11	12	13	14	15
3916.16	13 38	999 99	71.02	11.37	15.55	19.06	7.30	10.97	13.78	9.58	3.79	10.16	7.46	15.01
3021.04	21.80	999 99	48.79	15.40	6.23	16.15	15.82	3.87	19.04	4.23	13.02	13.87	13.19	4.20
3140.16	25.26	999 99	97.40	37.43	10.83	33.27	31.52	16.27	19.53	4.07	26.37	11.48	29.27	13.68
3121.08	12.28	999 99	75.80	16.57	10.47	22.33	12.92	16.00	37.37	10.27	26.91	14.48	29.16	19.24
3324.57	8.23	999 99	82.02	21.11	12.03	25.92	16.93	12.08	18.46	13.72	13.43	4.24	14.51	13.29
3435.61	25.25	999 99	77.77	29.05	12.74	28.53	27.99	13.09	32.74	13.02	23.39	12.98	25.71	10.30
3533.29	20.73	999 99	79.08	29.41	14.17	28.58	27.49	18.22	31.84	19.47	23.88	14.11	26.31	16.77
3628.74	19.97	999 99	61.65	20.46	15.86	23.88	25.44	19.16	26.06	19.53	23.71	16.44	24.34	18.29
3724.19	16.29	999 99	73.24	10.98	6.05	23.33	16.34	5.18	22.23	16.31	12.46	16.54	14.91	18.71
3812.01	26.46	999 99	47.35	6.43	14.36	11.64	7.18	8.95	10.22	4.11	6.46	16.62	4.22	12.92
3930.17	6.70	999 99	106.01	27.05	18.78	31.90	22.07	19.62	28.92	19.78	18.82	11.29	22.25	20.22
4032.85	24.08	999 99	75.61	26.06	3.26	26.68	24.91	9.06	30.07	13.34	20.46	10.71	22.74	6.68
3336.68	21.86	999 99	87.37	27.57	7.37	29.17	25.49	12.05	31.11	15.70	20.99	8.83	23.86	9.85
3525.27	4.40	999 99	47.44	21.93	15.03	28.19	16.81	17.80	23.58	17.34	13.75	9.55	17.55	20.07
3630.03	19.25	999 99	96.00	30.13	12.10	31.73	27.37	15.84	33.56	18.49	22.88	9.61	25.46	14.16
3909.04	20.25	999 99	71.49	22.93	3.31	24.95	21.24	6.17	26.80	19.76	16.90	7.39	19.17	4.04
4537.46	25.79	999 99	75.20	32.71	12.07	30.72	31.39	17.97	35.98	19.79	26.88	15.09	29.30	15.64
24.74	3.40	999 99	99.60	22.15	21.97	28.68	16.76	20.51	23.11	19.24	14.20	12.65	18.26	23.35
14.80	23.09	999 99	35.02	10.12	13.70	9.92	12.04	9.39	13.56	3.73	11.22	18.57	9.11	11.91
26.61	8.74	999 99	80.68	24.96	10.15	27.35	20.94	17.02	26.73	17.41	18.19	11.25	20.57	17.28
3943.33	23.15	999 99	111.73	32.63	11.82	35.25	29.72	16.34	36.49	19.50	24.52	9.10	27.90	14.27
5043.19	28.98	999 99	86.16	37.17	11.25	35.16	35.76	19.34	41.48	20.88	30.16	14.87	32.78	15.07
26.69	5.24	999 99	89.58	24.94	20.87	28.44	20.46	20.64	26.37	19.51	17.99	14.12	20.83	22.29
22.12	6.45	999 99	91.65	18.83	18.62	25.82	13.69	16.57	20.28	15.82	10.80	9.32	14.76	19.56
34.12	18.09	999 99	89.75	28.25	11.08	36.51	25.20	13.42	31.97	16.44	20.65	6.52	23.65	12.46
32.33	26.06	999 99	74.66	24.80	2.95	25.57	24.21	6.61	29.39	10.89	19.57	12.49	21.42	2.97
5512.34	34.63	999 99	13.08	15.35	28.57	3.83	16.68	24.35	15.71	16.34	26.77	34.57	16.81	27.63
9.52	25.44	999 99	26.17	7.94	18.98	4.58	11.11	14.73	10.10	18.27	12.36	23.79	8.79	17.75
43.92	27.43	999 99	97.88	38.00	15.99	36.90	35.67	21.33	41.90	23.89	30.61	16.37	33.73	19.13
35.26	22.24	999 99	91.76	28.69	7.54	30.76	26.34	11.78	32.66	15.72	7.65	21.44	24.35	9.63
43.18	29.39	999 99	85.99	36.74	12.30	34.68	35.23	18.81	40.83	21.95	16.05	29.97	32.95	16.11
6032.64	3.71	999 99	121.42	29.27	23.27	35.51	23.40	24.66	30.97	23.47	20.12	15.68	24.25	26.84

	16	17	18	19	20	21	22	23	24	25	26	27	28	29	30
16	00														
16	34	00													
24	95	13	00												
21	46	8	81												
20	7 10	9	67	20	23	16	40								
19	45	4	31	10	66	4	54	13	37	00					
26	87	14	13	5	75	22	01	10	10	00					
13	25	6	04	14	11	6	17	16	24	19	46				
20	98	9	59	16	96	8	00	8	14	0	14				
26	06	13	38	3	63	16	04	13	07	5	00				
35				10	30	21	23	9	07						
31	07	22	46	9	53	27	75	19	35	19	83	15	68		
12	78	7	76	12	16	8	34	4	76	8	48	16	57		
26	83	16	46	3	67	22	53	19	46	5	40	13	32		
22	60	9	97	4	19	17	53	16	60	4	11	7	50		
22	78	17	69	16	19	20	20	16	66	7	78	17	78		
40	40	33	57	18	53	37	89	30	08	13	62	19	96		
26	17	15	23	6	92	21	98	12	04	4	11	20	49		
28	54	18	74	10	70	25	07	15	16	5	93	6	94		
35	60	29	71	23	33	33	31	32	69	17	17	24	07		
35	97	28	36	22	27	31	31	31	78	19	77	21	87		
26	66	25	57	21	18	20	00	23	26	19	32	21	01		
28	66	18	66	11	10	12	04	15	82	8	10	13	53		
16	66	9	66	13	10	12	12	12	12	4	10	14	40		
32	55	23	27	14	66	29	27	19	14	17	38	11	04		
34	78	27	06	21	74	31	47	18	60	29	62	14	20		
35	67	27	44	21	94	32	32	24	27	30	93	15	64		
29	44	18	20	11	12	25	27	24	05	13	37	20	93		
37	26	29	24	21	61	34	37	18	16	18	16	20	81		
31	92	23	58	18	16	20	81	20	90	11	26	18	35		
37	19	33	53	20	56	35	89	29	75	21	10	26	24		
29	47	17	54	15	22	24	95	24	03	14	61	16	41		
16	23	17	35	11	07	13	98	11	35	8	34	17	92		
20	34	21	93	14	47	18	90	26	32	18	62	10	05		
40	86	31	89	10	53	37	79	36	36	18	90	23	08		
50	51	37	58	30	20	34	19	41	35	22	90	29	75		
27	72	21	19	15	63	27	72	22	27	17	31	10	47		
36	34	15	12	19	70	22	22	26	06	22	15	13	15		
54	15	26	71	13	95	33	64	33	11	16	14	18	92		
		12	14	22	14	24	25	24	25	12	48	22	98		

55	3.75	16.91	24.28	22.80	7.17	20.37	27.73	12.56	20.21	27.74	29.81	16.77	25.28	22.59	19.39
	10.21	11.01	14.87	15.55	7.85	13.39	18.39	7.29	11.45	19.37	20.42	3.87	15.52	14.02	11.66
	44.14	37.32	23.37	29.21	41.64	33.67	24.18	41.39	24.73	28.01	12.56	31.90	20.93	27.20	19.38
	37.55	29.66	13.71	21.66	34.04	25.24	15.71	32.34	15.73	21.43	3.24	23.99	10.92	18.11	11.87
	43.46	36.96	22.43	29.76	41.00	33.56	24.28	40.49	23.15	29.61	11.90	30.61	19.20	27.67	16.87
60	35.60	24.51	17.15	13.45	31.59	19.66	11.03	31.37	19.55	9.73	17.40	26.17	14.54	15.17	24.35
	16	17	18	19	20	21	22	23	24	25	26	27	28	29	30

INSTANCES BETWEEN CLUSTERS

31	0.00														
	15.86	5.00													
	14.07	5.29	0.00												
	5.91	14.95	14.88	0.00											
35	7.66	16.56	14.34	8.77	0.00										
	12.71	17.88	16.12	12.35	5.10	0.00									
	12.09	4.37	7.27	10.56	14.86	16.55	0.00								
	23.44	10.44	14.60	20.17	22.12	20.81	11.56	0.00							
	16.57	11.21	5.28	18.72	14.63	15.25	13.51	20.55	0.00						
40	7.75	11.72	12.63	4.44	11.93	14.82	7.18	17.29	18.37	0.00					
	4.05	11.72	11.24	4.00	9.23	13.06	8.27	19.08	15.78	4.22	0.00				
	21.83	8.33	4.94	21.98	19.07	19.21	12.44	16.97	5.93	20.27	18.37	0.00			
	3.53	12.90	10.13	8.66	7.95	12.02	10.93	21.48	12.44	9.35	5.90	16.93	0.00		
45	9.53	18.33	9.75	13.82	13.64	15.98	3.65	14.35	15.32	3.95	5.93	16.42	9.37	0.00	
	26.01	18.59	17.21	25.66	4.39	18.47	15.01	23.74	18.56	9.90	7.77	23.41	9.28	13.03	0.00
	21.79	13.07	8.33	25.29	21.55	20.57	13.34	18.24	8.64	23.93	21.95	3.94	20.88	19.93	26.34
			16.60	18.33	21.04	19.02	12.91	5.15	21.97	16.27	18.62	19.62	21.04	14.09	21.74
	13.10	11.65	7.16	15.13	11.31	12.16	12.69	18.39	3.29	15.03	12.86	8.27	9.68	13.50	14.82
	3.30	13.62	8.21	9.76	9.76	14.45	10.56	23.06	15.29	8.84	4.57	19.30	3.54	8.60	10.13
50	3.84	19.69	10.11	23.73	6.62	12.34	14.79	25.99	19.52	8.20	5.33	25.77	6.98	11.76	5.13
	21.71	12.89	8.38	22.66	17.42	17.36	15.63	19.54	4.70	21.28	19.22	6.83	16.40	18.40	22.80
	23.19	7.44	6.46	22.67	20.09	20.39	11.89	14.89	9.11	20.14	18.66	3.43	13.01	16.46	24.65
	7.53	10.29	7.44	10.26	11.70	14.57	8.44	19.32	10.52	9.48	7.07	14.57	4.76	7.80	12.64
	12.51	11.31	13.67	9.58	15.93	18.60	6.21	15.36	20.68	4.40	8.25	21.65	12.85	3.56	15.28
55	37.59	26.04	29.16	32.61	31.92	25.95	27.21	14.97	34.97	31.25	33.54	31.47	35.82	29.08	34.56
	27.80	16.78	20.05	23.63	24.61	21.37	17.55	6.89	25.64	21.62	23.81	22.41	26.05	19.33	26.22
	5.99	20.13	17.37	8.61	3.68	9.58	17.29	27.74	18.53	12.45	8.77	24.58	7.66	15.17	5.21
	5.73	11.28	10.75	6.38	11.54	15.11	7.32	19.37	15.46	5.24	3.18	18.31	6.25	4.96	10.64
	6.89	19.65	18.15	4.34	5.92	11.08	15.72	26.32	20.96	9.45	6.86	26.24	9.24	13.27	2.79
60	26.40	13.65	8.00	27.57	21.75	21.69	17.83	23.27	4.53	26.00	23.25	4.85	20.07	21.76	27.99

INSTANCES BETWEEN CLUSTERS

46	0.00														
	21.27	0.00													
	10.52	19.38	0.00												
	23.48	22.36	12.49	0.00											
50	29.68	23.23	15.68	6.95	0.00										
	7.77	21.31	4.70	20.44	25.78	0.00									
	4.03	18.21	10.53	20.57	27.82	9.16	0.00								
	18.98	19.49	8.57	4.56	10.69	14.86	15.55	0.00							
	25.47	14.04	17.08	13.24	14.55	23.38	21.34	11.73	0.00						
55	32.08	12.59	29.87	39.69	39.25	31.03	29.22	34.72	30.08	0.00					
	23.30	5.49	22.06	28.61	29.18	23.22	20.44	24.42	20.01	7.08	0.00				
	28.59	26.39	14.07	8.89	3.16	28.59	25.77	12.36	17.50	41.62	31.37	0.00			
	22.37	18.90	12.88	4.10	7.99	19.64	18.90	5.26	8.65	35.25	24.63	11.65	0.00		
	30.17	24.49	16.41	9.90	3.33	25.21	27.10	13.84	14.68	39.66	29.64	5.72	10.80	0.00	
60	6.48	25.68	6.63	24.23	31.17	3.62	8.33	17.67	28.44	38.84	28.76	28.26	23.48	31.31	0.00

Cluster Analysis

BAND SET = 1 2 3 4

CLASS	WEIGHTED DIVERGENCE CLASS PAIRS																		
	2	3	4	5	6	7	8	9	10	11	12	13	14	15	16	17	18	19	20
1	2000	2000	1981	2000	2000	2000	2000	1513	2000	2000	2000	2000	2000	2000	1990	2000	2000	1720	2000
2		2000	2000	2000	2000	2000	2000	2000	2000	2000	2000	2000	2000	2000	2000	2000	2000	2000	2000
3			2000	2000	2000	2000	2000	2000	2000	2000	2000	2000	2000	2000	2000	2000	2000	2000	2000
4				2000	2000	1855	2000	1687	2000	1998	2000	1578	2000	2000	1718	2000	2000	2000	1998
5					2000	2000	1934	2000	2000	2000	2000	2000	1520	2000	2000	2000	2000	2000	2000
6						2000	2000	2000	2000	2000	2000	2000	2000	1910	2000	2000	2000	1796	2000
7							2000	1984	2000	1519	2000	1503	2000	2000	1541	2000	1996	2000	1679
8								2000	1948	2000	2000	2000	1727	2000	2000	1994	2000	2000	2000
9									2000	2000	2000	1993	2000	2000	1612	2000	2000	1996	1999
10										2000	2000	2000	2000	2000	2000	1998	2000	2000	2000
11											2000	1742	2000	2000	1988	1983	1931	2000	1690
12												2000	2000	2000	2000	2000	2000	2000	2000
13													2000	2000	1959	2000	2000	2000	1994
14														2000	2000	2000	2000	2000	2000
15															2000	2000	2000	1984	2000
16																2000	2000	2000	1724
17																	1999	2000	2000
18																		2000	1682
19																			2000
20																			
21																			

	21	22	23	24	25	26	27	28	29	30	31	32	33	34	35	36	37	38	39	40
1	2000	1584	2000	2000	2000	1999	2000	2000	2000	2000	2000	2000	2000	2000	2000	2000	2000	2000	2000	2000
2	2000	2000	2000	1996	2000	2000	2000	2000	2000	2000	2000	2000	2000	2000	2000	2000	2000	1983	2000	2000
3	2000	2000	2000	2000	2000	2000	2000	2000	2000	2000	2000	2000	2000	2000	2000	2000	2000	2000	2000	2000
4	2000	1451	2000	2000	2000	1619	2000	2000	2000	2000	2000	2000	2000	2000	2000	2000	1974	2000	2000	2000
5	2000	2000	2000	2000	1995	2000	1998	2000	1989	2000	2000	2000	1996	2000	2000	1970	2000	2000	1574	1999
	2000	1999	2000	2000	2000	1972	2000	2000	2000	2000	2000	2000	2000	2000	2000	2000	2000	2000	2000	2000
	2000	1998	1995	2000	2000	1994	2000	1993	2000	2000	2000	2000	2000	2000	2000	2000	2000	2000	2000	2000
	2000	2000	1981	2000	2000	2000	1521	2000	1741	2000	1999	2000	2000	2000	2000	2000	1993	2000	2000	2000
	2000	1546	2000	2000	2000	1995	2000	2000	2000	2000	2000	2000	2000	2000	2000	2000	1927	1999	2000	2000
10	2000	2000	1905	2000	2000	1996	1993	2000	1698	2000	2000	2000	2000	2000	2000	2000	2000	2000	2000	2000
	2000	2000	1628	2000	2000	1999	2000	1531	2000	2000	2000	2000	2000	2000	2000	2000	2000	1649	2000	2000
	1975	2000	2000	2000	1723	2000	2000	2000	2000	2000	1883	1937	2000	2000	2000	1984	2000	2000	2000	2000
	2000	1983	1925	2000	2000	1850	2000	1992	2000	2000	2000	2000	2000	2000	2000	2000	1743	2000	2000	2000
	2000	2000	2000	2000	1999	2000	1977	2000	1703	2000	2000	2000	2000	2000	2000	1953	2000	2000	1973	2000
15	2000	2000	2000	2000	2000	2000	2000	2000	2000	2000	2000	2000	2000	2000	2000	2000	2000	2000	2000	2000
	2000	1951	2000	2000	2000	1994	2000	2000	2000	2000	2000	2000	2000	2000	2000	2000	1999	2000	2000	2000
	1970	2000	1601	2000	2000	2000	1550	1600	2000	2000	1415	2000	2000	2000	2000	1863	1997	2000	2000	2000
	1890	2000	1995	1685	2000	2000	2000	1676	2000	2000	1997	2000	2000	2000	2000	2000	2000	2000	2000	2000
	2000	1946	2000	2000	2000	1988	2000	2000	2000	2000	2000	2000	2000	2000	2000	2000	2000	2000	2000	2000
20	2000	2000	1993	2000	2000	2000	2000	1970	2000	2000	2000	2000	2000	2000	2000	2000	2000	2000	2000	2000
		2000	2000	1836	2000	2000	1999	1813	2000	2000	1662	1948	2000	2000	2000	2000	2000	2000	2000	2000
22			2000	2000	2000	1852	2000	2000	2000	2000	2000	2000	2000	2000	2000	2000	2000	2000	2000	2000

	41	42	43
1	2000	2000	2000
	1707	2000	2000
	2000	2000	2000
	2000	2000	2000
5	2000	2000	1461
	2000	2000	2000
	2000	2000	2000
	2000	2000	1962
	2000	2000	2000
10	2000	2000	2000
	2000	2000	2000
	2000	2000	1999
	2000	2000	2000
	2000	2000	1661
	2000	2000	2000
15	2000	2000	2000
	2000	2000	2000
	2000	2000	2000
	1998	2000	2000
	2000	2000	2000
	2000	2000	2000
20	1957	2000	2000
22	2000	2000	2000
39	40 1793	41 2000	42 2000
40			43 1693
41		2000	1978
42			1978
			2000
			2000

CLASS	44	45	46	47	48	49	50	51	52	53	54	55	56	57	58	59
1	2000	2000	2000	2000	2000	2000	2000	2000	2000	2000	2000	2000	2000	2000	2000	2000
2	2000	1633	2000	2000	2000	2000	1960	1997	2000	2000	2000	2000	2000	2000	2000	1770
3	2000	2000	2000	2000	2000	2000	2000	2000	2000	2000	2000	2000	2000	2000	2000	2000
4	2000	2000	2000	2000	2000	2000	2000	2000	2000	2000	2000	1999	2000	2000	2000	2000
5	2000	2000	2000	2000	2000	2000	2000	2000	2000	1802	2000	2000	2000	2000	2000	2000
6	2000	2000	1999	2000	2000	2000	2000	2000	2000	2000	1537	1592	2000	2000	2000	2000
7	2000	2000	2000	2000	2000	2000	2000	2000	2000	2000	2000	2000	2000	2000	2000	2000
8	2000	2000	1999	2000	2000	2000	2000	2000	2000	1949	2000	2000	2000	2000	2000	2000
9	2000	2000	2000	2000	2000	2000	2000	2000	2000	2000	2000	2000	2000	2000	2000	2000
10	2000	2000	1603	2000	2000	2000	2000	2000	2000	2000	2000	1997	2000	2000	2000	2000
11	2000	2000	2000	2000	2000	2000	2000	2000	2000	2000	2000	2000	2000	2000	2000	2000
12	2000	2000	2000	2000	2000	2000	2000	2000	1998	2000	2000	2000	2000	2000	2000	2000
13	2000	2000	2000	2000	2000	2000	2000	2000	2000	2000	2000	2000	2000	2000	2000	2000
14	2000	2000	2000	2000	2000	2000	2000	2000	2000	2000	1519	2000	2000	2000	2000	2000
15	2000	2000	2000	2000	2000	2000	2000	2000	2000	2000	1566	2000	2000	2000	2000	2000
16	2000	2000	2000	2000	2000	2000	2000	2000	2000	2000	2000	2000	2000	2000	2000	2000
17	2000	2000	2000	2000	2000	2000	2000	2000	2000	2000	2000	2000	2000	2000	2000	2000
18	2000	1999	2000	2000	2000	2000	2000	1905	2000	2000	2000	2000	2000	2000	2000	2000
19	2000	2000	2000	2000	2000	2000	2000	2000	2000	2000	1997	1996	2000	2000	2000	2000

	44	45	46	47	48	49	50	51	52	53	54	55	56	57	58	59
20	2000	2000	2000	2000	2000	2000	2000	2000	2000	2000	2000	2000	2000	2000	2000	2000
21	2000	1998	2000	2000	2000	2000	2000	1710	2000	2000	2000	2000	2000	2000	2000	2000
22	2000	2000	2000	2000	2000	2000	2000	2000	2000	2000	2000	1998	2000	2000	2000	2000
23	2000	2000	2000	2000	2000	2000	2000	2000	2000	2000	2000	2000	2000	2000	2000	2000
24	2000	1699	2000	2000	2000	2000	2000	1409	2000	2000	2000	2000	2000	2000	2000	2000
25	2000	2000	2000	2000	1972	2000	2000	2000	1918	1999	2000	2000	2000	1838	2000	2000
26	2000	2000	1973	2000	2000	2000	2000	2000	2000	2000	2000	1635	2000	2000	2000	2000
27	2000	2000	2000	2000	2000	2000	2000	2000	2000	1996	2000	2000	2000	2000	2000	2000
28	2000	2000	2000	2000	2000	2000	2000	1998	2000	2000	2000	2000	2000	2000	2000	2000
29	2000	2000	1956	2000	2000	2000	2000	2000	2000	1992	2000	2000	2000	2000	2000	2000
30	2000	2000	2000	2000	1735	1693	2000	2000	2000	2000	2000	2000	1987	2000	2000	2000
31	2000	2000	2000	2000	2000	2000	2000	1999	2000	2000	2000	2000	2000	2000	2000	2000
32	2000	1999	2000	1998	2000	2000	2000	1972	2000	2000	2000	2000	2000	2000	2000	2000
33	1955	2000	2000	2000	2000	1744	2000	2000	2000	2000	2000	2000	2000	1997	1913	2000
34	1848	2000	2000	2000	2000	1999	2000	2000	2000	2000	2000	2000	1987	2000	1999	2000
35	2000	2000	2000	2000	2000	2000	2000	2000	2000	2000	2000	2000	2000	2000	2000	2000
36	2000	2000	2000	2000	2000	2000	2000	2000	2000	1980	2000	2000	2000	2000	2000	2000
37	2000	2000	1902	2000	2000	2000	2000	2000	2000	2000	2000	1965	2000	2000	2000	2000

	44	45	46	47	48	49	50	51	52	53	54	55	56	57	58	59	
38	2000	2000	2000	1844	2000	2000	1873	2000	2000	2000	2000	2000	2000	2000	2000	1947	
39	2000	2000	2000	2000	2000	1999	2000	2000	2000	1910	2000	2000	2000	1918	2000	2000	
40	2000	2000	2000	2000	1804	1976	2000	2000	2000	1999	2000	2000	2000	1795	2000	2000	
41	2000	1536	2000	2000	2000	2000	1994	1447	2000	2000	2000	2000	2000	2000	2000	1912	
42	2000	2000	2000	2000	1888	1996	2000	2000	1991	2000	2000	2000	1978	2000	2000	2000	
43	2000	2000	2000	2000	2000	2000	2000	2000	2000	1749	2000	2000	2000	1997	2000	2000	
44		2000	2000	2000	2000	1983	2000	2000	2000	2000	2000	2000	1992	2000	1597	2000	
45			2000	2000	2000	2000	2000	1841	2000	2000	2000	2000	2000	2000	2000	1982	
46				2000	2000	2000	2000	2000	2000	2000	2000	2000	2000	2000	2000	2000	
47					2000	2000	1917	2000	2000	2000	2000	2000	1874	2000	2000	2000	
48						1997	2000	2000	1995	2000	2000	2000	2000	1971	2000	2000	
49							2000	2000	2000	2000	2000	2000	1977	2000	1808	2000	
50								2000	2000	2000	2000	2000	2000	2000	2000	1927	
51									2000	2000	2000	2000	2000	2000	2000	2000	
52										2000	2000	2000	2000	1996	2000	2000	
53											2000	2000	2000	2000	2000	2000	
54												2000	2000	2000	2000	2000	
55													1968	2000	2000	2000	
56														2000	2000	2000	
57															2000	1958	
58																2000	
																	2000

AVERAGE DIVERGENCE = 1981
MINIMUM DIVERGENCE = 1409 FOUND IN CLASS PAIR 24 51

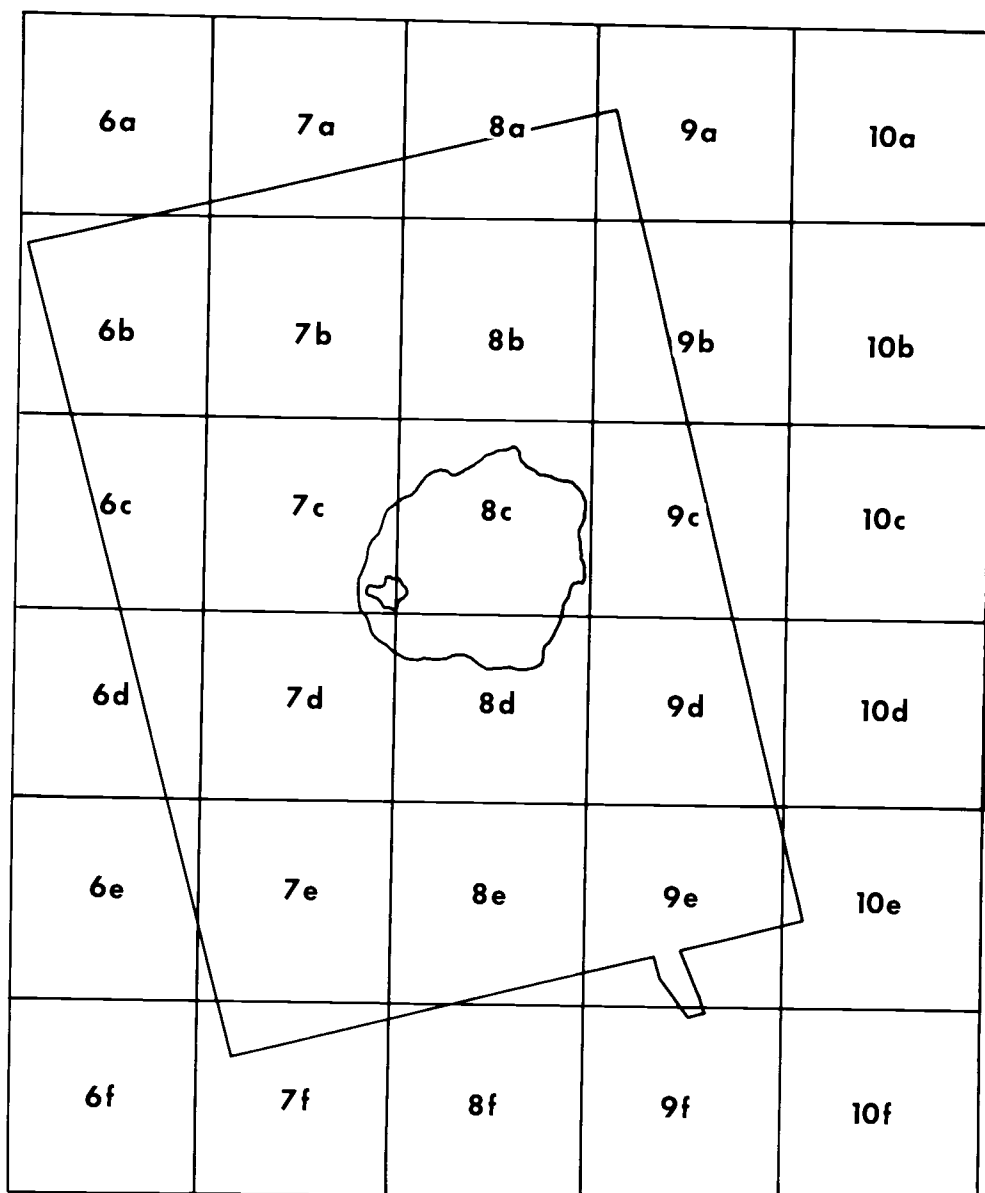
APPENDIX II

Classification Key

<u>Gray levels</u>	<u>Symbol</u>
0	
1	1
2	2
3	3
4	4
5	5
6	6
7	7
8	8
9	9
10	A
11	B
12	C
13	D
14	E
15	F
16	G
17	H
18	I
19	J
20	K
21	L
22	M
23	N
24	O
25	P
26	Q
27	R
28	S
29	T
30	U
31	V
32	W
33	X
34	Y
35	Z

A description of which surface cover types are represented by which symbol for the 59 classes is shown on pages 213 through 217.

Key to Appendix II, LANDSAT Classes 1 Through 35



NOTE:

THE OUTLINE OF CRATER LAKE NATIONAL PARK IS INSERTED IN THE ABOVE FIGURE TO INDICATE WHICH PORTIONS OF APPENDIX II COVER WHICH PORTIONS OF THE PARK.

Figure 45

Classification Key

<u>Gray levels</u>	<u>Symbol</u>
36	1
37	2
38	3
39	4
40	5
41	6
42	7
43	8
44	9
45	A
46	B
47	C
48	D
49	E
50	F
51	G
52	H
53	I
54	J
55	K
56	L
57	M
58	N
59	O

Key to Appendix II, LANDSAT Classes 36 Through 59

6aa	7ar	8aa	9aa	10aa
6bb	7bb	8bb	9bb	10bb
6cc	7cc	8cc	9cc	10cc
6dd	7dd	8dd	9dd	10dd
6ee	7ee	8ee	9ee	10ee
6ff	7ff	8ff	9ff	10ff

NOTE:

**THE OUTLINE OF CRATER LAKE NATIONAL PARK IS INSERTED
IN THE ABOVE FIGURE TO INDICATE WHICH PORTIONS OF
APPENDIX II COVER WHICH PORTIONS OF THE PARK.**


```

000000000000
155555555555
000000000111
123456789012
10a 1 400400 000000
2 40 000000
3 0 000000
4 0 000000
5 0 000000
6 0 000000
7 000000000000
8 400000000000
9 0 000000
10 0 000000
11 0 000000
12 400400 000000
13 0 000000
14 0 000000
15 0 000000
16 0 000000
17 0 000000
18 400400 000000
19 0 000000
20 0 000000
21 0 000000
22 0 000000
23 0 000000
24 400400 000000
25 0 000000
26 0 000000
27 0 000000
28 400400 000000
29 0 000000
30 0 000000
31 0 000000
32 0 000000
33 0 000000
34 0 000000
35 0 000000
36 0 000000
37 0 000000
38 0 000000
39 0 000000
40 0 000000
41 0 000000
42 0 000000
43 0 000000
44 0 000000
45 0 000000
46 0 000000
47 0 000000
48 0 000000
49 0 000000
50 0 000000
51 0 000000
52 0 000000
53 0 000000
54 400400 000000
55 0 000000
56 0 000000
57 0 000000
58 0 000000
59 0 000000
60 0 000000
61 0 000000
62 0 000000
63 0 000000
64 0 000000
65 0 000000
66 0 000000
67 0 000000
68 0 000000
69 0 000000
70 0 000000
71 0 000000
72 0 000000
73 0 000000
74 0 000000
75 0 000000
76 0 000000
77 0 000000
78 0 000000
79 0 000000
80 0 000000
81 0 000000
82 0 000000
83 0 000000

```

10.8

```

84 HHHHHHHHHH47
85 HHHHHHHHHHDD
86 HHHHHHHHHH4
87 HHHHHHHHHHDD
88 HHHHHHHHHH
89 HHHHHHHHHH
90 HHHHHHHHHH
91 DHHHHHHHHH
92 HHHHHHHHHH
93 HHHHHHHHHH
94 HHHHHHHHHH
95 HHHHHHHHHH
96 HHHHHHHHHH
97 HHHHHHHHHH
98 HHHHHHHHHH
99 HHHHHHHHHH
100 HHHHHHHHHH
101 HHHHHHHHHH
102 HHHHHHHHHH
103 HHHHHHHHHH
104 HHHHHHHHHH
105 HHHHHHHHHH
106 HHHHHHHHHH
107 HHHHHHHHHH
108 HHHHHHHHHH
109 HHHHHHHHHH
110 HHHHHHHHHH
111 HHHHHHHHHH
112 HHHHHHHHHH
113 HHHHHHHHHH
114 HHHHHHHHHH
115 HHHHHHHHHH
116 HHHHHHHHHH
117 HHHHHHHHHH
118 HHHHHHHHHH
119 HHHHHHHHHH
120 HHHHHHHHHH
121 HHHHHHHHHH
122 HHHHHHHHHH
123 HHHHHHHHHH
124 HHHHHHHHHH
125 HHHHHHHHHH
126 HHHHHHHHHH
127 HHHHHHHHHH
128 HHHHHHHHHH
129 HHHHHHHHHH
130 HHHHHHHHHH
131 HHHHHHHHHH
132 HHHHHHHHHH
133 HHHHHHHHHH
134 HHHHHHHHHH
135 HHHHHHHHHH
136 HHHHHHHHHH
137 HHHHHHHHHH
138 HHHHHHHHHH
139 HHHHHHHHHH
140 HHHHHHHHHH
141 HHHHHHHHHH
142 HHHHHHHHHH
143 HHHHHHHHHH
144 HHHHHHHHHH
145 HHHHHHHHHH
146 HHHHHHHHHH
147 HHHHHHHHHH
148 HHHHHHHHHH
149 HHHHHHHHHH
150 HHHHHHHHHH
151 HHHHHHHHHH
152 HHHHHHHHHH
153 HHHHHHHHHH
154 HHHHHHHHHH
155 HHHHHHHHHH
156 HHHHHHHHHH
157 HHHHHHHHHH
158 HHHHHHHHHH
159 HHHHHHHHHH
160 HHHHHHHHHH
161 HHHHHHHHHH
162 HHHHHHHHHH
163 HHHHHHHHHH
164 HHHHHHHHHH
165 HHHHHHHHHH
166 HHHHHHHHHH
167 HHHHHHHHHH
168 HHHHHHHHHH
169 HHHHHHHHHH
170 HHHHHHHHHH
171 HHHHHHHHHH
172 HHHHHHHHHH
173 HHHHHHHHHH
174 HHHHHHHHHH
175 HHHHHHHHHH

```

10c

176 S00U7#5U7439
177 BBBBHHND4444
178 BBBBHHND4444
179 SS7747444111
180 SS8819441111
181 C49919441111
182 4M1911111111
183 999911111111
184 99991111119C
185 91911111199C
186 91111111199C
187 11911111199K
188 9911111119CG
189 0N1J11119C77
190 911111119C87
191 99991761111G
192 844700885LLI
193 886881111111
194 888888881111
195 888888885555
196 558888885555
197 SVHHHNS5555S
198 888888885555
199 888888885555
200 478511111111
201 468888885555
202 700000008888
203 558888887777
204 888777888777
205 777888888877
206 788877888777
207 888888885555
208 888888888888
209 888888888888
210 888888888888
211 888888888888
212 N9C94449GG99
213 111111111111
214 111111111111
215 648888888888
216 700000004444
217 408888888888
218 708888888888
219 888888888888
220 888888888888
221 888888888888
222 888888888888
223 888888888888
224 677688888888
225 004888888888
226 888888888888
227 478888888888
228 065588888888
229 708888888888
230 788888888888
231 718888888888
232 888888888888
233 888888888888
234 777888888888
235 811888888888
236 888888888888
237 888888888888
238 888888888888
239 888888888888
240 888888888888
241 888888888888
242 888888888888
243 444888888888
244 400000000000
245 000000000000
246 000000000000
247 000000000000
248 000000000000
249 000000000000
250 888888888888
251 888888888888
252 888888888888
253 888888888888
254 888888888888
255 888888888888
256 888888888888
257 888888888888
258 888888888888
259 888888888888
260 888888888888
261 888888888888
262 888888888888
263 888888888888
264 888888888888
265 888888888888
266 888888888888
267 888888888888

10a

269 DDHND400M4
270 4400DDDD4440
271 44444040077
272 447MD477777
273 7D70DD7G777
274 MND48000000
275 DD4444M41170
276 DDHND4444447
277 DDD4409M444
278 44DD44DDG444
279 4DD44D7DGG7G
280 47447B7DHD00
281 7G704400NH
282 4MND444400
283 1M11M444G44
284 MND44047004
285 40DDDDDD777
286 4044070MBSR
287 DD444G777G
288 DD44M3MG7777
289 DD444MM4774
290 D4DM49G444
291 DD4044G449
292 MND4444444
293 194MM444077
294 MND44449MG
295 M4444440GKIS
296 M44440DD0DL
297 M40DDND0S1
298 M40DDND070
299 40DD8870BB7
300 70DD70DD00M
301 44G70DD0DD00
302 44777BDD00H0
303 4077DD00MND
304 4407DD00007
305 40DDDDDD777
306 G70DD00777
307 B0DDDD07G
308 77B07777777
309 GGGDD7780DD
310 9G704770DD
311 GGG7DD44440
312 G7G70DD049
313 B77790049
314 707772477G
315 707GG7C7777
316 7757777K7777
317 4L7H5878557
318 88778555700
319 8807KSL0G7K
320 507801S1SB
321 777781S5BBH
322 4778887K77KB
323 G7KKB7CK7
324 77B8777070
325 GDDGL770S7
326 44499G470ND
327 DD77000040
328 000000044M4
329 409949ND0444
330 409R4070044
331 49990M0000
332 M440MNDMND
333 MND4000ND
334 40ND040SRND4
335 4440 MGD0DDN
336 44404JM70M4
337 40ND04NB4440
338 537774D440LV
339 444M411M444
340 0 MNDMND00J
341 00004440044
342 M440MND4444M
343 0400001044
344 V VDN44440M
345 VEN40N M
346 H004R B
347 M4M4HP
348 VP R4M4HP
349 HC VR M40M
350 BV VRH DRR0M
351 MND MND RND
352 MNDMND R M
353 M4M4B M4
354 R M4D R
355 MND411 R
356 CMMR4MCC
357 KDMND R
358 R M440MND
359 MNDMND
360 M MNDMND

102

361 UK YHNNH H4N
362 VHO 4N4SP #4N
363 CHNNMMH R H
364 P DH4NDVP HM
365 E DN44VGFHM
366 PPHNNH4NP R
367 PPP D9MAD
368 VPP D9MADV
369 V CHNNH8
370 VPPRD1M4N R
371 HCC M499M9
372 HNV D4NNH9
373 M94DHN4NNHMM
374 R RHRH4NNHMM
375 E RDHNNHMM
376 PPHND1M4N
377 R PCHSS91H11
378 DNM77999199
379 HNN9999999
380 4M99999999
381 4M99999999
382 HNN9999999
383 4M99999999
384 4M99999999
385 4M99999999
386 4M99999999
387 944M999999
388 CH4M999999
389 KCG4M999999
390 KKK3M999999
391 KKK3M999999
392 1199999999
393 7911117K7DD4
394 111111111111
395 111111111111
396 111111111111
397 111111111111
398 111111111111
399 111111111111
400 111111111111
401 111111111111
402 77419CC774
403 91119CC774
404 KKK9999999
405 KKK9999999
406 SSS9999999
407 1199999999
408 1199999999
409 KKK9999999
410 KKK9999999
411 C9CC1M1K7C
412 C9CC1M1K7C
413 KKK11111111
414 KKK11111111
415 KKK11111111
416 KKK11111111
417 KKK11111111
418 SSS11111111
419 SSS11111111
420 SSS11111111
421 SSS11111111
422 SSS11111111
423 SSS11111111
424 SSS11111111
425 SSS11111111
426 SSS11111111
427 SSS11111111
428 SSS11111111
429 SSS11111111
430 SSS11111111
431 SSS11111111
432 SSS11111111
433 SSS11111111
434 SSS11111111
435 SSS11111111
436 SSS11111111
437 SSS11111111
438 SSS11111111
439 SSS11111111
440 SSS11111111
441 SSS11111111
442 SSS11111111
443 SSS11111111
444 SSS11111111
445 SSS11111111
446 SSS11111111
447 SSS11111111
448 SSS11111111
449 SSS11111111
450 SSS11111111
451 SSS11111111
452 SSS11111111
453 SSS11111111

10f

```

454 887868888888
455 C77878888888
456 C77878888888
457 869888888888
458 899888888888
459 866788788877
460 C77777857888
461 K47888888878
462 078888777778
463 888888888888
464 078871115888
465 867768888888
466 887788888877
467 757778888877
468 878878887777
469 868888887788
470 778888877788
471 478877778877
472 448877777777
473 884888888877
474 774477777788
475 744888887788
476 777887777777
477 888888888888
478 888888888888
479 888888888888
480 888888888888
481 888888888888
482 888888888888
483 888888888888
484 888888888888
485 888888888888
486 888888888888
487 888888888888
488 888888888888
489 888888888888
490 888888888888
491 888888888888
492 888888888888
493 888888888888
494 888888888888
495 888888888888
496 888888888888
497 888888888888
498 888888888888
499 888888888888
500 888888888888
501 888888888888
502 888888888888
503 888888888888
504 888888888888
505 888888888888
506 888888888888
507 888888888888
508 888888888888
509 888888888888
510 888888888888
511 888888888888
512 888888888888

```


6bb

83
84
85
86
87
88
89
90
91
92
93
94
95
96
97
98
99
100
101
102
103
104
105
106
107
108
109
110
111
112
113
114
115
116
117
118
119
120
121
122
123
124
125
126
127
128
129
130
131
132
133
134
135
136
137
138
139
140
141
142
143
144
145
146
147
148
149
150
151
152
153
154
155
156
157
158
159
160
161
162
163
164
165
166
167
168
169
170
171
172
173
174
175
176
177

2
810

2

1 1 1 1 22
H 1 1 1

2

2

G

GG
G

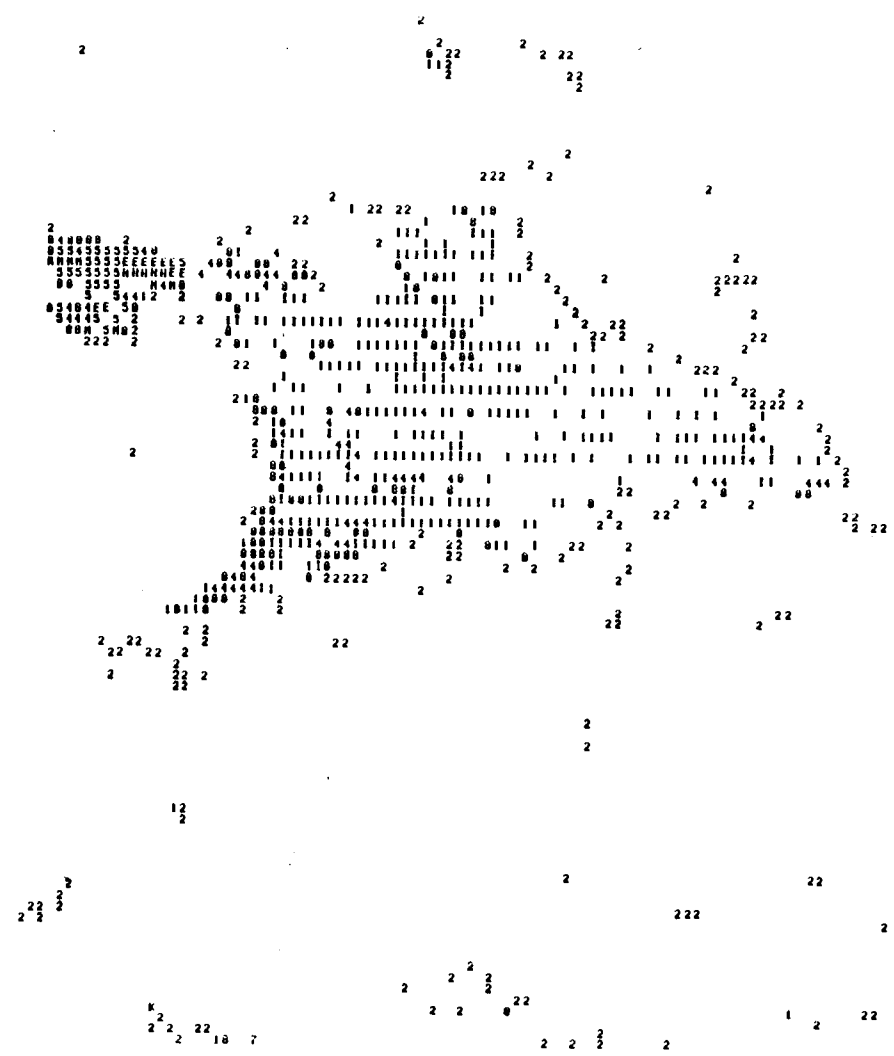
C AC

DF

GGG

766

85
 84
 87
 88
 89
 90
 91
 92
 93
 94
 95
 96
 97
 98
 99
 100
 101
 102
 103
 104
 105
 106
 107
 108
 109
 110
 111
 112
 113
 114
 115
 116
 117
 118
 119
 120
 121
 122
 123
 124
 125
 126
 127
 128
 129
 130
 131
 132
 133
 134
 135
 136
 137
 138
 139
 140
 141
 142
 143
 144
 145
 146
 147
 148
 149
 150
 151
 152
 153
 154
 155
 156
 157
 158
 159
 160
 161
 162
 163
 164
 165
 166
 167
 168
 169
 170
 171
 172
 173
 174
 175
 176
 177

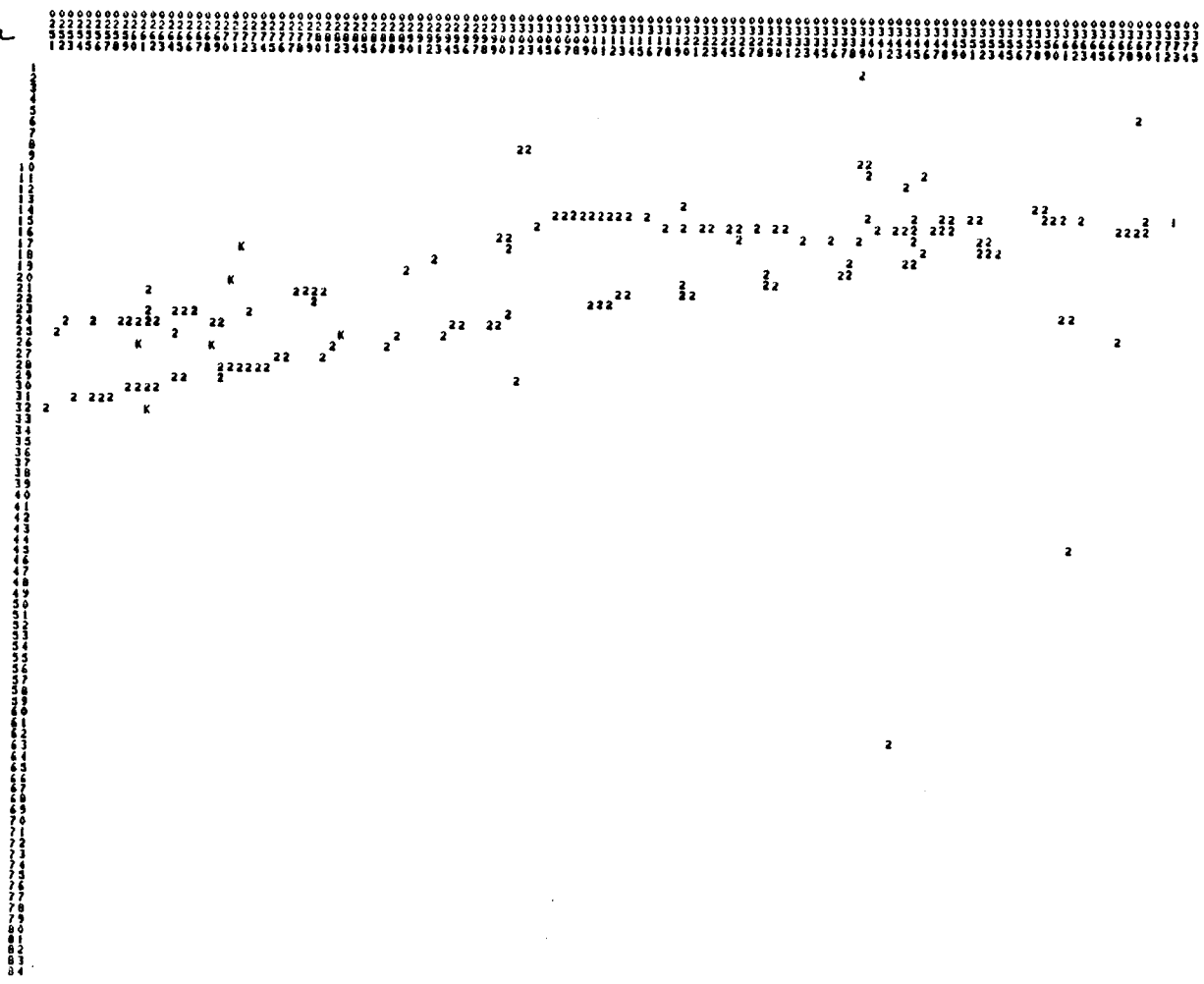


7FF
248
249
250
251
252
253
254
255
256
257
258
259
260
261
262
263
264
265
266
267
268
269
270
271
272
273
274
275
276
277
278
279
280
281
282
283
284
285
286
287
288
289
290
291
292
293
294
295
296
297
298
299
300
301
302
303
304
305
306
307
308
309
310
311
312

CC
C
A A
A
CC
A

2
2 2
1 2

Saa



866

85
86
87
88
89
90
91
92
93
94
95
96
97
98
99
100
101
102
103
104
105
106
107
108
109
110
111
112
113
114
115
116
117
118
119
120
121
122
123
124
125
126
127
128
129
130
131
132
133
134
135
136
137
138
139
140
141
142
143
144
145
146
147
148
149
150
151
152
153
154
155
156
157
158
159
160
161
162
163
164
165
166
167
168
169
170
171
172
173
174
175
176
177

22 22 2

22222222 2

2 2

2 2

1 22 2

2

2

2 2

2 2 2

2 2

2

2

2

2 2

22

2

2

2

2

2

2

2

22

2

2

2

2

2



1066

1066
1067
1068
1069
1070
1071
1072
1073
1074
1075
1076
1077
1078
1079
1080
1081
1082
1083
1084
1085
1086
1087
1088
1089
1090
1091
1092
1093
1094
1095
1096
1097
1098
1099
1100
1101
1102
1103
1104
1105
1106
1107
1108
1109
1110
1111
1112
1113
1114
1115
1116
1117
1118
1119
1120
1121
1122
1123
1124
1125
1126
1127
1128
1129
1130
1131
1132
1133
1134
1135
1136
1137
1138
1139
1140
1141
1142
1143
1144
1145
1146
1147
1148
1149
1150
1151
1152
1153
1154
1155
1156
1157
1158
1159
1160
1161
1162
1163
1164
1165
1166
1167
1168
1169
1170
1171
1172
1173
1174
1175
1176
1177
1178

1

2

1

2

2

1

1

1

11

66

103

424
223
224
225
226
227
228
229
230
231
232
233
234
235
236
237
238
239
240
241
242
243
244
245
246
247
248
249
250
251
252
253
254
255
256
257
258
259
260
261
262
263
264
265
266
267
268
269
270
271
272
273
274
275
276
277
278
279
280
281
282
283
284
285
286
287
288
289
290
291
292
293
294
295
296
297
298
299
300
301
302
303
304
305
306
307
308
309
310
311
312
313
314
315
316
317
318
319
320
321
322
323
324
325
326
327
328
329
330
331
332
333
334
335
336
337
338
339
340
341
342
343
344
345
346
347
348
349
350
351
352
353
354
355
356
357
358
359
360
361
362
363
364

2

2

2

2

2

2

2

K

2

2

2

2

2

2

2

2

2

2


```

460
461
10FF 462
463
464
465
466
467
468
469
470
471
472
473
474
475
476
477
478
479
480
481
482 43366
483 4
484 46
485 46 4 6
486 30566 6 33
487 44386333446
488 060FF60FFCF3
489 46 43 033C3
490 46CC43C346
491
492 46
493
494 43CC3F3
495 3F333CC310
496 CF333F33CC3C
497 C 03CC3FC
498 F0443FC33F3
499 C6 FCF064 0
500 FCF3FF00F3
501 FCCCF3FF33F
502 343CCF33CC
503 C443333343
504 CC3663606663
505 3CF36 03633
506 F333F633FFF
507 FCC3333CC3C
508 1CC3CC346 C
509 CCCC3CC3CC
510 33333FFCC3C
511 03CF 433C
512 00FFC3333F3

```